A compilation of charged-particle induced thermonuclear reaction rates

C. Angulo [a,1], M. Arnould [a], M. Rayet [a,2] P. Descouvemont [b,3], D. Baye [b],
C. Leclercq-Willain [b], A. Coc [c], S. Barhoumi [c,4], P. Aguer [c,5] C. Rolfs [d],
R. Kunz [e], J.W. Hammer [e], A. Mayer [e], T. Paradellis [f], S. Kossionides [f],
C. Chronidou [f], K. Spyrou [f], S. Degl'Innocenti [g,6], G. Fiorentini [g],
B. Ricci [g], S. Zavatarelli [g,7], C. Providencia [h,8], H. Wolters [h,9] J. Soares [h],
C. Grama [i], J. Rahighi [j,10], A. Shotter [j], M. Lamehi Rachti [j,10]

[a] Institut d'Astronomie et d'Astrophysique CP226, Université Libre de Bruxelles, B-1050 Bruxelles, Belgium
[b] Physique Nucléaire Théorique et Physique Mathématique CP229, Université Libre de Bruxelles,
B-1050 Bruxelles, Belgium
[c] Centre de Spectrométrie Nucléaire et Spectrométrie de Masse, IN2P3-CNRS, F-91405 Orsay, France
[d] Experimentalphysik III, Ruhr-Universität Bochum, D-44780 Bochum, Germany
[e] Institut für Strahlenphysik, Universität Stuttgart, D-70550 Stuttgart, Germany
[f] Laboratory for Material Analysis, Institute of Nuclear Physics, N.C.S.R. Demokritos,
GR-15310 Aghia Paraskevi, Greece
[g] Dipartimento di Fisica, Universita di Ferrara and INFN-Ferrara, I-44100 Ferrara, Italy
[h] Centro de Física Nuclear, Universidade de Lisboa, P-1699 Lisboa Cedex, Portugal
[i] Institute of Physics and Nuclear Engineering, P.O. Box MG-6, Bucharest, Romania
[j] Department of Physics and Astronomy, University of Edinburgh, EH9-3JZ Edinburgh, UK

Abstract

Low-energy cross section data for 86 charged-particle induced reactions involving light ($1 \leq Z \leq 14$), mostly stable, nuclei are compiled. The corresponding Maxwellian-averaged thermonuclear reaction rates of relevance in astrophysical plasmas at temperatures in the range from 10^6 K to 10^{10} K are calculated. These evaluations assume either that the target nuclei are in their ground state, or that the target states are thermally populated following a Maxwell–Boltzmann distribution, except in some cases involving isomeric states.

Adopted values complemented with lower and upper limits of the rates are presented in tabular form. Analytical approximations to the adopted rates, as well as to the inverse/direct rate ratios, are provided. © 1999 Elsevier Science B.V. All rights reserved.

1. Introduction

Since the fifties, astrophysics has advanced at a remarkable pace, and has achieved an impressive record of success. One of the factors contributing to these rapid developments is without any doubt a series of spectacular breakthroughs in *Nuclear Astrophysics*, which embodies the special interplay between nuclear physics and astrophysics.

The close relationship between these two major scientific disciplines comes about because of the clear demonstration that the structure, evolution and composition of a large variety of cosmic objects, including the Solar System, bear strong imprints of the properties of atomic nuclei, as well as of their interactions. In such conditions, careful and dedicated experimental and theoretical studies of a large variety of nuclear processes are indispensable tools for the modeling of ultra-macroscopic systems such as stars.

Thanks to the impressive skill and painstaking efforts of nuclear physicists involved in astrophysics, remarkable progress has been made over the years in order to evaluate reaction cross sections at energies that are as close as possible to those of astrophysical relevance. This is a highly challenging task indeed: for charged particle reactions, the energies of interest are much lower than the Coulomb barrier height, and the cross sections to be determined are among the smallest ones ever measured in the laboratory. The experimental problems nuclear physics has to face through astrophysics are even more severe as the properties and cross sections of a large variety of exotic (neutron-deficient or neutron-rich) nuclei are needed in some astrophysical modelings. The radioactive ion beam facilities in operation in some countries have already made some interesting data available. In a near future, many such facilities now under development all over the world will bring a wealth of new data of astrophysical interest.

In spite of much experimental effort and achievement, it is evident that nuclear models have to bring a substantial share to the evaluation of nuclear reaction rates in astrophysical plasmas. Theory has indeed (i) to provide as reliable extrapolations of experimental data as possible to low-energy regions of astrophysical relevance where this information is generally lacking, (ii) to extract purely nuclear effects from low-energy experimental data that may be "polluted" by atomic (screening) effects, or (iii) to provide reaction rates on excited nuclear states that are thermally populated in astrophysical conditions, or on nuclei away from the valley of nuclear stability. These

[1] Present address: Institut de Physique Nucléaire, Université catholique de Louvain, B-1348 Louvain-la-Neuve, Belgium.
[2] Chercheur qualifié FNRS.
[3] Directeur de Recherches FNRS.
[4] Permanent address: Institut de Physique, USTHB, B.P. 32, El-Alia, Bab Ezzouar, Algiers, Algeria.
[5] Present address: CENBG, IN2P3-CNRS, et Université de Bordeaux I, F-33175 Gradignan, France.
[6] Permanent address: Dipartimento di Fisica, Universita di Pisa, I-56100 Pisa, Italy.
[7] Permanent address: Dipartimento di Fisica, Universita di Genova and INFN-Genova, I-16146 Genova, Italy.
[8] Permanent address: Centro de Física Teórica, Universidade de Coimbra, P-3000 Coimbra, Portugal.
[9] Permanent address: Escola Superior de Ciencias e Tecnologia, Universidade Católica Portuguesa, P-3080 Figueira da Foz, Portugal.
[10] Permanent address: Van De Graaff Laboratory, Nuclear Research Centre, Atomic Energy Organisation of Iran, 14376 Tehran, Iran.

situations are not amenable to experiments at the present time, and will remain so for a long time to come.

Because of its very success and growth, in particular through the impressive achievements in experimental and theoretical nuclear physics mentioned above, nuclear astrophysics faces in fact a new and difficult challenge. The rapidly growing wealth of nuclear data becomes less and less easily accessible to the astrophysics community. Mastering this volume of information and making it available in an accurate and usable form for incorporation into stellar evolution or nucleosynthesis models become urgent goals of prime necessity. The establishment of the required level in the privileged communication between nuclear physicists and astrophysicists makes necessary the build-up of well documented and evaluated sets of experimental data or theoretical predictions of astrophysical relevance.

This has been the driving motivation for the setting-up in 1993 of a network of nuclear physics and astrophysics laboratories from Belgium, France, Germany, Greece, Italy, Portugal and the United Kingdom under the *Human Capital and Mobility* (HCM) Programme of the European Commission, this consortium being coordinated by the Institut d'Astronomie et d'Astrophysique of the Université Libre de Bruxelles. The aim of this collaborative effort is to provide a detailed evaluation and compilation of the rates for an ensemble of charged particle induced nuclear reactions on *stable* targets up to Silicon. Also included are several reactions on the unstable nuclei ^{7}Be, ^{13}N, ^{22}Na and ^{26}Al of special astrophysical significance. This work is meant to supersede the only compilation of such reactions for astrophysical purposes issued by W.A. Fowler and collaborators [FO67,FO75,HA83,CA85,CA88] (recent works give recommended values for the cross section of solar fusion reactions only [CA97,AD98]). The main innovative features with respect to this compilation that have been of constant concern during our work may be summarized as follows:

(1) detailed references are provided to the sources of the basic data (cross sections, resonance energies, spins, parities, ...) that are necessary in order to calculate the rates;

(2) the way these data have been evaluated is documented to a substantial extent;

(3) uncertainties have been analyzed in detail in order to provide realistic lower and upper bounds to the adopted rates;

(4) the evaluated/compiled rates are provided in tabular form. This format is considered to be especially well suited to modern computer use (as in the opacity tables [RO92]). However, analytical formulae approximating the rates might be wanted by some users, and have also been established.

Section 2 describes the formalism that has been adopted in order to derive the astrophysical rates of the charged particle induced reactions and of their reverse. In addition to the general formulae used for the calculation of the Maxwellian-averaged reaction rates, it contains a description of the data treatment, as well as the selected analytical expressions approximating the reaction rates. Section 3 explains the format adopted for the presentation of the results. Table 1 displays all the compiled reactions. Short write-ups are provided in Table 2 for the 86 reactions that have been analyzed. An-

alytical approximations of the reaction rates and the partition functions are given in Tables 3 and 4, respectively. More details are available electronically on the web site http://pntpm.ulb.ac.be/nacre.htm.

2. General formalism

2.1. Calculation of Maxwellian-averaged reaction rates $N_A\langle\sigma v\rangle$

Here, as well as in Sections 2.2–2.4, all equations apply to target nuclei in their ground state. Questions related to the thermal excitation of the targets are considered explicitly in Sections 2.5 and 2.6. We refer to Appendix A for the meaning of symbols and for the units used implicitly in some of the following formulae.

2.1.1. General definitions

For two-body reactions, the Maxwellian-averaged reaction rates $N_A\langle\sigma v\rangle$ are computed from [FO67]

$$N_A\langle\sigma v\rangle = N_A \frac{(8/\pi)^{1/2}}{\mu^{1/2}(k_B T)^{3/2}} \int_0^\infty \sigma E \exp(-E/k_B T)\,dE, \tag{1}$$

where N_A is the Avogadro number, μ the reduced mass of the system, k_B the Boltzmann constant, T the temperature, σ the cross section, v the relative velocity, and E the energy in the center-of-mass system. The only three-body reactions considered in this compilation are $^4\text{He}(\alpha n,\gamma)^9\text{Be}$ and $^4\text{He}(\alpha\alpha,\gamma)^{12}\text{C}$. The formulae to be applied in these cases are explained in the corresponding comments of Table 2.

When $N_A\langle\sigma v\rangle$ is expressed in $\text{cm}^3\,\text{mol}^{-1}\,\text{s}^{-1}$, the energies E and $k_B T$ in MeV, and the cross section σ in barn, Eq. (1) leads to

$$N_A\langle\sigma v\rangle = 3.7313 \times 10^{10} A^{-1/2} T_9^{-3/2} \int_0^\infty \sigma E \exp(-11.605 E/T_9)\,dE, \tag{2}$$

where A is the reduced mass in amu, and T_9 is the temperature in units of 10^9 K. The calculation of the rates is performed between $T_9 = 0.001$ and 10.

For charged-particle induced reactions, the cross section can be expressed as [FO67]

$$\sigma(E) = S(E)\exp(-2\pi\eta)\frac{1}{E}, \tag{3}$$

where $S(E)$, defined by this equation, is referred to as the astrophysical S-factor. The quantity

$$\eta = \frac{Z_1 Z_2 e^2}{\hbar v} = 0.1575 Z_1 Z_2 \left(\frac{A}{E}\right)^{1/2} \tag{4}$$

is the Sommerfeld parameter, Z_1 and Z_2 being the charge numbers of the interacting nuclei, and $\hbar$ the reduced Planck constant.

2.1.2. Numerical integration of the rates

Except for narrow resonances, the S-factor is a smooth function of energy, which is convenient for extrapolating measured cross sections down to astrophysical energies. When $S(E)$ is assumed to be a constant, the integrand in Eq. (1) is peaked at the "most effective energy" [FO67]

$$E_0 = \left(\frac{\mu}{2}\right)^{1/3} \left(\frac{\pi e^2 Z_1 Z_2 k_B T}{\hbar}\right)^{2/3} = 0.1220(Z_1^2 Z_2^2 A)^{1/3} T_9^{2/3} \text{ MeV} \tag{5}$$

and can be approximated by a Gaussian function centred at E_0, with full width at $1/e$ of the maximum given by

$$\Delta E_0 = 4(E_0 k_B T/3)^{1/2} = 0.2368(Z_1^2 Z_2^2 A)^{1/6} T_9^{5/6} \text{ MeV}. \tag{6}$$

With these approximations, the integral in Eq. (1) can be calculated analytically [FO67]. However, in the present compilation we do not rely on such approximations and perform numerically the integration of Eq. (1) for the non-resonant contribution to the rate, $N_A \langle \sigma v \rangle_{NR}$, as well as for the contribution of the broad resonances, $N_A \langle \sigma v \rangle_{BR}$. In those cases it is found that a good accuracy is reached by limiting the numerical integration for a given temperature to the energy domain $(E_0 - n\Delta E_0, E_0 + n\Delta E_0)$, with $n = 2$ or 3.

The main difficulty in evaluating the rates at the low temperatures in the range $0.001 \leqslant T_9 \leqslant 10$ is related to the necessity of extrapolating the S-factors down to very low energies, where cross sections are not available. General procedures are described in Section 2.2, that allow the rates to be calculated down to $T_9 = 0.001$. Their application to specific reactions is commented in Table 2. Similarly, for many of the reactions considered in this compilation, $N_A \langle \sigma v \rangle$ cannot be evaluated for temperatures as high as $T_9 = 10$ because of the lack of reliable cross section data at sufficiently high energies. In those case, we use theoretical estimates for $N_A \langle \sigma v \rangle$ to complement the experimentally based rates up to $T_9 = 10$ according to the procedure described in Section 2.5.

2.1.3. Treatment of narrow resonances

In the case of a narrow resonance, the resonant cross section $\sigma_r(E)$ is generally approximated by a Breit–Wigner expression [FO67,RO88]

$$\sigma_r(E) = \frac{\pi}{\kappa^2} \omega \frac{\Gamma_i(E) \, \Gamma_f(E)}{(E - E_r)^2 + \Gamma(E)^2/4}, \tag{7}$$

where κ is the wave number, $\Gamma_i(E)$ and $\Gamma_f(E)$ are the entrance and exit channel partial widths, respectively, $\Gamma(E)$ is the total width, and ω is the statistical factor given by

$$\omega = (1 + \delta_{12}) \frac{(2J + 1)}{(2I_1 + 1)(2I_2 + 1)}, \tag{8}$$

where I_1, I_2 and J are the spins of the interacting nuclei and of the resonance. The Kronecker symbol δ_{12} takes into account that the interacting nuclei can be identical.

The energy dependence of the particle widths $\Gamma_i(E)$ and $\Gamma_f(E)$ is given by [LA58]

$$\Gamma_{i,f}(E) = 2\gamma_{i,f}^2 P_\ell(E,a) = \Gamma_{i,f}\frac{P_\ell(E,a)}{P_\ell(E_r,a)},$$ (9)

where P_ℓ is the penetration factor associated with the relative angular momentum ℓ and with the channel radius, taken as $a = 1.4(A_1^{1/3} + A_2^{1/3})$ fm, $\Gamma_{i,f}$ are the partial widths at the resonance energy E_r, and $\gamma_{i,f}^2$ are the reduced widths. In absence of data, $\gamma_{i,f}^2 = 0.01\gamma_W^2$ are adopted as a first approximation, where $\gamma_W^2 = 3\hbar^2/2\mu a^2$ is the Wigner limit.

For radiative capture reactions, the energy dependence of the gamma width $\Gamma_\gamma(E)$ is given by

$$\Gamma_\gamma(E) = \Gamma_\gamma\left(\frac{E - E_f}{E_r - E_f}\right)^{2\lambda+1},$$ (10)

where Γ_γ is the gamma width at the resonance energy E_r, λ is the multipolarity of the electromagnetic transition, and E_f is the energy of the final state in the compound nucleus.

When the Breit–Wigner cross section (7) is inserted in Eq. (1), the integrand exhibits maxima at E_r and at E_0. The contribution of the former peak corresponds to the usual resonant term $N_A\langle\sigma v\rangle_r$, while the contribution of the latter represents the so-called "tail contribution" $N_A\langle\sigma v\rangle_{tail}$. We approximate those two contributions by functions which can be integrated analytically to obtain the resonant rate as a sum of two terms:

$$N_A\langle\sigma v\rangle_R = N_A\langle\sigma v\rangle_r + N_A\langle\sigma v\rangle_{tail}$$

$$= N_A\left(\frac{2\pi}{\mu k_B}\right)^{3/2}\hbar^2\omega\gamma T^{-3/2}\exp(-E_r/k_BT)$$

$$+ N_A\left(\frac{2}{\mu}\right)^{1/2}\frac{\Delta E_0}{(k_BT)^{3/2}}S(E_0)\exp(-C_0/T^{1/3}),$$ (11)

where $\omega\gamma$ is given by

$$\omega\gamma = \omega\frac{\Gamma_i\Gamma_f}{\Gamma(E_r)},$$ (12)

and $S(E_0)$ is the S-factor calculated at energy E_0 from Eqs. (3) and (7), and

$$C_0 = 3(\pi^2\mu/2k_B)^{1/3}(e^2Z_1Z_2/\hbar)^{2/3}.$$ (13)

When $N_A\langle\sigma v\rangle_R$ is expressed in $cm^3mol^{-1}s^{-1}$, E_r and $\omega\gamma$ in MeV, and $S(E_0)$ in MeV barn, Eq. (11) reads

$$N_A\langle\sigma v\rangle_R = 1.5394 \times 10^{11}A^{-3/2}(\omega\gamma)T_9^{-3/2}\exp(-11.605E_r/T_9)$$

$$+ 7.8318 \times 10^9(Z_1Z_2/A)^{1/3}S(E_0)T_9^{-2/3}\exp(-4.2486(Z_1^2Z_2^2A/T_9)^{1/3}).$$ (14)

The relative importance of these two terms depends on E_r and E_0, and hence on temperature. When $E_0 \geqslant E_r$, the tail contribution turns out to be negligible.

The above procedure is repeated for each narrow resonance, and their contributions to the total rate are simply added. Exceptions are made in some cases. For example, for the (α,n) reactions, the resonance data are abundant enough to allow a numerical integration of Eq. (1) in the whole energy range of interest and to avoid any of the approximations described above.

Eq. (14) is also valid for the calculation of the subthreshold state contribution $N_A\langle\sigma v\rangle_{SR}$. In such cases, $\Gamma_i = 0$ ($\omega\gamma = 0$), and only the second term of Eq. (14) remains.

2.2. Data treatment

2.2.1. Resonances

When several and different data on a given resonance are published, the adopted energies E_r and strengths $\omega\gamma$ are obtained using the method of weighted average. The central value, K, and the internal and external errors, e_{int} and e_{ext}, are calculated for a set N_{exp} of data points from OV69

$$K = \frac{\sum_i W_i K_i}{\sum_i W_i}, \qquad W_i = (\Delta K_i)^{-2},$$

$$e_{int} = \left(\sum_i W_i\right)^{-1/2}, \qquad e_{ext} = \left[\frac{1}{N_{exp} - 1}\frac{\sum_i W_i(K_i - K)^2}{\sum_i W_i}\right]^{1/2}. \tag{15}$$

Here, W_i are the weighting factors, taken as ΔK_i^{-2}, where ΔK_i is the standard deviation of the data K_i. The final error is taken as $\max(e_{int}, e_{ext})$.

2.2.2. Non-resonant data

Non-resonant data points (from either one or several publications) are first expressed in terms of S-factor data points, $S(E_k) \pm \Delta S(E_k)$, where E_k is the energy corresponding to the kth point. In general, these S-factor data are approximated by a polynomial of degree N, leading to

$$S(E) \simeq \sum_{i=0}^{N} S_i E^i. \tag{16}$$

The coefficients S_i of this polynomial are obtained from a χ^2-fit, where the individual data points are weighted by the errors, as explained in Section 2.2.1. This fit is expected to be the "best" fit to different data sets, where the lower and upper limits for the $S(E)$-curve are obtained using χ^2-procedures (i.e. taking into account the ΔS_k errors). The degree N can be chosen so as to improve the quality of the fit (typical values are $N = 2$ or 3). From the S-factor (16), the reaction rates (including lower and upper limits) are calculated by numerical integration of Eq. (1) using Eq. (3).

This procedure is the standard starting point. It is easily reproducible and avoids any subjective renormalization of the different experimental data sets. However, due to the large number of different cases, this standard procedure may have to be slightly modified

in specific situations (for example, renormalization might be necessary in some cases). Sometimes, a smooth spline fit to all data between the data points is adopted. These features are specified in the comments of each reaction (Table 2).

For the extrapolation of the data points to zero energy, laboratory cross sections have to be corrected for electron screening (see, for example, AS87) before including them in the calculations of the rates. This effect becomes significant typically for $E/U_e \leqslant 100$, where U_e is the so-called screening potential, and was first observed in the $^3\text{He}(\text{d},\text{p})^4\text{He}$ reaction below 15 keV [EN88]. On the other hand, in stellar conditions, the nuclei are surrounded by a dense electron gas that reduces the Coulomb repulsion and makes penetration of the Coulomb barrier easier. The cross sections are therefore enhanced in comparison with the cross sections between bare nuclei. This stellar screening effect can be evaluated by applying, for example, the Debye–Hückel theory [CL83]. The link between stellar and laboratory conditions therefore requires the bare-nucleus cross sections. The enhancement factor due to electron screening is taken as [AS87,SC89]

$$\frac{\sigma_s(E)}{\sigma(E)} \simeq \exp(\pi\eta U_e/E) \quad \text{for } U_e \ll E, \tag{17}$$

where $\sigma_s(E)$ and $\sigma(E)$ are the cross sections for the screened nuclei and for the bare nuclei, respectively. The electron screening potential U_e is determined from (17) with $\sigma(E)$ extrapolated down to zero energy. A first approximation is given by $U_e = Z_1 Z_2 e^2/R_a$, where $R_a \approx a_0/Z_h$ is the atomic radius of the innermost electrons of the heaviest of the interacting atoms 1 and 2, whose charged number is denoted Z_h, a_0 being the Bohr radius.

At the present time, the Coulomb breakup method, although promising, has not been demonstrated to be a fully reliable tool. Although available measurements of this type will be quoted, they will not be taken into account in the rate evaluation. On the other hand, when experimental data do not allow the calculation of reliable reaction rates in a certain temperature range, the data are complemented with theoretical information (see, for example, Section 2.3).

2.2.3. Treatment of endoergic reactions

Extrapolations to low energies of endoergic reactions between charged particles are difficult as experimental data exist only at energies far above the threshold, and the existing data at the lowest energies do not allow a clear picture of the behavior of the S-factor. This is the case for three of the reactions compiled in the present work: $^{14}\text{N}(\text{p},\alpha)^{11}\text{C}$, $^{20}\text{Ne}(\text{p},\alpha)^{17}\text{F}$ and $^{24}\text{Mg}(\text{p},\alpha)^{21}\text{Na}$.

The procedure for the calculation of the rates involves the S-factor of the reverse reactions S_{rev}, which smoothly depends on energy. The S-factor S_{rev} is approximated by an analytical function and extrapolated afterwards. The approximation can be a polynomial fit of the kind $S_{\text{rev}} = \sum_{i=0}^{N} S_i E_\alpha^i$. This is the case of the $^{14}\text{N}(\text{p},\alpha)^{11}\text{C}$ reaction. For the $^{20}\text{Ne}(\text{p},\alpha)^{17}\text{F}$ and $^{24}\text{Mg}(\text{p},\alpha)^{21}\text{Na}$ reactions, an exponential function $S_{\text{rev}} = a_1 \exp(-a_2 E_\alpha)$ gives a better fit. The coefficients S_i, a_1 and a_2 are obtained from a χ^2-fit. The energy E_α is the center of mass energy in the channel $\alpha+^{11}\text{C}$, $\alpha+^{17}\text{F}$, and $\alpha+^{21}\text{Na}$, respectively.

By means of the principle of time reversal [BL52], that relates the cross section $\sigma_{12\rightarrow34}$ for the reaction $1 + 2 \rightarrow 3 + 4$ to the cross section $\sigma_{34\rightarrow12}$ of the reverse $3 + 4 \rightarrow 1 + 2$ transformation (see also Section 2.7), the S-factor curves and the reaction rates for the direct reactions are calculated. Details are given in the comments of the corresponding reactions.

2.3. Potential model

At low energies, the non-resonant (also called direct capture) contribution can be significant. For some of the reactions studied here at astrophysical energies, it is even the dominant process. When data required to evaluate the non-resonant part are not available, a model calculation is performed. The radiative cross section

$$\sigma(E) = \sum_{J_f,\lambda} \sigma_{J_f,\lambda}(E) \tag{18}$$

is summed over final states J_f and electric multipoles $E\lambda$. For the direct radiative capture to a state with spin J_f, the cross section for the dominant electric $E\lambda$ transition is given by

$$\begin{aligned}
\sigma_{J_f,\lambda}(E) = {}& 8\pi\alpha\frac{c}{\upsilon\kappa^2}\left[Z_1\left(\frac{A_2}{A}\right)^\lambda + Z_2\left(\frac{-A_1}{A}\right)^\lambda \right]^2 C^2 S_{J_f} \\
& \times \sum_{J_i,I,\ell_i} \frac{(\kappa_\gamma)^{2\lambda+1}}{[(2\lambda+1)!!]^2} \frac{(\lambda+1)(2\lambda+1)}{\lambda} \\
& \times \frac{(2\ell_i+1)(2\ell_f+1)(2J_f+1)}{(2I_1+1)(2I_2+1)} \begin{pmatrix} \ell_f & \lambda & \ell_i \\ 0 & 0 & 0 \end{pmatrix}^2 \\
& \times (2J_i+1)\begin{Bmatrix} J_i & \ell_i & I \\ \ell_f & J_f & \lambda \end{Bmatrix}^2 \left(\int_0^\infty \phi_i(r)r^\lambda\phi_f(r)\,dr\right)^2,
\end{aligned} \tag{19}$$

where κ_γ is the photon wave number, ℓ_i and ℓ_f are the initial and final orbital angular momenta, I is the channel spin,

$$\begin{pmatrix} \ell_f & \lambda & \ell_i \\ 0 & 0 & 0 \end{pmatrix} \quad \text{and} \quad \begin{Bmatrix} J_i & \ell_i & I \\ \ell_f & J_f & \lambda \end{Bmatrix}$$

are the $3j$ and $6j$ symbols, and ϕ_i and ϕ_f are the initial and final wave functions, solutions of the radial Schrödinger equation

$$\left[-\frac{\hbar^2}{2\mu}\left(\frac{d^2}{dr^2} - \frac{\ell(\ell+1)}{r^2} \right) + V^{J\ell I}(r) \right] \phi(r) = E\phi(r), \tag{20}$$

where the potential $V^{J\ell I}(r)$ is adjusted so as to reproduce the energies of the final bound states. It has been shown in BA85 that adjusting the potential to the final bound state gives a good estimate. This equation is solved numerically. In Eq. (19), $C^2 S_{J_f}$ is

the spectroscopic factor of the final state, assumed to be $C^2 S_{J_f} = 1$ for the reactions considered here. The initial scattering wave function is normalized asymptotically as

$$\phi_i \underset{r \to \infty}{\to} \cos \delta^{J_i \ell_i I} F_{\ell_i}(\kappa r) + \sin \delta^{J_i \ell_i I} G_{\ell_i}(\kappa r), \tag{21}$$

where F_ℓ and G_ℓ are the regular and irregular Coulomb wave functions, and $\delta^{J\ell I}$ is the phase shift. The channel spin I is equal to the total spin of the final state. The orbital momentum of the initial state is chosen as the smallest value compatible with the orbital momentum ℓ_f of the bound state and the multipolarity λ.

2.4. Analytical approximation of reaction rates

The major goal of the present compilation is to provide numerical reaction rates in tabular form. This approach differs from the one promoted in previous compilations (CA88 and references therein), and is expected to lead to more accurate rates. However, for completeness, we also provide analytical approximations to the numerical adopted rates. For this purpose, the total rate is expressed as

$$N_A \langle \sigma v \rangle = N_A \langle \sigma v \rangle_{\mathrm{NR+tail}} + N_A \langle \sigma v \rangle_r + N_A \langle \sigma v \rangle_{\mathrm{MR}} + N_A \langle \sigma v \rangle_{\mathrm{SR}} + N_A \langle \sigma v \rangle_{\mathrm{BR}}, \tag{22}$$

where the various contributions are discussed in Sections 2.4.1–2.4.5 below.

2.4.1. Non-resonant and tail contribution to the rates

The non-resonant rate, $N_A \langle \sigma v \rangle_{\mathrm{NR}}$ (Section 2.1.2), and the tail contribution to the rate, $N_A \langle \sigma v \rangle_{\mathrm{tail}}$ (second term in the r.h.s. of Eq. (14)), are approximated by the same formula, and are lumped in a single contribution $N_A \langle \sigma v \rangle_{\mathrm{NR+tail}}$. For an exoergic reaction, with Q-value Q, it takes the form

$$N_A \langle \sigma v \rangle_{\mathrm{NR+tail}} = C_1 T_9^{-2/3} \exp(-C_0 T_9^{-1/3}) \left(1 + \sum_{i=1}^{N_{\mathrm{rate}}} c_i T_9^i \right) \quad [Q > 0]. \tag{23}$$

The coefficients C_1 and c_i are fitted to the rate contributions calculated as described in Sections 2.1.2 and 2.1.3, and $C_0 = 4.2486(Z_1^2 Z_2^2 A)^{1/3}$ (from Eq. (13)). The degree N_{rate} of the polynomial in Eq. (23) is chosen in order to obtain fits accurate to a few percent, and typically better than 10–15%. Eq. (23) is found to provide a better approximation than the $T_9^{1/3}$ expansion adopted in previous compilations (Eq. (50) in FO67).

For endoergic reactions, $N_A \langle \sigma v \rangle_{\mathrm{NR+tail}}$ is parametrized as [BA69a]

$$N_A \langle \sigma v \rangle_{\mathrm{NR+tail}} = C_1 T_9^{-2/3} \exp(-C_0' T_9^{-1/3} - D_0/T_9)$$

$$\times \left(1 + \sum_{i=1}^{N_{\mathrm{rate}}} c_i T_9^i \right) \quad [Q < 0], \tag{24}$$

where

$$D_0 = |Q|/k_B = 11.605|Q|,$$ (25)

Q being expressed in MeV and C_1 and c_i are adjustable parameters. The coefficient C_0' is computed from Eq. (13) with the nuclear charges and masses corresponding to the exit channel.

2.4.2. Isolated and narrow resonance rates

The contribution of isolated and narrow resonances is given by the first term of Eq. (14),

$$N_A \langle \sigma v \rangle_r = D_1 T_9^{-3/2} \exp(-D_2/T_9),$$ (26)

with

$$D_1 = N_A \left(\frac{2\pi}{\mu k_B} \right)^{3/2} \hbar^2 (\omega \gamma) = 1.5394 \times 10^{11} A^{-3/2} \omega \gamma$$ (27)

and

$$D_2 = E_r/k_B = 11.605 E_r.$$ (28)

The analytical approximations include the isolated and narrow resonances with the most significant contribution.

2.4.3. Multiresonant rates

For high densities of resonances (energy spacings of the order of the resonance widths, or even overlapping resonances), it is found that a continuum background is superimposed on some sharp resonances. While these narrow resonances can be accounted for by Eqs. (26)–(28), it is advisable to represent the continuum by one multiresonance (MR) term of the form

$$N_A \langle \sigma v \rangle_{MR} = D_3 T_9^{D_4} \exp(-D_5/T_9).$$ (29)

The parameters D_3, D_4 and D_5 are obtained from a fit to the numerical values of the rates.

2.4.4. Subthreshold states

When a subthreshold state is present, its contribution $N_A \langle \sigma v \rangle_{SR}$ to the rate is obtained through a modification of Eq. (23) which reads

$$N_A \langle \sigma v \rangle_{SR} = C_1 T_9^{-2/3} S(E_0) \exp(-C_0 T_9^{-1/3}) \left(1 + \sum_{i=1}^{N_{rate}} c_i T_9^i \right),$$ (30)

where C_1 and c_i are adjustable parameters. Using Eqs. (3) and (7), the S-factor is found to depend on energy as

$$S(E) = S_r \frac{1}{(E - E_r)^2 + \Gamma^2/4},$$ (31)

where $S_r = S(E_r)$. Taking into account that $E_r < 0$ and that Γ is very small, the energy dependence of the S-factor can be approximated by $1/E^2$. With this result, Eq. (30) is rewritten as

$$
N_A \langle \sigma v \rangle_{SR} = C_1 T_9^{-2} \exp(-C_0 T_9^{-1/3}) \left(1 + \sum_{i=1}^{N_{rate}} c_i T_9^i \right),
\tag{32}
$$

where C_1 and c_i are adjustable parameters.

2.4.5. Broad low energy resonances

When a broad low energy resonance ($\Gamma > E_r$) is present, the S-factor is not well approximated by a polynomial. In contrast to the case of subthreshold states, the denominator of Eq. (31) cannot be approximated by E^2. The contribution to the total reaction rate of a broad low energy resonance can be written as

$$
N_A \langle \sigma v \rangle_{BR} = C_1 T_9^{-2/3} \exp(-C_0 T_9^{-1/3}) \frac{1}{[E_0(T_9) - E_r]^2 + \Gamma^2/4} \left(1 + \sum_{i=1}^{N_{rate}} c_i T_9^i \right),
\tag{33}
$$

where C_1 and c_i are adjustable parameters.

2.5. Hauser–Feshbach rates

When cross section data do not allow the calculation of $N_A \langle \sigma v \rangle$ up to $T_9 = 10$, we use theoretical predictions obtained with the Hauser–Feshbach model in a range $T_{9,max} < T_9 \leqslant 10$, where $T_{9,max}$ is defined as follows. Let us denote E_{max} as the highest center-of-mass energy for which a cross section measurement is available. A reliable calculation of $N_A \langle \sigma v \rangle$ on the basis of the available measurements can be done at a given temperature if the contribution of the integrand of Eq. (2) for $E > E_{max}$ can be neglected at that temperature. This requirement is examined for each considered reaction, and is found to be satisfied if one takes $E_0 + n\Delta E_0 = E_{max}$ with $n = 1$ to 3, depending on the reaction. From this condition, $T_{9,max}$ is deduced with the help of Eqs. (5) and (6). Note that, in a few instances (specified in the comments of Table 2), it is considered that the mere use of a constant S-factor up to the energy $E_0 + n\Delta E_0$ corresponding to $T_9 = 10$ is sufficient, not leading to a significant loss of accuracy, so that the use of Hauser–Feshbach rates is not necessary.

In short, the Hauser–Feshbach (HF) calculations proceed as follows. Let us consider the reaction $1^\alpha + 2 \rightarrow 3^\beta + 4$, where α and β represent bound states in target nucleus 1 and residual nucleus 3 with excitation energies ϵ_1^α and ϵ_3^β and with spins I_1^α and I_3^β, respectively (the ground states of 1 and 3 correspond to $\alpha = 0$ and $\beta = 0$). We consider reactions where particles 2 and 4, with spins I_2 and I_4, are neutrons, protons, α-particles or photons and have no bound excited states. The HF theory assumes that the reaction proceeds through the formation of a compound nucleus and that the cross section is given by

$$\sigma_{\alpha\beta}(E^{\alpha}) = \frac{\pi\hbar^2/2\mu E^{\alpha}}{(2I_1^{\alpha}+1)(2I_2+1)} \sum_{J,\pi} (2J+1) \frac{T^{\alpha}(J^{\pi})T^{\beta}(J^{\pi})}{T_{\text{tot}}(J^{\pi})} W_{\alpha\beta}, \qquad (34)$$

where 1^{α} and 2 interact with center-of-mass energy $E^{\alpha} = E - \epsilon_1^{\alpha}$. The quantities $T^{\alpha}(J^{\pi})$ and $T^{\beta}(J^{\pi})$ are the transmission functions for forming the state J^{π} in the compound nucleus from $1^{\alpha} + 2$ and $3^{\beta} + 4$, respectively. The statistical model assumes that such a state exists for each orbital angular momentum of the relative motion between 1 and 2 at the corresponding excitation energy of the compound nucleus. Each T is a summation over all possible orbital and channel spins. The total transmission function $T_{\text{tot}}(J^{\pi})$ is the sum of all the transmission functions for the decay of the compound state J^{π} into any possible (bound or unbound) state energetically accessible from $1^{\alpha} + 2$ interacting with energy E^{α}, while $W_{\alpha\beta}$ is the width fluctuation correction factor.

The total cross section $\sigma_{\alpha}(E^{\alpha})$ for the reaction $1^{\alpha} + 2 \rightarrow 3 + 4$ to all bound states of the residual nucleus is obtained by summing over β both sides of Eq. (34), and the laboratory measurements provide the cross section $\sigma_0(E)$ on the target ground state. When the residual nucleus has an isomeric state, it may be of interest to distinguish the reaction leading to that state from the reaction producing the residual nucleus in its ground state. Such a distinction cannot be made in our HF calculations. The particular treatment of the reactions $^{25}\text{Mg}(p,\gamma)^{26}\text{Al}^{g,m}$ is described in the comments of Table 2.

We briefly describe here the nuclear physics ingredients used in our HF calculations. The γ-transmission functions include the dominant E1 and M1 transitions only. The transmission functions for neutrons and protons are calculated using optical potentials derived by JE77, while the phenomenological Woods–Saxon potential of MA78a is used for the calculation of α-particle transmission functions. We refer to TH86 for further references and details concerning the calculation of transmission functions. The summation over nuclear excited states which appears in Eq. (34) transforms into an integral over a nuclear level density as soon as the channel energy exceeds the energy of the last excited level for which energy, spin and parity are known experimentally. The experimental nuclear levels are taken from the Nuclear Data Sheets up to 1995, and a level density formula based on the back-shifted Fermi gas formalism with empirical shell corrections [TH86] is adopted. The nuclear masses are from AU97. The use of a statistical reaction theory may seem inappropriate in the case of very light nuclei. However, we observe that, for the 27 reactions requiring HF calculations, the rates derived from experiments differ from the theoretical ones at $T_9 = T_{9,\text{max}}$ by less than a factor 7, except in 2 cases, where they differ by factors 14 and 34.

In order to keep a reasonable balance between the reliability of our experimentally based rates and the relatively good quality of the HF predictions (being expected to be better at higher than at lower temperatures), we adopt the following procedure in the $T_{9,\text{max}} < T_9 \leqslant 10$ range. Let us denote $\langle \sigma v \rangle_a$, $\langle \sigma v \rangle_h$ and $\langle \sigma v \rangle_l$ the recommended rates and their estimated upper and lower limits, where the indices a, h and l stand for *adopt*, *high* and *low* as in Table 2 (see Section 3). Upper indices "max" and "10" refer to the values of those quantities at $T_9 = T_{9,\text{max}}$ and at $T_9 = 10$, respectively. A typical situation is shown in Fig. 1 for the case where the calculated HF rate is larger than the adopted one at $T_{9,\text{max}}$ (Fig. 1, upper panel).

In such a case,

(1) $\langle\sigma v\rangle_l$ is assumed to vary like the HF rate $\langle\sigma v\rangle_{HF}$. Having to be continuous at $T_{9,max}$, it is simply given by

$$\langle\sigma v\rangle_l = \langle\sigma v\rangle_{HF}\frac{\langle\sigma v\rangle_l^{max}}{\langle\sigma v\rangle_{HF}^{max}}; \tag{35}$$

(2) we consider that the upper limit of the rate at $T_9 = 10$ is given by $\langle\sigma v\rangle_{HF}^{10}$. To connect $\langle\sigma v\rangle_h^{max}$ to $\langle\sigma v\rangle_h^{10}$ we multiply $\langle\sigma v\rangle_{HF}$ according to

$$\langle\sigma v\rangle_h = \langle\sigma v\rangle_{HF}\left(\frac{10 - T_9}{10 - T_{9,max}}\frac{\langle\sigma v\rangle_h^{max}}{\langle\sigma v\rangle_{HF}^{max}} + \frac{T_9 - T_{9,max}}{10 - T_{9,max}}\right), \tag{36}$$

where the multiplicative factor varies linearly with T_9 and has the correct values at $T_{9,max}$ and 10;

(3) $\langle\sigma v\rangle_a$ is obtained by requiring that the ratio of the errors made on $\langle\sigma v\rangle$ remains constant in the $T_{9,max} < T_9 \leqslant 10$ range,

$$\frac{\langle\sigma v\rangle_h - \langle\sigma v\rangle_a}{\langle\sigma v\rangle_a - \langle\sigma v\rangle_l} = \frac{\langle\sigma v\rangle_h^{max} - \langle\sigma v\rangle_a^{max}}{\langle\sigma v\rangle_a^{max} - \langle\sigma v\rangle_l^{max}}. \tag{37}$$

Similar prescriptions are used for the determination of $\langle\sigma v\rangle_a$, $\langle\sigma v\rangle_h$ and $\langle\sigma v\rangle_l$ when $\langle\sigma v\rangle_{HF}^{max} < \langle\sigma v\rangle_a^{max}$, the treatment of $\langle\sigma v\rangle_l$ and $\langle\sigma v\rangle_h$ being interchanged in this case.
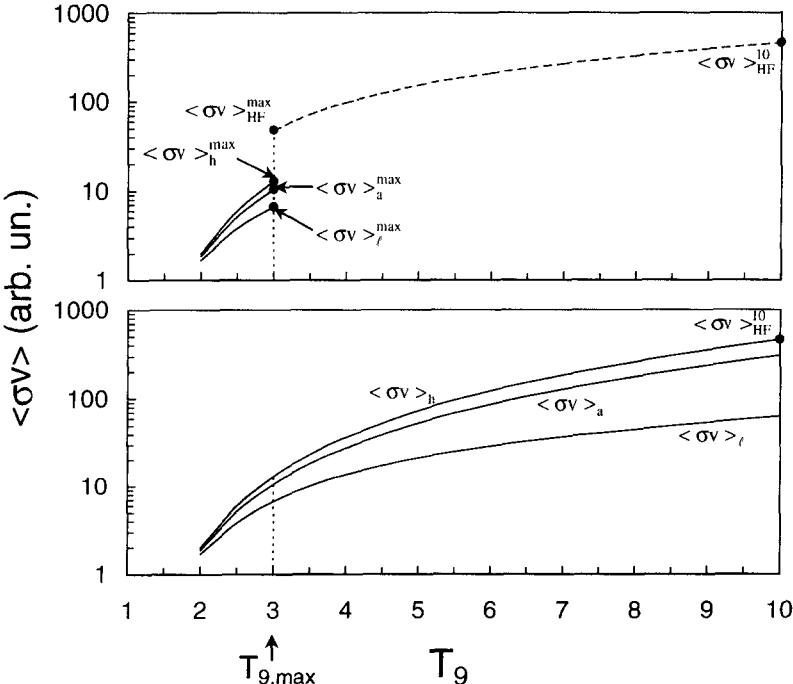
Fig. 1. Construction of the adopted rate and of its upper and lower limits in the range $T_{9,max} < T_9 \leqslant 10$. Upper panel: the evaluated rates $\langle\sigma v\rangle_a$, $\langle\sigma v\rangle_l$ and $\langle\sigma v\rangle_h$ for $T_9 \leqslant T_{9,max}$ and the HF estimate for $T_{9,max} < T_9 \leqslant 10$; lower panel: $\langle\sigma v\rangle_a$, $\langle\sigma v\rangle_l$ and $\langle\sigma v\rangle_h$ calculated up to $T_9 = 10$ by the procedure outlined in the text.

2.6. Effect of the thermal excitation of target nuclei

In a stellar plasma, the excited levels of a target nucleus are thermally populated, and thus contribute to the reaction mechanism. As a result, the stellar rates may differ from those obtained when the target nuclei are in their ground state. This correction cannot be predicted on grounds of experimental data, except in very specific situations (see e.g. [BA69b]). These are considered in [CA88] (Table 2) through appropriate corrections in their analytical expressions, whenever those authors consider it to be important. In the other instances, they evaluate the thermalization effects with the use of the so-called "equal strength approximation". In this rough approach, the rate on a thermalized target is just identical to the ground state rate (see [FO75], p. 90, for a thorough discussion of the [CA88] procedure). Here, we evaluate this effect in the framework of the HF model by calculating the population of the target excited states under the assumption that the stellar plasma is in local thermodynamic equilibrium (LTE). In this case the relative population of the various states is simply Maxwellian. The ratio of the HF rates on a thermalized target to the HF rates for a target in its ground state is then given by

$$r_{tt} = \frac{1}{G_1(T)} \sum_{\alpha} \frac{(2J_1^{\alpha} + 1)}{(2J_1^0 + 1)} \exp\left(-\frac{\epsilon_1^{\alpha}}{kT}\right) \frac{\langle \sigma_{\alpha} v \rangle_{HF}}{\langle \sigma_0 v \rangle_{HF}}, \tag{38}$$

where

$$G_i(T) = \frac{1}{2J_i^0 + 1} \sum_{\mu} (2J_i^{\mu} + 1) \exp\left(-\frac{\epsilon_i^{\mu}}{kT}\right) \tag{39}$$

is the temperature-dependent normalized partition function for nucleus i. The temperature dependent partition functions (39) are given in Table 4 in the form of analytical expressions in T_9 for all concerned target and residual nuclei.

The use of the HF theory to calculate r_{tt} is justified by the previous discussion on the validity of HF for describing the ground state rate $\langle \sigma_0 v \rangle$ since the reaction from a target excited level shifts the energy of the compound nucleus by the energy of that level, so that the number of available compound nucleus levels is increased. On the other hand, in all cases considered, the temperature dependence of the rates is very smooth at temperatures where thermal effects are expected to be important. As a result, very large variations of $\langle \sigma_{\alpha} v \rangle$ due to the presence of isolated resonances, which would be overlooked by using a statistical description of the involved nuclear spectra, are very improbable. Although one cannot exclude that the use of the HF model can accidentally introduce errors in r_{tt}, we consider that most of the uncertainty is removed by expressing r_{tt} as a ratio of two HF estimates.

For each reaction, the values of $N_A \langle \sigma v \rangle_{gs}$ given in the tables (see Section 3) have to be multiplied by r_{tt} in order to obtain the "thermalized" rates $N_A \langle \sigma v \rangle_{tt}$ which are of direct astrophysical relevance. The same correction applies to the *low*, *adopted* and *high* rates. For nuclei with $Z > 5$, and when r_{tt} differs from unity by more than 3% at one temperature at least of the considered range (r_{tt} can be either > 1 or < 1), r_{tt} is approximated by analytical formulae which are given in Table 3. In the other cases, we

just adopt $N_A\langle\sigma v\rangle_{tt} = N_A\langle\sigma v\rangle_{gs}$. The errors made by using the formulae of Table 3 are in general negligible, and can reach 5% only for large corrections (in excess of 50%).

Note that if the target nucleus has an isomeric state, its population relative to the others states is not always Maxwellian in the considered temperature range, and the above prescription has to be modified. We refer to the comments of Table 2 for the particular case of the reaction ^{26}Al(p, γ)^{27}Si.

The thermalization corrections are most pronounced when low lying excited states of the target nuclei can be strongly populated in the considered temperature range, and when the probability of an outgoing channel is strongly dependent on momentum-parity selection rules. This is particularly true for endoergic reactions which have particle channels as final states (see e.g. [AR72]). The corrections exceed 50% at some temperatures in the considered temperature range for 11 reactions: 7 of those are endoergic (p,n), (p,α) or (α,n) reactions, for which the corrections reach a factor 2 or more. Note that several large corrections are obtained for temperatures smaller than $T_9 = 10$, which shows the role played by the momentum-parity selection rules on the thermalization effect.

2.7. Reverse reaction rates

The principle of time-reversal invariance [BL52] relates the cross section $\sigma_{12\to34}$ for the reaction $1 + 2 \to 3 + 4$ to the cross section $\sigma_{34\to12}$ of the reverse $3 + 4 \to 1 + 2$ transformation. On these grounds, and provided that the rates for the direct and for the inverse reactions are thermalized, their ratio is given by

$$\frac{\langle\sigma v\rangle_{34\to12}}{\langle\sigma v\rangle_{12\to34}} = \frac{(2I_1 + 1)(2I_2 + 1)(1 + \delta_{34})}{(2I_3 + 1)(2I_4 + 1)(1 + \delta_{12})} \left(\frac{G_1 G_2}{G_3 G_4}\right) \left(\frac{A_1 A_2}{A_3 A_4}\right)^{3/2} \exp\left(-\frac{Q}{k_B T}\right),$$
(40)

where Q is the Q-value for reaction $1 + 2 \to 3 + 4$ and G_i are the temperature-dependent partition functions for nuclei $i = 1$ to 4, defined by Eq. (39). Note than $G_i(T) \equiv 1$ for nucleons and for nuclei which have no bound excited states.

The summation on the excited states μ of the nucleus i is performed as in the case of Eq. (34) (see Section 2.5). When "particle" 4 is a photon, the photodisintegration rate (in s^{-1}) for the reaction $3 + \gamma \to 1 + 2$ is written as

$$\lambda_{3\gamma\to12} = \frac{(2I_1 + 1)(2I_2 + 1)}{(2I_3 + 1)(1 + \delta_{12})} \left(\frac{G_1 G_2}{G_3}\right) \left(\frac{A_1 A_2}{A_3}\right)^{3/2} \left(\frac{k_B T}{2\pi N_A \hbar^2}\right)^{3/2}$$
$$\times \langle\sigma v\rangle_{12\to3\gamma} \exp\left(-\frac{Q}{k_B T}\right)$$
(41)

$$= 9.8686 \times 10^9 T_9^{3/2} \frac{(2I_1 + 1)(2I_2 + 1)}{(2I_3 + 1)(1 + \delta_{12})} \left(\frac{G_1 G_2}{G_3}\right) \left(\frac{A_1 A_2}{A_3}\right)^{3/2}$$
$$\times N_A \langle\sigma v\rangle_{12\to3\gamma} \exp\left(-11.605 Q/T_9\right).$$
(42)

A few of the compiled reactions involve three particles in the outgoing channel. Although the expression of $N_A \langle \sigma v \rangle$ for the direct reaction $1 + 2 \rightarrow 3 + 4 + 5$ is still given by Eq. (1), the reverse/direct rate ratio is given by

$$\frac{\langle \sigma v \rangle_{345 \rightarrow 12}}{\langle \sigma v \rangle_{12 \rightarrow 345}} = \frac{(2I_1 + 1)(2I_2 + 1) \, n_{345}!}{(2I_3 + 1)(2I_4 + 1)(2I_5 + 1)(1 + \delta_{12})}$$

$$\times \left(\frac{G_1 G_2}{G_3 G_4 G_5} \right) \left(\frac{A_1 A_2}{A_3 A_4 A_5} \right)^{3/2} \left(\frac{2 \pi N_A \hbar^2}{k_B T} \right) \exp \left(-\frac{Q}{k_B T} \right), \quad (43)$$

where n_{345} is the number of identical particles among 3, 4 and 5.

In Table 3 we give the reverse ratio for each reaction ("Rev. ratio") *without* the partition functions $G_i(T)$. The complete reverse ratio is obtained by using the partition functions of Table 4. The special cases of the two 3-body reactions are treated in comments of Table 2.

3. Presentation of results

The compilation is concerned only with reaction rates that are large enough for the target lifetime to be shorter than the age of the Universe, taken to be equal to 15×10^9 y. Assuming a density of 10^4 g cm^{-3}, reactions rates with values

$$N_A \langle \sigma v \rangle \leqslant 10^{-25} \; \text{cm}^3 \text{mol}^{-1} \text{s}^{-1}$$

can be considered as negligible in practically all astrophysical conditions. If $N_A \langle \sigma v \rangle$ is always larger than 10^{-25} cm^3 mol^{-1} s^{-1}, the lowest temperature T_9 is taken as 0.001, as in previous compilations. Larger densities can be met in various astrophysical phenomena, but only on a much shorter time scale.

Table 1 lists the compiled reactions. Reaction rates are given in Table 2. For each reaction, some comments concerning the adopted experimental data are given, along with the way the calculation of the rates has been performed. If necessary, a table of narrow resonances is given. It contains the energies E_r and strengths $\omega \gamma$ of an ensemble of relatively low energy resonances of relevance. For each of them, the source references are provided. In a variety of cases, more resonances than the explicitly tabulated ones are included in the rate calculation. Their taking into account is reminded in the resonance table, and the corresponding list of original references is given in the comments. A weighted average of the available resonance strengths is adopted for the calculation of the rates, except otherwise stated. For resonances where only an upper limit of the strength is reported, the adopted value is obtained by multiplying the upper limit by 0.1. The "error" on the adopted value corresponds to applying a factor 0 and 1 to obtain the lower and upper limits, respectively. The last column of the table shows whether the resonance has been treated as an isolated term (I), or included in a multiresonance term (M) in the analytical approximation. If its contribution is negligible (N), it is not included in the analytical approximation.

Figures of the S-factor versus energy are also given, where applicable. They show all published data sets, even those that are not adopted for the calculation of the rates. A temperature scale is also given. It is obtained by inverting Eq. (5), which gives the "most effective energy" E_0 as a function of temperatures. The solid curves correspond either to the adopted S-factor in the whole energy range covered by experiments, or to an extrapolation to lower energies. In the first case, the adopted curve is, in most cases, a polynomial fit. However, in some reactions, the adopted rate is calculated using the energy dependence given by theoretical calculations. Details about the adopted procedure are found in the comments. If only an extrapolation curve is shown, the rates are calculated using a spline curve though the experimental data and extrapolated to zero energy by the displayed curve. The Q-value is also shown for endoergic reactions.

The calculation of the reaction rates is performed as explained in Section 2. The results are presented in a tabular way in Table 2 as a function of T_9. The temperature steps are the same as in CA88. The columns labeled *low, adopt, high* display the lower limit, adopted value, and upper limit of $N_A \langle \sigma v \rangle_{gs}$. The column labeled *exp* is the exponent n of the factor 10^n that should multiply the three previous columns. Our adopted $N_A \langle \sigma v \rangle_{tt}$ rates can be calculated as the product of the entries of column *adopt* by the values of r_{tt}, an analytical approximation of which is given in Table 3. The column *ratio* displays the ratios between these adopted $N_A \langle \sigma v \rangle_{tt}$ and the *intermediate* rates proposed by CA88. This ratio may thus be affected by the respective predictions of both the ground state rate and the thermalized rate. Cases where our r_{tt} HF predictions differ from the CA88 equal strength approximation ($r_{tt} = 1$) by more than 10% are duly identified in the specific comments to the rates.

Analytical approximations for the adopted reaction rates $N_A \langle \sigma v \rangle_{gs}$ and $N_A \langle \sigma v \rangle_{tt}$ are given in Table 3, along with an analytical approximation of the factor (Rev. ratio) by which $N_A \langle \sigma v \rangle_{tt}$ has to be multiplied in order to derive the reverse rate on the corresponding thermalized nucleus.

Appendix A. Notations

Throughout this work, we use the following symbols and conventions. When symbols of physical quantities must be replaced by numerical values, the units given in brackets are used implicitly (unless otherwise stated) throughout this paper.

α	=	fine structure constant
γ^2	=	reduced resonance width
$\Gamma,\ \Gamma(E)$	=	total width in the center-of-mass system (MeV)
$\Gamma_i(E),\ \Gamma_f(E) =$		partial widths of the entrance and exit channels in the center-of-mass system (MeV)
δ_{ij}	=	Kronecker symbol
η	=	Sommerfeld parameter
κ	=	particle wave number
κ_γ	=	photon wave number
λ	=	order of the electric multipole moment
μ	=	reduced mass
$\sigma,\ \sigma(E)$	=	cross section (barn)
σ_r	=	resonant cross section (barn)
$\phi_i,\ \phi_f$	=	initial and final radial wave functions
$\omega\gamma$	=	resonance strength in the center-of-mass system (MeV)
a_0	=	first Bohr radius
A_i	=	mass of nucleus i (amu)
A	=	reduced mass (amu). For a two-body system $1 + 2$, $A = A_1 A_2 / (A_1 + A_2)$ (amu)
c	=	light velocity
e	=	proton charge
E	=	energy in the center-of-mass system (MeV)
E_γ	=	energy of the emitted gamma ray (MeV)
$E_{i,f}$	=	energy of the initial, final state in the compound nucleus (MeV)
E_r	=	resonant energy in the center-of-mass system (MeV)
E_0	=	most effective energy (MeV)
E_x	=	excitation energy with respect to the ground state (MeV)
ΔE_0	=	full $1/e$ width of the Gamow window (MeV)
$F_\ell,\ G_\ell$	=	regular, irregular Coulomb wave function
h	=	reduced Planck constant
I_i	=	spin of the interacting nucleus i in units of $\hbar$
I	=	channel spin in units of $\hbar$, $I = I_1 \otimes I_2$
J	=	resonance spin in units of $\hbar$
J_f	=	spin of a compound state in units of $\hbar$
k_B	=	Boltzmann constant
ℓ	=	relative orbital angular momentum in units of $\hbar$
$\ell_i,\ \ell_f$	=	initial, final orbital angular momentum in units of $\hbar$
N_A	=	Avogadro number

$N_A \langle \sigma v \rangle$ = reaction rate ($\text{cm}^3 \text{ mol}^{-1} \text{ s}^{-1}$)

$N_A \langle \sigma v \rangle_{gs}$ = reaction rate for the target nucleus in ground state ($\text{cm}^3 \text{ mol}^{-1} \text{ s}^{-1}$)

$N_A \langle \sigma v \rangle_{ms}$ = reaction rate for the target nucleus in isomeric state ($\text{cm}^3 \text{ mol}^{-1} \text{ s}^{-1}$)

$N_A \langle \sigma v \rangle_{tt}$ = reaction rate for a thermalized target nucleus ($\text{cm}^3 \text{ mol}^{-1} \text{ s}^{-1}$)

Q = reaction Q-value (MeV)

r = radial variable describing the relative motion of particles

R_a = atomic radius

$S(E)$ = astrophysical S-factor (MeV barn)

S_r = S-factor at the resonance energy E_r (MeV barn)

T = temperature

T_9 = temperature in 10^9 K

v = relative velocity

Z_i = charge number of interacting nucleus i

Appendix B. Physical constants and atomic masses

The following physical and conversion constants are used in all calculations related to the present compilation. They are taken from the 1996 report of the Particle Data Group [PA96] and, with the exception of c, are rounded to a maximum of 6 significant digits. For atomic masses, the central values of the AU97 compilation are used, rounded to the microamu level.

Although the physics involved in the cross section and reaction rate evaluation most often does not require the level of accuracy used for the atomic masses and for the following constants, any detailed comparison the reader wishes to make between his/her reaction rates and ours should use the same values in order to avoid artificial numerical discrepancies.

Note that, at the present level of accuracy, the last significant digit of our constants is neither affected by the 1-standard deviation uncertainties quoted in [PA96] (the quoted value of c is exact by definition, being used to define the meter), nor by the new recommended value for the constant ($2e/h$) used in [AU97].

c = 299792458 m s^{-1}

1 amu = 931.494 MeV/c^2

1 eV = 1.60218×10^{-19} J

$k_B T$ = $0.08617 T_9 = T_9/11.605$ MeV

N_A = 6.0221×10^{23} mol^{-1}

α = $e^2/\hbar c = 1/137.036$

$\hbar c$ = 197.327 MeV fm

Explanation of tables

Table 1. Summary of compiled reactions

Reaction	the reaction in conventional notation
Notation in refs.	notation used in references for each reaction

Table 2. Reaction rates

Reaction	the reaction in conventional notation	
Comments	specific comments on the compilation procedure	
S-factor figure	presentation of S-factor versus c.m. energy	
Resonance table	tabular presentation of resonance properties	
	E_r	resonance energy in c.m. system (in keV or MeV)
	J^π	resonance spin and parity
	$\omega\gamma$	resonance strength in c.m. system (in meV, eV or keV)
	adopt	adopted resonance strength in c.m. system
Table of rates	tabular presentation of rates	
	T_9	temperature in units of 10^9 K
	lower	lower limit of the rates
	adopt	recommended rates
	upper	upper limit of the rates
	exp	exponent n of the factor 10^n that should multiply the three previous columns
	ratio	ratio of the adopted rate $N_A\langle\sigma v\rangle_{tt}$ to the CA88 rate

Table 3. Analytical approximation of the reaction rates

Reaction	the reaction in conventional notation
Q	Q-value of the reaction in MeV
($n\%$)	accuracy of the analytical approximation with respect to the tabulated rates, "better than $n\%$"
gs, ms, tt	indicate reactions with target nuclei in ground state, isomeric state, or with thermalized target
g, m, t	indicate reactions leading to the ground state, isomeric state, or to both ground and isomeric states
Rev. ratio	factor by which the rate $N_A\langle\sigma v\rangle_{tt}$ has to be multiplied in order to get the rate of the reverse reaction on the corresponding thermalized nucleus

Table 4. Analytical approximation of the partition functions

$G(T_9)$ partition function

isotope   isotope in conventional notation

a_1, a_2, a_3, a_4, a_5 coefficients of the analytical approximation

The accuracy of the analytical approximations is better than 2%.

Table 1. List of compiled reactions

Reaction	Notation in refs.	Reaction	Notation in refs.	Reaction	Notation in refs.
^{1}H(p,νe$^+$)^{2}H	ppnu	^{11}B(p,α)^{8}Be	b11pa	^{20}Ne(p,α)^{17}F	ne20pa
^{2}H(p,γ)^{3}He	dpg	^{12}C(p,γ)^{13}N	c12pg	^{20}Ne(α,γ)^{24}Mg	ne20ag
^{2}H(d,γ)^{4}He	ddg	^{12}C(α,γ)^{16}O	c12ag	^{21}Ne(p,γ)^{22}Na	ne21pg
^{2}H(d,n)^{3}He	ddn	^{13}C(p,γ)^{14}N	c13pg	^{21}Ne(α,n)^{24}Mg	ne21an
^{2}H(d,p)^{3}H	ddp	^{13}C(p,n)^{13}N	c13pn	^{22}Ne(p,γ)^{23}Na	ne22pg
^{2}H(α,γ)^{6}Li	dag	^{13}C(α,n)^{16}O	c13an	^{22}Ne(α,γ)^{26}Mg	ne22ag
^{3}H(d,n)^{4}He	tdn	^{13}N(p,γ)^{14}O	n13pg	^{22}Ne(α,n)^{25}Mg	ne22an
^{3}H(α,γ)^{7}Li	tag	^{14}N(p,γ)^{15}O	n14pg	^{22}Na(p,γ)^{23}Mg	na22pg
^{3}He(^{3}He,2p)^{4}He	he3he3	^{14}N(p,n)^{14}O	n14pn	^{23}Na(p,γ)^{24}Mg	na23pg
^{3}He(α,γ)^{7}Be	he3ag	^{14}N(p,α)^{11}C	n14pa	^{23}Na(p,n)^{23}Mg	na23pn
^{4}He(αn,γ)^{9}Be	aang	^{14}N(α,γ)^{18}F	n14ag	^{23}Na(p,α)^{20}Ne	na23pa
^{4}He($\alpha\alpha$,γ)^{12}C	aaag	^{14}N(α,n)^{17}F	n14an	^{23}Na(α,n)^{26}Al^g	na23an
^{6}Li(p,γ)^{7}Be	li6pg	^{15}N(p,γ)^{16}O	n15pg	^{23}Na(α,n)^{26}Al^m	na23an
^{6}Li(p,α)^{3}He	li6pa	^{15}N(p,n)^{15}O	n15pn	^{23}Na(α,n)^{26}Al^t	na23an
^{7}Li(p,γ)^{8}Be	li7pg	^{15}N(p,α)^{12}C	n15pa	^{24}Mg(p,γ)^{25}Al	mg24pg
^{7}Li(p,α)^{4}He	li7pa	^{15}N(α,γ)^{19}F	n15ag	^{24}Mg(p,α)^{21}Na	mg24pa
^{7}Li(α,γ)^{11}B	li7ag	^{16}O(p,γ)^{17}F	o16pg	^{25}Mg(p,γ)^{26}Al^g	mg25pg
^{7}Li(α,n)^{10}B	li7an	^{16}O(α,γ)^{20}Ne	o16ag	^{25}Mg(p,γ)^{26}Al^m	mg25pg
^{7}Be(p,γ)^{8}B	be7pg	^{17}O(p,γ)^{18}F	o17pg	^{25}Mg(p,γ)^{26}Al^t	mg25pg
^{7}Be(α,γ)^{11}C	be7ag	^{17}O(p,α)^{14}N	o17pa	^{25}Mg(α,n)^{28}Si	mg25an
^{9}Be(p,γ)^{10}B	be9pg	^{17}O(α,n)^{20}Ne	o17an	^{26}Mg(p,γ)^{27}Al	mg26pg
^{9}Be(p,n)^{9}B	be9pn	^{18}O(p,γ)^{19}F	o18pg	^{26}Mg(α,n)^{29}Si	mg26an
^{9}Be(p,d)^{8}Be	be9pd	^{18}O(p,α)^{15}N	o18pa	^{26}Al^{gs}(p,γ)^{27}Si	al26pg
^{9}Be(p,α)^{6}Li	be9pa	^{18}O(α,γ)^{22}Ne	o18ag	^{26}Al^{ms}(p,γ)^{27}Si	al26pg
^{9}Be(α,n)^{12}C	be9an	^{18}O(α,n)^{21}Ne	o18an	^{27}Al(p,γ)^{28}Si	al27pg
^{10}B(p,γ)^{11}C	b10pg	^{19}F(p,γ)^{20}Ne	f19pg	^{27}Al(p,α)^{24}Mg	al27pa
^{10}B(p,α)^{7}Be	b10pa	^{19}F(p,n)^{19}Ne	f19pn	^{27}Al(α,n)^{30}P	al27an
^{11}B(p,γ)^{12}C	b11pg	^{19}F(p,α)^{16}O	f19pa	^{28}Si(p,γ)^{29}P	si28pg
^{11}B(p,n)^{11}C	b11pn	^{20}Ne(p,γ)^{21}Na	ne20pg		

The references of Sections 1, 2 and 3 are marked as "intro" in the reference list.

Table 2. Reaction rates

Reaction: ^{1}H(p,νe$^+$)^{2}H

The rates are essentially determined from theoretical calculations using the S-factor $S(E) = \mathcal{S}_0 + \mathcal{S}_1 E + \mathcal{S}_2 E^2$. Only $\mathcal{S}_0$ and $\mathcal{S}_1$ are available in the literature [BA69c,BR71, BA88a,GO90,CA91,BA92]. Following KA94, the S-factor at zero energy

$$S(0) = 3.89 \times 10^{-25} \left(\frac{\lambda^2(0)}{6.92}\right) \left(\frac{G_A/G_V}{1.2573}\right)^2 \left(\frac{1+\delta}{1.01}\right)^2 \left(\frac{f_{pp}(0)}{0.142}\right) \text{ MeV b} \quad \text{(B.1)}$$

is expressed in terms of the nuclear overlap $\lambda^2(0)$, the ratio of the axial vector to the vector coupling constant G_A/G_V, the correction $(1 + \delta)$ to the nuclear matrix element due to exchanges of π and ρ mesons, and the phase space factor $f_{pp}(0)$. The value $\lambda^2(0) = 6.9 \times (1^{+0.07}_{-0.015})$ is adopted, where the central value is from KA94, and the uncertainty is the range of published values [SA52,BA69c,BR71,GA72,BA79a,GO90,KA94]. A weighted mean of the available experimental results [BY95,PA96] gives $G_A/G_V = -1.268 \pm 0.004$. The value $\delta = 0.01 \pm 0.01$ is adopted on grounds of the most recent calculations [BA79a,CA91]. Former results [BL65,GA72,DA76] include only π contributions. The value $f_{pp}(0) = 0.142$ from BA69c is adopted. A 1.5% radiative correction taken from neutron decay is introduced empirically in AD98. As such a correction is sensitive to the varying endpoint energy and is not available for the present reaction, we do not include it here. For $\mathcal{S}_1/\mathcal{S}_0$, the most recent result of CA91, $\mathcal{S}_1/\mathcal{S}_0 = 11.7$ MeV^{-1}, is adopted (similar evaluations are presented in BA69c, BR71 and BA79a). For $\mathcal{S}_2/\mathcal{S}_0$, the cross section from $E = 0$ to 1 MeV is computed in the present work with two different nucleon–nucleon potentials [RE68,TH77], leading to $\mathcal{S}_2/\mathcal{S}_0 = 75 \pm 10$ MeV^{-2}. Finally, we adopt $S(E) = 3.94 \times 10^{-25} \times (1 + 11.7 E + 75 E^2)$ MeV b, with E in MeV. The corresponding adopted rates are in good agreement with the CA88 ones except at high temperatures. This is mainly due to the higher value for $\mathcal{S}_1/\mathcal{S}_0$ used here, and to the introduction of the $\mathcal{S}_2/\mathcal{S}_0$ term omitted in CA88.
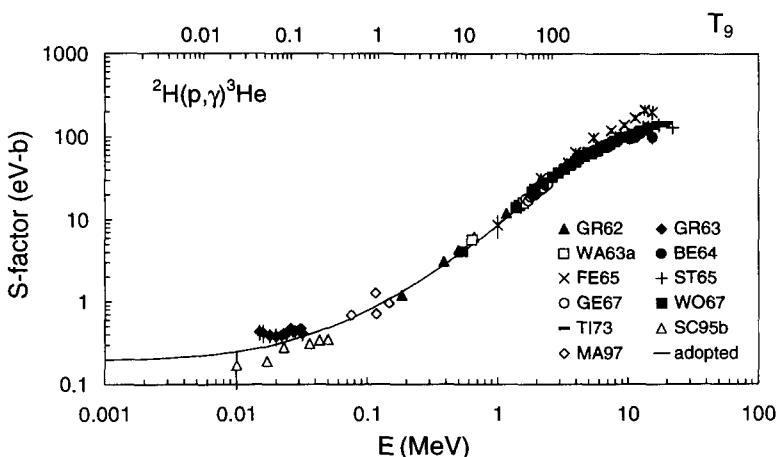
T_9	low	adopt	high	exp	ratio	T_9	low	adopt	high	exp	ratio
0.002	5.43	5.57	5.99	−25	1.0	0.15	3.84	3.99	4.34	−17	1.1
0.003	1.24	1.28	1.37	−23	1.0	0.16	4.32	4.49	4.89	−17	1.1
0.004	8.82	9.06	9.75	−23	1.0	0.18	5.31	5.53	6.04	−17	1.1
0.005	3.53	3.62	3.90	−22	1.0	0.2	6.37	6.64	7.27	−17	1.1
0.006	1.01	1.04	1.11	−21	1.0	0.25	9.24	9.69	10.6	−17	1.2
0.007	2.33	2.39	2.57	−21	1.0	0.3	1.24	1.31	1.44	−16	1.2
0.008	4.62	4.74	5.11	−21	1.0	0.35	1.59	1.68	1.86	−16	1.3
0.009	8.24	8.46	9.10	−21	1.0	0.4	1.96	2.08	2.31	−16	1.3
0.01	1.35	1.39	1.49	−20	1.0	0.45	2.35	2.51	2.80	−16	1.4
0.011	2.09	2.14	2.30	−20	1.0	0.5	2.77	2.96	3.32	−16	1.5
0.012	3.05	3.13	3.37	−20	1.0	0.6	3.67	3.96	4.47	−16	1.6
0.013	4.29	4.41	4.74	−20	1.0	0.7	4.67	5.06	5.74	−16	1.7
0.014	5.83	5.98	6.44	−20	1.0	0.8	5.75	6.27	7.15	−16	1.8
0.015	7.70	7.90	8.51	−20	1.0	0.9	6.92	7.58	8.68	−16	2.0

<div align="center">continued from previous page</div>

T_9	low	adopt	high	exp	ratio	T_9	low	adopt	high	exp	ratio
0.016	0.99	1.02	1.10	−19	1.0	1	8.17	8.99	10.3	−16	2.1
0.018	1.55	1.59	1.71	−19	1.0	1.25	1.16	1.29	1.50	−15	2.4
0.02	2.27	2.34	2.52	−19	1.0	1.5	1.56	1.75	2.03	−15	2.7
0.025	4.89	5.02	5.41	−19	1.0	1.75	2.00	2.25	2.64	−15	3.1
0.03	8.72	8.96	9.66	−19	1.0	2	2.49	2.81	3.31	−15	3.4
0.04	2.02	2.08	2.24	−18	1.0	2.5	3.59	4.09	4.83	−15	4.1
0.05	3.65	3.76	4.06	−18	1.0	3	4.85	5.55	6.59	−15	4.8
0.06	5.74	5.91	6.38	−18	1.0	3.5	6.26	7.19	8.56	−15	5.5
0.07	8.22	8.47	9.15	−18	1.0	4	7.81	9.00	10.7	−15	6.2
0.08	1.11	1.14	1.23	−17	1.0	5	1.13	1.31	1.57	−14	7.6
0.09	1.42	1.47	1.59	−17	1.0	6	1.53	1.77	2.13	−14	9.0
0.1	1.77	1.83	1.98	−17	1.0	7	1.97	2.30	2.76	−14	10
0.11	2.14	2.21	2.40	−17	1.0	8	2.46	2.87	3.46	−14	12
0.12	2.53	2.62	2.85	−17	1.0	9	2.98	3.48	4.21	−14	13
0.13	2.95	3.06	3.32	−17	1.1	10	3.54	4.15	5.01	−14	15
0.14	3.39	3.51	3.82	−17	1.1						

Reaction: ^{2}H(p,γ)^{3}He
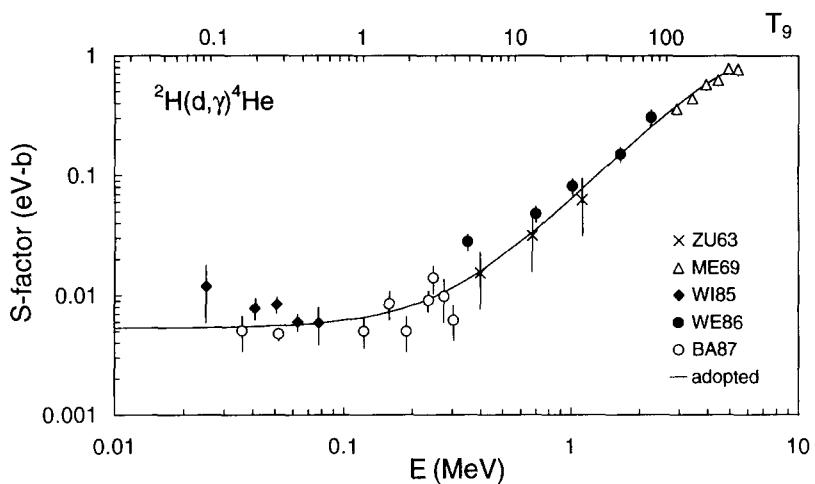
Cross section data from GR62, GR63, WA63a, BE64, FE65, ST65, GE67, WO67, TI73, SC95a and MA97 are used for the calculation of the rates. For WA63a, BE64, FE65, ST65 and TI73, the data given in the figure are obtained from those reported for the inverse reaction ^{3}He(γ,p)^{2}H. At low energy, the data sets of GR63 and SC95a differ by more than 50%, so that a unique extrapolation to zero energy is not possible. Therefore, the S-factor is fitted with a polynomial of degree 3, using the SC95a data for the calculation of the lower limits of the rates, and the GR63 data for the upper limits. The adopted rates are averages between the lower and upper limits. This procedure leads to $\mathcal{S}_0 = (0.20 \pm 0.07) \times 10^{-6}$ MeV b, $\mathcal{S}_1 = (5.60 \pm 2.00) \times 10^{-6}$ b, $\mathcal{S}_2 = (3.10 \pm 1.10) \times 10^{-6}$ MeV^{-1} b. For $T_9 < 1.5$, the present rates are about 20% lower than the CA88 values, as a result of our lower adopted S-factor. At higher temperatures, our rates are higher, probably due to the more extended data base used here.

T_9	low	adopt	high	exp	ratio	T_9	low	adopt	high	exp	ratio
0.001	0.83	1.30	1.77	−11	0.8	0.14	8.67	1.14	1.40	1	0.8
0.002	1.15	1.79	2.43	−8	0.8	0.15	1.01	1.32	1.62	1	0.8
0.003	3.75	5.80	7.85	−7	0.8	0.16	1.16	1.51	1.85	1	0.8
0.004	3.34	5.13	6.93	−6	0.8	0.18	1.49	1.91	2.34	1	0.8
0.005	1.57	2.41	3.24	−5	0.8	0.2	1.84	2.36	2.87	1	0.8
0.006	5.10	7.78	10.5	−5	0.8	0.25	2.85	3.60	4.34	1	0.8
0.007	1.30	1.98	2.66	−4	0.8	0.3	4.01	4.99	5.98	1	0.8
0.008	2.82	4.27	5.72	−4	0.8	0.35	5.28	6.51	7.74	1	0.8
0.009	5.41	8.17	10.9	−4	0.8	0.4	6.65	8.14	9.62	1	0.8
0.01	0.95	1.43	1.91	−3	0.8	0.45	8.11	9.85	11.6	1	0.8
0.011	1.55	2.32	3.09	−3	0.8	0.5	0.97	1.16	1.36	2	0.8
0.012	2.39	3.57	4.75	−3	0.8	0.6	1.29	1.54	1.79	2	0.8
0.013	3.51	5.24	6.96	−3	0.8	0.7	1.64	1.93	2.23	2	0.8
0.014	4.98	7.40	9.83	−3	0.8	0.8	2.00	2.35	2.69	2	0.8
0.015	0.68	1.01	1.34	−2	0.8	0.9	2.38	2.77	3.16	2	0.8
0.016	0.91	1.35	1.79	−2	0.8	1	2.77	3.20	3.64	2	0.8
0.018	1.52	2.24	2.96	−2	0.8	1.25	3.80	4.33	4.87	2	0.8
0.02	2.36	3.47	4.57	−2	0.8	1.5	4.87	5.50	6.13	2	0.9
0.025	5.71	8.29	10.9	−2	0.8	1.75	6.00	6.70	7.41	2	0.9
0.03	1.12	1.61	2.10	−1	0.8	2	7.15	7.93	8.71	2	0.9
0.04	2.98	4.23	5.47	−1	0.8	2.5	0.96	1.05	1.14	3	1.0
0.05	6.01	8.41	10.8	−1	0.8	3	1.21	1.30	1.40	3	1.0
0.06	1.03	1.42	1.81	0	0.8	3.5	1.46	1.57	1.68	3	1.0
0.07	1.58	2.16	2.75	0	0.8	4	1.73	1.84	1.95	3	1.1
0.08	2.25	3.06	3.87	0	0.8	5	2.27	2.38	2.50	3	1.1
0.09	3.05	4.11	5.17	0	0.8	6	2.83	2.94	3.05	3	1.2
0.1	3.96	5.30	6.65	0	0.8	7	3.39	3.50	3.60	3	1.2
0.11	4.98	6.63	8.28	0	0.8	8	3.96	4.06	4.15	3	1.3
0.12	6.11	8.09	10.1	0	0.8	9	4.53	4.61	4.69	3	1.3
0.13	7.34	9.66	12.0	0	0.8	10	5.09	5.16	5.23	3	1.4

Reaction: ^{2}H(d,γ)^{4}He
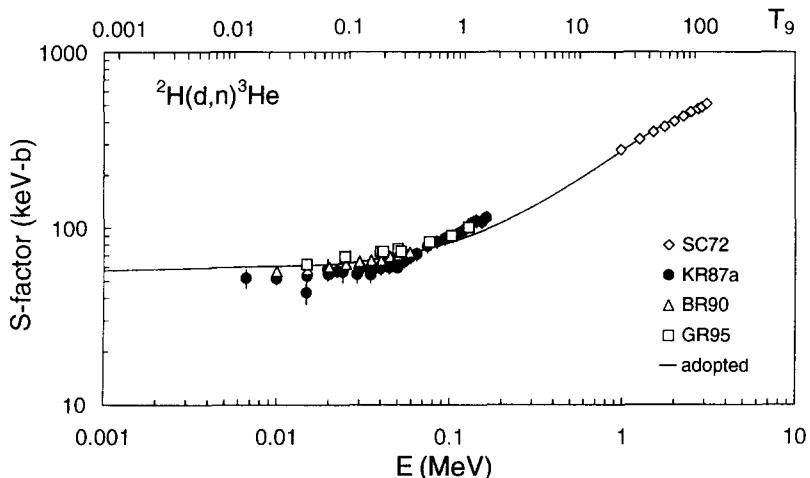
The non-resonant data are from ZU63, ME69, and WE86, and the relative data from WI85 and BA87. They often assume pure E2 transitions, which may be a cause of systematic error. The ^{2}H(d,γ)^{4}He cross sections of ME69 are obtained from those reported for the inverse reaction. The ratios σ(d,γ)/σ(d,p) of WI85 and BA87 are normalized here using the fit $S(E) = 56 + 0.203\,E$ (E in keV, $S(E)$ in keV b) for the S-factor of ^{2}H(d,p)^{3}H. For $T_9 < 0.2$, the recommended reaction rates are up to 10% lower than the rate given in CA88, probably due to a different σ(d,p) for the normalization of the WI85 and BA87 data. The differences at high temperatures come from the fact that our numerical integration of Eq. (1) is more accurate than the analytical approach of CA88.

^{2}H(d,γ)^{4}He

T_9	low	adopt	high	exp	ratio	T_9	low	adopt	high	exp	ratio
0.001	1.19	1.34	1.50	−15	0.9	0.14	3.89	4.64	5.40	−2	0.9
0.002	4.90	5.55	6.20	−12	0.9	0.15	4.48	5.37	6.26	−2	1.0
0.003	2.69	3.04	3.40	−10	0.9	0.16	5.10	6.13	7.16	−2	1.0
0.004	3.30	3.74	4.19	−9	0.9	0.18	6.41	7.74	9.07	−2	1.0
0.005	1.95	2.21	2.47	−8	0.9	0.2	7.80	9.46	11.1	−2	1.0
0.006	7.50	8.52	9.53	−8	0.9	0.25	1.15	1.41	1.67	−1	1.0
0.007	2.19	2.49	2.79	−7	0.9	0.3	1.54	1.91	2.28	−1	1.0
0.008	5.28	6.01	6.73	−7	0.9	0.35	1.95	2.44	2.93	−1	1.1
0.009	1.11	1.26	1.42	−6	0.9	0.4	2.37	2.99	3.61	−1	1.1
0.01	2.10	2.39	2.68	−6	0.9	0.45	2.80	3.55	4.31	−1	1.1
0.011	3.65	4.16	4.67	−6	0.9	0.5	3.23	4.14	5.04	−1	1.2
0.012	5.96	6.79	7.63	−6	0.9	0.6	4.14	5.34	6.55	−1	1.2
0.013	0.92	1.05	1.18	−5	0.9	0.7	5.08	6.62	8.15	−1	1.3
0.014	1.37	1.56	1.75	−5	0.9	0.8	6.07	7.95	9.83	−1	1.4
0.015	1.95	2.23	2.50	−5	0.9	0.9	7.11	9.35	11.6	−1	1.4
0.016	2.70	3.08	3.47	−5	0.9	1	0.82	1.08	1.34	0	1.5
0.018	4.78	5.47	6.16	−5	0.9	1.25	1.12	1.48	1.84	0	1.7
0.02	7.81	8.95	10.1	−5	0.9	1.5	1.47	1.93	2.39	0	1.8
0.025	2.07	2.38	2.69	−4	0.9	1.75	1.86	2.43	3.00	0	2.0
0.03	4.34	4.99	5.65	−4	0.9	2	2.29	2.97	3.66	0	2.1
0.04	1.26	1.45	1.65	−3	0.9	2.5	3.28	4.20	5.12	0	2.3
0.05	2.65	3.07	3.49	−3	0.9	3	4.45	5.61	6.77	0	2.4
0.06	4.64	5.40	6.17	−3	0.9	3.5	5.76	7.17	8.59	0	2.5
0.07	7.23	8.45	9.67	−3	0.9	4	7.21	8.88	10.6	0	2.6
0.08	1.04	1.22	1.40	−2	0.9	5	1.05	1.27	1.49	1	2.6
0.09	1.41	1.66	1.90	−2	0.9	6	1.41	1.68	1.96	1	2.7
0.1	1.82	2.15	2.48	−2	0.9	7	1.81	2.13	2.46	1	2.7
0.11	2.28	2.70	3.12	−2	0.9	8	2.23	2.60	2.97	1	2.6
0.12	2.78	3.31	3.83	−2	0.9	9	2.66	3.08	3.50	1	2.6
0.13	3.32	3.95	4.59	−2	0.9	10	3.10	3.56	4.02	1	2.5

Reaction: ^{2}H(d,n)^{3}He

The non-resonant data of SC72, KR87a, BR90, and GR95 are used. The S-factor is fitted at low energies by $S(E) = S_0 + S_1 E + S_2 E^2$, with $S_0 = 0.055$ MeV b, $S_1 = 0.308$ b and $S_2 = -0.094$ MeV^{-1} b (E in MeV). Below $E = 10$ keV, the extrapolation of the S-factor depends on the degree of the polynomial. This sensitivity is taken into account in the uncertainties on the rate. The lower limit is calculated with the KR87a data only, while the upper limit is derived from the GR95 data only. At low temperatures ($T_9 < 0.3$), the present rates are slightly larger than the CA88 ones, obtained by using $S_0 = 0.050$ MeV b, $S_1 = 0.170$ b, and $S_2 = 2.12$ MeV^{-1} b. The large difference in S_2 also leads to an important reduction of the rate above $T_9 \approx 0.5$. The CA88 values have been obtained from a fit to the KR87a data only, restricted to energies lower than 200 keV. The high-energy data of SC72 (from 1 to 3 MeV) included in our calculation allow for a more precise determination of the S-factor at high energies. The present reaction rates agree within a few percent with the BO92 compilation.
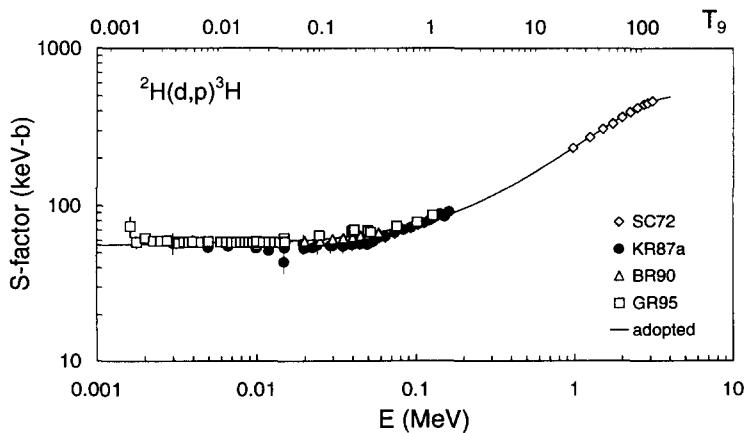
T_9	low	adopt	high	exp	ratio	T_9	low	adopt	high	exp	ratio
0.001	1.26	1.39	1.52	−8	1.1	0.14	5.14	5.64	6.15	5	1.1
0.002	5.22	5.75	6.30	−5	1.1	0.15	5.98	6.57	7.16	5	1.1
0.003	2.87	3.17	3.47	−3	1.1	0.16	6.87	7.54	8.22	5	1.1
0.004	3.55	3.91	4.28	−2	1.1	0.18	8.78	9.63	10.5	5	1.1
0.005	2.10	2.32	2.53	−1	1.1	0.2	1.08	1.19	1.29	6	1.1
0.006	8.11	8.94	9.79	−1	1.1	0.25	1.65	1.80	1.96	6	1.1
0.007	2.38	2.62	2.87	0	1.1	0.3	2.27	2.48	2.70	6	1.0
0.008	5.75	6.34	6.93	0	1.1	0.35	2.93	3.20	3.48	6	1.0
0.009	1.21	1.33	1.46	1	1.1	0.4	3.61	3.94	4.28	6	1.0
0.01	2.30	2.53	2.77	1	1.1	0.45	4.31	4.71	5.11	6	0.9
0.011	4.01	4.42	4.83	1	1.1	0.5	5.03	5.49	5.95	6	0.9
0.012	6.56	7.23	7.91	1	1.1	0.6	6.48	7.06	7.65	6	0.9

T_9	low	adopt	high	exp	ratio	T_9	low	adopt	high	exp	ratio
0.013	1.02	1.12	1.23	2	1.1	0.7	7.95	8.64	9.35	6	0.8
0.014	1.51	1.66	1.82	2	1.1	0.8	0.94	1.02	1.10	7	0.8
0.015	2.16	2.38	2.61	2	1.1	0.9	1.09	1.18	1.27	7	0.7
0.016	3.00	3.30	3.62	2	1.1	1	1.23	1.33	1.44	7	0.7
0.018	5.34	5.89	6.44	2	1.1	1.25	1.58	1.71	1.84	7	0.6
0.02	8.77	9.66	10.6	2	1.1	1.5	1.91	2.06	2.21	7	0.5
0.025	2.35	2.59	2.84	3	1.1	1.75	2.23	2.40	2.57	7	0.5
0.03	4.97	5.48	5.99	3	1.1	2	2.54	2.73	2.91	7	0.4
0.04	1.47	1.61	1.76	4	1.1	2.5	3.12	3.33	3.54	7	0.4
0.05	3.14	3.46	3.78	4	1.1	3	3.64	3.87	4.11	7	0.3
0.06	5.59	6.15	6.72	4	1.1	3.5	4.13	4.37	4.61	7	0.3
0.07	8.84	9.72	10.6	4	1.1	4	4.58	4.83	5.08	7	0.2
0.08	1.29	1.41	1.54	5	1.1	5	5.39	5.63	5.88	7	0.2
0.09	1.76	1.94	2.12	5	1.1	6	6.11	6.33	6.55	7	0.2
0.1	2.31	2.54	2.78	5	1.1	7	6.76	6.95	7.14	7	0.1
0.11	2.93	3.22	3.51	5	1.1	8	7.36	7.51	7.66	7	0.1
0.12	3.61	3.97	4.33	5	1.1	9	7.95	8.05	8.14	7	0.1
0.13	4.35	4.77	5.21	5	1.1	10	8.53	8.57	8.60	7	0.1
T_9	low	adopt	high	exp	ratio	T_9	low	adopt	high	exp	ratio

Reaction: ^{2}H(d,p)^{3}H

The non-resonant data of SC72, KR87a, BR90, and GR95 are used. The lowest energy data point of GR95 that might be affected by screening effects has been corrected (U_e = 10 eV). An additional 3% error, due to the assumption of a polynomial description of the S-factor curve, is added to the experimental errors. The S-factor is fitted by $S(E) = S_0 + S_1 E + S_2 E^2$, with $S_0 = 0.056$ MeV b, $S_1 = 0.204$ b, $S_2 = -0.0251$ MeV^{-1} b. At low temperatures ($T_9 < 0.4$), the present rate is slightly larger than the rate of CA88, based on $S_0 = 0.053$ MeV b, $S_1 = 0.019$ b, and $S_2 = 1.92$ MeV^{-1} b. The large difference in S_2 yields an important reduction of our rates with respect to the CA88 ones above $T_9 \approx 0.7$. The CA88 values have been obtained from a fit to the KR87a data [see the ^{2}H(d,n)^{3}He reaction]. The present reaction rates agree within a few percent with the BO92 compilation.
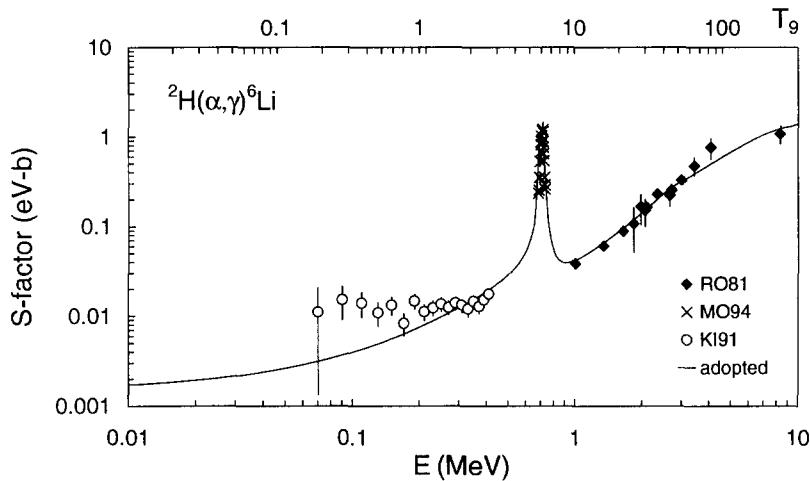
T_9	low	adopt	high	exp	ratio	T_9	low	adopt	high	exp	ratio
0.001	1.35	1.41	1.47	−8	1.1	0.14	5.16	5.37	5.59	5	1.1
0.002	5.60	5.85	6.09	−5	1.1	0.15	5.99	6.23	6.48	5	1.1
0.003	3.08	3.21	3.35	−3	1.1	0.16	6.86	7.14	7.42	5	1.1
0.004	3.80	3.96	4.13	−2	1.1	0.18	8.72	9.07	9.42	5	1.1
0.005	2.25	2.34	2.44	−1	1.1	0.2	1.07	1.11	1.16	6	1.1
0.006	8.67	9.04	9.42	−1	1.1	0.25	1.61	1.67	1.74	6	1.1
0.007	2.54	2.65	2.76	0	1.1	0.3	2.19	2.28	2.36	6	1.1
0.008	6.13	6.40	6.66	0	1.1	0.35	2.80	2.91	3.02	6	1.1
0.009	1.29	1.35	1.40	1	1.1	0.4	3.43	3.56	3.69	6	1.0
0.01	2.44	2.55	2.66	1	1.1	0.45	4.07	4.22	4.38	6	1.0
0.011	4.26	4.45	4.63	1	1.1	0.5	4.71	4.89	5.07	6	1.0
0.012	6.97	7.27	7.57	1	1.1	0.6	6.01	6.22	6.45	6	0.9
0.013	1.08	1.13	1.17	2	1.1	0.7	7.29	7.55	7.82	6	0.9
0.014	1.60	1.67	1.74	2	1.1	0.8	8.55	8.86	9.17	6	0.8
0.015	2.29	2.39	2.49	2	1.1	0.9	0.98	1.01	1.05	7	0.8
0.016	3.18	3.31	3.45	2	1.1	1	1.10	1.14	1.18	7	0.7
0.018	5.65	5.89	6.14	2	1.1	1.25	1.40	1.44	1.49	7	0.6
0.02	9.27	9.66	10.1	2	1.1	1.5	1.68	1.73	1.79	7	0.6
0.025	2.48	2.59	2.69	3	1.1	1.75	1.94	2.01	2.07	7	0.5
0.03	5.22	5.44	5.67	3	1.1	2	2.20	2.27	2.35	7	0.5
0.04	1.53	1.60	1.66	4	1.1	2.5	2.68	2.76	2.85	7	0.4
0.05	3.26	3.40	3.54	4	1.1	3	3.11	3.22	3.32	7	0.3
0.06	5.78	6.02	6.27	4	1.1	3.5	3.52	3.64	3.75	7	0.3
0.07	9.10	9.48	9.86	4	1.1	4	3.90	4.03	4.16	7	0.3
0.08	1.32	1.37	1.43	5	1.1	5	4.59	4.74	4.89	7	0.2
0.09	1.80	1.88	1.95	5	1.1	6	5.19	5.36	5.53	7	0.2
0.1	2.36	2.45	2.55	5	1.1	7	5.72	5.91	6.10	7	0.1
0.11	2.97	3.09	3.22	5	1.1	8	6.20	6.40	6.61	7	0.1
0.12	3.65	3.80	3.95	5	1.1	9	6.62	6.84	7.06	7	0.1
0.13	4.38	4.56	4.74	5	1.1	10	7.00	7.22	7.45	7	0.1

Reaction: ^{2}H$(\alpha,\gamma)^6$Li

Direct measurements of the non-resonant cross section have been performed only at energies $E = 1$ to 8.4 MeV [RO81], while MO94a is limited to the 3^+ resonance at $E_r = 0.711$ MeV. An upper limit for the cross section at $E = 53$ keV has been established by CE96, but this limit is much higher than any theoretical estimate, and it has been disregarded. At lower energies, the break-up results of KI91 (see, however, Section 2.2.2) and theoretical calculations [RO81,LA86a,LA86b,CR89,BU90,CR90,TY91,MO94a, TY94] are available (see NO97 for an extended discussion). The data of KI91 are obtained from the author and, due to a problem in the graphic representation, they differ from those given in their paper. For the 0.711 MeV resonance, the adopted resonance strength is taken here as the weighted average of BA60, EI69 and MO94a [$\omega\gamma = (10.2 \pm 0.6) \times 10^{-4}$ eV], while the total width is taken as the weighted average of MO94a and BA79b: $\Gamma = 22 \pm 2$ keV. At low energies ($E < 0.7$ MeV), we use the more recent calculation of MO94a. The rates are calculated by adding the 0.711 MeV resonant contribution to the non-resonant one. The lower and upper limits are calculated by taking into account the lower and upper limits in the theoretical calculations. At low temperatures ($T_9 < 0.09$), our rates are up to a factor of 2 lower than the CA88 ones, which correspond to those

derived by RO81, due to a different low energy extrapolation adopted here.
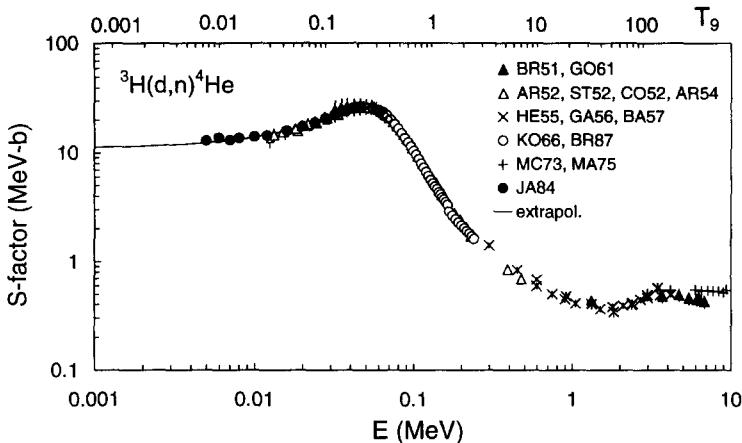
T_9	low	adopt	high	exp	ratio	T_9	low	adopt	high	exp	ratio
0.002	0.17	2.13	12.3	−23	0.5	0.15	1.59	8.76	30.5	−5	1.0
0.003	0.24	2.87	16.4	−20	0.5	0.16	0.22	1.17	3.98	−4	1.0
0.004	0.23	2.68	15.1	−18	0.5	0.18	0.37	1.93	6.34	−4	1.1
0.005	0.59	6.71	37.5	−17	0.5	0.2	0.60	3.00	9.47	−4	1.1
0.006	0.70	7.80	43.3	−16	0.5	0.25	1.61	7.28	21.1	−4	1.1
0.007	0.50	5.52	30.4	−15	0.5	0.3	0.35	1.45	3.90	−3	1.1
0.008	0.26	2.77	15.2	−14	0.5	0.35	0.65	2.53	6.34	−3	1.0
0.009	0.10	1.08	5.88	−13	0.6	0.4	1.10	4.03	9.48	−3	1.0
0.01	0.33	3.50	18.9	−13	0.6	0.45	1.75	6.02	13.3	−3	1.0
0.011	0.94	9.74	52.3	−13	0.6	0.5	2.63	8.56	17.9	−3	1.0
0.012	0.24	2.41	12.9	−12	0.6	0.6	0.53	1.57	2.93	−2	1.0
0.013	0.54	5.42	28.7	−12	0.6	0.7	0.96	2.64	4.46	−2	1.0
0.014	0.11	1.12	5.93	−11	0.6	0.8	1.63	4.24	6.56	−2	1.0
0.015	0.22	2.18	11.4	−11	0.6	0.9	2.64	6.56	9.52	−2	1.0
0.016	0.41	4.00	20.9	−11	0.6	1	4.07	9.81	13.6	−2	1.1
0.018	0.12	1.17	6.04	−10	0.6	1.25	0.98	2.27	3.01	−1	1.1
0.02	0.31	2.94	15.0	−10	0.6	1.5	1.87	4.22	5.58	−1	1.1
0.025	0.21	1.87	9.33	−9	0.7	1.75	3.02	6.67	8.85	−1	1.0
0.03	0.88	7.65	37.3	−9	0.7	2	4.35	9.40	12.5	−1	1.0
0.04	0.73	5.96	28.0	−8	0.8	2.5	0.73	1.51	2.02	0	1.0
0.05	0.33	2.57	11.6	−7	0.8	3	1.05	2.06	2.75	0	1.0
0.06	1.07	7.84	34.3	−7	0.9	3.5	1.39	2.57	3.41	0	1.0
0.07	0.27	1.91	8.12	−6	0.9	4	1.75	3.07	4.03	0	1.0
0.08	0.59	4.00	16.5	−6	0.9	5	2.56	4.07	5.23	0	1.1
0.09	1.15	7.48	30.0	−6	1.0	6	3.52	5.17	6.49	0	1.1
0.1	0.20	1.28	5.02	−5	1.0	7	4.62	6.41	7.89	0	1.2
0.11	0.34	2.06	7.85	−5	1.0	8	5.85	7.81	9.47	0	1.3
0.12	0.53	3.14	11.7	−5	1.0	9	7.20	9.35	11.2	0	1.5
0.13	0.79	4.57	16.6	−5	1.0	10	0.86	1.10	1.31	1	1.6
0.14	1.14	6.43	22.9	−5	1.0						

Reaction: ^{3}H(d,n)^{4}He
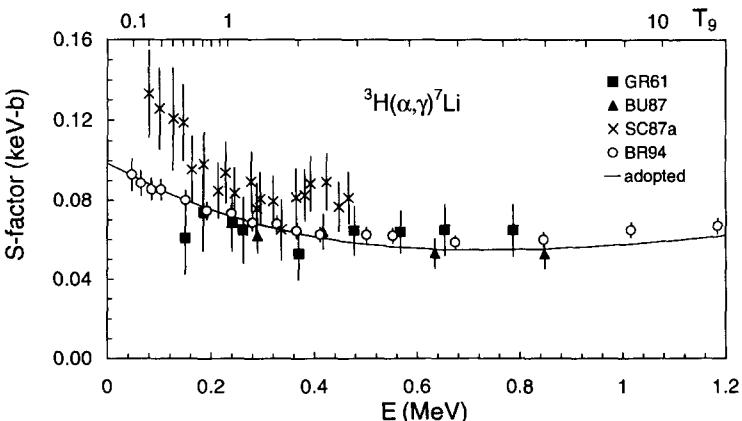
Experimental data are available from $E = 0.005$ to 10 MeV [BR51a,AR52,CO52, ST52,AR54,HE55,GA56,BA57,GO61,KO66,MC73,MA75,JA84,BR87a]. The data below 0.1 MeV are fitted and extrapolated to energies below 0.005 MeV using a Breit–Wigner expression, the parameters of which have been fitted to the experimental data. Screening effects are neglected. Present and previous compilations are in good agreement (about 10%). Small differences around $T_9 = 0.05$ are probably due to the numerical approach used here compared to the analytical procedure of CA88.

T_9	low	adopt	high	exp	ratio	T_9	low	adopt	high	exp	ratio
0.001	1.82	1.90	1.97	−7	1.0	0.09	3.27	3.37	3.48	7	1.0
0.0011	7.06	7.35	7.64	−7	1.0	0.1	4.41	4.55	4.69	7	1.0
0.0012	2.34	2.43	2.53	−6	1.0	0.11	5.69	5.87	6.05	7	0.9
0.0013	6.81	7.09	7.37	−6	1.0	0.12	7.09	7.31	7.53	7	0.9
0.0014	1.79	1.86	1.93	−5	1.0	0.13	8.58	8.85	9.12	7	0.9
0.0015	4.29	4.47	4.64	−5	1.0	0.14	1.01	1.05	1.08	8	0.9
0.0016	9.55	9.94	10.3	−5	1.0	0.15	1.18	1.21	1.25	8	0.9
0.0018	3.93	4.09	4.25	−4	1.0	0.16	1.34	1.38	1.42	8	0.9
0.002	1.33	1.38	1.44	−3	1.0	0.18	1.67	1.72	1.78	8	0.9
0.0025	1.52	1.58	1.64	−2	1.0	0.2	1.99	2.06	2.12	8	1.0
0.003	0.97	1.01	1.05	−1	1.0	0.25	2.74	2.83	2.92	8	1.0
0.004	1.43	1.49	1.55	0	1.0	0.3	3.35	3.47	3.58	8	1.0
0.005	0.97	1.00	1.04	1	1.0	0.35	3.83	3.97	4.11	8	1.0
0.006	4.13	4.30	4.46	1	1.0	0.4	4.19	4.35	4.51	8	1.0
0.007	1.32	1.37	1.42	2	1.0	0.45	4.45	4.63	4.81	8	1.0
0.008	3.42	3.55	3.68	2	1.1	0.5	4.64	4.84	5.04	8	1.0
0.009	7.64	7.94	8.24	2	1.1	0.6	4.85	5.07	5.30	8	1.0
0.01	1.53	1.59	1.65	3	1.1	0.7	4.90	5.15	5.41	8	1.0
0.011	2.80	2.91	3.02	3	1.1	0.8	4.87	5.14	5.42	8	1.0
0.012	4.78	4.96	5.15	3	1.1	0.9	4.78	5.07	5.37	8	1.0
0.013	7.71	8.01	8.31	3	1.1	1	4.66	4.97	5.29	8	1.0
0.014	1.19	1.23	1.28	4	1.1	1.25	4.31	4.66	5.02	8	0.9
0.015	1.76	1.82	1.89	4	1.1	1.5	3.95	4.34	4.74	8	0.9
0.016	2.51	2.61	2.70	4	1.1	1.75	3.63	4.05	4.47	8	0.9
0.017	3.50	3.63	3.76	4	1.1	2	3.34	3.79	4.23	8	0.9
0.018	4.74	4.92	5.10	4	1.1	2.5	2.87	3.36	3.85	8	0.9
0.02	8.18	8.49	8.79	4	1.1	3	2.50	3.02	3.55	8	0.9
0.025	2.44	2.53	2.62	5	1.1	3.5	2.21	2.77	3.32	8	0.9
0.03	5.64	5.84	6.05	5	1.1	4	1.98	2.56	3.14	8	0.8
0.035	1.10	1.14	1.18	6	1.2	5	1.65	2.26	2.87	8	0.8
0.04	1.91	1.98	2.05	6	1.2	6	1.41	2.05	2.69	8	0.9
0.05	4.57	4.72	4.88	6	1.2	7	1.23	1.90	2.56	8	0.9
0.06	8.85	9.15	9.45	6	1.2	8	1.10	1.78	2.46	8	0.9
0.07	1.50	1.55	1.59	7	1.1	9	1.00	1.69	2.38	8	0.9
0.08	2.29	2.37	2.44	7	1.0	10	0.92	1.62	2.32	8	0.9

Reaction: $^3H(\alpha,\gamma)^7Li$
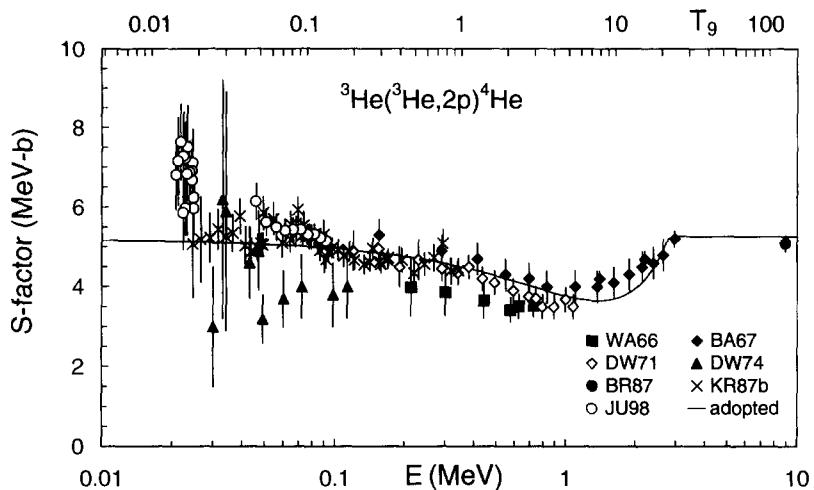
Non-resonant cross section data from GR61, BU87 and BR94 covering the energy range $0.047 \leqslant E \leqslant 1.18$ MeV are used. The data of SC87a, which have an inconsistent normalization, are disregarded. Nuclear models explain well the low energy dependence without the inclusion of electron screening [KA86,LA86a,MO93]. Up to 2.5 MeV, we use the energy dependence given by the microscopic calculation of KA86. A renormalization factor 1.01 ± 0.11 is obtained from a χ^2 analysis of the data. The recommended S-factor at zero energy is $S_0 = 0.10 \pm 0.02$ keV b. For $E \leqslant 0.4$ MeV, the S-factor can be well approximated by the expression $S(E) = 0.10 - 0.15\,E + 0.13\,E^2$ (E in MeV, $S(E)$ in keV b). The present rate is in perfect agreement with the CA88 compilation in the temperature range $T_9 \leqslant 1$. However, for $T_9 > 1$, the present rates are significantly lower, up to a factor 5 near $T_9 = 10$. This difference is due to the S-factor used by CA88, which fits well the experimental data up to about 0.2 MeV, while it increases unphysically at higher energies. The present results are in good agreement with the rates given in BR94.

T_9	low	adopt	high	exp	ratio	T_9	low	adopt	high	exp	ratio
0.002	6.51	7.30	8.10	−21	1.0	0.15	5.93	6.66	7.38	−1	1.0
0.003	1.65	1.85	2.05	−17	1.0	0.16	7.82	8.77	9.73	−1	1.0
0.004	2.28	2.56	2.84	−15	1.0	0.18	1.27	1.43	1.58	0	1.0
0.005	7.55	8.48	9.40	−14	1.0	0.2	1.92	2.16	2.39	0	1.0
0.006	1.08	1.22	1.35	−12	1.0	0.25	4.37	4.91	5.44	0	1.0
0.007	0.91	1.02	1.13	−11	1.0	0.3	8.09	9.08	10.1	0	1.0
0.008	5.21	5.85	6.48	−11	1.0	0.35	1.31	1.47	1.63	1	1.0
0.009	2.28	2.56	2.84	−10	1.0	0.4	1.94	2.18	2.42	1	1.0
0.01	0.81	9.11	1.01	−9	1.0	0.45	2.70	3.03	3.36	1	1.0
0.011	2.46	2.76	3.06	−9	1.0	0.5	3.57	4.00	4.44	1	1.0
0.012	6.55	7.35	8.15	−9	1.0	0.6	5.60	6.28	6.97	1	1.0
0.013	1.57	1.76	1.96	−8	1.0	0.7	7.96	8.93	9.90	1	1.0
0.014	3.46	3.88	4.30	−8	1.0	0.8	1.06	1.19	1.32	2	1.0
0.015	7.07	7.93	8.80	−8	1.0	0.9	1.34	1.50	1.67	2	1.0
0.016	1.36	1.53	1.69	−7	1.0	1	1.64	1.84	2.04	2	1.0
0.018	4.31	4.84	5.36	−7	1.0	1.25	2.42	2.72	3.02	2	0.9
0.02	1.16	1.31	1.45	−6	1.0	1.5	3.25	3.64	4.04	2	0.9
0.025	8.43	9.46	1.05	−6	1.0	1.75	4.09	4.59	5.08	2	0.8
0.03	3.80	4.26	4.72	−5	1.0	2	4.93	5.54	6.14	2	0.8
0.04	3.36	3.77	4.18	−4	1.0	2.5	6.63	7.44	8.26	2	0.6
0.05	1.56	1.75	1.94	−3	1.0	3	8.34	9.36	10.4	2	0.5
0.06	5.01	5.63	6.24	−3	1.0	3.5	1.00	1.13	1.25	3	0.5
0.07	1.26	1.42	1.57	−2	1.0	4	1.18	1.32	1.47	3	0.4
0.08	2.70	3.03	3.36	−2	1.0	5	1.54	1.73	1.91	3	0.3
0.09	5.11	5.73	6.36	−2	1.0	6	1.95	2.19	2.43	3	0.2
0.1	8.83	9.91	11.0	−2	1.0	7	2.49	2.79	3.10	3	0.2
0.11	1.42	1.59	1.77	−1	1.0	8	3.26	3.66	4.06	3	0.2
0.12	2.16	2.42	2.69	−1	1.0	9	4.41	4.95	5.49	3	0.2
0.13	3.13	3.52	3.90	−1	1.0	10	6.13	6.88	7.62	3	0.2
0.14	4.38	4.92	5.45	−1	1.0						

Reaction: $^3\mathrm{He}(^3\mathrm{He},2p)^4\mathrm{He}$
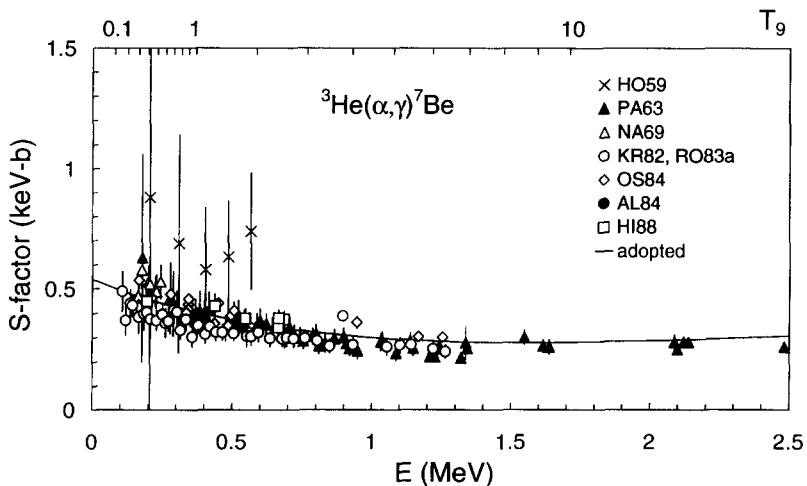
For the determination of the S-factor, the non-resonant data of WA66, BA67, DW71, DW74, KR87b, BR87b and JU98 are used. The AR96 data are superseded by the JU98 data. Low energy data are corrected by electron screening with $U_e = 330$ eV. The results of GO54 (a factor 2-3 smaller than all the more recent data, without error estimate) and ZU65 (where only a proton spectrum is shown) are not considered. The adopted data are well approximated by $S(E) = 5.18 - 2.22 E + 0.804 E^2$ (E in MeV, $S(E)$ in MeV b). The S_0 value is close to the recommended of AD98 (5.4 ± 0.4 MeV b). At higher energies ($E > 2.8$ MeV), we assume a constant value $S(E) = 5.26$ MeV b. The existence of a low energy resonance [FE72,FO72] is not observed up to now [JU98]. In the $0.003 < T_9 < 0.02$ range, the present rates are slightly ($\leqslant 10\%$) smaller than the CA88 ones, due to the smaller value of S_0 used here than the KR87b value adopted in the CA88 compilation. For $T_9 > 1$, the present rates are significantly lower than the CA88 one. In this temperature region, the CA88 values are based entirely on the extrapolation given in KR87b, which is valid only for $E < 0.3$ MeV.

^{3}He(^{3}He,2p)^{4}He

S-factor (MeV-b) vs E (MeV) / T_9

Legend: ■ WA66 ◆ BA67 ◇ DW71 ▲ DW74 ● BR87 × KR87b ○ JU98 — adopted

T_9	low	adopt	high	exp	ratio	T_9	low	adopt	high	exp	ratio
0.003	2.74	2.91	3.08	−25	0.9	0.15	1.68	1.78	1.89	1	1.0
0.004	5.44	5.76	6.10	−22	0.9	0.16	2.62	2.79	2.96	1	1.0
0.005	1.20	1.27	1.34	−19	0.9	0.18	5.77	6.14	6.52	1	1.0
0.006	7.31	7.75	8.20	−18	0.9	0.2	1.14	1.21	1.28	2	1.0
0.007	1.94	2.06	2.18	−16	0.9	0.25	4.37	4.65	4.95	2	1.0
0.008	2.91	3.08	3.26	−15	0.9	0.3	1.21	1.29	1.37	3	1.0
0.009	2.85	3.02	3.20	−14	0.9	0.35	2.72	2.90	3.08	3	1.0
0.01	2.04	2.16	2.29	−13	0.9	0.4	5.27	5.62	5.99	3	1.0
0.011	1.14	1.20	1.28	−12	0.9	0.45	9.18	9.81	10.4	3	1.0
0.012	5.20	5.51	5.83	−12	0.9	0.5	1.48	1.58	1.68	4	1.0
0.013	2.02	2.14	2.27	−11	0.9	0.6	3.22	3.44	3.67	4	1.0
0.014	6.87	7.29	7.71	−11	1.0	0.7	5.95	6.37	6.80	4	1.0
0.015	2.09	2.22	2.34	−10	1.0	0.8	0.98	1.05	1.13	5	0.9
0.016	5.77	6.12	6.48	−10	1.0	0.9	1.49	1.60	1.72	5	0.9
0.018	3.48	3.69	3.91	−9	1.0	1	2.14	2.30	2.46	5	0.9
0.02	1.63	1.73	1.83	−8	1.0	1.25	4.35	4.68	5.02	5	0.8
0.025	3.60	3.81	4.04	−7	1.0	1.5	7.39	7.96	8.56	5	0.7
0.03	3.78	4.01	4.25	−6	1.0	1.75	1.12	1.21	1.30	6	0.6
0.04	1.15	1.22	1.30	−4	1.0	2	1.58	1.70	1.84	6	0.5
0.05	1.30	1.38	1.46	−3	1.0	2.5	2.68	2.90	3.13	6	0.4
0.06	8.20	8.70	9.22	−3	1.0	3	3.99	4.32	4.67	6	0.3
0.07	3.55	3.77	3.99	−2	1.0	3.5	5.49	5.95	6.42	6	0.2
0.08	1.19	1.26	1.33	−1	1.0	4	7.15	7.75	8.36	6	0.2
0.09	3.27	3.48	3.69	−1	1.0	5	1.09	1.18	1.27	7	0.1
0.1	7.84	8.33	8.83	−1	1.0	6	1.51	1.63	1.75	7	0.1
0.11	1.68	1.78	1.89	0	1.0	7	1.97	2.12	2.27	7	0.1
0.12	3.29	3.49	3.71	0	1.0	8	2.46	2.63	2.81	7	0.1
0.13	5.99	6.37	6.76	0	1.0	9	2.95	3.15	3.36	7	0.1
0.14	1.03	1.09	1.16	1	1.0	10	3.46	3.68	3.91	7	0.1

Reaction: $^3\text{He}(\alpha,\gamma)^7\text{Be}$

Non-resonant data from HO59, PA63, NA69, KR82, RO83a, AL84, OS84 and HI88 are used. The VO83 data are omitted, since only the extrapolated value of the S-factor at zero energy is given. The PA63 data at $E < 400$ keV are taken from the values reported in NA69. Following HI88, the data of KR82 are renormalized by a factor 1.4. Up to 2.5 MeV, we use the energy dependence given by the microscopic calculation of KA86. A renormalization factor 1.08 ± 0.18 is obtained from a χ^2 analysis of the data. The recommended S-factor at zero energy is then $S_0 = 0.54 \pm 0.09$ keV b (AD98 gives $S_0 = 0.53 \pm 0.05$ keV b). For $E \leqslant 0.2$ MeV, the S-factor can be well approximated by the expression $S(E) = 0.54 - 0.52\,E - 0.52\,E^2$ (E in MeV, $S(E)$ in keV b). Beyond 2.5 MeV, a constant value of $S(E) = 0.31$ keV b is assumed, as suggested by direct capture calculations [TO63,LI81,LA86a,MO93,WA84]. The resulting rates are in good agreement with those from CA88, except at the highest temperatures, where the adopted rates are significantly larger. The CA88 rates are obtained with an exponentially decreasing S-factor [WI81] which falls below the experimental data above $E \approx 2$ MeV.

T_9	low	adopt	high	exp	ratio	T_9	low	adopt	high	exp	ratio
0.005	4.14	4.97	5.80	−25	1.0	0.16	7.94	9.52	11.1	−4	1.0
0.006	3.05	3.66	4.28	−23	1.0	0.18	1.81	2.17	2.53	−3	1.0
0.007	0.95	1.13	1.32	−21	1.0	0.2	3.67	4.40	5.14	−3	1.0
0.008	1.60	1.92	2.24	−20	1.0	0.25	1.50	1.80	2.10	−2	1.0
0.009	1.75	2.10	2.45	−19	1.0	0.3	4.35	5.22	6.09	−2	1.0
0.01	1.37	1.64	1.91	−18	1.0	0.35	1.01	1.21	1.41	−1	1.0
0.011	8.25	9.90	11.5	−18	1.0	0.4	2.01	2.42	2.82	−1	1.0
0.012	4.04	4.85	5.66	−17	1.0	0.45	3.59	4.31	5.03	−1	1.0
0.013	1.68	2.01	2.35	−16	1.0	0.5	5.90	7.07	8.25	−1	1.0
0.014	6.03	7.24	8.44	−16	1.0	0.6	1.32	1.59	1.85	0	1.0
0.015	1.93	2.32	2.70	−15	1.0	0.7	2.50	3.01	3.51	0	1.0

continued from previous page

T_9	low	adopt	high	exp	ratio	T_9	low	adopt	high	exp	ratio
0.016	5.59	6.71	7.83	−15	1.0	0.8	4.21	5.06	5.90	0	1.0
0.018	3.66	4.40	5.13	−14	1.0	0.9	6.51	7.81	9.11	0	1.0
0.02	1.85	2.22	2.59	−13	1.0	1	0.94	1.13	1.32	1	1.0
0.025	4.70	5.64	6.57	−12	1.0	1.25	1.96	2.35	2.75	1	1.0
0.03	5.51	6.61	7.71	−11	1.0	1.5	3.39	4.07	4.74	1	1.0
0.04	1.97	2.37	2.76	−9	1.0	1.75	5.21	6.25	7.29	1	1.0
0.05	2.49	2.98	3.48	−8	1.0	2	7.39	8.87	10.3	1	1.0
0.06	1.71	2.05	2.39	−7	1.0	2.5	1.27	1.52	1.78	2	1.0
0.07	7.92	9.50	11.1	−7	1.0	3	1.91	2.29	2.67	2	1.1
0.08	2.80	3.36	3.91	−6	1.0	3.5	2.64	3.16	3.69	2	1.1
0.09	8.10	9.72	11.3	−6	1.0	4	3.44	4.12	4.81	2	1.1
0.1	2.02	2.42	2.83	−5	1.0	5	5.22	6.26	7.30	2	1.3
0.11	4.48	5.37	6.27	−5	1.0	6	7.16	8.60	10.0	2	1.4
0.12	0.91	1.09	1.27	−4	1.0	7	0.92	1.10	1.29	3	1.5
0.13	1.69	2.03	2.37	−4	1.0	8	1.13	1.35	1.58	3	1.7
0.14	2.98	3.58	4.17	−4	1.0	9	1.34	1.60	1.87	3	1.8
0.15	4.97	5.97	6.96	−4	1.0	10	1.54	1.85	2.16	3	1.9
T_9	low	adopt	high	exp	ratio	T_9	low	adopt	high	exp	ratio

Reaction: $^4\mathrm{He}(\alpha n,\gamma)^9\mathrm{Be}$

We assume that the capture proceeds in two steps: a metastable $^8\mathrm{Be}$ is formed, which then captures a neutron. The formation of $^5\mathrm{He}$ followed by an α capture is neglected because of the short lifetime of $^5\mathrm{He}$. The rate is calculated with an extension of the model presented in NO85 (see also GÖ95 for a simple, but crude approximation),

$$N_A^2 \langle \sigma v \rangle^{\alpha\alpha n} = N_A \left(\frac{8\pi\hbar}{\mu_{\alpha\alpha}^2} \right) \left(\frac{\mu_{\alpha\alpha}}{2\pi k_B T} \right)^{3/2}$$

$$\times \int_0^\infty \frac{\sigma_{\alpha\alpha}(E)}{\Gamma_\alpha(^8\mathrm{Be},E)} \exp(-E/k_B T) N_A \langle \sigma v \rangle^{n^8\mathrm{Be}} E\, dE,$$

where $\mu_{\alpha\alpha}$ is the reduced mass of the $\alpha + \alpha$ system, and E is the energy with respect to threshold. The elastic cross section and the corresponding parameters are discussed in the comments related to the $^4\mathrm{He}(\alpha\alpha,\gamma)^{12}\mathrm{C}$ reaction. The $N_A\langle\sigma v\rangle^{n^8\mathrm{Be}}$ rate assumes that $^8\mathrm{Be}$ is formed at an energy E different from the energy $E_{8\mathrm{Be}}$ of the $^8\mathrm{Be}$ ground-state resonance, and that it is bound. This rate is given by

$$N_A\langle\sigma v\rangle^{n^8\mathrm{Be}} = N_A \frac{8\pi}{\mu_{n^8\mathrm{Be}}^2} \left(\frac{\mu_{n^8\mathrm{Be}}}{2\pi k_B T} \right)^{3/2} \int_0^\infty \sigma_{n^8\mathrm{Be}}(E';E) \exp(-E'/k_B T)\ E'\, dE',$$

where $\mu_{n^8\mathrm{Be}}$ is the reduced mass of the n + $^8\mathrm{Be}$ system and E' is the energy with respect to its threshold (which varies with the formation energy E). We parametrize $\sigma_{n^8\mathrm{Be}}(E';E)$ as

$$\sigma_{n^8\mathrm{Be}}(E';E) = \sum_{J=1/2,5/2} \frac{1}{8}(2J+1)\frac{\pi\hbar^2}{2\mu_{n^8\mathrm{Be}}E'}$$

$$\times \frac{\Gamma_n(^9\mathrm{Be}^J,E')\Gamma_\gamma(^9\mathrm{Be}^J,E'+E)}{(E'-E_r^J+E-E_{^8\mathrm{Be}})^2+\frac{1}{4}\Gamma_n(^9\mathrm{Be}^J,E')^2},$$

where the sum runs over the $1/2^+$, $1/2^-$ and $5/2^+$ resonances at energies E_r^J. This expression is related to the measured $^9\mathrm{Be}(\gamma,n)^8\mathrm{Be}$ photoneutron cross section. Early experimental data for the photoneutron cross section are summarized in LA66 and in BE67. The BE67 data are criticized in BA68a. We adopt the FU82 data around the $1/2^+$ resonance and the HU75 data at higher energies. For the $1/2^+$ resonance located just above threshold, we take the BA83 parametrization of the FU82 data. The neutron width of this s wave resonance is given by $\Gamma_n(^9\mathrm{Be}^J,E') = \sqrt{E'/E_r^J}\,\Gamma_n$, and its E1 γ width by $\Gamma_\gamma(^9\mathrm{Be}^J,E'+E) = (E_T+E'+E-E_{^8\mathrm{Be}})^3/(E_T+E_r^J)^3\,\Gamma_\gamma$, where the photon threshold energy E_T is 1.644 MeV and $E_r^J = 67$ keV, $\Gamma_n = 0.227$ MeV, $\Gamma_\gamma = 0.51\pm0.10$ eV. The error is deduced from Table 3 of FU82. The adopted γ width differs from the value in KU87, which is not consistent with the KU87 electron scattering data (F.C. Barker, private communication). The $5/2^-$ resonance is neglected [BU98]. The broad $1/2^-$ resonance at $E_r^J = 1.12\pm0.12$ MeV should be important at high temperatures [BU98]. Its total width is 1.08 ± 0.11 MeV and we assume $\Gamma_\gamma = 1$ WU for an M1 decay (0.45 eV) with an error of 80% (see also DE89). For the $5/2^+$ resonance at $E_r^J = 1.385$ MeV, we assume constant widths ($\Gamma_n = 0.282\pm0.011$ MeV from AJ88). The γ width obtained from electron scattering in CL68 does not allow reproducing the photoneutron cross section of HU75. The adopted value $\Gamma_\gamma = 0.90\pm0.45$ eV is derived from this cross section with an increased error because of the smaller value in CL68. The differences with CA88 are due to many factors. We perform all integrations numerically. The adopted α-width of the $^8\mathrm{Be}$ ground state is reduced [see $^4\mathrm{He}(\alpha\alpha,\gamma)^{12}\mathrm{C}$]. Our rate is significantly larger below $T_9 = 0.025$ because of the energy dependence of $\Gamma_\alpha(^8\mathrm{Be},E)$, which is neglected in CA88. At higher temperatures, the rates differ because the photoneutron cross section in CA88 is parametrized as $\sigma_{\gamma n} = 1.6\exp(-4E)$ mb (with E in MeV), rather than as a sum over resonances.

T_9	low	adopt	high	exp	ratio	T_9	low	adopt	high	exp	ratio
0.001	2.14	3.90	5.80	−59	-	0.14	2.80	3.57	4.34	−8	0.6
0.002	1.43	2.50	3.66	−47	-	0.15	4.11	5.23	6.35	−8	0.6
0.003	0.79	1.35	1.95	−41	-	0.16	5.70	7.25	8.80	−8	0.6
0.004	3.35	5.58	8.00	−38	-	0.18	0.96	1.22	1.49	−7	0.6
0.005	1.28	2.11	3.00	−35	1E58	0.2	1.43	1.82	2.21	−7	0.6
0.006	1.21	1.96	2.78	−33	1E45	0.25	2.74	3.48	4.22	−7	0.6
0.007	4.61	7.39	10.4	−32	1E36	0.3	3.93	4.99	6.06	−7	0.7
0.008	0.94	1.48	2.07	−30	1E29	0.35	4.84	6.14	7.45	−7	0.7
0.009	1.20	1.88	2.62	−29	1E24	0.4	5.44	6.90	8.37	−7	0.7
0.01	1.08	1.69	2.34	−28	1E20	0.45	5.77	7.33	8.89	−7	0.7
0.011	0.75	1.16	1.60	−27	1E17	0.5	5.90	7.50	9.09	−7	0.7

continued from previous page

T_9	low	adopt	high	exp	ratio	T_9	low	adopt	high	exp	ratio
0.012	4.15	6.37	8.77	−27	1E14	0.6	5.78	7.34	8.91	−7	0.7
0.013	1.93	2.95	4.04	−26	1E12	0.7	5.38	6.84	8.30	−7	0.7
0.014	0.78	1.18	1.61	−25	1E10	0.8	4.89	6.22	7.56	−7	0.7
0.015	2.76	4.17	5.69	−25	1E8	0.9	4.40	5.60	6.80	−7	0.7
0.016	0.89	1.33	1.81	−24	1E7	1	3.93	5.00	6.08	−7	0.8
0.018	0.70	1.05	1.42	−23	1E5	1.25	2.96	3.78	4.60	−7	0.8
0.02	4.27	6.29	8.48	−23	1E3	1.5	2.26	2.89	3.52	−7	0.8
0.025	2.11	2.99	3.92	−21	2.0	1.75	1.76	2.26	2.75	−7	0.8
0.03	3.88	5.05	6.24	−19	0.4	2	1.40	1.80	2.20	−7	0.8
0.04	1.48	1.90	2.33	−15	0.4	2.5	0.93	1.21	1.49	−7	0.8
0.05	2.01	2.58	3.15	−13	0.4	3	6.69	8.87	11.0	−8	0.9
0.06	5.01	6.43	7.84	−12	0.4	3.5	5.05	6.83	8.61	−8	1.0
0.07	4.80	6.14	7.48	−11	0.5	4	3.97	5.48	6.99	−8	1.0
0.08	2.53	3.24	3.94	−10	0.5	5	2.67	3.83	5.01	−8	1.2
0.09	0.90	1.15	1.40	−9	0.5	6	1.94	2.88	3.83	−8	1.5
0.1	2.44	3.12	3.79	−9	0.5	7	1.48	2.26	3.04	−8	1.7
0.11	5.42	6.92	8.41	−9	0.5	8	1.16	1.81	2.47	−8	1.9
0.12	1.04	1.33	1.61	−8	0.5	9	0.94	1.48	2.03	−8	2.1
0.13	1.78	2.27	2.76	−8	0.5	10	0.77	1.23	1.70	−8	2.3
T_9	low	adopt	high	exp	ratio	T_9	low	adopt	high	exp	ratio

Reaction: ^{4}He$(\alpha\alpha,\gamma)^{12}$C

The rate is calculated with a variant of the model presented in NO85 and LA86c,

$$N_A^2 \langle\sigma v\rangle^{\alpha\alpha\alpha} = 3N_A \left(\frac{8\pi\hbar}{\mu_{\alpha\alpha}^2}\right) \left(\frac{\mu_{\alpha\alpha}}{2\pi k_B T}\right)^{3/2}$$

$$\times \int_0^\infty \frac{\sigma_{\alpha\alpha}(E)}{\Gamma_\alpha(^8\text{Be},E)} \exp(-E/k_B T)\, N_A \langle\sigma v\rangle^{\alpha^8\text{Be}}\, E\, dE,$$

where $\mu_{\alpha\alpha}$ is the reduced mass of the $\alpha + \alpha$ system, and E is the energy with respect to the $\alpha + \alpha$ threshold. The elastic cross section of $\alpha + \alpha$ scattering is given by Eq. (7) with $\Gamma_i = \Gamma_f = \Gamma_\alpha(^8\text{Be},E)$. The energy-dependent width of the ^{8}Be ground state is defined in Eq. (9). The energy $E_{^8\text{Be}}$ and width $\Gamma_\alpha(^8\text{Be})$ of the ^{8}Be ground state are displayed in the table. The $N_A\langle\sigma v\rangle^{\alpha^8\text{Be}}$ rate assumes that ^{8}Be has been formed at an energy E different from $E_{^8\text{Be}}$, and that it is bound [LA86c]. This rate is given by

$$N_A\langle\sigma v\rangle^{\alpha^8\text{Be}} = N_A \frac{8\pi}{\mu_{\alpha^8\text{Be}}^2} \left(\frac{\mu_{\alpha^8\text{Be}}}{2\pi k_B T}\right)^{3/2} \int_0^\infty \sigma_{\alpha^8\text{Be}}(E';E) \exp(-E'/k_B T)\, E'\, dE',$$

where $\mu_{\alpha^8\text{Be}}$ is the reduced mass of the $\alpha + {}^8$Be system, and E' is the energy with respect to its threshold (which varies with the formation energy E). As in NO85 and LA86c, we parametrize $\sigma_{\alpha^8\text{Be}}(E';E)$ as

$$\sigma_{\alpha^8\text{Be}}(E';E) = \sum_{J=0,2} (2J+1) \frac{\pi\hbar^2}{2\mu_{\alpha^8\text{Be}}E'}$$

$$\times \frac{\Gamma_\alpha(^{12}C^J, E')\Gamma_\gamma(^{12}C^J, E'+E)}{(E' - E_r^J + E - E_{^8\text{Be}})^2 + \frac{1}{4}\Gamma(^{12}C^J, E';E)^2},$$

where the sum runs over the 0_2^+ resonance and an assumed 2^+ resonance at energies E_r^J. The widths are given by $\Gamma = \Gamma_\alpha + \Gamma_\gamma$, $\Gamma_\alpha(^{12}C^J, E') = \Gamma_\alpha(^{12}C^J)\, P_l(E')/P_l(E_r^J)$ and $\Gamma_\gamma(^{12}C^J, E'+E) = \Gamma_\gamma(^{12}C^J)(E_T + E' + E - E_{^8\text{Be}})^5/(E_T + E_r^J)^5$, where, for $J = 0$, the photon threshold energy E_T is $7.367 - 4.439 = 2.928$ MeV and E_r^J, $\Gamma_\alpha(^{12}C^J)$ and $\Gamma_\gamma(^{12}C^J)$ are given in the table. In these expressions, we follow DE87 in not including a separate non-resonant contribution as in LA86c. Indeed, such a contribution interferes with the tail of a broad resonance, and the microscopic calculation in DE87 shows that a Breit–Wigner expression provides a fair approximation of the global terms. For $J = 2$, we assume the existence of a broad resonance belonging to the same rotational band as the 0_2^+ state. The capture to the ^{12}C ground state is calculated with $E_T = 7.367$ MeV and the theoretical values [DE87] $E_r^J = 1.75$ MeV, $\Gamma_\alpha = 0.56$ MeV and $\Gamma_\gamma = 0.2$ eV. An 80% uncertainty is adopted on the γ width. The various integrals are calculated numerically. The weak influence of higher resonances is restricted to a contribution of the 3^- resonance, for which we use $\Gamma_\gamma = 2$ meV. The experimental bound and the Γ_{γ_0} value given in the table are used as upper and lower bounds. The rate of CA88 (which is the rate of NO85 with an additional resonance term) is always smaller than the present one, in spite of the fact that our adopted α-width of the ^{8}Be ground state is smaller. Our rate is significantly larger at low temperatures because NO85 uses $\Gamma_\alpha(^{12}C^J, E';E) = \Gamma_\alpha(^{12}C^J)\, P_l(E')/P_l(E_r^J - E + E_{^8\text{Be}})$. Their reduced α-width then depends in an unrealistic way on the threshold energy E. At high temperatures, our rate is much larger because of the assumed 2^+ contribution.

Nucleus	J^π	E_r (keV)	Γ_α (eV)	Γ_γ (meV)	Ref.
^{8}Be	0^+	92.12	6.8 ± 1.7	–	BE68
		92.03	5.57 ± 0.25	–	WÜ92
		92.08	5.60 ± 0.25	–	adopt
^{12}C	0_2^+	287.7	8.3 ± 1.0	3.7 ± 0.5	AJ90
	3_1^-	2274	$(34 \pm 5) \times 10^3$	$< 14\ (\Gamma_{\gamma_0} = 0.31 \pm 0.04)$	AJ90
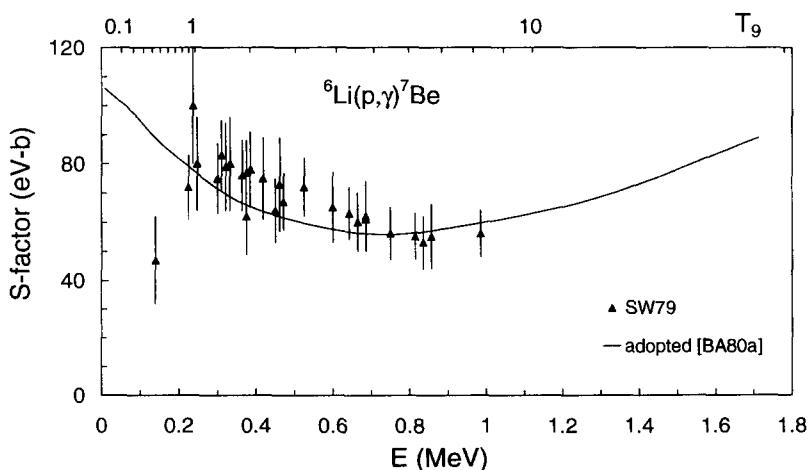
T_9	low	adopt	high	exp	ratio	T_9	low	adopt	high	exp	ratio
0.01	2.13	2.93	3.89	−71	11	0.25	3.65	4.22	4.79	−14	1.1
0.011	4.32	5.94	7.90	−69	11	0.3	3.95	4.57	5.18	−13	1.0
0.012	4.79	6.59	8.75	−67	11	0.35	2.01	2.33	2.64	−12	1.0
0.013	3.24	4.46	5.92	−65	11	0.4	6.48	7.49	8.50	−12	1.0
0.014	1.46	2.01	2.66	−63	12	0.45	1.54	1.78	2.02	−11	1.0
0.015	4.65	6.40	8.50	−62	12	0.5	2.98	3.45	3.91	−11	1.0
0.016	1.11	1.53	2.03	−60	12	0.6	7.46	8.62	9.79	−11	1.0

T_9	low	adopt	high	exp	ratio	T_9	low	adopt	high	exp	ratio
0.018	3.07	4.22	5.61	−58	11	0.7	1.34	1.55	1.75	−10	1.0
0.02	3.96	5.45	7.23	−56	8.9	0.8	1.96	2.27	2.58	−10	1.0
0.025	0.81	1.11	1.47	−51	4.1	0.9	2.54	2.93	3.33	−10	1.0
0.03	1.10	1.46	1.86	−47	2.3	1	3.01	3.48	3.95	−10	1.0
0.04	4.04	5.31	6.76	−41	1.8	1.25	3.71	4.30	4.89	−10	1.0
0.05	0.79	1.04	1.32	−36	1.7	1.5	3.87	4.49	5.12	−10	1.0
0.06	0.91	1.20	1.52	−33	1.7	1.75	3.72	4.37	5.02	−10	1.0
0.07	2.33	3.00	3.75	−31	1.7	2	3.44	4.16	4.87	−10	1.1
0.08	8.18	9.68	11.2	−29	1.3	2.5	2.86	3.92	4.99	−10	1.3
0.09	2.18	2.52	2.87	−26	1.2	3	2.45	4.16	5.90	−10	1.7
0.1	2.05	2.38	2.70	−24	1.1	3.5	2.22	4.77	7.39	−10	2.6
0.11	8.34	9.64	10.9	−23	1.1	4	2.11	5.55	9.10	−10	3.8
0.12	1.79	2.07	2.35	−21	1.1	5	2.05	7.04	12.2	−10	7.0
0.13	2.35	2.72	3.09	−20	1.1	6	2.05	8.03	14.3	−10	10
0.14	2.10	2.43	2.76	−19	1.1	7	2.01	8.48	15.3	−10	13
0.15	1.38	1.60	1.82	−18	1.1	8	1.94	8.52	15.5	−10	15
0.16	7.11	8.22	9.34	−18	1.1	9	1.84	8.28	15.1	−10	15
0.18	1.05	1.22	1.38	−16	1.1	10	1.73	7.90	14.5	−10	15
0.2	0.88	1.02	1.16	−15	1.1						
T_9	low	adopt	high	exp	ratio	T_9	low	adopt	high	exp	ratio

Reaction: ^{6}Li$(p,\gamma)^7$Be

The non-resonant data from SW79 in the $0.25 \leqslant E \leqslant 1$ MeV range are adopted, along with the direct capture calculation of BA80. The zero energy S-factor $S_0 = 65 \pm 10$ eV b from CE92 is omitted, since this value is not presently understood. For $T_9 \leqslant 1.5$, the adopted rates are higher than the CA88 ones, due to the different S-factor extrapolation at low energies adopted here. The large differences for $T_9 > 5$ are due to a very rapid decrease of the CA88 rates at high temperatures. The CA88 rates are obtained from an exponentially decreasing S-factor which falls below the BA80 estimate above 1 MeV.
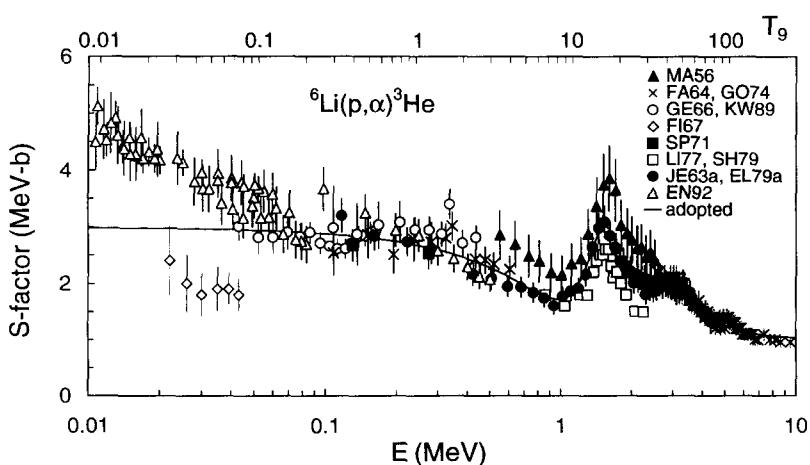
T_9	low	adopt	high	exp	ratio	T_9	low	adopt	high	exp	ratio
0.001	2.88	3.60	4.32	−29	1.9	0.14	3.24	4.05	4.86	−1	1.6
0.002	6.29	7.86	9.43	−22	1.9	0.15	4.45	5.57	6.68	−1	1.6
0.003	2.23	2.79	3.35	−18	1.9	0.16	5.95	7.44	8.93	−1	1.6
0.004	3.82	4.78	5.74	−16	1.9	0.18	0.99	1.24	1.49	0	1.6
0.005	1.47	1.84	2.21	−14	1.9	0.2	1.53	1.91	2.29	0	1.6
0.006	2.38	2.97	3.56	−13	1.9	0.25	3.62	4.52	5.42	0	1.5
0.007	2.18	2.73	3.27	−12	1.9	0.3	6.92	8.62	10.3	0	1.5
0.008	1.35	1.69	2.03	−11	1.9	0.35	1.15	1.43	1.71	1	1.4
0.009	6.32	7.90	9.48	−11	1.9	0.4	1.75	2.17	2.59	1	1.4
0.01	2.38	2.97	3.57	−10	1.9	0.45	2.48	3.07	3.66	1	1.3
0.011	7.56	9.45	11.3	−10	1.8	0.5	3.34	4.13	4.91	1	1.3
0.012	2.10	2.63	3.16	−9	1.9	0.6	5.43	6.68	7.94	1	1.3
0.013	5.25	6.56	7.87	−9	1.9	0.7	7.94	9.75	11.6	1	1.2
0.014	1.20	1.49	1.79	−8	1.9	0.8	1.08	1.33	1.57	2	1.2
0.015	2.52	3.15	3.78	−8	1.9	0.9	1.40	1.71	2.02	2	1.1
0.016	4.99	6.24	7.49	−8	1.8	1	1.75	2.13	2.52	2	1.1
0.018	1.67	2.08	2.50	−7	1.8	1.25	2.66	3.24	3.82	2	1.1
0.02	4.70	5.88	7.05	−7	1.8	1.5	3.63	4.41	5.19	2	1.0
0.025	3.73	4.66	5.60	−6	1.8	1.75	4.65	5.63	6.61	2	1.0
0.03	1.80	2.25	2.70	−5	1.8	2	5.65	6.84	8.03	2	1.0
0.04	1.76	2.20	2.64	−4	1.8	2.5	7.64	9.24	10.8	2	1.0
0.05	0.88	1.10	1.32	−3	1.8	3	0.98	1.18	1.39	3	1.0
0.06	2.98	3.73	4.47	−3	1.8	3.5	1.18	1.43	1.68	3	1.1
0.07	7.86	9.82	11.8	−3	1.7	4	1.38	1.68	1.98	3	1.3
0.08	1.74	2.18	2.61	−2	1.7	5	1.79	2.18	2.57	3	1.9
0.09	3.40	4.25	5.10	−2	1.7	6	2.17	2.66	3.14	3	3.2
0.1	6.03	7.54	9.05	−2	1.7	7	2.54	3.12	3.70	3	6.5
0.11	0.99	1.24	1.49	−1	1.7	8	2.89	3.56	4.23	3	17
0.12	1.54	1.93	2.31	−1	1.7	9	3.21	3.96	4.71	3	70
0.13	2.28	2.85	3.42	−1	1.7	10	3.49	4.32	5.15	3	2800

Reaction: ^{6}Li$(p,\alpha)^3$He
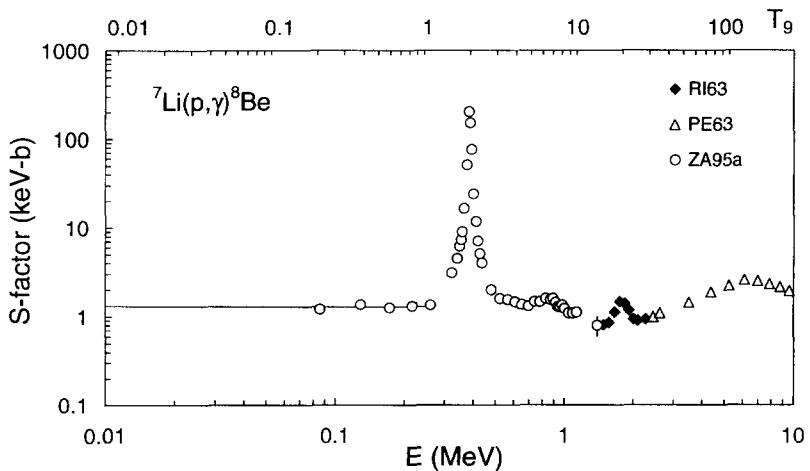
Total cross sections are adopted from MA56, JE63a, FA64, GE66, SP71, GO74, LI77, EL79a, SH79 and KW89 from $E = 0.043$ to 12.08 MeV. The low-energy data from FI67 are omitted due to what appears to be normalization problems. Those from EN92 are corrected for electron screening effects ($U_e = 470$ eV and 440 eV for atomic and molecular target data, respectively). We used the extrapolation performed by KW89, $S_0 = 2.97 \pm 0.03$ MeV b and we fitted the S-factor data in the whole energy range. The fitted S-factor curve is shown in the figure. For $E \leqslant 0.1$ MeV, the S-factor can be well approximated by the expression $S(E) = 2.97 - 0.67\,E - 5.49\,E^2$ (E in MeV, $S(E)$ in MeV b). The differences between the adopted rates and the CA88 ones at high temperatures (about 30% at $T_9 = 10$) are probably due to the better accuracy of the numerical integration of the rate equation used here.

T_9	low	adopt	high	exp	ratio	T_9	low	adopt	high	exp	ratio
0.001	0.90	1.00	1.10	−24	0.9	0.14	1.06	1.18	1.30	4	0.9
0.002	1.97	2.19	2.41	−17	0.9	0.15	1.47	1.63	1.79	4	0.9
0.003	6.98	7.76	8.53	−14	0.9	0.16	1.97	2.19	2.41	4	0.9
0.004	1.20	1.33	1.46	−11	0.9	0.18	3.30	3.66	4.03	4	0.9
0.005	4.61	5.12	5.63	−10	0.9	0.2	5.13	5.70	6.27	4	0.9
0.006	7.43	8.25	9.08	−9	0.9	0.25	1.23	1.37	1.51	5	0.9
0.007	6.82	7.58	8.33	−8	0.9	0.3	2.38	2.65	2.91	5	0.9
0.008	4.23	4.70	5.17	−7	0.9	0.35	4.01	4.46	4.91	5	0.9
0.009	1.98	2.20	2.42	−6	0.9	0.4	6.14	6.82	7.50	5	0.9
0.01	7.45	8.27	9.10	−6	0.9	0.45	8.76	9.73	10.7	5	0.9
0.011	2.37	2.63	2.90	−5	0.9	0.5	1.19	1.32	1.45	6	0.9
0.012	6.60	7.33	8.06	−5	0.9	0.6	1.94	2.15	2.37	6	0.9
0.013	1.65	1.83	2.01	−4	0.9	0.7	2.85	3.16	3.48	6	0.9
0.014	3.75	4.17	4.58	−4	0.9	0.8	3.88	4.31	4.75	6	0.9
0.015	7.92	8.80	9.68	−4	0.9	0.9	5.03	5.58	6.14	6	0.9
0.016	1.57	1.74	1.92	−3	0.9	1	6.25	6.95	7.64	6	0.9
0.018	5.25	5.83	6.41	−3	0.9	1.25	0.95	1.06	1.17	7	0.9
0.02	1.48	1.65	1.81	−2	0.9	1.5	1.30	1.45	1.59	7	0.9
0.025	1.18	1.31	1.44	−1	0.9	1.75	1.66	1.84	2.03	7	0.9
0.03	5.69	6.32	6.95	−1	0.9	2	2.02	2.24	2.46	7	0.9
0.04	5.58	6.20	6.82	0	0.9	2.5	2.73	3.03	3.33	7	0.9
0.05	2.80	3.11	3.43	1	0.9	3	3.44	3.82	4.20	7	0.9
0.06	0.95	1.06	1.17	2	0.9	3.5	4.14	4.60	5.06	7	0.9
0.07	2.52	2.80	3.08	2	0.9	4	4.83	5.37	5.91	7	0.9
0.08	5.61	6.23	6.85	2	0.9	5	6.14	6.82	7.50	7	0.9
0.09	1.10	1.22	1.34	3	0.9	6	7.32	8.13	8.94	7	1.0
0.1	1.96	2.17	2.39	3	0.9	7	8.34	9.27	10.2	7	1.0
0.11	3.23	3.59	3.95	3	0.9	8	0.92	1.03	1.13	8	1.1
0.12	5.03	5.59	6.15	3	0.9	9	1.00	1.11	1.22	8	1.2
0.13	7.47	8.30	9.13	3	0.9	10	1.06	1.18	1.30	8	1.3

Reaction: ^{7}Li(p,γ)^{8}Be

Experimental data from RI63, PE63 and ZA95a are adopted, covering the energy range $0.086 \leqslant E \leqslant 10$ MeV. The relative cross sections of RI63 and PE63 are normalized to the absolute values of ZA95a in the overlapping energy region (with an assumed 100% error). Several experiments using polarized proton beams [CH92,GO96,GO97] show that the reaction ^{7}Li(p,γ)^{8}B proceeds by both s-wave and p-wave capture. The anisotropic cross section has been confirmed by HA96. At energies $E < 100$ keV, estimations of the M1/E1 cross section ratio ranges between 12% lower and 20% higher than obtained when a constant S-factor is assumed. However, no clear results are given until now [see GO97 for an extended discussion]. Therefore, we consider an additional uncertainty of 20% to the constant S-factor equal to $S(E) = 1.5 \pm 0.2$ keV b [CE92] adopted for the extrapolation to low energies. The present rates are significantly higher than those of CA88 at low temperatures. This results mainly from a different extrapolation [ZA95a]. At high temperatures, the differences are probably due to the omission by CA88 of the contribution of the resonance around 2 MeV [RI63,PE63] and of the giant dipole resonance around 7.3 MeV [PE63,FI76].
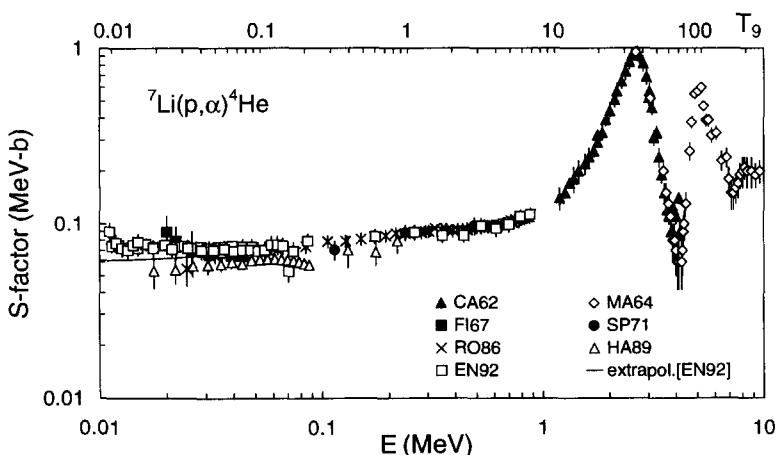
T_9	low	adopt	high	exp	ratio	T_9	low	adopt	high	exp	ratio
0.001	1.95	2.81	3.82	−28	109	0.14	4.27	4.71	5.16	0	46
0.002	4.79	6.90	9.37	−21	107	0.15	5.92	6.52	7.12	0	44
0.003	1.80	2.59	3.52	−17	105	0.16	7.98	8.77	9.55	0	43
0.004	3.19	4.59	6.23	−15	104	0.18	1.35	1.48	1.61	1	40
0.005	1.26	1.81	2.46	−13	102	0.2	2.13	2.32	2.51	1	38
0.006	2.07	2.97	4.03	−12	101	0.25	5.31	5.72	6.14	1	30
0.007	1.93	2.77	3.76	−11	100	0.3	1.09	1.16	1.24	2	17
0.008	1.21	1.74	2.35	−10	99	0.35	2.05	2.18	2.32	2	7.8
0.009	5.71	8.20	11.1	−10	98	0.4	3.76	3.99	4.23	2	4.1
0.01	2.17	3.11	4.21	−9	97	0.45	6.77	7.17	7.56	2	2.7
0.011	6.96	9.98	13.6	−9	96	0.5	1.17	1.24	1.30	3	2.1

continued on next page

T_9	low	adopt	high	exp	ratio	T_9	low	adopt	high	exp	ratio
0.012	1.95	2.79	3.78	−8	95	0.6	2.96	3.12	3.27	3	1.6
0.013	4.89	7.01	9.48	−8	94	0.7	6.02	6.32	6.62	3	1.4
0.014	1.12	1.60	2.17	−7	93	0.8	1.03	1.08	1.13	4	1.3
0.015	2.38	3.40	4.60	−7	92	0.9	1.55	1.63	1.70	4	1.3
0.016	4.73	6.76	9.14	−7	92	1	2.14	2.24	2.35	4	1.3
0.018	1.59	2.27	3.07	−6	90	1.25	3.69	3.86	4.04	4	1.2
0.02	4.51	6.45	8.71	−6	88	1.5	5.11	5.35	5.60	4	1.2
0.025	3.63	5.18	6.98	−5	85	1.75	6.26	6.56	6.86	4	1.3
0.03	1.77	2.52	3.38	−4	82	2	7.17	7.53	7.88	4	1.3
0.04	2.18	2.48	2.78	−3	76	2.5	8.31	8.75	9.20	4	1.3
0.05	1.10	1.25	1.40	−2	71	3	8.89	9.43	9.97	4	1.4
0.06	3.76	4.24	4.73	−2	67	3.5	9.07	9.74	10.4	4	1.5
0.07	0.99	1.12	1.25	−1	63	4	9.15	9.98	10.8	4	1.6
0.08	2.21	2.48	2.76	−1	60	5	8.72	9.96	11.2	4	1.8
0.09	4.33	4.86	5.38	−1	57	6	8.08	9.82	11.6	4	2.0
0.1	7.72	8.63	9.54	−1	54	7	7.47	9.79	12.1	4	2.2
0.11	1.28	1.43	1.57	0	52	8	6.83	9.76	12.7	4	2.5
0.12	2.00	2.22	2.44	0	49	9	6.31	9.88	13.5	4	2.8
0.13	2.98	3.30	3.62	0	47	10	0.58	1.00	1.42	5	3.2
T_9	low	adopt	high	exp	ratio	T_9	low	adopt	high	exp	ratio

Reaction: $^7\text{Li}(p,\alpha)^4\text{He}$

Experimental cross section data from CA62, MA64, FI67, SP71, RO86, HA89 and EN92 are adopted. The low energy data of EN92 are corrected for electron screening with $U_e = 300$ eV. The original data of SP71 and HA89 represent the number of α-particles emitted per proton. In order to obtain the total cross section, we divide their values by a factor of 2. For the calculation of the rates, a smooth spline fit to all data is adopted. For $E \leqslant 0.9$ MeV, the approximation of the "bare" nucleus S-factor given in EN92 is adopted, $S(E) = 0.0593 + 0.193\,E - 0.355\,E^2 + 0.236\,E^3$ (E in MeV, $S(E)$ in MeV b). The differences between the adopted rates and the CA88 ones (about 30%) are probably due to the higher accuracy of the numerical integration used here.

T_9	low	adopt	high	exp	ratio	T_9	low	adopt	high	exp	ratio
0.001	0.98	1.13	1.28	−26	1.1	0.14	2.32	2.62	2.91	2	1.0
0.002	2.42	2.79	3.16	−19	1.1	0.15	3.24	3.65	4.05	2	1.0
0.003	0.91	1.05	1.19	−15	1.1	0.16	4.38	4.93	5.48	2	1.0
0.004	1.63	1.88	2.13	−13	1.1	0.18	7.47	8.40	9.34	2	1.0
0.005	6.47	7.45	8.44	−12	1.1	0.2	1.18	1.33	1.47	3	1.0
0.006	1.07	1.23	1.39	−10	1.1	0.25	2.94	3.30	3.66	3	1.0
0.007	1.00	1.15	1.30	−9	1.1	0.3	5.89	6.60	7.31	3	1.0
0.008	6.32	7.27	8.22	−9	1.1	0.35	1.02	1.14	1.26	4	1.0
0.009	2.99	3.44	3.89	−8	1.1	0.4	1.61	1.80	1.99	4	1.0
0.01	1.14	1.31	1.48	−7	1.1	0.45	2.35	2.62	2.89	4	1.0
0.011	3.68	4.23	4.77	−7	1.1	0.5	3.29	3.65	4.01	4	1.0
0.012	1.03	1.19	1.34	−6	1.1	0.6	5.60	6.20	6.79	4	1.0
0.013	2.61	2.99	3.38	−6	1.1	0.7	8.55	9.44	1.03	4	1.0
0.014	5.99	6.88	7.76	−6	1.1	0.8	1.21	1.33	1.45	5	1.0
0.015	1.28	1.46	1.65	−5	1.1	0.9	1.61	1.77	1.93	5	1.0
0.016	2.55	2.92	3.30	−5	1.1	1	2.07	2.27	2.47	5	1.0
0.018	8.64	9.90	11.2	−5	1.1	1.25	3.38	3.70	4.02	5	1.0
0.02	2.47	2.83	3.19	−4	1.1	1.5	4.87	5.33	5.79	5	1.0
0.025	2.02	2.31	2.60	−3	1.1	1.75	6.56	7.18	7.80	5	1.0
0.03	1.00	1.14	1.28	−2	1.1	2	8.38	9.19	10.00	5	1.1
0.04	1.01	1.16	1.30	−1	1.1	2.5	1.25	1.38	1.50	6	1.1
0.05	5.25	5.97	6.70	−1	1.1	3	1.75	1.93	2.11	6	1.2
0.06	1.83	2.08	2.33	0	1.1	3.5	2.35	2.60	2.85	6	1.3
0.07	4.95	5.62	6.29	0	1.1	4	3.10	3.43	3.77	6	1.3
0.08	1.12	1.27	1.42	1	1.0	5	4.94	5.48	6.02	6	1.1
0.09	2.24	2.53	2.83	1	1.0	6	7.05	7.81	8.58	6	1.0
0.1	4.05	4.58	5.11	1	1.0	7	0.92	1.02	1.12	7	0.9
0.11	6.80	7.68	8.55	1	1.0	8	1.13	1.25	1.37	7	0.9
0.12	1.07	1.21	1.35	2	1.0	9	1.33	1.48	1.62	7	0.8
0.13	1.61	1.82	2.02	2	1.0	10	1.52	1.68	1.84	7	0.8

Reaction: $^7\text{Li}(\alpha,\gamma)^{11}\text{B}$
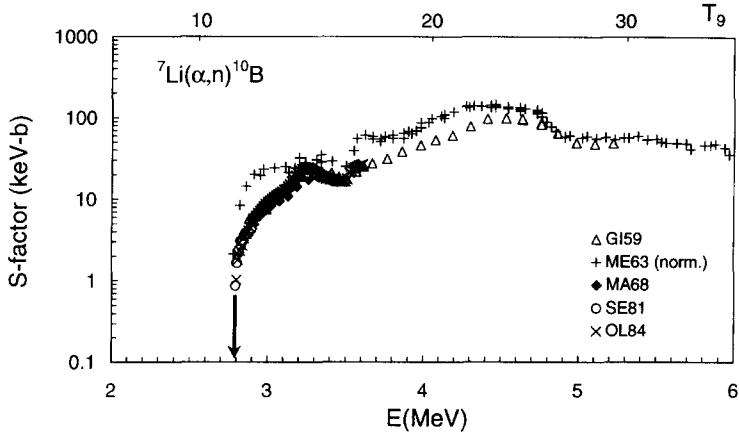
The parameters reported by PA67 and HA84 for the resonances at $E_r = 0.255$, 0.518, 0.607, 1.590, 1.667, 1.782, and 1.936 MeV are adopted (for a discussion of the BE51 data, see HA84). In DE95, the non-resonant capture is shown to be well approximated by the tail of low-energy resonances only. The difference between our adopted rates and the CA88 ones at low temperatures are mainly due to the contribution of the resonance at $E_r = 1.590$ MeV, for which CA88 use a total width of 200 keV [PA63], whereas our adopted width is 433 keV [PA67]. Although PA67 reports in one table a width of 200 keV, this value is rejected in the text, and the value $\Gamma = 433$ keV is recommended there. A small difference in energy of the $E_r = 0.255$ MeV resonance (0.2565 MeV in CA88) has also a significant effect at higher temperatures.

E_r (MeV)	$\omega\gamma$ (eV)	Ref.	
0.255 ± 0.002	0.0088 ± 0.0013	HA84	I
0.518 ± 0.001	$0.31^{+0.12}_{-0.09}$	HA84	M
0.607 ± 0.001	1.73 ± 0.24	HA84	M
1.590 ± 0.012	17.0 ± 3.4	PA67	M
1.667 ± 0.012	1.5 ± 0.3	PA67	M
1.782 ± 0.032	2.5 ± 0.5	PA67	M
1.936 ± 0.032	$0.04^{+0.36}_{-0.04}$	PA67	M

T_9	low	adopt	high	exp	ratio	T_9	low	adopt	high	exp	ratio
0.015	1.95	3.06	4.40	−25	2.7	0.4	6.98	8.31	9.66	−1	1.1
0.016	0.98	1.53	2.21	−24	2.7	0.45	1.38	1.64	1.92	0	1.1
0.018	1.69	2.65	3.83	−23	2.7	0.5	2.42	2.89	3.39	0	1.1
0.02	1.98	3.09	4.45	−22	2.7	0.6	6.15	7.45	8.88	0	1.1
0.025	2.70	4.21	6.09	−20	2.7	0.7	1.38	1.69	2.04	1	1.1
0.03	1.15	1.79	2.59	−18	2.7	0.8	2.80	3.44	4.19	1	1.1
0.04	2.68	4.18	6.07	−16	2.7	0.9	5.13	6.28	7.67	1	1.1
0.05	1.30	2.02	2.93	−14	2.6						
0.06	2.49	3.88	5.63	−13	2.6	1	0.85	1.04	1.27	2	1.1
0.07	2.64	4.11	5.95	−12	2.6	1.25	2.14	2.62	3.19	2	1.1
0.08	1.95	2.99	4.30	−11	2.5	1.5	3.91	4.78	5.79	2	1.0
0.09	1.49	2.13	2.91	−10	2.1	1.75	5.90	7.21	8.70	2	1.0
0.1	1.62	2.10	2.63	−9	1.7	2	7.95	9.71	11.7	2	1.0
0.11	1.71	2.11	2.54	−8	1.5	2.5	1.20	1.48	1.77	3	1.0
0.12	1.34	1.63	1.93	−7	1.4	3	1.63	2.00	2.43	3	1.1
0.13	7.83	9.45	11.1	−7	1.4	3.5	2.08	2.57	3.17	3	1.1
0.14	3.55	4.26	5.00	−6	1.3	4	2.57	3.15	3.95	3	1.2
0.15	1.31	1.57	1.83	−5	1.3	5	3.52	4.21	5.45	3	1.4
0.16	4.06	4.87	5.70	−5	1.3	6	4.21	4.91	6.45	3	1.5
0.18	2.66	3.18	3.71	−4	1.2	7	4.48	5.30	6.79	3	1.7
0.2	1.17	1.40	1.63	−3	1.2	8	4.48	5.52	6.79	3	1.9
0.25	1.62	1.93	2.25	−2	1.2	9	4.43	5.61	6.76	3	2.2
0.3	0.89	1.06	1.23	−1	1.1	10	4.46	5.58	6.77	3	2.4
0.35	2.91	3.47	4.03	−1	1.1						

Reaction: ^{7}Li$(\alpha,n)^{10}$B

Experimental data from GI59, MA68, SE81 and OL84 covering the energy range from threshold ($Q = -2.790$ MeV) to $E = 5.22$ MeV are adopted. From threshold to $E = 3.61$ MeV, OL84 and SE81 are selected, as a careful and complete discussion of possible sources of errors is provided. At higher energies up to 5.22 MeV, the GI59 data are used, following the suggestion of SE81 and OL84. Differential cross sections are reported by ME63 for a wide energy range. We have converted them into total cross sections assuming isotropy and 100% error. All these resulting values are shown in the figure, but only those above $E = 5.22$ MeV are adopted. The CA88 rates rely only on a continuum term, which is in contradiction with the experimental data. At energies close to threshold, the cross sections used in CA88 are much higher than the experimental ones.
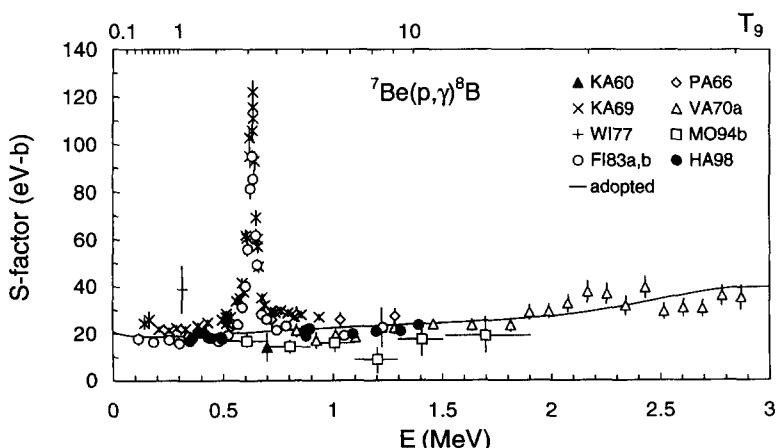
T_9	low	adopt	high	exp	ratio	T_9	low	adopt	high	exp	ratio
0.45	1.33	1.46	1.60	−24	0.1	2.5	1.30	1.38	1.46	2	0.2
0.5	1.82	2.00	2.18	−21	0.1	3	1.30	1.37	1.45	3	0.2
0.6	0.94	1.03	1.11	−16	0.1	3.5	6.95	7.35	7.75	3	0.2
0.7	2.22	2.41	2.60	−13	0.1	4	2.50	2.65	2.79	4	0.2
0.8	7.62	8.25	8.87	−11	0.1	5	1.54	1.65	1.76	5	0.3
0.9	7.22	7.79	8.36	−9	0.1	6	5.23	5.74	6.24	5	0.3
1	2.78	2.99	3.20	−7	0.1	7	1.25	1.41	1.58	6	0.4
1.25	2.02	2.17	2.31	−4	0.1	8	2.38	2.80	3.22	6	0.4
1.5	1.69	1.80	1.92	−2	0.1	9	3.91	4.81	5.71	6	0.5
1.75	4.02	4.29	4.56	−1	0.1	10	5.67	7.37	9.07	6	0.5
2	4.39	4.68	4.96	0	0.1						

Reaction: ^{7}Be(p,γ)^{8}B

Experimental data from KA60, PA66, KA69, VA70a, FI83a, FI83b and HA98 are available. All data sets, with the exception of the HA98 ones, are renormalized to the ^{7}Li(d,p)^{8}Li cross section, for which the recommended value of ST96a, obtained by analysing previous experiments also, is adopted. However, the error quoted by ST96a is increased to take into account uncertainties in the absolute data normalization, $\sigma(^7$Li(d,p)^{8}Li)= 146 ± 11 mb. The data point from WI77 is omitted. Data obtained in Coulomb break-up experiments [MO94b] are also disregarded (see Section 2.2.2). For the calculation of the rates, we adopt the energy dependence predicted by the microscopic calculation of DE94a with a renormalization factor of 0.69 ± 0.07 obtained from a χ^2 analysis of the experimental data. The recommended S-factor at zero energy is then $\mathcal{S}_0 = 21 ± 2$ eV b. This value is slightly larger than the value recommended by AD98 ($\mathcal{S}_0 = 19^{+4}_{-2}$ eV b) who exclude the KA69 data. For $E \leqslant 0.1$ MeV, the S-factor can be well approximated by the expression $S(E) = 21 - 18E + 38E^2$ (E in MeV, $S(E)$ in eV b). For the $E_r = 633 ± 10$ keV resonance, we adopt a strength $\omega\gamma = 0.011 ± 0.002$ eV following the renormalization of the original values of KA69 and FI83 (see above). The differences between the present rates and the CA88 ones relate to the influence of

T_9	low	adopt	high	exp	ratio	T_9	low	adopt	high	exp	ratio
0.003	1.43	1.60	1.77	−24	0.9	0.15	3.25	3.64	4.03	−3	0.8
0.004	7.90	8.83	9.78	−22	0.9	0.16	4.70	5.25	5.81	−3	0.8
0.005	7.00	7.83	8.67	−20	0.9	0.18	0.90	1.00	1.11	−2	0.8
0.006	2.13	2.38	2.64	−18	0.9	0.2	1.56	1.75	1.93	−2	0.8
0.007	3.25	3.64	4.03	−17	0.8	0.25	4.73	5.29	5.85	−2	0.8
0.008	3.07	3.44	3.80	−16	0.8	0.3	1.09	1.22	1.35	−1	0.8
0.009	2.05	2.29	2.53	−15	0.8	0.35	2.13	2.38	2.63	−1	0.8
0.01	1.05	1.17	1.29	−15	0.8	0.4	3.67	4.10	4.54	−1	0.8
0.011	4.35	4.86	5.38	−14	0.8	0.45	5.82	6.50	7.20	−1	0.8
0.012	1.53	1.71	1.90	−13	0.8	0.5	8.64	9.66	10.7	−1	0.8
0.013	4.73	5.29	5.85	−13	0.8	0.6	1.66	1.86	2.07	0	0.8
0.014	1.30	1.46	1.61	−12	0.8	0.7	2.82	3.17	3.54	0	0.8
0.015	3.28	3.66	4.05	−12	0.8	0.8	4.40	4.98	5.59	0	0.8
0.016	7.60	8.50	9.40	−12	0.8	0.9	6.46	7.36	8.31	0	0.8
0.018	3.37	3.76	4.16	−11	0.8	1	0.91	1.04	1.18	1	0.8
0.02	1.21	1.35	1.50	−10	0.8	1.25	1.79	2.07	2.37	1	0.8
0.025	1.56	1.74	1.93	−9	0.8	1.5	2.97	3.45	3.96	1	0.8
0.03	1.09	1.22	1.35	−8	0.8	1.75	4.38	5.10	5.85	1	0.9
0.04	1.84	2.05	2.27	−7	0.8	2	5.95	6.91	7.91	1	0.9
0.05	1.35	1.51	1.67	−6	0.8	2.5	0.94	1.08	1.23	2	0.9
0.06	6.17	6.90	7.64	−6	0.8	3	1.29	1.49	1.69	2	0.9
0.07	2.06	2.31	2.55	−5	0.8	3.5	1.66	1.90	2.15	2	0.9
0.08	5.56	6.22	6.88	−5	0.8	4	2.04	2.32	2.62	2	1.0
0.09	1.28	1.43	1.59	−4	0.8	5	2.82	3.20	3.58	2	1.0
0.1	2.63	2.94	3.25	−4	0.8	6	3.65	4.12	4.60	2	1.1
0.11	4.92	5.49	6.08	−4	0.8	7	4.53	5.11	5.69	2	1.1
0.12	8.54	9.54	10.6	−4	0.8	8	5.45	6.13	6.82	2	1.2
0.13	1.40	1.56	1.73	−3	0.8	9	6.42	7.21	8.00	2	1.3
0.14	2.18	2.43	2.69	−3	0.8	10	7.41	8.32	9.23	2	1.4

the new value for the ^{7}Li(d,p)^{8}Li cross section, and to the use of a different low energy extrapolation.

Reaction: $^7\mathrm{Be}(\alpha,\gamma)^{11}\mathrm{C}$
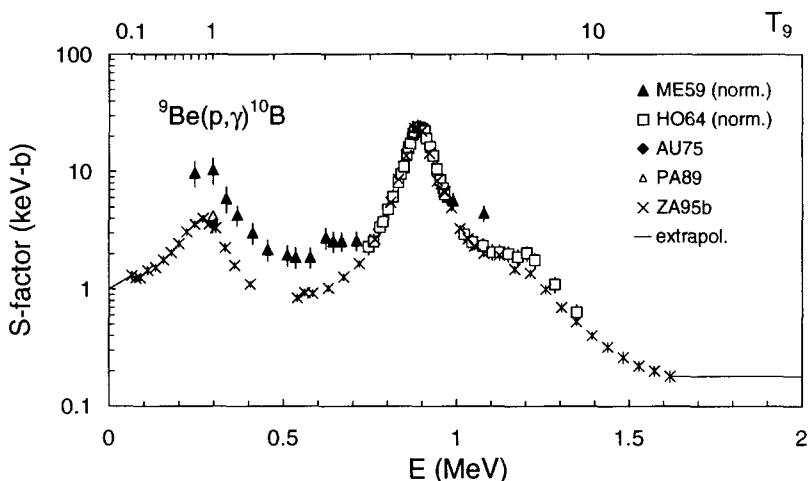
Experimental data are available only for the first two resonances at $E_r = 0.560$ and 0.877 MeV [HA84]. For the non-resonant rates, theoretical information is available up to $T_9 = 0.7$ only ($E_0 = 0.53$ MeV, $\Delta E_0 = 0.41$ MeV), since calculated cross sections [DE95], which also include a subthreshold resonance ($J^\pi = 3/2^+$, $E_r = -43$ keV), are restricted to $E \leqslant 1$ MeV. In [BU88], the S-factor is computed with a potential model, but some parameters of this model can not be determined with precision. Beyond $T_9 = 2$, higher-energy resonances should contribute (the first one is a $7/2^+$ resonance at $E_r = 1.11$ MeV), but $\omega\gamma$ values are not available. Consequently, HF rates have been used for $T_9 \geqslant 2$. The origin of the non-resonant term of CA88 is unknown (the positive S_0' value does not correspond to the tail of a subthreshold state). The strong enhancement at low temperatures is due the presence of the subthreshold state, which is not included in CA88. Between $T_9 = 0.3$ and $T_9 = 5$, the resonant term dominates, and both reaction rates are similar. Beyond $T_9 = 5$, our HF calculation yields larger rates than the CA88 ones.

E_r	J^π	$\omega\gamma$ (eV)	Γ_α (eV)	Γ_γ (eV)	Ref	
0.560	$3/2^-$	0.331±0.041	11±7	0.350±0.056	HA84	1
0.877	$5/2^-$	3.80±0.57	12.6±3.8	3.1±1.3	HA84	1

T_9	low	adopt	high	exp	ratio	T_9	low	adopt	high	exp	ratio
0.02	0.81	1.16	1.50	−26	133	0.45	1.65	2.32	3.09	−2	1.1
0.025	3.05	4.36	5.67	−24	126	0.5	6.03	8.40	11.1	−2	1.1
0.03	2.79	3.98	5.17	−22	119	0.6	4.12	5.65	7.31	−1	1.1
0.04	1.96	2.80	3.63	−19	108	0.7	1.60	2.18	2.79	0	1.1
0.05	2.02	2.89	3.76	−17	99	0.8	4.41	6.01	7.66	0	1.1
0.06	6.84	9.78	12.7	−16	91	0.9	0.97	1.33	1.70	1	1.1
0.07	1.12	1.61	2.09	−14	84	1	1.84	2.54	3.26	1	1.1
0.08	1.12	1.60	2.08	−13	78	1.25	5.64	8.01	10.4	1	1.0
0.09	0.78	1.11	1.44	−12	73	1.5	1.25	1.78	2.34	2	1.0
0.10	4.09	5.85	7.61	−12	69	1.75	2.13	3.17	4.21	2	0.9
0.11	1.74	2.49	3.24	−11	65	2	3.21	4.84	6.46	2	0.9
0.12	6.27	8.96	11.7	−11	61	2.5	4.64	7.61	10.6	2	0.8
0.13	1.97	2.81	3.65	−10	58	3	0.59	1.05	1.50	3	0.7
0.14	5.50	7.86	10.2	−10	55	3.5	0.70	1.33	1.96	3	0.7
0.15	1.40	2.00	2.60	−9	53	4	0.80	1.61	2.43	3	0.7
0.16	3.28	4.69	6.10	−9	51	5	0.93	2.15	3.36	3	0.8
0.18	1.49	2.13	2.77	−8	44	6	1.03	2.66	4.28	3	0.9
0.2	5.52	7.90	10.3	−8	28	7	1.10	3.15	5.18	3	1.0
0.25	1.08	1.58	2.15	−6	3.1	8	1.16	3.63	6.08	3	1.2
0.3	2.57	3.82	5.34	−5	1.3	9	1.21	4.10	6.97	3	1.3
0.35	3.93	5.73	7.89	−4	1.1	10	1.25	4.58	7.88	3	1.6
0.4	3.22	4.61	6.23	−3	1.1						

Reaction: ^{9}Be(p,γ)^{10}B

The data from ZA95b are adopted. They cover the energy region from 65 to 1620 keV, and are in agreement with the data of HO64, AU75 and PA89. The data of ME59 are omitted due to discrepancies in the quoted partial cross sections. The narrow resonance at E_r = 974.2 keV ($\omega\gamma$ = 0.73 ± 0.10 eV) [FO49,HO53,MO56,BO64,HO64,ZA95b], not shown in the figure, has a negligible contribution to the rates. The reliability of the reaction rates below T_9 = 0.1 depends on the validity of the extrapolated value S_0 = 1 keV b proposed by ZA95b. This S_0 value is not supported by the data of CE92 (S_0 = 4.2 keV b), which indicate a constant S-factor below 150 keV. The reason for this discrepancy is not clear, and we adopted the data of ZA95b because they are in agreement with the rest of the existing data in the energy range of overlapping data. Between T_9 = 3.5 and 10, the rates are calculated by assuming that $S(E > 1.62$ MeV) has a constant value equal to the measured one at 1.62 MeV with 50% of uncertainty. The present reaction rates are about 2 to 5 times lower than the CA88 ones in the region $0.3 \leqslant T_9 \leqslant 2$. This is due to the use by CA88 of the ME59 data, which overestimate the contribution of the E_r = 296.8 keV resonance by similar factors.

T_9	low	adopt	high	exp	ratio	T_9	low	adopt	high	exp	ratio
0.003	2.93	4.03	5.13	−23	0.9	0.15	1.99	2.16	2.34	−1	0.8
0.004	1.75	2.39	3.03	−20	0.9	0.16	2.95	3.2	3.45	−1	0.8
0.005	1.64	2.23	2.82	−18	0.9	0.18	5.93	6.42	6.91	−1	0.8
0.006	5.25	7.07	8.9	−17	0.9	0.2	1.09	1.18	1.27	0	0.8
0.007	0.83	1.12	1.4	−15	0.9	0.25	3.79	4.08	4.38	0	0.7
0.008	0.81	1.09	1.36	−14	0.9	0.3	0.99	1.07	1.15	1	0.6
0.009	5.59	7.41	9.23	−14	0.9	0.35	2.14	2.31	2.47	1	0.5
0.01	2.94	3.87	4.81	−13	0.9	0.4	4	4.3	4.61	1	0.4
0.011	1.25	1.64	2.03	−12	0.9	0.45	6.66	7.16	7.67	1	0.3
0.012	4.51	5.9	7.28	−12	0.9	0.5	1.02	1.09	1.17	2	0.3

continued from previous page
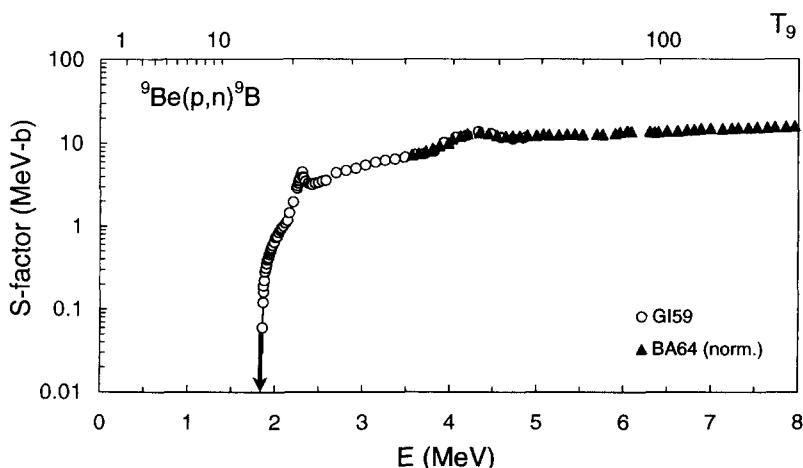
T_9	low	adopt	high	exp	ratio	T_9	low	adopt	high	exp	ratio
0.013	1.42	1.85	2.27	−11	0.9	0.6	1.96	2.11	2.27	2	0.2
0.014	4	5.18	6.35	−11	0.9	0.7	3.2	3.44	3.68	2	0.2
0.015	1.02	1.32	1.62	−10	0.9	0.8	4.68	5.04	5.39	2	0.2
0.016	2.41	3.1	3.79	−10	0.9	0.9	6.46	6.95	7.44	2	0.2
0.018	1.1	1.41	1.71	−9	0.9	1	8.55	9.2	9.84	2	0.2
0.02	4.09	5.17	6.26	−9	0.9	1.25	1.59	1.7	1.82	3	0.3
0.025	5.62	6.99	8.37	−8	0.9	1.5	2.73	2.92	3.12	3	0.4
0.03	4.15	5.08	6.02	−7	0.9	1.75	4.31	4.61	4.92	3	0.5
0.04	7.63	9.11	10.6	−6	0.9	2	6.31	6.75	7.18	3	0.6
0.05	6.04	7.05	8.07	−5	0.9	2.5	1.08	1.16	1.23	4	0.7
0.06	2.91	3.34	3.77	−4	0.9	3	1.53	1.64	1.75	4	0.8
0.07	1.02	1.15	1.29	−3	0.9	3.5	1.94	2.07	2.21	4	0.8
0.08	2.84	3.18	3.52	−3	0.9	4	2.29	2.46	2.62	4	0.8
0.09	6.75	7.5	8.24	−3	0.8	5	2.7	2.9	3.11	4	0.9
0.1	1.42	1.57	1.72	−2	0.8	6	2.92	3.15	3.38	4	0.9
0.11	2.73	2.99	3.26	−2	0.8	7	3.04	3.29	3.54	4	0.9
0.12	4.85	5.31	5.76	−2	0.8	8	3	3.26	3.52	4	0.9
0.13	8.14	8.88	9.62	−2	0.8	9	2.94	3.23	3.52	4	1.0
0.14	1.3	1.41	1.53	−1	0.8	10	2.93	3.24	3.55	4	1.0
T_9	low	adopt	high	exp	ratio	T_9	low	adopt	high	exp	ratio

Reaction: $^9\text{Be}(p,n)^9\text{B}$
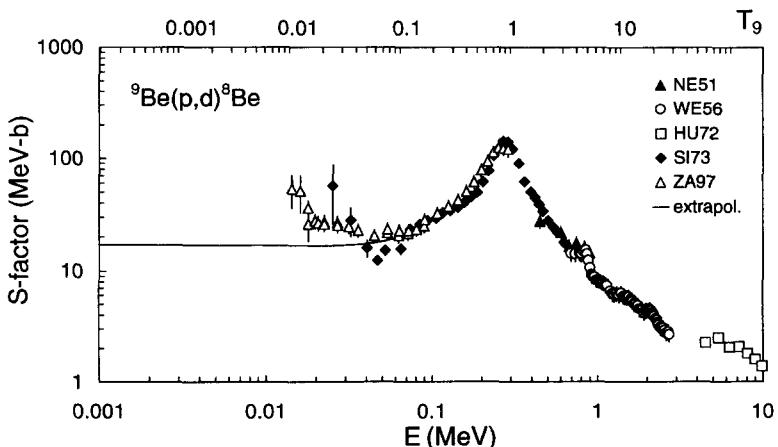
The experimental data from GI59 are used from threshold ($Q = -1.851$ MeV) to $E = 3.5$ MeV. For $E \geqslant 4.8$ MeV, the relative yield data of BA64 are adopted, after normalization to the value $\sigma = 0.511$ b at $E = 4.33$ MeV from GI59. In the intermediate region, the χ^2 average of both data sets is adopted. In GI59, the total error is 5%, and includes uncertainties in detector efficiency and target thickness. In BA64, the corresponding error is 8%. The recommended reaction rates are in good agreement with the CA88 ones.

T_9	low	adopt	high	exp	ratio	T_9	low	adopt	high	exp	ratio
0.3	5.49	5.84	6.07	−24	1.0	1.75	7.03	7.40	7.77	2	0.9
0.35	1.58	1.68	1.75	−19	1.0	2	3.59	3.78	3.97	3	0.9
0.4	3.52	3.73	3.89	−16	1.0	2.5	3.61	3.80	3.99	4	0.9
0.45	1.42	1.50	1.57	−13	1.0	3	1.71	1.81	1.90	5	0.9
0.5	1.72	1.82	1.91	−11	1.0	3.5	5.30	5.58	5.86	5	0.9
0.6	2.34	2.48	2.59	−8	1.0	4	1.25	1.32	1.38	6	0.9
0.7	4.11	4.34	4.55	−6	0.9	5	4.26	4.50	4.74	6	0.9
0.8	2.01	2.13	2.23	−4	0.9	6	0.99	1.05	1.11	7	0.9
0.9	4.21	4.44	4.65	−3	0.9	7	1.85	1.95	2.07	7	0.9
1	4.84	5.11	5.36	−2	0.9	8	2.98	3.16	3.34	7	0.9
1.25	4.08	4.30	4.52	0	0.9	9	4.35	4.62	4.90	7	0.9
1.5	8.13	8.56	8.99	1	0.9	10	5.93	6.30	6.70	7	0.9

Reaction: ^{9}Be(p,d)^{8}Be

For the (p,d$_0$) channel, the data of SI73 and ZA97 are adopted below $E = 0.63$ MeV. The S-factor quoted in SI73 refers to the combined (p,d$_0$) and (p,α_0) reactions, its adopted values being a weighted average of the corresponding cross sections. Between $E = 0.67$ and 2.7 MeV, the data of NE51 and WE56 are adopted, while the data of HU72 are used between $E = 4.4$ MeV and 9.8 MeV. The low energy extrapolation ($E \leqslant 0.07$ MeV) is made assuming a constant S-factor, based on the S_0 value of SI73, $S_0 = 17^{+25}_{-7}$ MeV b. However, it should be pointed out that the low energy data from ZA97 show an enhancement that cannot be explained only by electron screening, but no clear explanation is given in ZA97. We have calculated the contribution of several subthreshold states in ^{10}B, but none of them is sufficiently important to explain the enhancement. Therefore, we follow SI73 for the extrapolation. The adopted reaction rates are in good agreement with the CA88 ones, except at the highest temperatures. This is probably due to the fact that CA88 did not use the high energy data adopted in the present compilation. The differences around $T_9 = 0.25$ reflect differences between our numerical integrations and the CA88 analytical approximation.
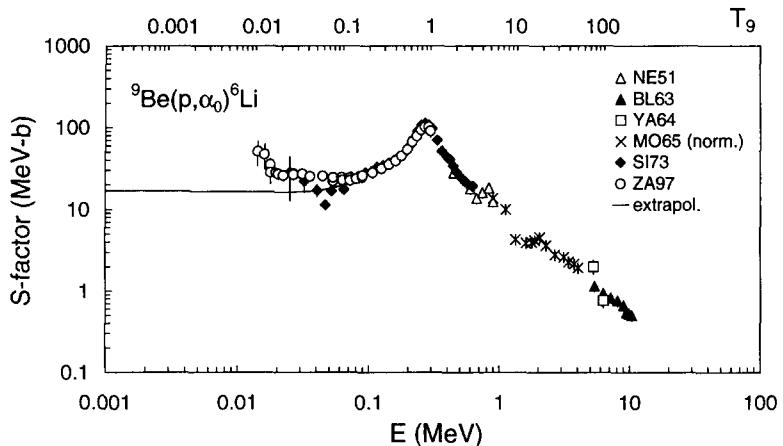
T_9	low	adopt	high	exp	ratio	T_9	low	adopt	high	exp	ratio
0.002	1.52	2.67	7.30	−23	1.0	0.15	3.64	4.20	4.66	3	1.0
0.003	3.77	6.66	17.8	−19	1.0	0.16	5.57	6.36	7.03	3	1.1
0.004	2.20	3.92	10.3	−16	1.0	0.18	1.19	1.34	1.46	4	1.1
0.005	2.03	3.63	9.32	−14	1.0	0.2	2.31	2.55	2.78	4	1.2
0.006	0.63	1.14	2.88	−12	1.0	0.25	8.86	9.62	10.4	4	1.2
0.007	0.99	1.80	4.44	−11	1.0	0.3	2.52	2.71	2.90	5	1.1
0.008	0.95	1.73	4.22	−10	1.0	0.35	5.81	6.22	6.62	5	1.0
0.009	0.64	1.18	2.81	−9	1.0	0.4	1.14	1.22	1.30	6	1.0
0.01	3.31	6.12	14.4	−9	1.0	0.45	1.99	2.12	2.25	6	0.9
0.011	1.39	2.58	5.96	−8	1.0	0.5	3.14	3.34	3.55	6	0.9
0.012	4.94	9.22	21.0	−8	1.0	0.6	6.38	6.79	7.19	6	0.9
0.013	1.53	2.88	6.43	−7	0.9	0.7	1.07	1.14	1.21	7	0.9
0.014	4.26	8.02	17.6	−7	0.9	0.8	1.58	1.68	1.79	7	0.9
0.015	1.08	2.04	4.40	−6	0.9	0.9	2.15	2.28	2.42	7	0.9
0.016	2.51	4.77	10.2	−6	0.9	1	2.73	2.91	3.09	7	0.9
0.018	1.12	2.15	4.43	−5	0.9	1.25	4.20	4.49	4.77	7	0.9
0.02	4.09	7.84	15.7	−5	0.9	1.5	5.55	5.95	6.35	7	0.9
0.025	0.55	1.05	1.96	−3	0.9	1.75	6.73	7.24	7.75	7	0.9
0.03	4.00	7.56	13.3	−3	0.9	2	7.75	8.37	8.99	7	0.9
0.04	0.74	1.35	2.13	−1	0.9	2.5	0.94	1.02	1.10	8	0.9
0.05	0.61	1.05	1.51	0	0.9	3	1.05	1.15	1.26	8	0.9
0.06	3.12	5.04	6.77	0	0.9	3.5	1.14	1.26	1.38	8	1.0
0.07	1.17	1.78	2.26	1	0.9	4	1.21	1.34	1.47	8	1.0
0.08	3.52	5.04	6.17	1	0.9	5	1.30	1.45	1.61	8	1.0
0.09	0.90	1.23	1.46	2	0.9	6	1.35	1.53	1.70	8	1.1
0.1	2.02	2.64	3.08	2	0.9	7	1.39	1.58	1.76	8	1.1
0.11	4.13	5.20	5.97	2	1.0	8	1.42	1.61	1.80	8	1.2
0.12	7.76	9.51	10.8	2	1.0	9	1.43	1.63	1.83	8	1.2
0.13	1.37	1.64	1.84	3	1.0	10	1.44	1.65	1.85	8	1.3
0.14	2.28	2.68	2.99	3	1.0						

Reaction: ^{9}Be(p,α)^{6}Li

For the (p,α_0) channel, the data of SI73 and ZA97 are adopted for $E \leqslant 0.63$ MeV. The S-factor quoted in SI73 refers to the combined (p,d_0) and (p,α_0) reactions, its adopted values being a weighted average of the corresponding cross sections. Between $E = 0.67$ and 0.9 MeV, the NE51 data are used, renormalized by a factor 1.1, derived from the average of WE56 and the differential cross section measured at 98.5° by TH49. Between $E = 0.9$ and 4 MeV, the relative data of MO65 are used, normalized to the adopted value for the cross section at 0.899 MeV. For energies above 5 MeV, the data of BL63 and YA64 are selected. For the (p,α_2) channel, the data of DA52 and the relative values of MA59 (normalized to DA52) are adopted. The energies of MA59 are corrected for the target thickness. The low energy S-factor is assumed to be constant, based on the $\mathcal{S}_0$ factor of SI73, $\mathcal{S}_0 = 17^{+25}_{-7}$ MeV b. However, ZA97 point out that the low energy data show an enhancement that cannot be explained only by electron screening, but no clear explanation is given in ZA97. We have calculated the contribution of several subthreshold states in ^{10}B, but none of them is sufficiently important to explain the enhancement. Therefore, we follow SI73 for the extrapolation [see also ^{9}Be(p,d)^{8}Be]. The adopted reaction rates are in good agreement with the CA88 ones, except at the
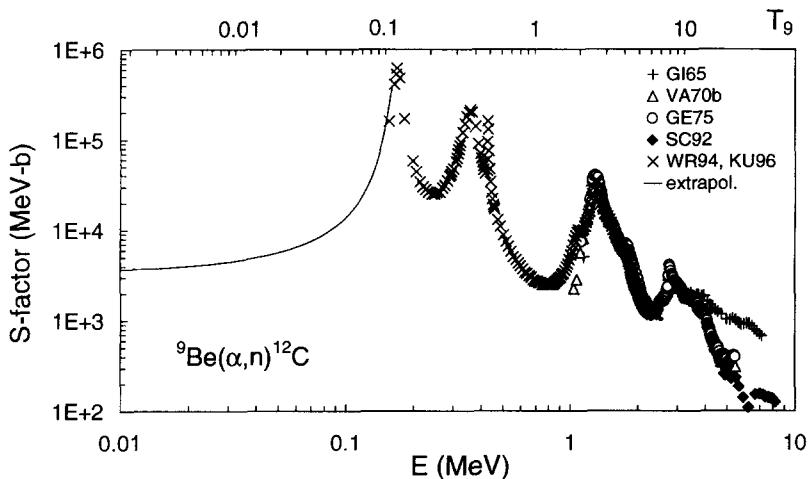
highest temperatures. This is probably due to the fact that CA88 did not use the high-energy data adopted in the present compilation. The differences around $T_9 = 0.25$ reflect differences between our numerical integrations and the CA88 analytical approximation.


T_9	low	adopt	high	exp	ratio	T_9	low	adopt	high	exp	ratio
0.002	1.52	2.56	7.30	−23	1.0	0.15	3.63	4.18	4.66	3	1.0
0.003	3.77	6.39	17.8	−19	1.0	0.16	5.56	6.33	7.01	3	1.1
0.004	2.20	3.76	10.3	−16	1.0	0.18	1.18	1.33	1.45	4	1.1
0.005	2.02	3.49	9.32	−14	1.0	0.2	2.28	2.52	2.75	4	1.1
0.006	0.63	1.10	2.88	−12	0.9	0.25	8.59	9.33	10.1	4	1.2
0.007	0.99	1.73	4.44	−11	0.9	0.3	2.38	2.57	2.75	5	1.2
0.008	0.95	1.67	4.22	−10	0.9	0.35	5.36	5.74	6.12	5	1.1
0.009	0.64	1.14	2.81	−9	0.9	0.4	1.03	1.10	1.17	6	1.0
0.01	3.31	5.91	14.4	−8	0.9	0.45	1.77	1.88	2.00	6	1.0
0.011	1.39	2.50	5.96	−8	0.9	0.5	2.75	2.93	3.11	6	0.9
0.012	4.93	8.93	21.0	−8	0.9	0.6	5.50	5.85	6.20	6	0.9
0.013	1.53	2.79	6.43	−7	0.9	0.7	9.13	9.71	10.3	6	0.9
0.014	4.25	7.78	17.6	−7	0.9	0.8	1.34	1.43	1.52	7	0.9
0.015	1.07	1.97	4.40	−6	0.9	0.9	1.82	1.93	2.05	7	0.9
0.016	2.50	4.63	10.2	−6	0.9	1	2.31	2.47	2.62	7	0.9
0.018	1.12	2.09	4.43	−5	0.9	1.25	3.58	3.83	4.08	7	0.9
0.02	4.08	7.61	15.7	−5	0.9	1.5	4.79	5.15	5.51	7	0.9
0.025	0.55	1.02	1.96	−3	0.9	1.75	5.91	6.38	6.85	7	0.9
0.03	3.99	7.34	13.3	−3	0.9	2	6.91	7.50	8.09	7	1.0
0.04	0.74	1.31	2.13	−1	0.9	2.5	8.61	9.43	10.3	7	1.0
0.05	0.61	1.02	1.51	0	0.9	3	0.99	1.10	1.20	8	1.0
0.06	3.12	4.93	6.77	0	0.9	3.5	1.10	1.22	1.34	8	1.1
0.07	1.17	1.74	2.26	1	0.9	4	1.18	1.32	1.46	8	1.1
0.08	3.52	4.97	6.17	1	0.9	5	1.29	1.46	1.62	8	1.2
0.09	0.90	1.21	1.46	2	0.9	6	1.36	1.55	1.73	8	1.3
0.1	2.02	2.62	3.08	2	0.9	7	1.41	1.61	1.81	8	1.4
0.11	4.12	5.17	5.97	2	0.9	8	1.45	1.65	1.86	8	1.4
0.12	7.76	9.46	10.8	2	1.0	9	1.47	1.68	1.90	8	1.5
0.13	1.37	1.63	1.84	3	1.0	10	1.48	1.70	1.93	8	1.6
0.14	2.28	2.67	2.99	3	1.0						

Reaction: $^9\text{Be}(\alpha,\text{n})^{12}\text{C}$

The reaction rate is determined using the experimental cross sections of GI65, VA70b, GE75, SC92, WR94 and KU96. In the energy range $E \leqslant 0.254$ MeV, data of WR94 for the $E_r = 166$ keV resonance are used. Tails from resonances at higher energies are also taken into account. The width of the resonance at $E_r = 106$ keV is adopted from CI80, and the upper limit in its strength is estimated by the Wigner limit. This strength is multiplied by 0.1 in order to obtain the extrapolation to zero energy and the recommended rate. The lower limit of the rates is calculated by neglecting this resonance. For the $0.254 \leqslant E \leqslant 2.5$ MeV range, the data of GE75, WR94 and KU96 are used. The data of VA70b are omitted because they deviate from these data sets at low energies ($E < 1.5$ MeV). Even the resonance at $E_r = 1.085$ MeV, which has a clear signature, is not observed in the VA70b data. For $2.5 \leqslant E \leqslant 4.86$ MeV, the VA70b and GE75 data are used. These two sets are in agreement within experimental errors. For $4.86 \leqslant E \leqslant 10.87$ MeV, the SC92 data are used. The uncertainty on the reaction rate is evaluated from the experimental uncertainties, except for the $E_r = 166$ keV resonance, which is treated as described above. The large difference between our rates and the CA88 ones near $T_9 \approx 0.15$ arises probably from the underestimate by CA88 of the 166 keV resonance contribution.
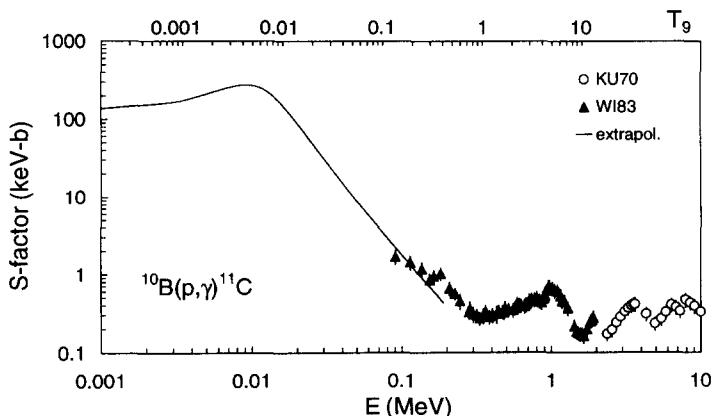
T_9	low	adopt	high	exp	ratio	T_9	low	adopt	high	exp	ratio
0.018	2.58	3.98	16.6	−25	1.2	0.4	1.11	1.24	1.38	1	0.9
0.02	5.85	9.23	39.7	−24	1.3	0.45	3.00	3.35	3.70	1	0.9
0.025	3.12	5.27	24.6	−21	1.5	0.5	6.67	7.43	8.21	1	0.9
0.03	3.88	7.04	35.5	−19	1.5	0.6	2.23	2.49	2.74	2	1.0
0.04	4.90	9.74	53.3	−16	0.6	0.7	5.40	6.01	6.62	2	1.1
0.05	0.98	1.78	8.93	−13	0.5	0.8	1.09	1.21	1.33	3	1.2
0.06	0.77	1.09	4.04	−11	0.7	0.9	2.01	2.24	2.46	3	1.4
0.07	2.88	3.43	8.40	−10	1.4	1	3.61	4.02	4.44	3	1.5

continued from previous page

T_9	low	adopt	high	exp	ratio	T_9	low	adopt	high	exp	ratio
0.08	5.39	5.91	10.6	−9	2.5	1.25	1.55	1.74	1.93	4	1.4
0.09	5.72	6.04	8.90	−8	3.5	1.5	5.75	6.47	7.20	4	1.2
0.1	3.91	4.06	5.37	−7	4.3	1.75	1.64	1.86	2.07	5	1.1
0.11	1.92	1.97	2.46	−6	4.9	2	3.75	4.25	4.74	5	1.0
0.12	7.31	7.48	8.98	−6	5.5	2.5	1.22	1.38	1.55	6	0.9
0.13	2.29	2.34	2.75	−5	6.1	3	2.69	3.06	3.42	6	0.9
0.14	6.16	6.29	7.30	−5	6.7	3.5	4.76	5.40	6.04	6	0.9
0.15	1.48	1.51	1.74	−4	7.1	4	7.35	8.33	9.30	6	0.8
0.16	3.23	3.32	3.81	−4	7.1	5	1.38	1.56	1.74	7	0.8
0.18	1.30	1.35	1.55	−3	5.4	6	2.17	2.44	2.71	7	0.9
0.2	4.52	4.81	5.48	−3	3.3	7	3.06	3.43	3.79	7	0.9
0.25	7.01	7.73	8.72	−2	1.4	8	4.01	4.48	4.94	7	0.9
0.3	6.10	6.79	7.59	−1	1.0	9	4.99	5.55	6.11	7	1.0
0.35	3.15	3.52	3.91	0	0.9	10	5.95	6.60	7.26	7	1.0
T_9	low	adopt	high	exp	ratio	T_9	low	adopt	high	exp	ratio

Reaction: ^{10}B(p,γ)^{11}C

The experimental data from KU70 and WI83 are adopted. They cover the reaction rate region from $T_9 = 0.15$ to 10. For $T_9 < 0.15$, the reaction rates are influenced by a low energy resonance ($\ell = 0$) resonance at $E_r = (9 \pm 2)$ keV [WI83] [see also ^{10}B(p,α)^{7}Be]. For $E < 0.09$ MeV, the S-factor is approximated by a Breit–Wigner expression using the parameters of the 9 keV resonance given by WI83, ($\sigma_r = (2.07 \pm 0.40) \times 10^{-14}$ μb, $\Gamma_\gamma/\Gamma_{tot} = (2.6 \pm 0.15) \times 10^{-4}$ and $\Gamma_{tot} = 15 \pm 1$ keV). From these parameters we obtain $\Gamma_p = (1.0 \pm 0.2) \times 10^{-17}$ keV and $\Gamma_\gamma = (3.9 \pm 0.3) \times 10^{-3}$ keV. We have studied the influence of the energy error by calculating the reduced width γ^2 corresponding to an energy of 9 keV, and the S-factor curves for 7 and 11 keV and this γ^2. The error of σ_r, $\Gamma_\gamma/\Gamma_{tot}$ and Γ_{tot} is also added. The results show that the uncertainty in the rates is large at temperatures below 0.001, but for $T_9 \geqslant 0.003$ and in the region of the Breit–Wigner approximation, the error is not larger than 30%. The large differences between the adopted rates and the CA88 ones at low temperatures are mainly due to the contribution of this low energy resonance, which is not included in CA88.
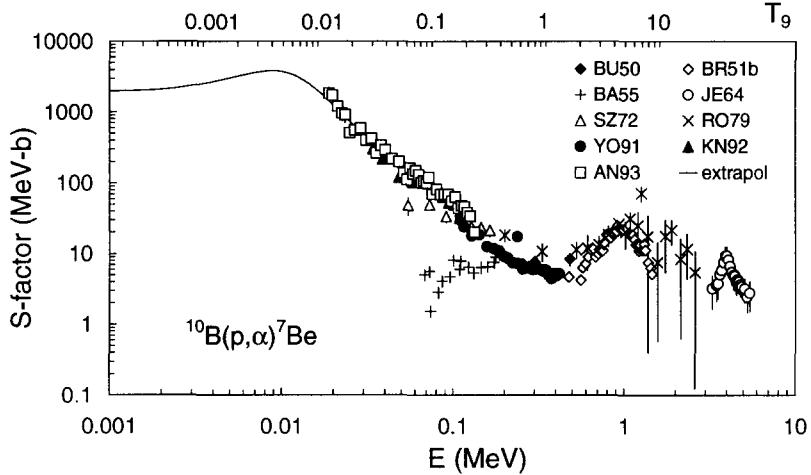
T_9	low	adopt	high	exp	ratio	T_9	low	adopt	high	exp	ratio
0.16	1.58	2.00	2.47	−2	48	0.004	1.14	1.45	1.87	−22	7800
0.18	2.99	3.78	4.64	−2	41	0.005	2.21	2.81	3.59	−20	7500
0.2	5.20	6.55	8.02	−2	36	0.006	1.16	1.47	1.87	−18	6900
0.25	1.58	1.98	2.40	−1	28	0.007	2.61	3.31	4.20	−17	6200
0.3	3.65	4.57	5.51	−1	23	0.008	3.29	4.17	5.29	−16	5500
0.35	7.03	8.79	10.6	−1	19	0.009	2.74	3.46	4.38	−15	4800
0.4	1.19	1.49	1.79	0	16	0.01	1.66	2.10	2.66	−14	4200
0.45	1.85	2.31	2.77	0	14	0.011	7.90	9.98	12.6	−14	3700
0.5	2.69	3.36	4.03	0	12	0.012	3.11	3.93	4.97	−13	3300
0.6	4.98	6.22	7.46	0	9.9	0.013	1.05	1.32	1.68	−12	2900
0.7	0.82	1.03	1.23	1	8.3	0.014	3.12	3.94	4.99	−12	2600
0.8	1.26	1.58	1.89	1	7.1	0.015	0.83	1.05	1.34	−11	2300
0.9	1.84	2.30	2.76	1	6.1	0.016	2.04	2.58	3.27	−11	2100
1	2.57	3.21	3.86	1	5.2	0.018	0.99	1.24	1.58	−10	1700
1.25	5.22	6.53	7.84	1	3.2	0.02	3.78	4.77	6.06	−10	1500
1.5	0.92	1.15	1.38	2	2.1	0.025	5.42	6.86	8.72	−9	1000
1.75	1.45	1.81	2.17	2	1.5	0.03	4.03	5.11	6.49	−8	730
2	2.10	2.62	3.15	2	1.2	0.04	7.20	9.13	11.6	−7	450
2.5	3.67	4.58	5.50	2	0.9	0.05	5.41	6.87	8.76	−6	310
3	5.43	6.78	8.13	2	0.8	0.06	2.47	3.14	4.00	−5	230
3.5	7.25	9.05	10.9	2	0.8	0.07	0.82	1.04	1.32	−4	180
4	0.91	1.13	1.36	3	0.8	0.08	2.16	2.74	3.49	−4	140
5	1.25	1.56	1.87	3	0.8	0.09	4.86	6.18	7.84	−4	120
6	1.58	1.98	2.37	3	1.0	0.1	0.97	1.24	1.56	−3	98
7	1.91	2.38	2.86	3	1.1	0.11	1.77	2.25	2.84	−3	84
8	2.23	2.79	3.34	3	1.3	0.12	3.02	3.83	4.82	−3	73
9	2.56	3.19	3.83	3	1.6	0.13	4.85	6.16	7.71	−3	65
10	2.88	3.60	4.31	3	1.9	0.14	7.45	9.45	11.8	−3	58
0.15	1.10	1.40	1.74	-2	52						

Reaction: ^{10}B(p,α)^{7}Be

The experimental data from BU50, BR51b, JE64, SZ72, RO79, YO91, KN93 and AN93 are used. The thick target yields from RO79 are converted into cross section data using stopping power information [ZI85]. The data from BA55a are in strong disagreement with the other low energy data, and are omitted. The S-factor shows a steep increase with decreasing energy due to the presence of a low energy ($\ell = 0$) resonance at $E_r = (9 \pm 2)$ keV [WI83]. This resonance dominates the S-factor up to an energy of about 400 keV [see also ^{10}B(p,γ)^{11}C]. From the parameters $\sigma_r = (2.07 \pm 0.40) \times 10^{-14}$ μb, $\Gamma_\gamma/\Gamma_{tot} = (2.6 \pm 0.15) \times 10^{-4}$ and $\Gamma_{tot} = 15 \pm 1$ keV [WI83], we obtain $\Gamma_p = (1.0 \pm 0.2) \times 10^{-17}$ keV ($\Gamma_\alpha \simeq \Gamma_{tot}$). For $E < 18.7$ keV, the S-factor is approximated by a Breit–Wigner expression using these parameters. We have studied the influence of the energy error by calculating the reduced width γ^2 corresponding to an energy of 9 keV, and the S-factor curves for 7 and 11 keV and this γ^2. The error of σ_r, $\Gamma_\gamma/\Gamma_{tot}$ and Γ_{tot} is also added. The results show that the uncertainty in the rates is large at temperatures below 0.001, but for $T_9 \geqslant 0.003$ and in the region of the Breit–Wigner approximation, the error is not larger than 30%. At higher energies, a broad resonant structure dominates the S-factor. The reaction rates are
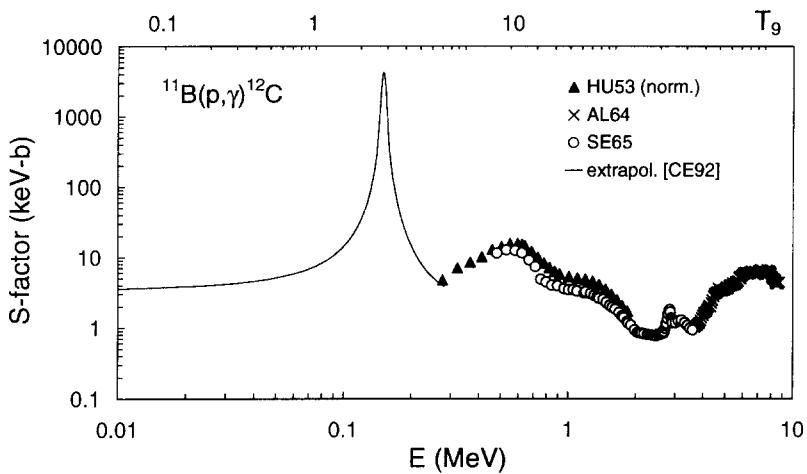
calculated by interpolating linearly the data points. The large differences between the adopted rates and the CA88 ones at low temperatures are due to the contribution of the 10 keV resonance, which is not included in CA88.

T_9	low	adopt	high	exp	ratio	T_9	low	adopt	high	exp	ratio
0.003	0.96	1.25	1.53	−21	430	0.15	3.23	3.56	3.89	2	6.5
0.004	1.72	2.23	2.74	−18	450	0.16	4.55	5.02	5.50	2	5.9
0.005	3.30	4.29	5.27	−16	430	0.18	8.45	9.37	10.3	2	5.1
0.006	1.72	2.23	2.75	−14	400	0.2	1.42	1.57	1.73	3	4.4
0.007	3.86	5.01	6.16	−13	360	0.25	3.99	4.44	4.89	3	3.4
0.008	4.85	6.30	7.74	−12	320	0.3	8.49	9.44	10.4	3	2.7
0.009	4.04	5.24	6.43	−11	280	0.35	1.47	1.64	1.81	4	2.1
0.01	2.47	3.19	3.91	−10	250	0.4	2.53	2.81	3.10	4	1.9
0.011	1.18	1.52	1.86	−9	220	0.45	3.78	4.22	4.66	4	1.6
0.012	4.70	6.02	7.34	−9	195	0.5	5.58	6.23	6.87	4	1.5
0.013	1.59	2.02	2.46	−8	170	0.6	1.03	1.17	1.30	5	1.3
0.014	4.73	5.98	7.23	−8	155	0.7	1.71	1.98	2.24	5	1.2
0.015	1.27	1.59	1.91	−7	140	0.8	2.64	3.13	3.61	5	1.1
0.016	3.08	3.84	4.59	−7	120	0.9	4.03	4.92	5.82	5	1.1
0.018	1.50	1.83	2.16	−6	100	1	5.69	7.15	8.61	5	1.1
0.02	5.78	6.94	8.09	−6	83	1.25	1.29	1.71	2.14	6	1.2
0.025	8.61	9.97	11.3	−5	58	1.5	2.44	3.35	4.26	6	1.1
0.03	6.70	7.60	8.50	−4	44	1.75	4.22	5.91	7.59	6	1.1
0.04	1.29	1.43	1.58	−2	29	2	6.54	9.35	12.2	6	1.1
0.05	1.06	1.17	1.29	−1	22	2.5	1.26	1.87	2.47	7	1.0
0.06	5.18	5.70	6.23	−1	18	3	2.00	3.06	4.12	7	0.9
0.07	1.84	2.03	2.21	0	15	3.5	2.75	4.35	5.96	7	0.9
0.08	5.28	5.79	6.31	0	13	4	3.50	5.73	7.95	7	0.9
0.09	1.24	1.36	1.48	1	12	5	4.80	8.29	11.8	7	0.9
0.1	2.52	2.76	3.00	1	10	6	0.58	1.05	1.51	8	1.1
0.11	4.88	5.36	5.83	1	9.2	7	0.65	1.23	1.80	8	1.2
0.12	8.63	9.48	10.3	1	8.4	8	0.70	1.36	2.01	8	1.4
0.13	1.41	1.54	1.68	2	7.7	9	0.79	1.52	2.25	8	1.7
0.14	2.16	2.38	2.60	2	7.0	10	0.85	1.63	2.42	8	2.0

Reaction: ^{11}B(p,γ)^{12}C

The experimental data of AL64 and SE65 are used for $E \geqslant 481$ keV. Below $E = 481$ keV, the data of HU53 normalized to $\sigma = 45$ μb at $E = 623$ keV [SE65] and a linear extrapolation to the S_0 value determined by direct capture calculations from CE92 are used ($S_0 = 3.3 \pm 0.5$ keV b). The 149 keV resonance ($J^\pi = 2^+$) is also included. The adopted resonance strength is the averaged value of HU53 and AN74 ($\omega\gamma = 0.0393 \pm 0.0056$ eV). The derived reaction rates are lower than the CA88 ones for most considered temperatures. This is due mainly to the adoption by CA88 of the HU53 data, which are higher than the presently adopted values.
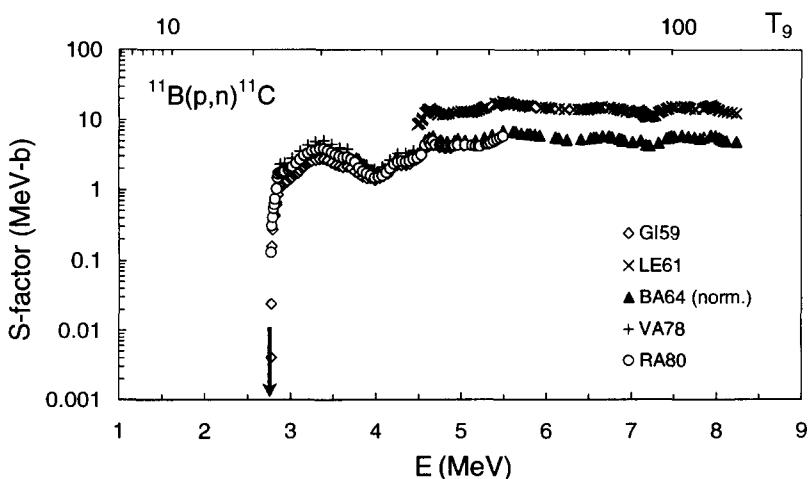

T_9	low	adopt	high	exp	ratio	T_9	low	adopt	high	exp	ratio
0.004	1.23	1.45	1.67	−24	0.9	0.16	1.73	2.07	2.40	0	0.8
0.005	2.48	2.92	3.36	−22	0.9	0.18	4.83	5.77	6.70	0	0.8
0.006	1.37	1.61	1.85	−20	0.8	0.2	1.08	1.29	1.50	1	0.8
0.007	3.63	4.28	4.93	−19	0.9	0.25	4.40	5.25	6.10	1	0.8
0.008	5.28	6.22	7.17	−18	0.9	0.3	1.07	1.28	1.48	2	0.9
0.009	5.00	5.89	6.78	−17	0.9	0.35	1.95	2.32	2.70	2	0.9
0.01	3.46	4.07	4.69	−16	0.8	0.4	2.98	3.56	4.13	2	0.9
0.011	1.88	2.21	2.55	−15	0.8	0.45	4.08	4.87	5.65	2	0.9
0.012	8.39	9.89	11.4	−15	0.8	0.5	5.18	6.18	7.17	2	0.9
0.013	3.20	3.77	4.34	−14	0.8	0.6	7.27	8.66	10.1	2	0.9
0.014	1.07	1.26	1.45	−13	0.8	0.7	0.92	1.09	1.27	3	0.9
0.015	3.20	3.77	4.34	−13	0.8	0.8	1.10	1.31	1.52	3	1.0
0.016	0.87	1.03	1.18	−12	0.8	0.9	1.29	1.53	1.77	3	1.0
0.018	5.11	6.02	6.94	−12	0.8	1	1.50	1.77	2.04	3	1.0
0.02	2.35	2.76	3.18	−11	0.8	1.25	2.12	2.47	2.82	3	1.0
0.025	4.94	5.82	6.70	−10	0.7	1.5	2.89	3.33	3.78	3	1.0
0.03	5.03	5.92	6.82	−9	0.7	1.75	3.77	4.31	4.85	3	0.9
0.04	1.46	1.72	1.98	−7	0.7	2	4.70	5.35	5.99	3	0.9
0.05	1.60	1.88	2.17	−6	0.6	2.5	6.59	7.44	8.30	3	0.8
0.06	0.99	1.17	1.35	−5	0.6	3	8.38	9.42	10.5	3	0.7

T_9	low	adopt	high	exp	ratio	T_9	low	adopt	high	exp	ratio
0.07	4.68	5.52	6.36	−5	0.6	3.5	1.00	1.12	1.24	4	0.7
0.08	2.29	2.72	3.14	−4	0.6	4	1.14	1.28	1.42	4	0.7
0.09	1.24	1.47	1.70	−3	0.7	5	1.38	1.54	1.70	4	0.7
0.1	5.97	7.11	8.25	−3	0.8	6	1.57	1.75	1.93	4	0.7
0.11	2.33	2.78	3.22	−2	0.8	7	1.74	1.94	2.14	4	0.7
0.12	7.38	8.79	10.2	−2	0.8	8	1.90	2.12	2.34	4	0.7
0.13	1.96	2.34	2.72	−1	0.8	9	2.08	2.32	2.56	4	0.7
0.14	4.52	5.39	6.26	−1	0.8	10	2.29	2.54	2.80	4	0.7
0.15	0.93	1.11	1.29	0	0.8						
T_9	low	adopt	high	exp	ratio	T_9	low	adopt	high	exp	ratio

Reaction: $^{11}B(p,n)^{11}C$
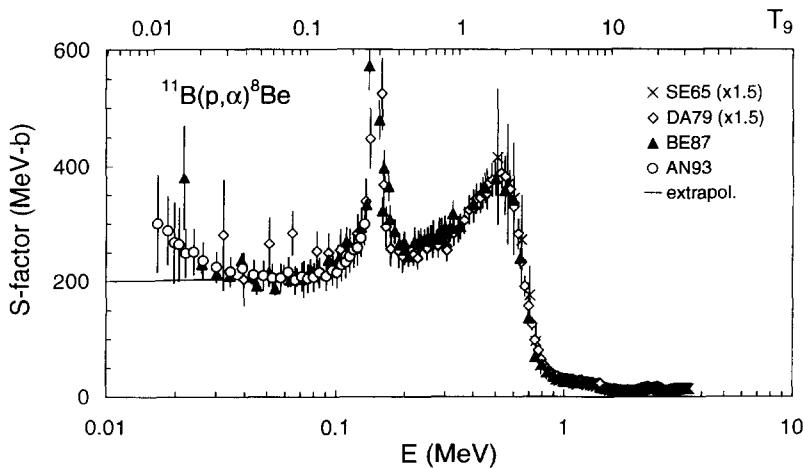
From the threshold ($Q = -2.765$ MeV) to $E = 3.4$ MeV, the data of VA78 and RA80 are used, normalized to their averaged value of $\sigma = 100 \pm 10$ mb at $E = 3.3$ MeV. These renormalized data are in excellent agreement with the thick target yield data of BA81, which are not used here. Above $E = 3.4$ MeV, the data of LE61 and BA64 are used, normalized to $\sigma = 137$ mb at $E = 4.7$ MeV from VA78 and RA80. The GI59 data are not included, since the authors warned against the quality of the used target. The available experimental data are complete for the calculation of the reaction rates. The recommended reaction rates are larger than the CA88 ones. This may come from the adoption by CA88 of the GI59 data, which are lower than the adopted values by a factor of 2, but no clear statement can be set.

| T_9	low	adopt	high	exp	ratio	T_9	low	adopt	high	exp	ratio
0.45	1.75	1.95	2.14	−23	1.1	2.5	6.86	7.62	8.38	2	1.8
0.5	2.30	2.56	2.82	−20	1.1	3	5.87	6.53	7.18	3	1.8
0.6	1.10	1.22	1.35	−15	1.2	3.5	2.71	3.01	3.31	4	1.8
0.7	2.42	2.69	2.96	−12	1.3	4	8.47	9.41	10.4	4	1.8
0.8	7.79	8.66	9.53	−10	1.4	5	4.17	4.63	5.09	5	1.8
0.9	6.95	7.73	8.50	−8	1.4	6	1.21	1.34	1.47	6	1.8
1	2.53	2.81	3.09	−6	1.5	7	2.59	2.87	3.16	6	1.8
1.25	1.64	1.82	2.00	−3	1.6	8	4.61	5.12	5.63	6	1.8
1.5	1.23	1.36	1.50	−1	1.6	9	7.24	8.05	8.85	6	1.8
1.75	2.68	2.98	3.28	0	1.7	10	1.04	1.16	1.27	7	1.8
2	2.71	3.01	3.31	1	1.7						

Reaction: ^{11}B$(p,\alpha)2^4$He
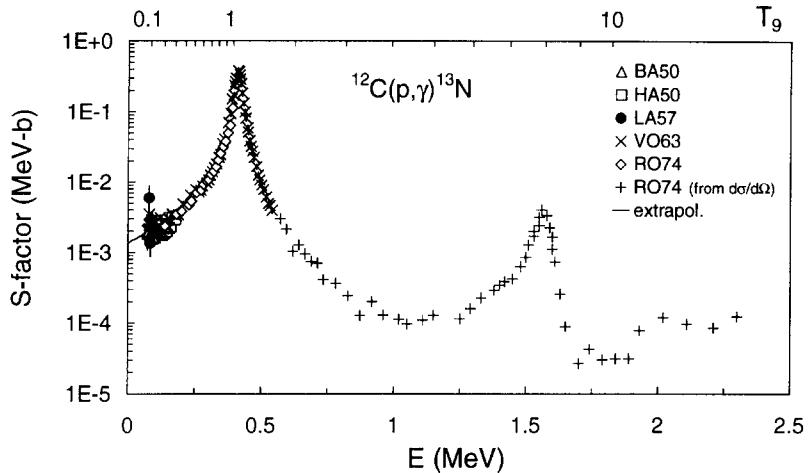
Experimental data from BE87 and AN93 are used for the calculation of the adopted rates and their upper limits. This follows the recommendation of BE87, who show that the reaction proceeds predominantly by a sequential decay, so that the observed yields should be divided by 2 and not by 3, as in SE65 and DA79. The original data from SE65 and DA79 are used for obtaining the lower limits of the rates. The S-factor is dominated by a broad resonance structure near 600 keV. A narrow resonance at $E_r = 148.6 \pm 0.4$ keV [AN74,DA79,BE87] is superimposed to this structure (adopted resonance strength $\omega\gamma = 14 \pm 2$ eV [SE61,AN74,DA79]). For the calculation of the reaction rates, data at $E < 60$ keV are corrected for electron screening with $U_e = 430$ eV [BE87,AN93]. For the low energy extrapolation, the recommended "bare" nuclei curve ($S_0 = 187 \pm 30$ MeV b) from AN93 is adopted. Our adopted rates are within about 20% of the CA88 ones at $T_9 < 5$. CA88 used probably the original SE65 and DA79 data sets, and extrapolated to zero energy. The differences are larger at higher T_9.

| T_9	low	adopt	high	exp	ratio	T_9	low	adopt	high	exp	ratio
0.003	3.57	4.90	5.15	−23	1.2	0.15	1.15	1.91	2.41	3	1.1
0.004	6.25	8.68	9.12	−20	1.2	0.16	1.84	3.12	4.00	3	1.1
0.005	1.26	1.77	1.86	−17	1.2	0.18	4.20	7.36	9.64	3	1.0
0.006	0.72	1.01	1.07	−15	1.2	0.2	0.85	1.51	2.00	4	1.0
0.007	1.80	2.57	2.70	−14	1.2	0.25	3.27	5.95	7.87	4	1.0
0.008	2.57	3.69	3.88	−13	1.2	0.3	0.87	1.60	2.07	5	1.0
0.009	2.42	3.51	3.69	−12	1.2	0.35	1.89	3.42	4.30	5	1.1
0.01	1.67	2.43	2.56	−11	1.2	0.4	3.55	6.36	7.79	5	1.2
0.011	0.90	1.32	1.39	−10	1.2	0.45	0.61	1.08	1.29	6	1.2
0.012	4.00	5.91	6.22	−10	1.2	0.5	0.98	1.70	2.00	6	1.2
0.013	1.51	2.26	2.37	−9	1.2	0.6	2.12	3.66	4.16	6	1.2
0.014	5.02	7.54	7.93	−9	1.2	0.7	3.96	6.76	7.54	6	1.2
0.015	1.49	2.25	2.37	−8	1.2	0.8	0.66	1.12	1.23	7	1.1
0.016	4.03	6.14	6.46	−8	1.2	0.9	1.01	1.70	1.86	7	1.0
0.018	2.33	3.61	3.80	−7	1.2	1	1.43	2.40	2.62	7	0.9
0.02	1.06	1.66	1.74	−6	1.2	1.25	2.75	4.59	4.99	7	0.8
0.025	2.16	3.49	3.67	−5	1.2	1.5	4.30	7.12	7.73	7	0.8
0.03	2.17	3.55	3.74	−4	1.2	1.75	5.84	9.70	10.5	7	0.8
0.04	0.66	1.04	1.09	−2	1.2	2	0.74	1.21	1.32	8	0.8
0.05	0.77	1.13	1.20	−1	1.2	2.5	0.99	1.64	1.77	8	0.9
0.06	4.98	7.02	7.51	−1	1.2	3	1.18	1.97	2.14	8	1.0
0.07	2.17	3.02	3.26	0	1.2	3.5	1.33	2.22	2.42	8	1.1
0.08	0.72	1.01	1.10	1	1.2	4	1.41	2.43	2.65	8	1.2
0.09	1.99	2.82	3.12	1	1.3	5	1.51	2.76	3.04	8	1.3
0.1	4.79	6.94	7.82	1	1.2	6	1.57	3.03	3.38	8	1.4
0.11	1.04	1.55	1.78	2	1.2	7	1.66	3.28	3.72	8	1.5
0.12	2.08	3.19	3.76	2	1.2	8	1.67	3.54	4.09	8	1.6
0.13	3.88	6.12	7.41	2	1.2	9	1.67	3.80	4.47	8	1.8
0.14	0.68	1.11	1.38	3	1.1	10	1.67	4.04	4.85	8	1.9

Reaction: $^{12}C(p,\gamma)^{13}N$
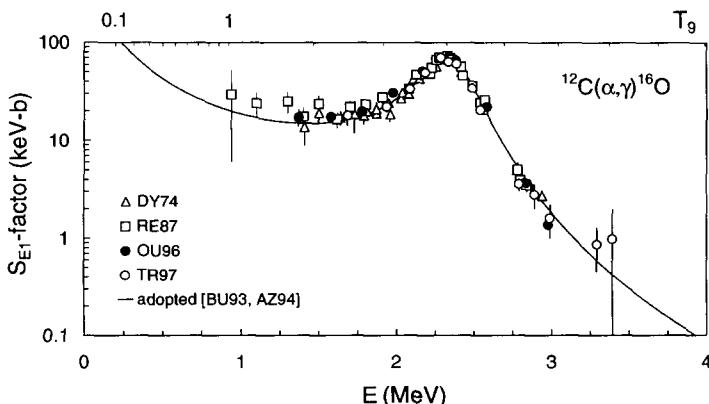
Experimental data from BA50, HA50, LA57a, VO63 and RO74a, covering the energy range from 72 to 541 keV, are adopted. For the calculation of the rates, a smooth spline fit to all data is adopted. For the extrapolation to $E = 0$, the direct capture results from [RO74a] are adopted. At higher energies, the $0°$ and $90°$ differential cross sections from RO74a multiplied by 4π are adopted, assuming a 40% error. The derived values are in very good agreement with the overlapping adopted data at lower energies. For $E > 2.3$ MeV, the S-factor is assumed to be energy independent, as suggested by direct capture studies [RO74a]. The adopted rates are very close to the CA88 ones, except around $T_9 = 0.3$. This is probably due to the numerical approach used here compared to the analytical approximation used by CA88.
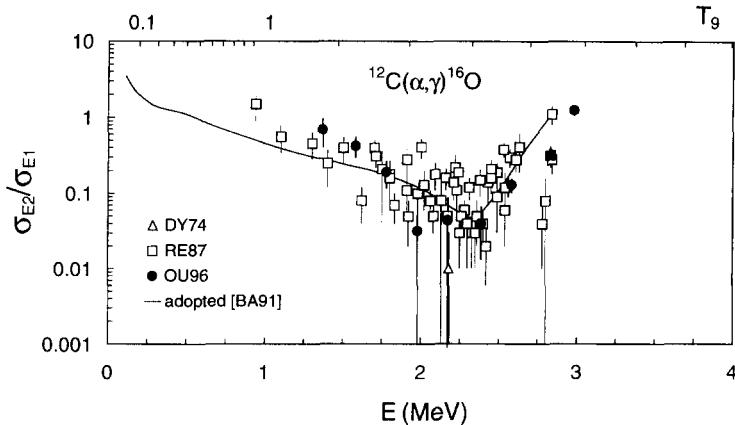
T_9	low	adopt	high	exp	ratio	T_9	low	adopt	high	exp	ratio
0.006	1.10	1.22	1.34	−24	1.0	0.16	1.25	1.39	1.53	−3	1.1
0.007	4.35	4.83	5.32	−23	1.0	0.18	3.30	3.67	4.04	−3	1.2
0.008	0.90	1.00	1.10	−21	1.0	0.2	7.80	8.66	9.53	−3	1.2
0.009	1.17	1.30	1.43	−20	1.0	0.25	4.95	5.50	6.05	−2	1.4
0.01	1.07	1.18	1.30	−19	1.0	0.3	2.50	2.78	3.05	−1	1.6
0.011	7.33	8.15	8.96	−19	1.0	0.35	1.04	1.15	1.27	0	1.5
0.012	4.04	4.49	4.94	−18	1.0	0.4	3.43	3.81	4.19	0	1.4
0.013	1.86	2.06	2.27	−17	1.0	0.45	0.92	1.02	1.12	1	1.3
0.014	7.35	8.17	8.99	−17	1.0	0.5	2.05	2.28	2.51	1	1.2
0.015	2.57	2.85	3.14	−16	1.0	0.6	6.90	7.67	8.44	1	1.1
0.016	8.06	8.96	9.85	−16	1.0	0.7	1.62	1.81	1.99	2	1.0
0.018	6.10	6.78	7.46	−15	1.0	0.8	3.04	3.38	3.72	2	1.0
0.02	3.49	3.88	4.27	−14	1.0	0.9	4.87	5.42	5.97	2	0.9
0.025	1.15	1.28	1.40	−12	1.0	1	7.01	7.80	8.60	2	0.9
0.03	1.65	1.83	2.02	−11	1.0	1.25	1.29	1.44	1.59	3	0.9
0.035	1.38	1.54	1.69	−10	1.0	1.5	1.86	2.08	2.30	3	0.8
0.04	7.97	8.86	9.75	−10	1.0	1.75	2.34	2.62	2.89	3	0.8
0.05	1.26	1.40	1.54	−8	1.0	2	2.70	3.02	3.35	3	0.8
0.06	1.03	1.14	1.26	−7	1.0	2.5	3.16	3.56	3.96	3	0.8
0.07	5.52	6.13	6.75	−7	1.1	3	3.35	3.80	4.25	3	0.9
0.08	2.21	2.45	2.70	−6	1.1	3.5	3.41	3.90	4.39	3	0.9
0.09	7.13	7.93	8.72	−6	1.1	4	3.41	3.94	4.47	3	0.9
0.1	1.96	2.18	2.40	−5	1.1	5	3.28	3.88	4.48	3	0.9
0.11	4.76	5.29	5.82	−5	1.1	6	3.14	3.81	4.48	3	1.0
0.12	1.05	1.16	1.28	−4	1.1	7	2.97	3.69	4.42	3	1.0
0.13	2.13	2.36	2.60	−4	1.1	8	2.86	3.64	4.41	3	1.0
0.14	4.04	4.49	4.94	−4	1.1	9	2.70	3.52	4.34	3	1.0
0.15	7.27	8.08	8.88	−4	1.1	10	2.69	3.55	4.42	3	1.1

Reaction: $^{12}C(\alpha,\gamma)^{16}O$

For the E1 contribution, the S-factor $S_{E1}(300 \text{ keV}) = 79 \pm 21$ keV b resulting from an R-matrix fit [BU93,AZ94] is used. This fit involves experimental data on capture [DY74,RE87,KR88,OU92,OU96,TR97], elastic scattering [PL87] and β-delayed α-spectrum of ^{16}N [BU93,AZ94]. Significant improvements on the $^{12}C(\alpha,\gamma)^{16}O$ rate have been performed through the analysis of the ^{16}N β decay [BU93,ZH93,FR97]. The E1 S-factor, which includes the contribution of the 1_1^- subthreshold state and of the 1_2^- broad resonance, is used to determine the reaction rate by numerical integration. The data of KE82 and KR88 do not separate E1 and E2 contributions, and are not included in the figure. The error on this fit is estimated as $\Delta S/S(E = 0.3 \text{ MeV}) = 0.27$ (given in AZ94), $\Delta S/S(E = 2.34 \text{ MeV}) = 0.05$ (lowest experimental error) and $\Delta S/S(E = 2.94 \text{ MeV}) = 0.13$ (estimated from the experimental data). Between these points, the shape of $\Delta S/S$ is assumed to be linear with E. Recent data of OU96 supersede erroneous ones [OU92], and do not change the fit within the error bars. For the E2 contribution, we use the R-matrix fit of BA91 [$S_{E2}(300 \text{ keV}) = 120 \pm 60$ keV b], which involves experimental data on capture [RE87] and on elastic scattering [PL87]. This 300 keV value is consistent with the upper limit recommended by BU96 [$S_{E2}(300 \text{ keV}) \leqslant 140$ keV b] from R-matrix fits. The low-energy S-factor is mainly determined by the properties of the 2_1^+ subthreshold state. Recent E2 data [OU96] are consistent with the fit. The E2 cross sections are deduced from σ_{E2}/σ_{E1} data; therefore, the errors on E2 are also affected by the errors on E1. At low energy, statistics is the main source of errors. At higher energy (≈ 2.5 MeV), the σ_{E2}/σ_{E1} ratio is small owing to the broad 1_2^- resonance, which enhances the E1 cross section. From these considerations, a constant uncertainty of 50% is used for the E2 component. Contributions from other resonances up to $E = 6$ MeV are treated separately, with energies and widths given in TI93. The contribution of cascade transitions is small (7–10% from RE87), and is therefore neglected. For $T_9 \leqslant 2$, the differences between our adopted rates and the CA88 ones arise from the S-factor $S_{E1}(300 \text{ keV})$ adopted by CA88, which is a factor of about 2 lower than the value adopted here.
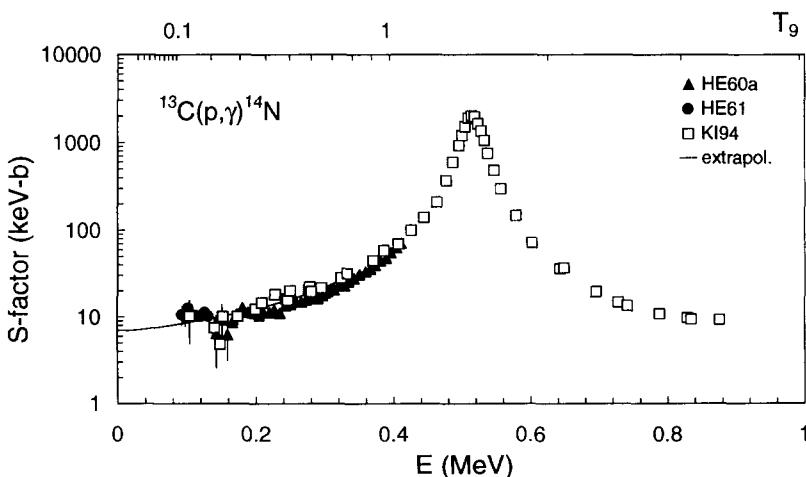
T_9	low	E1	E2	adopt	high	exp	ratio
0.06	0.60	0.43	0.59	1.02	1.44	-25	1.9
0.07	2.93	2.06	2.92	4.98	7.03	-24	1.9
0.08	0.72	0.50	0.72	1.22	1.72	-22	1.9
0.09	1.06	0.73	1.07	1.80	2.54	-21	2.0
0.1	1.06	0.73	1.08	1.81	2.55	-20	2.0
0.11	0.80	0.55	0.81	1.35	1.91	-19	2.0
0.12	4.71	3.23	4.75	7.98	11.3	-19	2.0
0.13	2.30	1.58	2.31	3.89	5.48	-18	2.0
0.14	0.96	0.66	0.96	1.61	2.27	-17	2.0
0.15	3.48	2.41	3.47	5.86	8.42	-17	1.9
0.16	1.13	0.79	1.12	1.91	2.68	-16	1.9
0.18	0.91	0.64	0.89	1.53	2.14	-15	1.9
0.2	5.44	3.84	5.27	9.11	12.8	-15	1.9
0.25	1.93	1.38	1.83	3.21	4.48	-13	1.9
0.3	2.88	2.10	2.66	4.75	6.62	-12	1.9
0.35	2.46	1.82	2.20	4.03	5.59	-11	1.9
0.4	1.43	1.08	1.23	2.31	3.20	-10	1.9
0.45	0.63	0.48	0.52	1.00	1.38	-9	1.9
0.5	2.22	1.75	1.77	3.52	4.82	-9	1.9
0.6	1.76	1.46	1.29	2.75	3.73	-8	1.9
0.7	0.92	0.79	0.62	1.40	1.89	-7	1.9
0.8	3.58	3.16	2.20	5.36	7.14	-7	1.9
0.9	1.13	1.02	0.64	1.66	2.19	-6	1.9
1	3.05	2.82	1.59	4.41	5.77	-6	2.0
1.25	2.31	2.22	0.97	3.19	4.08	-5	2.2
1.5	1.16	1.14	0.39	1.53	1.90	-4	2.2
1.75	4.55	4.44	1.18	5.76	6.97	-4	2.0
2	1.51	1.41	0.30	1.84	2.17	-3	1.7
2.5	1.09	0.86	0.14	1.27	1.46	-2	1.3
3	5.04	3.12	0.49	5.81	6.58	-2	1.2
3.5	1.69	0.80	0.14	1.94	2.20	-1	1.1
4	4.50	1.61	0.33	5.22	5.95	-1	1.1
5	2.09	0.42	0.13	2.51	2.96	0	1.0
6	6.78	0.77	0.37	8.53	10.5	0	0.9
7	1.71	0.12	0.08	2.24	2.86	1	0.8
8	3.55	0.15	0.15	4.83	6.32	1	0.7
9	6.35	0.19	0.25	8.87	11.9	1	0.6
10	1.01	0.02	0.04	1.45	1.96	2	0.5

Reaction: $^{13}C(p,\gamma)^{14}N$

The experimental data from HE60a, HE61 and KI94 are adopted. Since the data of HE60a and HE61 are limited to the capture cross section to the ^{14}N ground state, a renormalization factor 1.18, suggested by the authors [HE60a,HE61,KI94], is used to obtain the total cross section. For this reaction, the S-factor has been extrapolated by using a R-matrix fit involving the 1^- ($E_r = 0.511$ MeV) resonance and a background contribution. This procedure yields $S_0 = 7.0 \pm 1.5$ keV b. This value is consistent with the recommendation of AD98 (7.6 ± 1 keV b), who use the extrapolation of KI94. Resonance properties are taken from SE52, WO53, DE65, BI81, ZI86, PR85, and KI94. For the resonant data, a conservative error of 100% is adopted when no error is given by the authors. The 1^- resonance ($E_r = 0.511$ MeV) is the most important one. The present rates are slightly larger than the CA88 rates up to $T_9 \approx 0.5$, since the S_0 value used in CA88 (5.5 keV b) is lower than the present extrapolated value [KI94]. For $T_9 \geqslant 5$, the difference probably relates to the larger number of resonances included in the present rates.
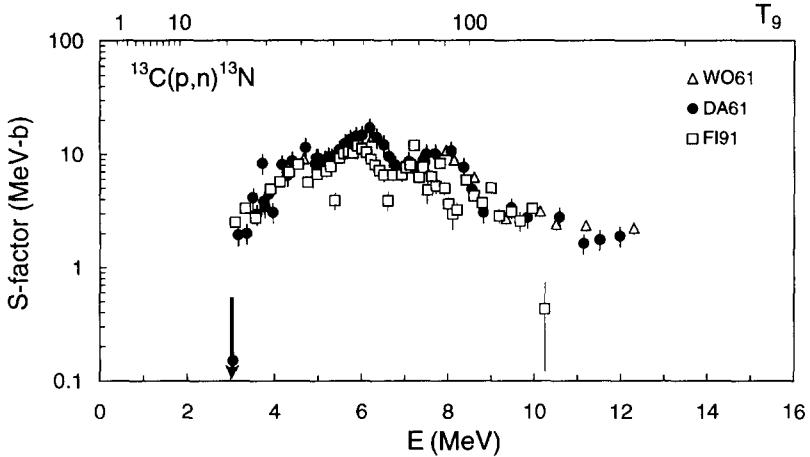
E_r (MeV)	J^π	$\omega\gamma$ (eV)	Ref.		E_r (MeV)	J^π	$\omega\gamma$ (eV)	Ref.	
0.416 ± 0.005	2^-	0.020 ± 0.002	KI94	M	1.429 ± 0.003	2^+	0.13 ± 0.13	WO53	N
0.511 ± 0.001	1^-	8.8 ± 1.1	KI94	I	1.578 ± 0.001	3^+	0.03 ± 0.03	DE65	N
0.939 ± 0.002	4^-	0.01 ± 0.01	DE65	N	1.621 ± 0.001	2^+	9.1 ± 0.5	BI81	M
1.069 ± 0.002	0^+	1.3 ± 1.3	WO53	M	1.958 ± 0.003	2^-	7.0 ± 1.0	PR85	M
1.225 ± 0.007	0^-	12.8 ± 12.8	SE52	M	2.152 ± 0.004	1^+	0.11 ± 0.01	PR85	N
1.356 ± 0.003	3^-	0.67 ± 0.07	ZI86	M	2.545	$1,2^+$	0.37 ± 0.03	PR85	N
1.413 ± 0.002	5^+	0.003 ± 0.003	DE65	N	2.881 ± 0.005	2^+	22.8 ± 1.3	PR85	M

T_9	low	adopt	high	exp	ratio	T_9	low	adopt	high	exp	ratio
0.007	1.59	2.00	2.40	−22	1.2	0.18	1.09	1.30	1.51	−2	1.2
0.008	3.30	4.15	5.00	−21	1.2	0.2	2.47	2.93	3.40	−2	1.2
0.009	4.29	5.39	6.49	−20	1.2	0.25	1.31	1.54	1.77	−1	1.3
0.010	3.90	4.90	5.89	−19	1.2	0.3	5.04	5.81	6.58	−1	1.3
0.011	2.69	3.37	4.05	−18	1.2	0.35	1.75	1.96	2.17	0	1.3
0.012	1.48	1.86	2.23	−17	1.2	0.4	5.54	6.04	6.53	0	1.2
0.013	6.81	8.54	10.3	−17	1.2	0.45	1.58	1.69	1.79	1	1.1
0.014	2.69	3.38	4.06	−16	1.2	0.5	3.85	4.20	4.54	1	1.0
0.015	0.94	1.18	1.42	−15	1.2	0.6	1.64	1.82	2.00	2	0.9
0.016	2.95	3.69	4.44	−15	1.2	0.7	4.74	5.41	6.09	2	0.9
0.018	2.23	2.79	3.34	−14	1.2	0.8	1.12	1.27	1.43	3	0.9
0.020	1.27	1.59	1.90	−13	1.2	0.9	2.13	2.43	2.74	3	0.9
0.025	4.15	5.18	6.21	−12	1.2	1	3.51	4.01	4.51	3	0.9
0.03	5.93	7.38	8.84	−11	1.2	1.25	8.21	9.40	10.6	3	0.9
0.04	2.85	3.54	4.22	−9	1.2	1.5	1.38	1.58	1.79	4	0.9
0.05	4.48	5.53	6.59	−8	1.2	1.75	1.92	2.23	2.54	4	0.9
0.06	3.65	4.50	5.36	−7	1.2	2	2.40	2.82	3.24	4	0.8
0.07	1.95	2.40	2.85	−6	1.2	2.5	3.11	3.78	4.46	4	0.8
0.08	7.80	9.57	11.3	−6	1.2	3	3.53	4.47	5.41	4	0.9
0.09	2.52	3.08	3.64	−5	1.2	3.5	3.73	4.94	6.15	4	0.9
0.10	6.91	8.43	9.95	−5	1.2	4	3.81	5.27	6.72	4	0.9
0.11	1.67	2.04	2.40	−4	1.2	5	3.77	5.62	7.46	4	1.0
0.12	3.66	4.45	5.23	−4	1.2	6	3.64	5.74	7.84	4	1.1
0.13	7.40	8.95	10.5	−3	1.2	7	3.49	5.74	7.99	4	1.1
0.14	1.40	1.69	1.98	−3	1.2	8	3.35	5.67	7.98	4	1.2
0.15	2.49	3.00	3.51	−3	1.2	9	3.23	5.55	7.88	4	1.2
0.16	4.23	5.08	5.94	−3	1.2	10	3.12	5.42	7.72	4	1.2

# Reaction: ^{13}C(p,n)^{13}N
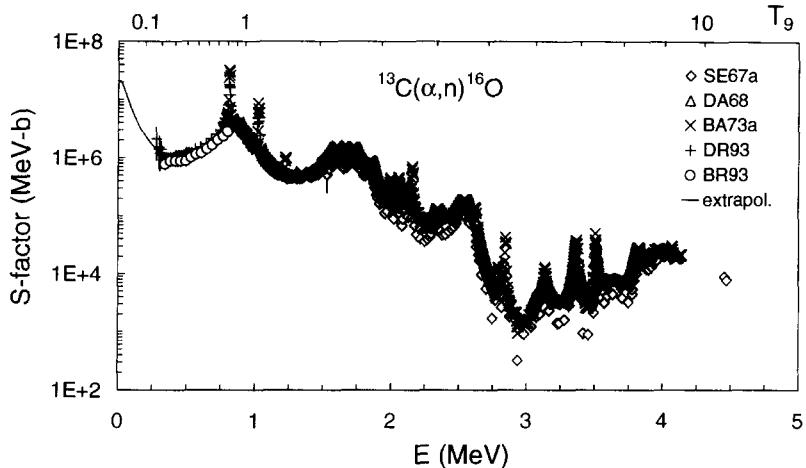
The rates of this reaction ($Q = -3.003$ MeV) are obtained by numerical integration of the experimental data of WO61, DA61 and FI91, with a linear interpolation between the data points. Above the neutron threshold in ^{14}N (10.55 MeV), the level density is very high (47 levels between $E_x = 10.55$ MeV and $E_x = 15$ MeV, as indicated by the experimental data). Below $T_9 = 1$, the present rates are slightly smaller than the CA88 ones, due to the new data of FI91, which are in general lower than the data of WO61 and DA61 used in CA88. Above $T_9 = 1$, the present rates are larger (up to a factor of 2.6 at $T_9 = 10$) due to the numerical integration of the rate formula, which is more accurate than the analytical treatment of CA88, especially at high temperatures, and to our thermalization corrections which are larger ($r_{tt} = 1.10$ to 1.36 at $T_9 = 5$ to 10) than the CA88 ones ($r_{tt} = 1$ at all T_9).

T_9	low	adopt	high	exp	ratio	T_9	low	adopt	high	exp	ratio
0.5	5.00	6.39	7.78	−23	0.7	2.5	1.42	1.69	1.96	2	1.2
0.6	6.40	7.91	9.41	−18	0.8	3	1.51	1.80	2.09	3	1.3
0.7	2.81	3.41	4.02	−14	0.9	3.5	8.20	9.79	11.4	3	1.4
0.8	1.51	1.81	2.12	−11	0.9	4	2.95	3.52	4.09	4	1.5
0.9	2.00	2.39	2.77	−9	1.0	5	1.81	2.16	2.52	5	1.7
1	0.99	1.18	1.37	−7	1.0	6	6.17	7.38	8.59	5	1.8
1.25	1.11	1.32	1.52	−4	1.0	7	1.49	1.79	2.08	6	2.0
1.5	1.20	1.42	1.64	−2	1.1	8	2.99	3.57	4.14	6	2.3
1.75	3.41	4.03	4.65	−1	1.1	9	5.03	6.00	6.98	6	2.4
2	4.19	4.97	5.75	0	1.2	10	7.74	9.23	10.7	6	2.6

Reaction: $^{13}C(\alpha,n)^{16}O$

The rates are determined using experimental cross sections of SE67a, DA68, BA73a, DR93 and BR93 covering the energy range between $E = 0.28$ and 4.47 MeV. For $E < 0.28$ MeV, the S-factor is extrapolated by fitting the data of DR93 with the tail of a $1/2^+$ subthreshold resonance at $E_x = 6.356$ MeV ($E_r = -3$ keV), using Eq. (31) with $\Gamma = 124 \pm 12$ keV [FO73,JO73] and $S_r = 2.30 \times 10^7$ MeV b. This extrapolation agrees with the R-matrix calculation of HA97. For $T_9 > 4$, HF rates are used following the procedure explained in Section 2.5. At low temperatures, the adopted rates are up to a factor of 8 higher than the CA88 ones. This large difference is caused by the inclusion of the subthreshold resonance. For $0.4 \leqslant T_9 \leqslant 2.5$, the adopted rates are up to factor of 2 higher, due to the new data of DR93 and BR93. At high temperatures, the HF rates are larger than the CA88 estimates.

T_9	low	adopt	high	exp	ratio	T_9	low	adopt	high	exp	ratio
0.04	0.65	5.34	6.45	−24	8.4	0.5	7.35	8.42	9.49	−2	1.6
0.05	0.49	3.24	3.91	−21	6.5	0.6	0.91	1.06	1.21	0	1.8
0.06	0.77	4.19	5.06	−19	5.2	0.7	6.07	7.18	8.30	0	1.9
0.07	0.44	2.00	2.42	−17	4.3	0.8	2.66	3.18	3.70	1	1.9
0.08	1.22	4.80	5.80	−16	3.6	0.9	0.86	1.04	1.22	2	1.9
0.09	2.03	6.99	8.45	−15	3.1	1	2.27	2.75	3.23	2	1.8
0.1	2.28	6.99	8.49	−14	2.7	1.25	1.41	1.73	2.05	3	1.6
0.11	1.90	5.24	6.41	−13	2.4	1.5	5.46	6.74	8.01	3	1.4
0.12	1.23	3.12	3.88	−12	2.2	1.75	1.60	1.99	2.37	4	1.2
0.13	0.66	1.55	1.95	−11	2.0	2	3.89	4.84	5.79	4	1.2
0.14	2.99	6.57	8.40	−11	1.8	2.5	1.50	1.87	2.24	5	1.1
0.15	1.18	2.44	3.16	−10	1.7	3	3.91	4.88	5.85	5	1.0
0.16	4.15	8.12	10.6	−10	1.6	3.5	7.85	9.81	11.8	5	1.0
0.18	3.85	6.77	8.88	−9	1.4	4	1.33	1.66	2.00	6	0.9
0.2	2.64	4.21	5.46	−8	1.3	5	3.02	3.86	4.72	6	1.0
0.25	1.28	1.70	2.08	−6	1.1	6	5.36	7.02	8.73	6	1.2
0.3	2.61	3.14	3.65	−5	1.0	7	0.82	1.10	1.40	7	1.3
0.35	3.11	3.57	4.03	−4	1.1	8	1.14	1.58	2.03	7	1.6
0.4	2.54	2.88	3.22	−3	1.3	9	1.49	2.12	2.78	7	1.8
0.45	1.55	1.76	1.97	−2	1.4	10	1.85	2.72	3.61	7	2.1
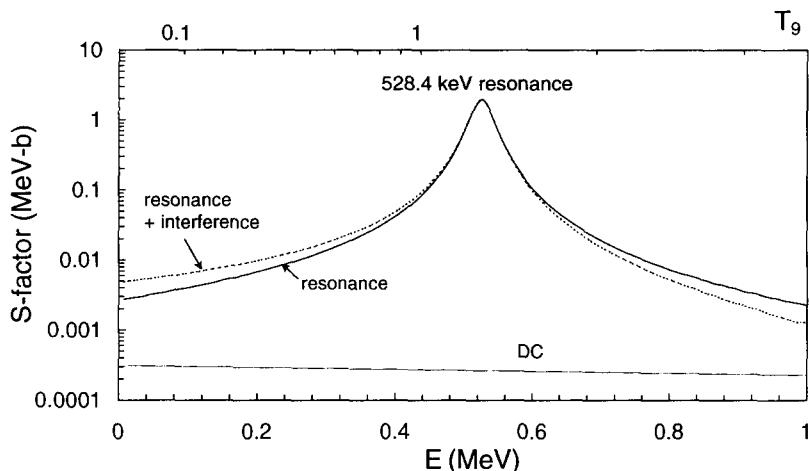
# Reaction: $^{13}N(p,\gamma)^{14}O$

The reaction rates are dominated by the contribution of the $J^{\pi} = 1^-$ resonance at $E_r = 528.4$ keV (weighted average value of GR72a, DE93a and MA94). The width of the resonance, $\Gamma = 37.3 \pm 0.9$ keV, is taken from CH85, DE93a and MA94. The resonance strength, $\omega\gamma = 2.5 \pm 0.6$ eV, is the weighted average value obtained from the indirect methods of FE89 and SM93 and the direct result of DE93a. The result from AG89 is disregarded since the authors warn against a possible ^{13}C contamination of the target. The two available results from Coulomb break-up experiments [MO91,KI93] are not included either (see Section 2.2.2). The rates are computed from the resonance

parameters and include the tail contribution of the 528.4 keV resonance. The constructive interference with the direct capture below the resonance, as suggested by DE93b, is also taken into account in order to obtain the upper limit of the rates. The present rates are up to factor of 2.6 (at $T_9 \approx 0.45$) larger than the theoretical estimates of LA85 used by CA88.

Method	Ref.	Γ_γ/Γ	Γ_γ (eV)
^{12}C(^{3}He,nγ)^{14}O	FE89	$(0.72 \pm 0.35) \times 10^{-4}$	
^{12}C(^{3}He,nγ)^{14}O	AG89	$(2.0 \pm 1.0) \times 10^{-4*}$	
^{14}N(p,n)^{14}O	SM93	$(3.1 \pm 1.7) \times 10^{-4}$	
	averaged	$0.82 \pm 0.47 \times 10^{-4}$	3.1 ± 1.8
Coulomb break up	MO91	–	$3.1 \pm 0.6^*$
Coulomb break up	KI93	–	$2.4 \pm 0.9^*$
^{13}N(p,γ)^{14}O	DE93b	–	3.3 ± 0.9
	adopted		3.3 ± 0.8

* See comments.

T_9	low	adopt	high	exp	ratio	T_9	low	adopt	high	exp	ratio
0.008	0.81	1.05	1.85	−24	1.1	0.2	1.03	1.34	1.99	−3	1.6
0.009	1.40	1.82	3.21	−23	1.1	0.25	7.10	9.23	13.1	−3	1.7
0.01	1.64	2.13	3.75	−22	1.1	0.3	3.55	4.61	6.17	−2	2.0
0.011	1.41	1.83	3.21	−21	1.1	0.35	1.56	2.03	2.50	−1	2.3
0.012	0.94	1.22	2.15	−20	1.1	0.4	6.15	7.98	9.82	−1	2.6
0.013	5.16	6.70	11.7	−20	1.1	0.45	2.05	2.67	3.28	0	2.6
0.014	2.39	3.11	5.44	−19	1.1	0.5	5.73	7.45	9.16	0	2.5
0.015	0.96	1.25	2.19	−18	1.1	0.6	2.83	3.67	4.52	1	2.3
0.016	3.45	4.47	7.81	−18	1.1	0.7	0.89	1.16	1.43	2	2.1
0.018	3.28	4.26	7.42	−17	1.2	0.8	2.10	2.73	3.35	2	2.0
0.02	2.29	2.97	5.16	−16	1.2	0.9	4.03	5.23	6.44	2	1.9

<div align="center">continued from previous page</div>

T_9	low	adopt	high	exp	ratio	T_9	low	adopt	high	exp	ratio
0.025	1.12	1.45	2.51	−14	1.2	1	6.71	8.71	10.7	2	1.9
0.03	2.17	2.82	4.84	−13	1.2	1.25	1.62	2.10	2.58	3	1.8
0.04	1.64	2.13	3.61	−11	1.3	1.5	2.78	3.61	4.44	3	1.7
0.05	3.56	4.62	7.76	−10	1.3	1.75	3.97	5.16	6.34	3	1.7
0.06	3.73	4.84	8.05	−9	1.3	2	5.06	6.58	8.09	3	1.7
0.07	2.44	3.17	5.22	−8	1.3	2.5	6.78	8.80	10.8	3	1.8
0.08	1.15	1.50	2.45	−7	1.4	3	0.79	1.02	1.26	4	1.8
0.09	4.29	5.58	9.03	−7	1.4	3.5	0.85	1.10	1.35	4	1.8
0.1	1.34	1.74	2.79	−6	1.4	4	0.87	1.13	1.40	4	1.8
0.11	3.62	4.70	7.48	−6	1.4	5	0.87	1.13	1.39	4	1.8
0.12	0.88	1.14	1.80	−5	1.4	6	0.83	1.07	1.32	4	1.9
0.13	1.93	2.51	3.94	−5	1.5	7	0.77	1.00	1.23	4	1.9
0.14	3.96	5.14	8.01	−5	1.5	8	7.17	9.31	11.5	3	1.9
0.15	7.62	9.90	15.3	−5	1.5	9	6.64	8.63	10.6	3	1.9
0.16	1.39	1.81	2.77	−4	1.5	10	6.16	8.00	9.83	3	2.0
0.18	4.06	5.27	7.95	−4	1.5						
T_9	low	adopt	high	exp	ratio	T_9	low	adopt	high	exp	ratio
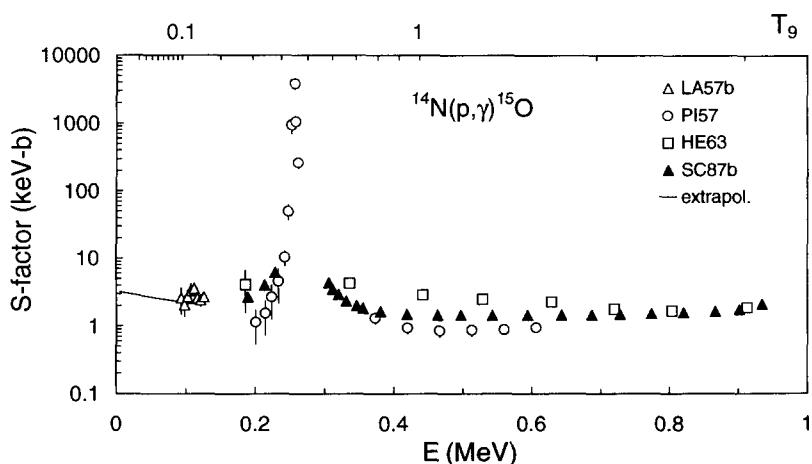
# Reaction: $^{14}N(p,\gamma)^{15}O$

The experimental data from LA57b, PI57 (as cited by SC87b), HE63 and SC87b are adopted for the calculation of the non-resonant contribution to the reaction rates. For the four data sets, a systematic error is added to the statistical error given in the figures or Tables (23% in LA57b, 33% in PI57, 12% in HE63, 15% in SC87b). For the extrapolation to energies below $E = 93$ keV, a subthreshold state at $E_r = -504$ keV is included. This extrapolation is in agreement with the one given in SC87b. Our recommended $S_0 = 3.2 \pm 0.8$ keV b, in agreement with the value given by AD98 within the error bars ($S_0 = 3.5^{+0.4}_{-1.6}$ keV b). The resonant data include 13 resonances. The strengths of the resonances between $E_r = 2185 \pm 7$ keV and $E_r = 4272 \pm 14$ keV are the reported values of DU51, PH72, KU77 and SC87b. The $1/2^+$ resonance ($E_r = 259.4 \pm 0.4$ keV) dominates the reaction rates at $T_9 \leqslant 1$. All resonance tails have a negligible contribution to the total reaction rates. Good agreement with the CA88 rates is obtained.

E_r (MeV)	J^π	$\omega\gamma$ (eV)					
		DU51	BA55b	HA57a	HE63	SC87b	adopt
0.2594 ± 0.0004	$1/2^+$	0.020±0.004	0.013±0.003		0.014±0.003	0.014±0.001	0.014±0.001 I
0.983 ± 0.002	$3/2^+$	0.63±0.13		0.39±0.13	0.39±0.08	0.31±0.04	0.35±0.05 M
1.440 ± 0.006	$1/2^+$	0.16±0.06		0.11±0.02		0.093±0.020	0.104±0.014 M
$1.623 \pm 0.002^\star$	$1/2^+$	0.21±0.06		0.76±0.19			0.26±0.16 M
1.684 ± 0.005	$(3/2)^-$	0.52±0.11		0.30±0.07			0.36±0.10 M
Res. 2.185–4.272 MeV				see comments			

*A $1/2^+$ and $5/2^+$ doublet separated by 0.5±0.5 keV
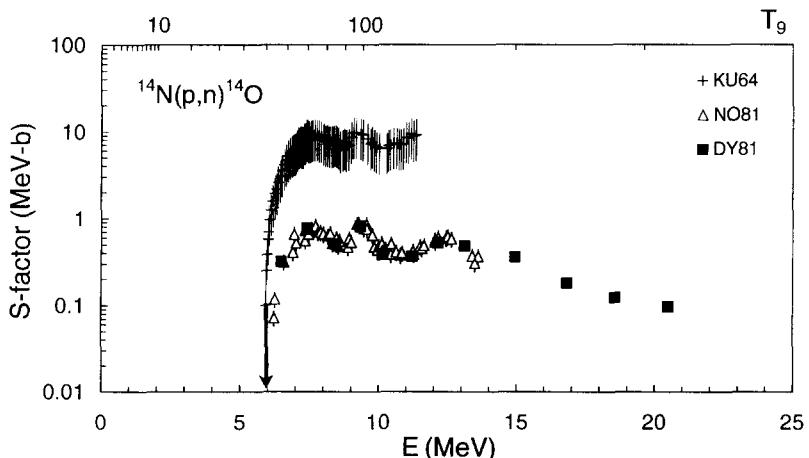
T_9	low	adopt	high	exp	ratio	T_9	low	adopt	high	exp	ratio
0.008	0.74	1.03	1.32	−24	1.0	0.2	7.41	8.26	9.14	−3	1.0
0.009	1.28	1.78	2.29	−23	1.0	0.25	1.04	1.14	1.25	−1	1.0
0.01	1.49	2.08	2.67	−22	1.0	0.3	5.84	6.40	6.98	−1	1.0
0.011	1.27	1.77	2.28	−21	1.0	0.35	1.94	2.12	2.31	0	1.0
0.012	0.85	1.18	1.52	−20	1.0	0.4	4.67	5.09	5.53	0	1.0
0.013	4.62	6.44	8.27	−20	1.0	0.45	9.04	9.85	10.7	0	1.0
0.014	2.13	2.97	3.81	−19	1.0	0.5	1.51	1.64	1.78	1	1.0
0.015	0.85	1.19	1.53	−18	1.0	0.6	3.14	3.42	3.70	1	1.0
0.016	3.04	4.24	5.43	−18	1.0	0.7	5.05	5.48	5.91	1	1.0
0.018	2.87	4.00	5.12	−17	1.0	0.8	7.09	7.68	8.27	1	1.0
0.02	1.98	2.76	3.53	−16	1.0	0.9	9.04	9.79	10.5	1	1.0
0.025	0.95	1.31	1.68	−14	1.0	1	1.08	1.17	1.26	2	1.0
0.03	1.79	2.48	3.18	−13	1.0	1.25	1.45	1.57	1.69	2	0.9
0.04	1.29	1.78	2.28	−11	1.0	1.5	1.74	1.89	2.05	2	0.9
0.05	2.67	3.68	4.69	−10	1.0	1.75	2.02	2.22	2.42	2	0.9
0.06	2.67	3.68	4.68	−9	1.0	2	2.35	2.61	2.88	2	0.9
0.07	1.67	2.30	2.92	−8	1.0	2.5	3.23	3.70	4.19	2	0.8
0.08	0.76	1.04	1.32	−7	1.0	3	4.54	5.39	6.27	2	0.7
0.09	2.71	3.70	4.69	−7	1.0	3.5	6.38	7.84	9.33	2	0.7
0.1	0.82	1.11	1.40	−6	1.0	4	0.88	1.11	1.34	3	0.7
0.11	2.18	2.95	3.71	−6	1.0	5	1.52	1.97	2.43	3	0.8
0.12	5.56	7.37	9.19	−6	1.0	6	2.27	2.99	3.71	3	0.9
0.13	1.44	1.85	2.27	−5	1.0	7	3.06	4.03	5.03	3	1.0
0.14	3.93	4.85	5.78	−5	1.0	8	3.80	5.02	6.26	3	1.1
0.15	1.09	1.30	1.51	−4	1.0	9	4.46	5.90	7.36	3	1.1
0.16	2.92	3.40	3.88	−4	1.0	10	5.03	6.65	8.29	3	1.1
0.18	1.71	1.93	2.16	−3	1.0						

Reaction: $^{14}N(p,n)^{14}O$

For this endoergic reaction ($Q = -5.926$ MeV), the reaction rates are obtained from the data of DY81 and NO81, with a linear interpolation between the experimental data points. The data from KU64 differ by more than one order of magnitude from the DY81 and NO81 data, which are in excellent agreement. This large discrepancy may be due to the technique used in KU64 for determining the nitrogen content in the foil targets, but no definite conclusion can be drawn from the paper. The KU64 data are used for the determination of the upper limits of the rates, while the data from DY81 and NO81 are used for the adopted rates and the lower limits. Our thermalization corrections give up to a factor 2.9 at $T_9 = 10$ (CA88 adopted $r_{tt} = 1$ at all T_9). The adopted rates are about 5 to 10 times lower than the CA88 rates, which are probably based on the KU64 data only.
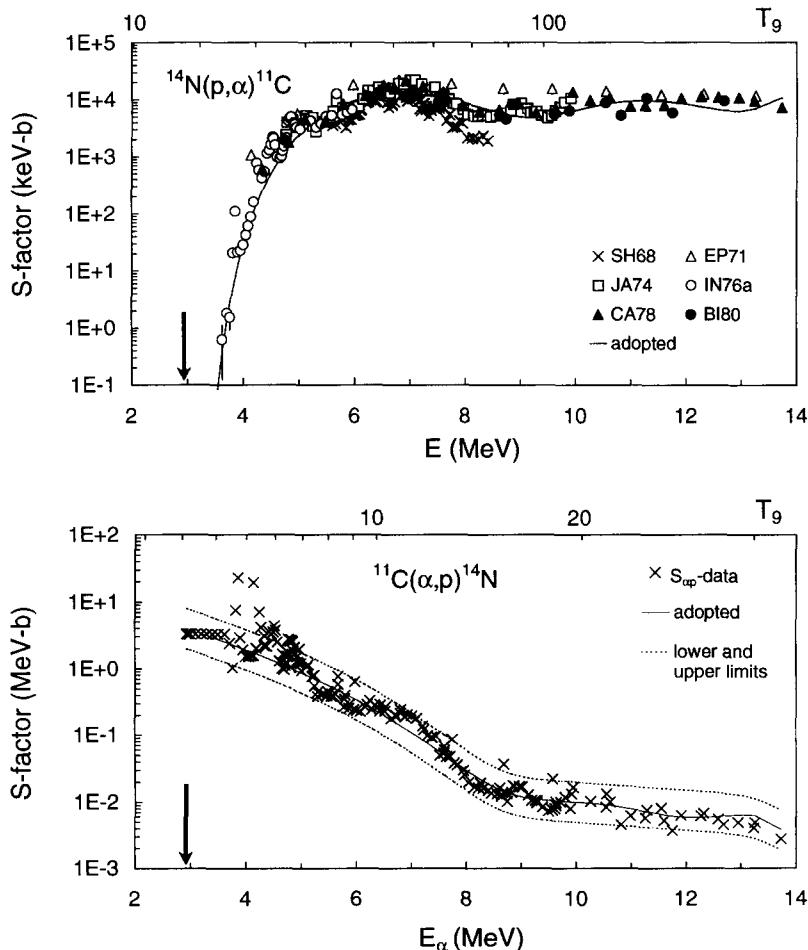
T_9	low	adopt	high	exp	ratio	T_9	low	adopt	high	exp	ratio
1	5.14	6.37	266	−24	0.1	4	4.93	5.99	129	−1	0.2
1.25	6.03	7.41	273	−18	0.1	5	1.79	2.18	45.1	1	0.2
1.5	7.02	8.56	283	−14	0.1	6	1.97	2.41	48.5	2	0.2
1.75	5.78	7.02	212	−11	0.1	7	1.09	1.34	26.5	3	0.2
2	0.90	1.09	30.7	−8	0.1	8	3.93	4.82	94.7	3	0.2
2.5	1.09	1.32	33.3	−5	0.1	9	1.06	1.31	25.5	4	0.2
3	1.27	1.53	36.0	−3	0.1	10	2.35	2.89	56.3	4	0.2
3.5	3.81	4.62	103	−2	0.2						

Reaction: $^{14}N(p,\alpha)^{11}C$

For this endoergic reaction ($Q = -2.922$ MeV), data from EP71, JA74, IN76a, CA78 and BI80 are used. Data from SH68 are omitted because they correspond only to the α_0 channel and are systematically lower than the other data sets. Experimental data are missing at energies between the threshold and $E = 3.6$ MeV. The existing data at the lowest energies do not allow a clear picture of the behavior of the S-factor curve. Below

$E = 4.77$ MeV, only the ^{14}N + p and ^{11}C + α channels are open, and hence the energy dependence of the cross section is dominated by the Coulomb barrier of the α channel. Therefore, for the calculation of the reaction rates, the S-factor for the reverse reaction ^{11}C$(\alpha,$p$)^{14}$N, which smoothly depends on energy, is approximated by a polynomial of degree 5. Neither low energy resonances, nor subthreshold states affect the S-factor. Due to the uncertainty in absolute values of the different data sets, a conservative uncertainty of a factor 2 is adopted for the lower and upper limits of the S-factor of the reverse reaction ^{11}C$(\alpha,$p$)^{14}$N. Below $T_9 = 5$, the recommended reaction rates are about 20–30% lower than the CA88 ones, due to a different expression for the S-factor of the reverse reaction. For $T_9 > 5$, our thermalization corrections are larger (r_{tt} is up to 2.04 at $T_9 = 10$) than the CA88 ones ($r_{tt} = 1$ at all T_9).

T_9	low	adopt	high	exp	ratio	T_9	low	adopt	high	exp	ratio
0.6	0.81	1.61	3.22	−25	0.7	3	3.22	6.43	12.9	0	0.9
0.7	1.50	3.00	6.00	−21	0.7	3.5	3.72	7.44	14.9	1	0.9
0.8	2.70	5.39	10.8	−18	0.7	4	2.42	4.83	9.66	2	0.9
0.9	1.00	2.00	4.00	−15	0.7	5	3.51	7.01	14.0	3	1.0
1	1.22	2.43	4.86	−13	0.7	6	2.16	4.31	8.62	4	1.1
1.25	0.83	1.65	3.30	−9	0.8	7	0.80	1.60	3.20	5	1.2
1.5	3.49	6.97	13.9	−7	0.8	8	2.15	4.30	8.60	5	1.3
1.75	2.92	5.83	11.7	−5	0.8	9	4.65	9.30	18.6	5	1.5
2	0.87	1.73	3.46	−3	0.8	10	0.86	1.72	3.44	6	1.7
2.5	1.13	2.26	4.52	−1	0.8						

Reaction: ^{14}N$(\alpha,\gamma)^{18}$F

Below T_9 = 2, the calculation of the reaction rates is performed by adding the contribution of 15 resonances at energies $E_r \leqslant$ 2.232 MeV [PA68,CO72, RO73b,BE82]. Among these resonances, only the ones at E_r = 0.237, 0.435, 0.883, 1.088, 1.189 and 1.258 MeV make a significant contribution to the total reaction rates. Only an upper limit of 8×10^{-15} eV for the strength of the E_r = 0.237 MeV resonance is known [CO72]; the adopted value, the upper limit and the lower limit are taken as a factor 0.1, 1.0 and 0 of this upper limit, respectively. It should be pointed out that the Wigner limit strongly depends on the nuclear radius. We obtain 2.56×10^{-19} MeV for a = 4.5 fm, while for a = 6 fm, the Wigner limit is 4.60×10^{-18} MeV. For the resonance at E_r = 0.535 MeV, the adopted value is a factor 0.1 of the upper limit of CO72 (see table), while the upper and lower limit are a factor 1 and 0, respectively. The $\omega\gamma$ values cited as PA68 are the numbers revised by RO73b taking into account stopping power corrections. Also the CO72 values are corrected here taken into account new values of the stoppping power. Above E_r = 1.373 MeV, the adopted resonance strength are from RO73b. A non-resonant contribution with $\mathcal{S}_0$ = 0.7 keV b [CO72], arising from the direct capture process and the tails of the low energy resonances, has a negligible effect on the total reaction rates. Above T_9 = 2, HF estimates are used, following the procedure explained in Section 2.5. Below T_9 = 2, the differences between the adopted rates and the CA88 ones arise from different resonance parameters. Above T_9 = 2, there are larger differences between the CA88 rates and the HF calculations.

T_9	low	adopt	high	exp	ratio	T_9	low	adopt	high	exp	ratio
0.07	4.E-4	1.05	10.5	−26	0.2	0.7	2.41	2.83	3.32	−3	1.0
0.08	0.03	1.19	11.7	−24	0.2	0.8	7.62	8.75	10.0	−3	1.1
0.09	2.36	7.27	47.7	−23	0.2	0.9	2.41	2.71	3.04	−2	1.2
0.1	5.47	7.37	1.57	−21	0.6	1	7.03	7.81	8.66	−2	1.2
0.11	4.65	5.67	7.36	−19	0.8	1.25	5.98	6.57	7.18	−1	1.2
0.12	1.87	2.24	2.67	−17	0.9	1.5	2.65	2.90	3.15	0	1.2
0.13	4.20	5.04	5.91	−16	0.9	1.75	7.65	8.36	9.09	0	1.2
0.14	6.00	7.21	8.42	−15	0.9	2	1.69	1.84	2.00	1	1.2
0.15	5.98	7.18	8.38	−14	0.9	2.5	3.82	5.14	5.97	1	1.1

continued from previous page

T9	low	adopt	high	exp	ratio	T9	low	adopt	high	exp	ratio
0.16	4.44	5.33	6.22	−13	0.9	3	0.67	1.05	1.29	2	1.1
0.18	1.24	1.48	1.73	−11	0.9	3.5	1.00	1.81	2.31	2	1.2
0.2	1.74	2.09	2.44	−10	0.9	4	1.36	2.77	3.66	2	1.3
0.25	1.93	2.32	2.71	−8	0.9	5	2.12	5.30	7.31	2	1.6
0.3	4.25	5.10	5.96	−7	0.9	6	2.90	8.59	12.2	2	1.9
0.35	3.72	4.47	5.24	−6	0.9	7	0.37	1.27	1.84	3	2.3
0.4	1.85	2.22	2.61	−5	0.8	8	0.45	1.77	2.59	3	2.9
0.45	6.31	7.58	8.92	−5	0.9	9	0.54	2.36	3.51	3	3.5
0.5	1.67	2.00	2.36	−4	0.9	10	0.64	3.07	4.60	3	4.2
0.6	7.31	8.73	10.3	−4	0.9						

E_r (MeV)	J^π	$\omega\gamma$ (eV)				
		PA68[1]	CO72[2]	RO73b	adopt	
0.237	4^+		$< 8 \times 10^{-15}$		$8^{+72}_{-8} \times 10^{-16}$	I
0.435	1		$(0.6 \pm 0.1) \times 10^{-4}$		$(0.6 \pm 0.1) \times 10^{-4}$	I
0.535	2^+		$< 1 \times 10^{-5}$		$1^{+9}_{-1} \times 10^{-6}$	M
0.883 ± 0.002	4^+	0.024 ± 0.001	0.024 ± 0.003	0.020 ± 0.007	0.024 ± 0.001	M
1.088 ± 0.003	$3^{(-)}$	0.008 ± 0.001		0.006 ± 0.001	0.007 ± 0.001	M
1.189 ± 0.002	1^-	1.3 ± 0.1		1.3 ± 0.1	1.3 ± 0.1	M
1.258 ± 0.002	1^-	0.38 ± 0.04	0.45 ± 0.02 [BE82]	0.5 ± 0.1	0.44 ± 0.02	M
Res. 1.373–2.232 MeV			see comments			

[1] Values revised by RO73b.

[2] Including stopping power corrections.
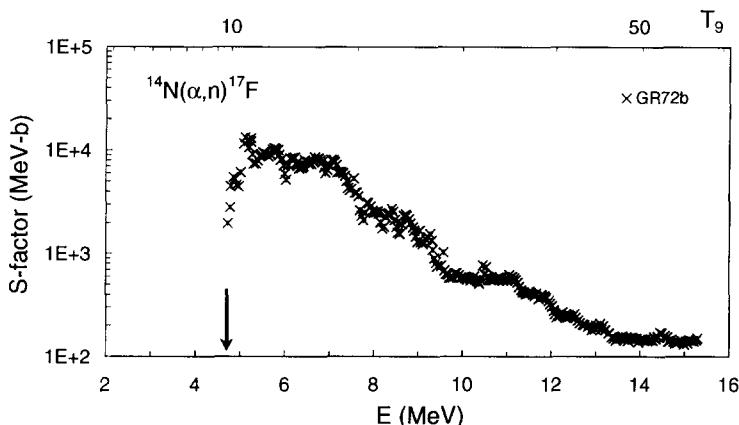
# Reaction: $^{14}\mathrm{N}(\alpha,n)^{17}\mathrm{F}$

For this endoergic reaction ($Q = -4.735$ MeV), the rates are determined by using the cross section data of GR72b, which cover the energy range from threshold to 15.5 MeV. At low temperatures, the difference between the adopted rates and the CA88 ones is most likely due to the use by CA88 of the 8 data points of RO83b, which correspond to thick-target yields. At high temperatures, thermalizations corrections increase the ratio of our adopted rates to the CA88 ones (our r_{tt} goes up to 1.3 at $T_9 = 10$, while CA88 adopt $r_{tt} = 1$ at all T_9).

T9	low	adopt	high	exp	ratio	T9	low	adopt	high	exp	ratio
0.7	1.04	1.10	1.15	−26	0.1	3	1.43	1.50	1.58	0	0.7
0.8	1.84	1.94	2.04	−22	0.1	3.5	1.99	2.10	2.20	1	0.8
0.9	3.71	3.91	4.11	−19	0.1	4	1.44	1.52	1.60	2	0.8
1	1.64	1.73	1.81	−16	0.1	5	2.32	2.45	2.57	3	0.9
1.25	0.96	1.01	1.06	−11	0.2	6	1.49	1.57	1.65	4	0.9
1.5	1.47	1.54	1.62	−8	0.2	7	5.61	5.91	6.21	4	0.9
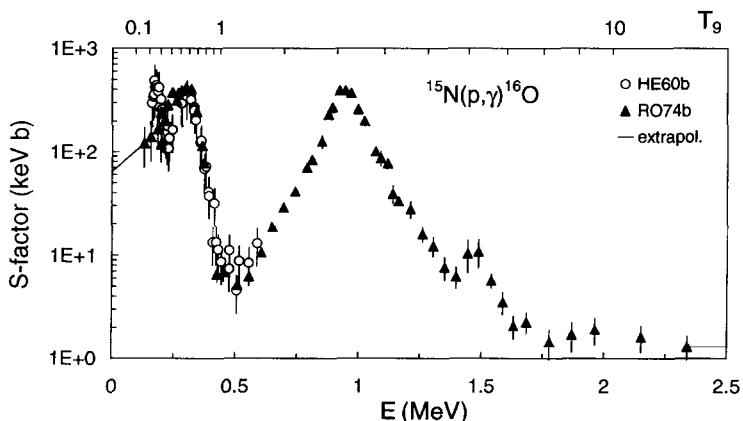
T_9	low	adopt	high	exp	ratio	T_9	low	adopt	high	exp	ratio
1.75	2.78	2.93	3.07	−6	0.3	8	1.52	1.60	1.68	5	0.9
2	1.43	1.50	1.58	−4	0.4	9	3.28	3.46	3.63	5	0.9
2.5	3.57	3.76	3.95	−2	0.6	10	6.07	6.39	6.71	5	1.0

Reaction: $^{15}N(p,\gamma)^{16}O$

Cross section data from HE60b and RO74b are available. The data of HE60b are omitted in the calculation of the rates, because they are in disagreement with RO74b and with the resonance data of SC52 and RE82. For the extrapolation to low energies, the S-factor is interpolated linearly between $S_0 = 64 \pm 6$ keV b [RO74b] and the lowest energy data point. This procedure is consistent with the RO74b extrapolation. Above $E = 2.3$ MeV, the S-factor is assumed to be a constant, and equal to its value at the last data point. No resonance parameters are needed for the calculation. The differences between the present rates and those from CA88 are most likely due to the use of HE60b data by CA88.

T_9	low	adopt	high	exp	ratio	T_9	low	adopt	high	exp	ratio
0.007	5.85	7.01	8.17	−25	1.1	0.18	0.91	1.35	1.79	−2	1.3
0.008	1.73	2.08	2.44	−23	1.1	0.2	2.49	3.52	4.55	−2	1.2
0.009	3.02	3.67	4.32	−22	1.1	0.25	1.90	2.44	2.97	−1	0.9
0.01	3.54	4.33	5.12	−21	1.1	0.3	0.87	1.05	1.23	0	0.7
0.011	3.05	3.75	4.46	−20	1.1	0.35	2.71	3.17	3.63	0	0.6
0.012	2.05	2.54	3.03	−19	1.1	0.4	6.51	7.48	8.44	0	0.6
0.013	1.13	1.40	1.68	−18	1.1	0.45	1.32	1.49	1.67	1	0.5
0.014	5.23	6.55	7.87	−18	1.1	0.5	2.30	2.58	2.87	1	0.5
0.015	2.11	2.66	3.20	−17	1.1	0.6	5.28	5.90	6.51	1	0.5
0.016	7.56	9.56	11.6	−17	1.1	0.7	0.96	1.07	1.17	2	0.5
0.018	7.21	9.22	11.2	−16	1.2	0.8	1.52	1.68	1.85	2	0.5
0.02	5.03	6.50	7.96	−15	1.2	0.9	2.23	2.46	2.70	2	0.5
0.025	2.46	3.25	4.03	−13	1.2	1	3.17	3.50	3.83	2	0.6
0.03	4.76	6.41	8.06	−12	1.2	1.25	7.27	7.96	8.65	2	0.6
0.04	3.55	4.96	6.36	−10	1.2	1.5	1.54	1.67	1.81	3	0.7
0.05	0.76	1.09	1.43	−8	1.3	1.75	2.84	3.09	3.34	3	0.7
0.06	0.78	1.16	1.53	−7	1.3	2	4.64	5.05	5.45	3	0.7
0.07	5.04	7.64	10.2	−7	1.3	2.5	0.92	1.00	1.08	4	0.7
0.08	2.34	3.63	4.91	−6	1.3	3	1.42	1.55	1.68	4	0.7
0.09	0.86	1.36	1.85	−5	1.3	3.5	1.89	2.06	2.23	4	0.8
0.1	2.64	4.23	5.81	−5	1.3	4	2.09	2.27	2.46	4	0.7
0.11	0.71	1.15	1.58	−4	1.3	5	2.40	2.61	2.81	4	0.7
0.12	1.71	2.78	3.84	−4	1.3	6	2.64	2.86	3.08	4	0.7
0.13	3.81	6.16	8.51	−4	1.4	7	2.83	3.06	3.29	4	0.7
0.14	0.79	1.27	1.75	−3	1.4	8	2.99	3.23	3.47	4	0.8
0.15	1.56	2.46	3.36	−3	1.4	9	3.13	3.37	3.62	4	0.8
0.16	2.92	4.53	6.13	−3	1.4	10	3.26	3.51	3.76	4	0.9
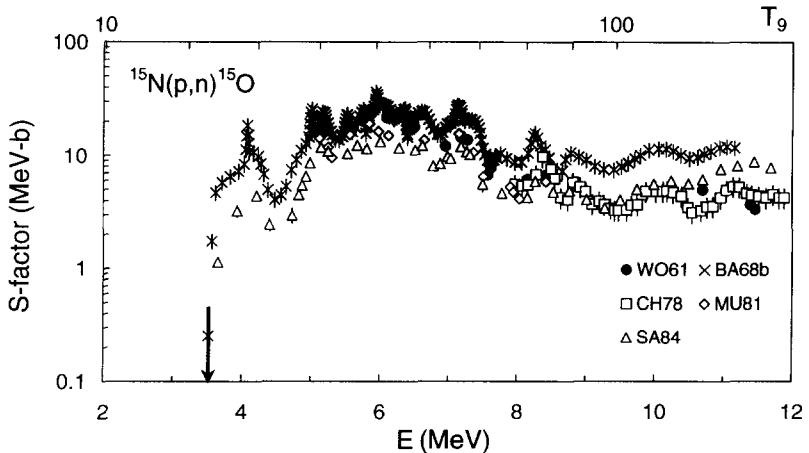
# Reaction: $^{15}N(p,n)^{15}O$

For this endoergic reaction ($Q = -3.536$ MeV), the reaction rates are obtained from the data of WO61, CH78, MU81 and SA84, with a linear interpolation between the data points. Data from BA68b differ by a factor of about 2 from the other data sets, and are normalized using the average value of CH78 and SA84 at $E = 9.5$ MeV. The original BA68b data are used to obtain the upper limits of the rates. At low temperatures, the large differences with CA88 are probably due to their use of the BA68b data. Thermalization effects cannot account for the increase of the ratio of our adopted rates to the CA88 ones at high temperatures (our r_{tt} goes up to about 1.1 only at $T_9 = 10$; CA88 adopt $r_{tt} = 1$ for all T_9).

T_9	low	adopt	high	exp	ratio	T_9	low	adopt	high	exp	ratio
0.6	2.14	2.50	6.41	−22	0.3	3	1.62	1.89	4.62	2	0.4
0.7	3.90	4.54	11.7	−18	0.3	3.5	1.16	1.36	3.28	3	0.4
0.8	6.11	7.12	18.4	−15	0.3	4	5.13	5.97	14.4	3	0.4
0.9	1.87	2.18	5.64	−12	0.3	5	4.17	4.85	11.5	4	0.5
1	1.82	2.12	5.49	−10	0.3	6	1.73	2.01	4.74	5	0.6
1.25	6.97	8.12	20.8	−7	0.3	7	4.85	5.64	13.2	5	0.7

				continued from previous page					
1.5	1.71	1.99	5.06	−4	0.3	8	1.07	1.24	2.87	6	0.8
1.75	0.87	1.02	2.56	−2	0.4	9	1.95	2.27	5.27	6	1.0
2	1.67	1.94	4.85	−1	0.4	10	3.24	3.76	8.62	6	1.4
2.5	1.03	1.21	2.97	1	0.4						
T_9	low	adopt	high	exp	ratio	T_9	low	adopt	high	exp	ratio
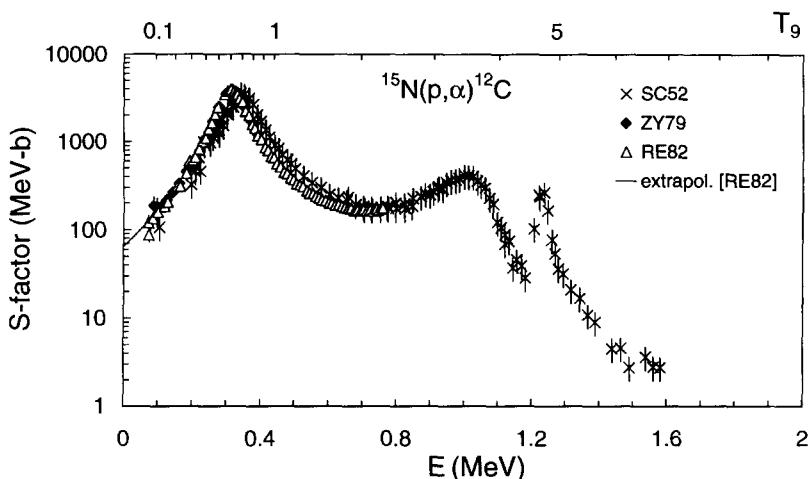
Reaction: $^{15}N(p,\alpha)^{12}C$

Data from ZY79 and RE82 between $E = 0.07$ and 0.76 MeV are used. The data of SC52 are used between $E = 0.76$ and 1.6 MeV. Below $E = 0.8$ MeV, the S-factor is dominated by the 1^- resonance at $E_r = 313.9$ keV with $\omega\gamma = 0.67 \pm 0.07$ keV [RE82], showing an interference effect with the other 1^- resonance at $E_r = 963$ keV ($\omega\gamma = 23 \pm 6$ keV [HA57b]). For $T_9 \leqslant 2.5$, the reaction rates are calculated using a linear interpolation between the experimental data [SC52,ZY79,RE82] and adding the contribution of the resonances at $E_r = 1537$ keV ($\omega\gamma = 6.9 \pm 1.0$ keV [HA57b]) and 2.798 keV ($\omega\gamma = 15 \pm 3$ keV [SN83,DA84]). At low energies, the Breit–Wigner extrapolation from RE82 is adopted ($S_0 = 65 \pm 7$ MeV b). For $T_9 > 2.5$, HF rates are used as explained in Section 2.5. Around $T_9 = 0.2$, the difference with the CA88 rates is probably due to the different resonance parameters adopted by CA88. At high temperatures, the HF rates are larger than the CA88 rates.

T_9	low	adopt	high	exp	ratio	T_9	low	adopt	high	exp	ratio
0.005	6.38	7.12	7.87	−26	1.0	0.16	7.99	9.75	11.9	0	1.9
0.006	1.10	1.24	1.37	−23	1.0	0.18	2.60	3.28	4.13	1	2.1
0.007	6.73	7.59	8.45	−22	1.0	0.2	7.32	9.64	12.7	1	2.0
0.008	2.00	2.27	2.53	−20	1.0	0.25	6.20	8.80	12.5	2	1.5
0.009	3.52	4.01	4.49	−19	1.0	0.3	3.28	4.66	6.63	3	1.1
0.01	4.17	4.76	5.35	−18	1.0	0.35	1.13	1.66	2.43	4	0.9

continued on next page

<div align="center">continued from previous page</div>

0.011	3.61	4.14	4.67	−17	1.0	0.4	3.15	4.48	6.38	4	0.8
0.012	2.44	2.81	3.18	−16	1.0	0.45	7.04	9.86	13.8	4	0.8
0.013	1.35	1.56	1.77	−15	1.0	0.5	1.35	1.88	2.63	5	0.8
0.014	6.31	7.31	8.31	−15	1.0	0.6	3.47	4.91	6.94	5	0.8
0.015	2.56	2.98	3.39	−14	1.0	0.7	7.52	9.85	12.9	5	0.9
0.016	0.92	1.08	1.23	−13	1.0	0.8	1.29	1.64	2.08	6	0.9
0.018	0.89	1.04	1.20	−12	1.0	0.9	1.56	2.35	3.54	6	1.0
0.02	6.27	7.39	8.52	−12	1.0	1	2.41	3.37	4.72	6	1.1
0.025	3.14	3.74	4.35	−10	1.0	1.25	4.43	6.20	8.6 8	6	1.2
0.03	6.20	7.48	8.76	−9	1.0	1.5	6.93	9.71	13.6	6	1.4
0.04	4.78	5.87	6.95	−7	1.1	1.75	0.84	1.34	2.14	7	1.5
0.05	1.06	1.31	1.57	−5	1.1	2	1.14	1.77	2.75	7	1.5
0.06	1.15	1.45	1.74	−4	1.1	2.5	1.66	2.59	4.05	7	1.5
0.07	0.80	1.00	1.21	−3	1.2	3	2.44	3.81	5.95	7	1.6
0.08	4.05	5.04	6.04	−3	1.2	3.5	3.29	5.13	7.99	7	1.7
0.09	1.62	1.99	2.36	−2	1.3	4	4.21	6.52	10.1	7	1.7
0.1	5.43	6.53	7.62	−2	1.3	5	6.09	9.43	14.6	7	1.9
0.11	1.58	1.87	2.16	−1	1.4	6	0.81	1.25	1.92	8	2.2
0.12	4.07	4.77	5.48	−1	1.5	7	1.01	1.55	2.39	8	2.4
0.13	0.95	1.12	1.29	0	1.6	8	1.21	1.86	2.86	8	2.7
0.14	2.04	2.44	2.83	0	1.7	9	1.42	2.17	3.32	8	3.0
0.15	4.01	4.97	5.94	0	1.8	10	1.62	2.47	3.77	8	3.3
T_9	low	adopt	high	exp	ratio	T_9	low	adopt	high	exp	ratio

Reaction: $^{15}\mathrm{N}(\alpha, \gamma)^{19}\mathrm{F}$

The main contribution to the rates below $T_9 = 0.2$ comes from the $E_r = 364$ keV resonance, for which we use the experimental strength $\omega\gamma$ of OL96. Uncertainties on this strength is adopted from OL97, following the discussions of OL96 and WI97. Adopted resonance strengths come mainly from RO72a, RO73d, DI77, SY78 and WI97 for a total of 48 resonances. For those at 1413, 1452, 1486 and 1524 keV, the $\omega\gamma$ values

from AI70 are used, renormalized to the revised strength of the resonance at 1326 keV from DI71a. For the resonances from $E = 1607$ to 2149 keV the resonance strengths of RO72b and WI97 are used. From $E = 2268$ to 2912 keV, those of DI77 are adopted. The data of SY78 are used for the resonances from $E = 4358$ to 5823 keV, and from $E = 5914$ to 6398 keV. The contribution of the direct capture to the first six levels of ^{19}F is calculated; it only affects the rates near $T_9 = 0.08$ [OL96]. Tails of higher lying resonances make negligible contributions to the rates, when compared with the direct capture. For $T_9 \leqslant 0.2$, our rates are about 50 times lower than the CA88 ones, as a result of our adoption of the OL96 strength of the $E_r = 364$ keV resonance, which is 60 times smaller than the value selected by CA88. Around $T_9 = 0.5$, the difference between the present rates and the CA88 ones is probably related to the $E_r = 669$ keV resonance, which has been neglected in CA88.
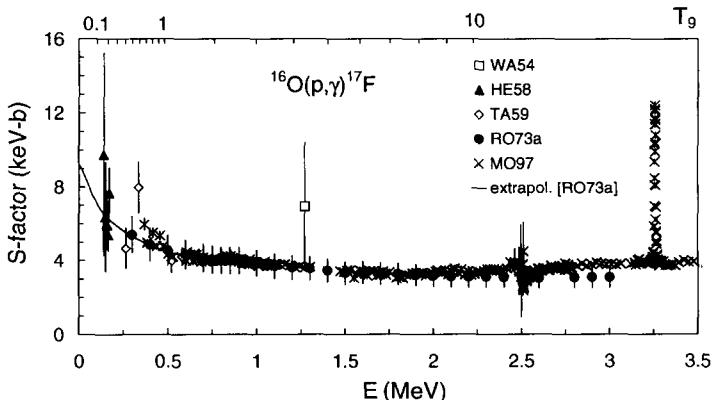
E_r (MeV)	J^π	$\omega\gamma$ (eV)			
		W197	others	adopt	
0.364 ± 0.002	$7/2^+$		$(6^{+6}_{-3}) \times 10^{-9}$ [OL96,OL97]	$(6^{+6}_{-3}) \times 10^{-9}$	I
0.536 ± 0.002	$5/2^+$	$(9.6 \pm 1.2) \times 10^{-5}$	$(9.6 \pm 2.1) \times 10^{-5}$ [MA87]	$(9.6 \pm 1.0) \times 10^{-5}$	I
0.542 ± 0.002	$3/2^-$	$(6.4 \pm 2.5) \times 10^{-6}$	$< 1 \times 10^{-5}$ [MA87]	$(6.4 \pm 2.5) \times 10^{-6}$	M
0.669 ± 0.002	$5/2^-$	$(5.6 \pm 0.6) \times 10^{-3}$	$(5.9 \pm 1.5) \times 10^{-3}\star$	$(5.7 \pm 0.6) \times 10^{-3}$	I
			$(6.3 \pm 2.1) \times 10^{-3}$ [RO72b]		
1.093 ± 0.003	$5/2^+$	$(9.7 \pm 1.6) \times 10^{-3}$	$\approx 10^{-2}\star$	$(9.7 \pm 1.6) \times 10^{-3}$	M
1.326 ± 0.003	$1/2^+$	1.69 ± 0.14	1.64 ± 0.16 [DI71b]	1.67 ± 0.11	M
Res. 1.607–2.912 MeV			see comments		
		UN74			
3.152 ± 0.002	$11/2^-$	0.95 ± 0.14	1.5 ± 0.2 [DI71b]	1.00 ± 0.15	M
			1.15 ± 0.23 [RO73d]		
3.525 ± 0.003	$(5/2^+)$	17.9 ± 2.1	17.0 ± 2.7 [RO76]	17.6 ± 1.7	M
3.645 ± 0.003	$3/2^+$		3.7 ± 0.9 [RO76]	3.7 ± 0.9	M
		SY78			
3.915 ± 0.003	$7/2^+$		2.3 ± 0.4 [DI71b]	2.3 ± 0.4	M
3.924 ± 0.003	$11/2^+$		3.1 ± 0.5 [DI71b]	3.1 ± 0.5	M
4.273 ± 0.005	$13/2^-$	0.58 ± 0.1	0.53 ± 0.08 [UN74]	0.53 ± 0.08	M
			0.51 ± 0.07 [RO76]		
4.295 ± 0.005	$5/2^+$	2.1 ± 0.5	1.37 ± 0.18 [RO76]	1.45 ± 0.17	M
Res. 4.358–5.823 MeV			see comments		
5.860 ± 0.004	$11/2^-$	3.6 ± 0.6	3.48 ± 0.47 [RO76]	3.5 ± 0.4	M
Res. 5.914–6.398 MeV			see comments		

$\star$From AI70, and renormalized to the 1.326 MeV resonance in DI71a

T_9	low	adopt	high	exp	ratio	T_9	low	adopt	high	exp	ratio
0.08	1.85	2.68	4.53	−25	0.06	0.7	4.11	4.77	5.46	−3	4.8
0.09	1.33	2.94	7.04	−23	0.02	0.8	1.34	1.54	1.76	−2	2.5
0.1	0.99	2.41	6.00	−21	0.02	0.9	3.45	3.97	4.51	−2	1.5
0.11	3.89	9.54	23.5	−20	0.02	1	7.82	8.99	10.2	−2	1.0
0.12	0.85	2.05	4.96	−18	0.02	1.25	4.82	5.59	6.40	−1	0.7
0.13	1.14	2.73	6.50	−17	0.02	1.5	2.26	2.65	3.06	0	0.8
0.14	1.07	2.50	5.87	−16	0.02	1.75	7.62	9.00	10.4	0	0.9
0.15	0.75	1.71	3.95	−15	0.02	2	1.95	2.31	2.68	1	1.0
0.16	4.24	9.36	21.1	−15	0.02	2.5	7.29	8.67	10.1	1	1.1
0.18	0.89	1.74	3.61	−13	0.02	3	1.74	2.08	2.42	2	1.2
0.2	1.32	2.22	4.01	−12	0.03	3.5	3.23	3.85	4.48	2	1.2
0.25	3.39	4.47	6.06	−10	0.13	4	5.12	6.10	7.10	2	1.2
0.3	1.85	2.29	2.84	−8	0.5	5	0.97	1.16	1.35	3	1.1
0.35	3.60	4.36	5.24	−7	1.6	6	1.49	1.78	2.07	3	1.0
0.4	3.56	4.25	5.03	−6	4.2	7	2.01	2.40	2.80	3	0.9
0.45	2.18	2.58	3.03	−5	8.8	8	2.51	3.00	3.50	3	0.8
0.5	0.94	1.11	1.29	−4	13	9	2.97	3.55	4.15	3	0.8
0.6	8.56	9.98	11.5	−4	10	10	3.38	4.05	4.74	3	0.7

Reaction: $^{16}O(p,\gamma)^{17}F$

The non-resonant data from WA54, HE58, TA59, RO73a and MO97 are adopted. At energies $E \leqslant 160$ keV, only one set of data [HE58] is available, with large experimental errors. The data from RO73a result from a normalization to one data point of TA59. For the extrapolation to zero energy, the potential model calculation of RO73a confirmed by MO97 is adopted. The recommended S-factor at zero energy is $S_0 = 9.3 \pm 2.8$ keV b. We adopt 30% overall uncertainty for the low energy extrapolation, which includes 10% of systematic error and 20% of error due to model assumptions. Beyond $T_9 = 4$, a reliable calculation of the reaction rates requires experimental data at $E > 3.5$ MeV. Since these data are missing, the S-factor is considered as a constant, equal to the value measured at the highest energy, with 20% uncertainty. In this case, HF rates are not adequate as the level density of ^{17}F is not high enough for a statistical model. The resonances at $E_r = 2503 \pm 7$ keV [RO73a] and $E_r = 3556 \pm 4$ keV [SE63] contribute for less than 1% to the total rates. Good agreement is found between the present rates and those from CA88.

T_9	low	adopt	high	exp	ratio	T_9	low	adopt	high	exp	ratio
0.01	4.71	6.73	8.75	−25	1.0	0.25	5.29	7.57	9.84	−4	1.0
0.011	4.97	7.10	9.23	−24	1.0	0.3	2.16	3.09	4.02	−3	1.0
0.012	4.00	5.71	7.42	−23	1.0	0.35	6.63	9.44	12.3	−3	1.0
0.013	2.57	3.68	4.78	−22	1.0	0.4	1.66	2.36	3.05	−2	1.0
0.014	1.38	1.97	2.56	−21	1.0	0.45	3.61	5.09	6.57	−2	1.0
0.015	6.35	9.06	11.8	−21	1.0	0.5	7.04	9.84	12.6	−2	1.0
0.016	2.56	3.65	4.75	−20	1.0	0.6	2.11	2.90	3.96	−1	1.0
0.018	3.01	4.30	5.59	−19	1.0	0.7	5.08	6.83	8.58	−1	1.0
0.02	2.51	3.59	4.66	−18	1.0	0.8	1.04	1.38	1.72	0	1.0
0.025	1.75	2.50	3.25	−16	1.0	0.9	1.91	2.49	3.07	0	1.0
0.03	4.42	6.32	8.21	−15	1.0	1	3.21	4.13	5.05	0	1.0
0.04	4.82	6.89	8.96	−13	1.0	1.25	0.90	1.13	1.36	1	1.0
0.05	1.34	1.91	2.49	−11	1.0	1.5	1.94	2.42	2.89	1	1.0
0.06	1.68	2.39	3.11	−10	1.0	1.75	3.56	4.40	5.25	1	1.1
0.07	1.25	1.79	2.33	−9	1.0	2	5.84	7.19	8.54	1	1.1
0.08	6.56	9.37	12.2	−9	1.0	2.5	1.26	1.54	1.82	2	1.0
0.09	2.65	3.78	4.92	−8	1.0	3	2.23	2.73	3.22	2	1.0
0.1	0.88	1.26	1.63	−7	1.0	3.5	3.50	4.30	5.05	2	1.0
0.11	2.50	3.57	4.65	−7	1.0	4	5.06	6.24	7.29	2	1.0
0.12	6.30	9.01	11.7	−7	1.0	5	0.90	1.12	1.29	3	1.0
0.13	1.44	2.06	2.67	−6	1.0	6	1.38	1.75	1.99	3	1.0
0.14	3.02	4.32	5.62	−6	1.0	7	1.94	2.49	2.79	3	1.0
0.15	5.93	8.48	11.0	−6	1.0	8	2.57	3.34	3.69	3	1.0
0.16	1.10	1.57	2.04	−5	1.0	9	3.24	4.27	4.67	3	1.0
0.18	3.25	4.65	6.04	−5	1.0	10	3.96	5.27	5.71	3	1.0
0.2	0.83	1.18	1.53	−4	1.0						

Reaction: $^{16}O(\alpha,\gamma)^{20}Ne$

The contribution of 23 resonances is considered, the parameters of which are taken from PE64, DI71c, RO71, AL72b, IN76b, ST78, FI80, HA87, KN94 and KU97. An upper limit for the non-resonant contribution is also available from experiments [KN94,KU97]. These data are complemented with many theoretical evaluations of the non-resonant cross section [DE83,LA83, DE86, BA88b,DU94]. The upper limits of the rates are derived from the upper limits of the experimental resonance parameters and of the non-resonant contribution of KN94. The lower limits of the rates are obtained from the use of the lower limits of the resonance parameters and of the non-resonant contribution reported by HA87. All resonance tails are found to have a negligible contribution to the rates. Compared to CA88, the present rates are enhanced at $T_9 < 0.25$ because our adopted S-factor is larger at 300 keV (here: $S(0) = 2$ MeV b; CA88: $S(0) = 0.7$ MeV b).

E_r (keV)	J^π	$\omega\gamma$ (eV)				
		HA87	KN94	others	adopt	
890 ± 3	3^-		$(1.9 \pm 0.3) \times 10^{-3}$		$(1.9 \pm 0.3) \times 10^{-3}$	I
1054 ± 3	1^-	$(2.0 \pm 0.4) \times 10^{-2}$	$(2.3 \pm 0.3) \times 10^{-2}$		$(2.3 \pm 0.3) \times 10^{-2}$	I
1991 ± 3	0^+	$(7.1 \pm 1.2) \times 10^{-2}$	$(7.4 \pm 0.9) \times 10^{-2}$		$(7.4 \pm 0.9) \times 10^{-2}$	M
2424 ± 3	3^-		$(1.08 \pm 0.15) \times 10^{-2}$		$(1.08 \pm 0.15) \times 10^{-2}$	M
2457 ± 3	0^+		$(5.9 \pm 0.9) \times 10^{-2}$		$(5.9 \pm 0.9) \times 10^{-2}$	M
2688 ± 3	2^+		$(1.6 \pm 0.2) \times 10^{-1}$		$(1.6 \pm 0.2) \times 10^{-1}$	M
3094 ± 3	2^+			$(3.4 \pm 0.4) \times 10^{-1}$ [AL72b]	$(3.4 \pm 0.4) \times 10^{-1}$	M
		PE64	FI80			
3975 ± 3	1^-		$(2.1 \pm 0.5) \times 10^{-1}$		$(2.1 \pm 0.5) \times 10^{-1}$	M
4040 ± 10	6^+			1.8 ± 0.4 [LI67] 1.4 ± 0.7 [DI71c] 1.3 ± 0.2 [RO71]	1.35 ± 0.15	M
4291 ± 1	4^+	3.05 ± 0.31		3.05 ± 0.31 [AL72b]	3.05 ± 0.31	M
4382 ± 4	3^-		$(1.8 \pm 0.2) \times 10^{-1}$		$(1.8 \pm 0.2) \times 10^{-1}$	M
4742 ± 30	2^+	1.3 ± 0.5			1.3 ± 0.5	M
5288 ± 30	4^+	8 ± 3			8 ± 3	M
5539 ± 7	2^+	29 ± 4		19.7 ± 1.6 [IN76b] 19.7 ± 2.0 [FI77] 19.2 ± 1.9 [ST78]	19.5 ± 1.5	M
		ST78				
6358 ± 1	4^+	30 ± 4	30 ± 4		30 ± 4	M
6544 ± 5	1^-		2.06 ± 0.25		2.06 ± 0.25	M
6838 ± 6	0^+	$(4.1 \pm 0.5) \times 10^{-1}$	$(4.1 \pm 0.5) \times 10^{-1}$		$(4.1 \pm 0.5) \times 10^{-1}$	M
7193 ± 8	4^+		$(2.3 \pm 0.5) \times 10^{-1}$		$(2.3 \pm 0.5) \times 10^{-1}$	M
7210 ± 10	8^+			$(1.3 \pm 0.2) \times 10^{-1}$ [HU80]	$(1.3 \pm 0.2) \times 10^{-1}$	M
7480 ± 5	2^+		1.4 ± 0.2		1.4 ± 0.2	M
7520 ± 4	3^-		6.6 ± 0.8		6.6 ± 0.8	M
7656 ± 10	3^-	1.94 ± 0.15			1.94 ± 0.15	M
7768 ± 30	3^-	$(1.7 \pm 0.5) \times 10^{-1}$			$(1.7 \pm 0.5) \times 10^{-1}$	M

T_9	low	adopt	high	exp	ratio	T_9	low	adopt	high	exp	ratio
0.1	1.59	7.96	13.4	−27	2.9	0.8	3.07	3.74	4.46	−4	0.9
0.11	0.22	1.09	1.83	−25	2.9	0.9	1.26	1.52	1.81	−3	1.0
0.12	0.22	1.10	1.85	−24	2.9	1	3.89	4.67	5.51	−3	1.0
0.13	1.74	8.68	14.6	−24	2.9	1.25	2.88	3.43	4.00	−2	1.0
0.14	1.12	5.60	9.43	−23	2.9	1.5	1.06	1.25	1.45	−1	1.0
0.15	0.61	3.04	5.13	−22	2.9	1.75	2.61	3.07	3.55	−1	1.1
0.16	0.29	1.43	2.41	−21	2.9	2	5.04	5.91	6.81	−1	1.1
0.18	0.45	2.22	3.74	−20	2.9	2.5	1.23	1.43	1.64	0	1.1
0.2	0.62	2.55	4.22	−19	2.3	3	2.19	2.54	2.91	0	1.1
0.25	3.49	4.96	6.69	−16	0.8	3.5	3.33	3.86	4.40	0	1.1
0.3	2.66	3.56	4.63	−13	0.7	4	4.66	5.40	6.14	0	1.1
0.35	3.03	3.97	5.07	−11	0.8	5	8.32	9.62	11.0	0	0.9
0.4	1.06	1.36	1.72	−9	0.8	6	1.46	1.70	1.94	1	0.8
0.45	1.68	2.14	2.67	−8	0.8	7	2.56	2.99	3.45	1	0.7
0.5	1.55	1.96	2.42	−7	0.8	8	4.34	5.12	5.92	1	0.7
0.6	4.45	5.53	6.73	−6	0.9	9	6.96	8.24	9.56	1	0.7
0.7	4.99	6.12	7.36	−5	0.9	10	1.05	1.24	1.44	2	0.7

Reaction: $^{17}O(p,\gamma)^{18}F$

Direct capture contribution comes from a low energy extrapolation of experimental cross sections [RO73a,RO75a] with about 20% quoted uncertainty. The contribution of the 1^+ $E_r = -3.12$ keV subthreshold resonance is negligible with respect to the direct capture process. Between $T_9 = 0.1$ and 0.2, the rates are dominated by the contribution of the $E_r = 66$ keV resonance. Its strength is calculated using the values $\Gamma = 131 \pm 5$ eV [MA80], $\Gamma_\gamma = 1.4 \pm 0.3$ eV [MA80] and $\Gamma_p = 22^{+7}_{-4}$ neV, as suggested by BL95. This Γ_p value lies between the one obtained by LA89 through a proton transfer experiment and the upper limit of TR95. The strength of the $E_r = 179.5$ keV resonance is unknown. We use the upper limit for its proton width [LA89], the total width $\Gamma = 44 \pm 30$ meV and the average radiative width $\Gamma_\gamma = 22$ meV from RO73c to obtain an upper limit for the strength (in good agreement with RO73b). With these assumptions, it dominates the total rates between $T_9 = 0.1$ and 0.5. In RO73b and KI79a, the measurements are relative to the strength of the 633 keV resonance in $^{27}Al(p,\gamma)^{28}Si$. The adopted values come from the weighted average of the SE73 values and the renormalized ones from RO73b and KI79a (according to the revised $J^\pi = 3^-$, 633 keV resonance strength in $^{27}Al(p,\gamma)^{28}Si$ [EN90]). Resonances at energies $E_r \geqslant 1270$ keV are from SE78. Above $T_9 = 3$, HF estimates are used (see Section 2.5). The enhancements with respect to the CA88 rates near $T_9 = 0.05$ reflect the contribution of the $E_r = 66$ keV resonance, which is not included in CA88. Those near $T_9 = 0.25$ are due to the revised upper limit of the $E_r = 179.5$ keV resonance strength.

E_r (keV)	J^π	$\omega\gamma$ (eV)				
		SE73	RO73b*	Others	adopt	
66.0 ± 0.3	1⁻			$19^{+11}_{-16} \times 10^{-11}$ [LA89] $5.9^{+1.9}_{-1.1} \times 10^{-11}$ [BL95] $\leq 8.60 \times 10^{-11}$ [TR95]	$5.9^{+1.9}_{-1.1} \times 10^{-11*}$	1
179.5 ± 2.4	2⁻		$< 0.42 \times 10^{-3}$	$< 0.6 \times 10^{-3}$ [LA89]	$2.5^{+22}_{-2.5} \times 10^{-5}$	1
489.9 ± 1.1	4⁻	$(6.8 ± 2.0) \times 10^{-3}$	$(21 ± 4) \times 10^{-3}$		$(9 ± 1.6) \times 10^{-3}$	M
501.5 ± 3.0	1⁺		< 0.33		$2^{+18}_{-2} \times 10^{-2}$	M
529.97 ± 0.33	0⁺	$(62 ± 18) \times 10^{-3}$	$(18 ± 5) \times 10^{-2}$		$(75 ± 16) \times 10^{-3}$	M
556.7 ± 0.9	3⁺	$(18 ± 5) \times 10^{-2}$	$(5.6 ± 1.5) \times 10^{-1}$		$(22 ± 5) \times 10^{-2}$	M
633.9 ± 0.8	3⁻	$(11 ± 3) \times 10^{-2}$	$(27 ± 5) \times 10^{-2}$	$(17 ± 4) \times 10^{-2}$ [KI79a]	$(10.6 ± 1.9) \times 10^{-2}$	M
635.5 ± 3.0	3⁻			$(9.7 ± 2.2) \times 10^{-2}$ [KI79a]	$(6.0 ± 1.3) \times 10^{-2}$	M
655.5 ± 2.5	1⁺		$< 1.1 \times 10^{-3}$		$6.5^{+58}_{-6.5} \times 10^{-5}$	M
676.7 ± 0.9	2⁺	$(20.6 ± 6.5) \times 10^{-2}$	$(7.6 ± 1.9) \times 10^{-1}$		$(2.7 ± 0.6) \times 10^{-1}$	M
704.0 ± 0.8	3⁺	$(19.2 ± 6.7) \times 10^{-3}$	$(53 ± 14) \times 10^{-3}$		$(24 ± 5) \times 10^{-3}$	M
779.0 ± 1.7	2⁺	$(17.5 ± 5.4) \times 10^{-3}$	$(50 ± 15) \times 10^{-3}$		$(20.9 ± 4.7) \times 10^{-3}$	M
878.4 ± 1.5	3⁺	$(10 ± 5) \times 10^{-3}$	$(30 ± 12) \times 10^{-3}$		$(12.5 ± 4.2) \times 10^{-3}$	M
960.5 ± 1.5	5⁺	$< 4.2 \times 10^{-3}$	$< 0.2 \times 10^{-3}$		$1.2^{+10}_{-1.2} \times 10^{-5}$	M
1037.2 ± 0.8	2⁻	$(130 ± 43) \times 10^{-3}$	$(3.6 ± 1.0) \times 10^{-1}$		$(160 ± 36) \times 10^{-3}$	M
1170.5 ± 1.4	4⁺	$(52 ± 15) \times 10^{-3}$	$(23 ± 6) \times 10^{-2}$		$(65 ± 14) \times 10^{-3}$	M
1196.6 ± 1.5	1⁺, 2, 3⁺	$(18 ± 5) \times 10^{-3}$	$(45 ± 17) \times 10^{-3}$		$(20.4 ± 4.8) \times 10^{-3}$	M
1270.9 ± 1.7	3, 4⁻	$(16.7 ± 5.4) \times 10^{-3}$	$(83 ± 33) \times 10^{-3}$		$(18.9 ± 5.2) \times 10^{-3}$	M
Res. 1729.5–1977.5 keV				see comments		

*see comments

T_9	low	adopt	high	exp	ratio	T_9	low	adopt	high	exp	ratio
0.009	3.61	4.52	5.42	−26	0.8	0.2	0.05	1.46	15.7	−3	1.5
0.01	5.39	6.73	8.08	−25	0.8	0.25	0.20	8.24	87.8	−3	1.6
0.011	5.71	7.14	8.57	−24	0.8	0.3	0.06	2.52	26.4	−2	1.5
0.012	4.61	5.77	6.92	−23	0.8	0.35	0.36	5.78	57.0	−2	1.3
0.013	2.99	3.73	4.48	−22	0.8	0.4	0.24	1.28	10.5	−1	0.9
0.014	1.61	2.01	2.41	−21	0.8	0.45	1.16	3.11	18.8	−1	0.7
0.015	7.43	9.29	11.1	−21	0.8	0.5	4.07	7.90	34.6	−1	0.6
0.016	3.01	3.76	4.51	−20	0.8	0.6	2.65	4.12	11.9	0	0.5
0.018	3.57	4.47	5.37	−19	0.9	0.7	0.99	1.45	3.45	1	0.5
0.02	3.05	3.82	4.62	−18	0.9	0.8	2.63	3.74	8.06	1	0.5
0.025	2.95	3.83	4.99	−16	1.3	0.9	5.55	7.75	15.7	1	0.5
0.03	1.62	2.17	3.05	−14	2.8	1	1.00	1.38	2.67	2	0.5
0.04	4.89	6.54	9.30	−12	7.8	1.25	2.76	3.75	6.77	2	0.4
0.05	1.62	2.13	2.98	−10	9.0	1.5	5.26	7.06	12.2	2	0.4
0.06	1.65	2.14	2.96	−9	7.1	1.75	0.81	1.08	1.81	3	0.4
0.07	0.87	1.12	1.56	−8	4.8	2	1.10	1.45	2.38	3	0.4
0.08	3.11	4.06	6.57	−8	3.1	2.5	1.61	2.11	3.36	3	0.4
0.09	0.88	1.25	3.29	−7	1.9	3	2.00	2.61	4.07	3	0.4
0.1	2.15	3.89	18.8	−7	1.3	3.5	2.59	3.25	4.77	3	0.4
0.11	0.48	1.28	9.32	−6	1.1	4	3.11	3.87	5.46	3	0.4
0.12	0.98	4.12	37.2	−6	1.1	5	4.01	5.14	7.15	3	0.4
0.13	0.19	1.21	12.1	−5	1.1	6	4.78	6.59	9.55	3	0.5
0.14	0.35	3.17	33.2	−5	1.2	7	5.48	8.29	12.9	3	0.6
0.15	0.62	7.41	79.4	−5	1.3	8	0.62	1.03	1.74	4	0.6
0.16	0.10	1.57	16.9	−4	1.3	9	0.68	1.25	2.31	4	0.7
0.18	0.25	5.43	58.9	−4	1.4	10	0.75	1.50	3.01	4	0.8

Reaction: $^{17}O(p,\alpha)^{14}N$

For $0.02 \leqslant T_9 \leqslant 0.1$, the rates are dominated by the contribution of the $E_r = 66$ keV resonance [MA80, LA89, BL95, NI97] for which strength we adopt the value of BL95. A lower value of the upper limit is reported by BE92a, but a recent analysis of BE92a data following a different hypothesis for the experimental background [NI97], leads an upper limit which is not in contradiction with BL95 [see also $^{17}O(p,\gamma)^{18}F$]. For $T_9 < 0.02$, the contributions from the tails of high energy resonances and of a 1^+ subthreshold state ($E_r = -3.12$ keV, $\Gamma_\alpha = 42.8 \pm 1.6$ eV [MA80], $\gamma^2 = 0.12\gamma_W^2$ at 3.6 fm) must also be considered. The strength of the $E_r = 179.5$ keV resonance is calculated using $\Gamma_p \leqslant 2.8$ meV from LA89, and $\Gamma = 44 \pm 30$ meV and $\Gamma_\alpha = 22$ meV from RO73c. In the $489.9 \leqslant E_r \leqslant 1202.5$ keV range, the resonance strengths measured by BR62, KI79a and KI79b are in fair agreement. Above $E_r = 1594.5$ keV, the only available data come from SE78. Above $T_9 = 6$, HF estimates are used (see Section 2.5). The ratio between the adopted rates and the CA88 ones shows enhancements by a factor of up to about 100 at $T_9 \leqslant 0.2$, due to the strengths of the two lowest resonances adopted here, and the contribution of the subthreshold state. The differences at the highest temperatures are due to our use of HF rates.

E_r (keV)	J^π	$\omega\gamma$ (eV)				
		BR62	KI79a	Others	adopt	
66.0 ± 0.3	1−			$5.5^{+1.8}_{-1.5} \times 10^{-9}$ [BL95] $18.3^{+9.9}_{-14.1} \times 10^{-9}$ [LA89] $\leqslant 22 \times 10^{-9}$ [NI97]	$5.5^{+1.8}_{-1.5} \times 10^{-9}$ ★	I
179.5 ± 2.4	2−	50 ± 5	47.9 ± 5.4	$\leqslant 5.8 \times 10^{-4}$ ★ $\leqslant 4.2 \times 10^{-4}$ [RO73c]	$5.8^{+52}_{-5.8} \times 10^{-5}$ ★	I
489.9 ± 1.1	4−				49.0 ± 3.7	I
529.97 ± 0.33	0+			$\leqslant 0.17$ [RO73c]	$1.7^{+1.5}_{-1.7} \times 10^{-2}$	M
556.7 ± 0.9	3+			2.25 ± 0.42 [RO73c]	2.25 ± 0.42	M
633.9 ± 0.8	3−	43 ± 4	29.8 ± 3.5 [KI79b]		35.5 ± 2.6	M
635.5 ± 3	3−		19.7 ± 2.3 [KI79b]		19.7 ± 2.3	M
655.5 ± 2.5	1+		5.0 ± 0.6		5.0 ± 0.6	M
676.7 ± 0.9	2+			5.8 ± 1.2 [RO73c]	5.8 ± 1.2	M
704.0 ± 0.8	3+	100 ± 10	97.0 ± 10.4		98.6 ± 7.2	M
779.0 ± 1.7	2+	23 ± 2	24.3 ± 2.7		23.4 ± 1.6	M
878.4 ± 1.5	3+	39 ± 4	37.6 ± 4.2		38.4 ± 2.9	M
960.5 ± 1.5	5+		1.04 ± 0.22		1.04 ± 0.22	M
1037.2 ± 0.8	2−	36 ± 4	38.9 ± 4.8		37.2 ± 3.1	M
1040.5 ± 4	1−	150 ± 16			150 ± 16	M
1170.5 ± 1.4	4+		109 ± 15		109 ± 15	M
1202.5 ± 5	2−	$(4.93 \pm 0.34) \times 10^3$			$(4.93 \pm 0.34) \times 10^3$	M
Res. 1594.5–2602.5 keV				see comments		

*see comments

T_9	low	adopt	high	exp	ratio	T_9	low	adopt	high	exp	ratio
0.009	0.91	1.27	1.65	−25	20	0.2	0.31	3.60	37.7	−3	2.9
0.01	1.22	1.71	2.21	−24	18	0.25	0.87	2.85	21.9	−2	0.8
0.011	1.19	1.65	2.13	−23	16	0.3	2.65	3.55	9.59	−1	0.6
0.012	0.89	1.23	1.59	−22	14	0.35	3.15	3.66	5.27	0	0.7
0.013	5.43	7.46	9.63	−22	13	0.4	1.99	2.25	2.70	1	0.8
0.014	2.78	3.80	4.91	−21	12	0.45	8.25	9.23	10.5	1	0.9
0.015	1.23	1.68	2.17	−20	11	0.5	2.55	2.84	3.18	2	1.0
0.016	4.91	6.63	8.56	−20	10	0.6	1.36	1.51	1.67	3	1.0
0.018	6.60	8.71	11.3	−19	10	0.7	4.45	4.93	5.43	3	1.0
0.02	1.07	1.35	1.77	−17	13	0.8	1.08	1.19	1.31	4	1.0
0.025	0.92	1.13	1.49	−14	28	0.9	2.14	2.37	2.60	4	1.0
0.03	1.12	1.37	1.81	−12	39	1	3.72	4.11	4.50	4	1.0
0.04	4.28	5.23	6.90	−10	57	1.25	1.03	1.13	1.24	5	0.9
0.05	1.41	1.73	2.28	−8	71	1.5	2.12	2.34	2.57	5	0.9
0.06	1.38	1.69	2.23	−7	81	1.75	3.75	4.16	4.57	5	0.9
0.07	6.82	8.34	11.0	−7	88	2	5.99	6.69	7.40	5	1.0
0.08	2.20	2.69	3.58	−6	86	2.5	1.24	1.42	1.59	6	1.1
0.09	5.37	6.59	9.09	−6	72	3	2.13	2.49	2.84	6	1.2
0.1	1.08	1.35	2.10	−5	47	3.5	3.21	3.82	4.44	6	1.3
0.11	1.89	2.47	5.08	−5	25	4	4.41	5.35	6.31	6	1.4
0.12	2.99	4.33	13.3	−5	13	5	7.39	9.12	10.9	6	1.5
0.13	4.40	7.63	35.2	−5	8.3	6	1.05	1.37	1.74	7	1.7
0.14	0.61	1.38	8.76	−4	5.9	7	1.46	1.90	2.40	7	1.8
0.15	0.82	2.54	20.0	−4	4.8	8	1.89	2.46	3.12	7	1.9
0.16	1.06	4.63	41.6	−4	4.3	9	2.35	3.06	3.87	7	2.0
0.18	0.17	1.40	14.2	−3	3.7	10	2.83	3.67	4.64	7	2.1

Reaction: $^{17}O(\alpha,n)^{20}Ne$
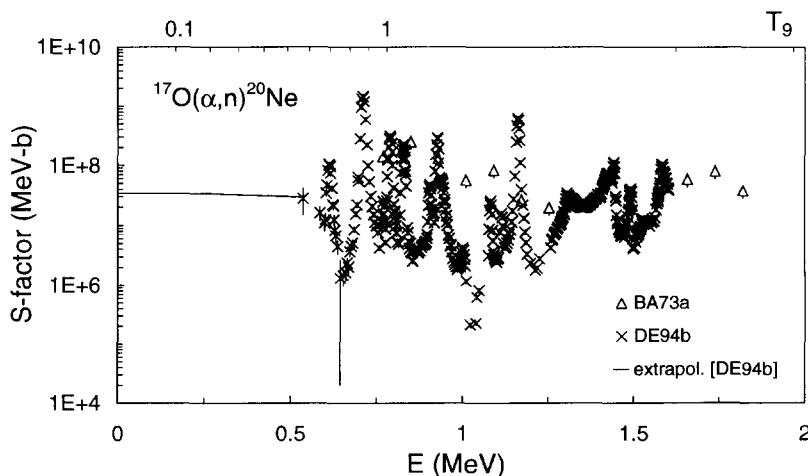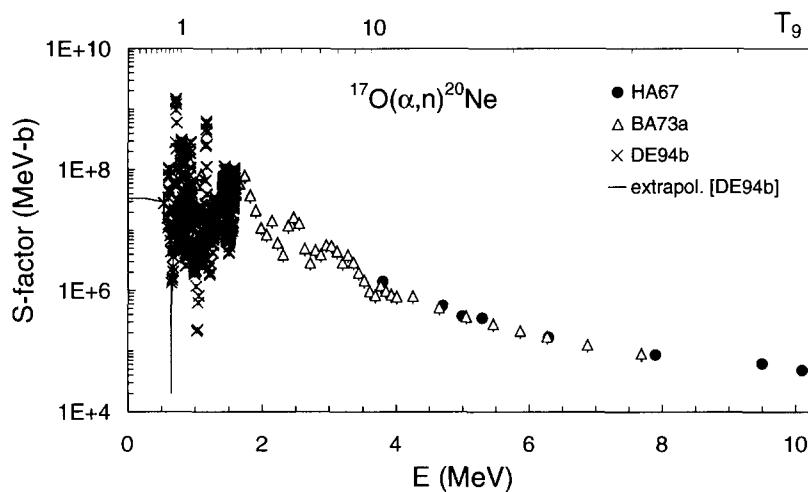
Data from HA67, BA73a and DE94b covering the energy range $0.56 \leqslant E \leqslant 10.1$ MeV are adopted. The results of DE94b are partially documented in KU95. Below 0.56 MeV, the extrapolation of DE94b, based on a statistical model calculation, is adopted for the recommended rates. The lower limit of the rates relies on a three-cluster microscopic calculation by DE93c. The upper limit of the rates is obtained by including all possible resonances with strengths equal to the Wigner limit. The differences between the CA88 and adopted rates at low temperatures are probably due to a different extrapolation, while the discrepancy at high temperatures likely results from the higher accuracy of our numerical treatment.

T_9	low	adopt	high	exp	ratio	T_9	low	adopt	high	exp	ratio
0.07	0.09	2.27	38.9	−24	0.5	0.7	2.49	2.74	3.00	−2	1.1
0.08	0.06	1.41	30.0	−22	0.5	0.8	1.29	1.42	1.55	−1	1.0
0.09	0.21	4.60	105	−21	0.5	0.9	5.33	5.87	6.41	−1	0.9
0.1	0.46	9.25	210	−20	0.5	1	1.87	2.07	2.28	0	0.9
0.11	0.07	1.27	27.5	−18	0.5	1.25	2.43	2.79	3.14	1	0.9

continued from previous page

T_9	low	adopt	high	exp	ratio	T_9	low	adopt	high	exp	ratio
0.12	0.08	1.30	25.7	−17	0.5	1.5	1.68	1.98	2.29	2	1.0
0.13	0.07	1.03	18.3	−16	0.5	1.75	7.35	8.91	10.5	2	1.0
0.14	0.55	6.67	105	−16	0.5	2	2.34	2.90	3.45	3	1.0
0.15	0.34	3.63	51.5	−15	0.5	2.5	1.30	1.65	2.00	4	1.0
0.16	0.18	1.71	22.3	−14	0.5	3	4.38	5.65	6.93	4	0.9
0.18	0.36	2.64	31.2	−13	0.5	3.5	1.11	1.44	1.78	5	0.9
0.2	0.48	2.79	31.1	−12	0.5	4	2.30	3.02	3.74	5	0.9
0.25	1.16	3.33	27.5	−10	0.5	5	6.90	9.12	11.3	5	1.1
0.3	1.01	1.64	6.95	−8	0.7	6	1.53	2.02	2.52	6	1.3
0.35	3.30	4.21	9.30	−7	1.0	7	2.80	3.73	4.65	6	1.6
0.4	4.92	5.77	8.74	−6	1.4	8	4.56	6.06	7.57	6	2.0
0.45	4.16	4.72	6.01	−5	1.6	9	6.80	9.05	11.3	6	2.6
0.5	2.34	2.62	3.09	−4	1.6	10	0.95	1.27	1.58	7	3.4
0.6	3.34	3.69	4.12	−3	1.4						
T_9	low	adopt	high	exp	ratio	T_9	low	adopt	high	exp	ratio

Reaction: ^{18}O(p,γ)^{19}F

The contribution of 20 resonances between $E_r = 20$ and 1893 keV is considered. At higher energies, most data come from WI80, where the reaction has been investigated for $76 \leqslant E \leqslant 2083$ keV, while BE82 and VO90 have studied the low energy resonances. The main contribution to the rates comes from the three low energy resonances at $E_r = 20$, 89 and 143.5 keV. In CA88, CH86a is quoted as the source of data for the $E_r = 20$ keV resonance. However, CH86a only gives the proton width $\Gamma_p = 2 \times 10^{-19}$ eV from a DWBA analysis of a ^{18}O(^{3}He,d)^{19}F measurement. Another value, $\Gamma_p = 6.7 \times 10^{-19}$ eV, is reported in WI80 from the analysis of a direct capture transition to that state. No published values of Γ_γ or Γ exist, but $\Gamma_\gamma = 2.3$ eV and $\Gamma_\alpha \sim 2.5$ keV are estimated in WI80. The first value corresponds to 28 Weisskopf units and the second to 1% of the Wigner limit. In the absence of other data, we use these values together with the CH86a data to obtain a rough estimate of $\omega\gamma = 6 \times 10^{-22}$ eV with an uncertainty of a factor 100. Consequently, below $T_9 = 0.02$, the present rates are lower than the CA88 ones by one order of magnitude, but the CA88 rates are within the proposed upper and lower limits. A non-resonant contribution (direct capture [WI80] and low energy tail of the $E_r = 143.5$ keV resonance) is also added, being important between $T_9 = 0.014$ and 0.03. Above $T_9 = 2$, the rates are calculated using HF rates (see Section 2.5). Around $T_9 = 0.05$, the adopted rates are higher than the CA88 ones because of the $E_r = 89$ keV isolated resonance, which is missing in CA88.

T_9	low	adopt	high	exp	ratio	T_9	low	adopt	high	exp	ratio
0.009	1.11	8.54	2660	−25	0.1	0.2	4.61	4.87	5.12	−1	1.1
0.01	0.17	1.01	263	−23	0.1	0.25	1.59	1.68	1.77	0	1.0
0.011	1.79	7.84	1690	−23	0.1	0.3	3.65	3.85	4.05	0	1.0
0.012	1.45	4.59	791	−22	0.1	0.35	6.39	6.74	7.10	0	1.0
0.013	0.95	2.21	289	−21	0.1	0.4	0.95	1.00	1.06	1	1.0
0.014	5.15	9.39	871	−21	0.2	0.45	1.27	1.34	1.42	1	1.0
0.015	2.40	3.64	226	−20	0.2	0.5	1.59	1.69	1.78	1	1.0
0.016	0.98	1.31	51.8	−19	0.3	0.6	2.22	2.36	2.50	1	1.0
0.018	1.18	1.39	21.0	−18	0.5	0.7	2.90	3.11	3.33	1	0.9
0.02	1.01	1.13	6.90	−17	0.7	0.8	3.84	4.20	4.57	1	0.9
0.025	7.55	8.24	12.6	−16	1.0	0.9	5.35	5.97	6.61	1	0.8
0.03	2.05	2.30	2.98	−14	1.0	1	7.74	8.81	9.91	1	0.8
0.04	2.67	5.39	15.1	−12	2.0	1.25	1.96	2.28	2.62	2	0.8
0.05	1.50	4.75	14.4	−10	3.6	1.5	4.17	4.89	5.63	2	0.9
0.06	1.25	2.07	4.08	−8	2.0	1.75	7.39	8.67	9.98	2	0.9
0.07	4.60	5.55	7.40	−7	1.4	2	1.13	1.32	1.51	3	0.9
0.08	7.06	7.81	8.95	−6	1.2	2.5	2.27	2.71	3.14	3	1.0
0.09	5.84	6.28	6.85	−5	1.2	3	3.79	4.62	5.46	3	1.1
0.1	3.12	3.32	3.55	−4	1.1	3.5	5.64	7.03	8.43	3	1.3
0.11	1.21	1.28	1.36	−3	1.1	4	7.71	9.86	12.0	3	1.4
0.12	3.72	3.93	4.16	−3	1.1	5	1.22	1.64	2.07	4	1.6
0.13	0.95	1.00	1.06	−3	1.1	6	1.65	2.36	3.07	4	1.7
0.14	2.11	2.23	2.35	−2	1.1	7	2.01	3.08	4.16	4	1.8
0.15	4.17	4.40	4.64	−2	1.1	8	2.27	3.77	5.27	4	1.9
0.16	7.54	7.96	8.38	−2	1.1	9	2.40	4.39	6.37	4	1.9
0.18	1.99	2.10	2.21	−1	1.0	10	2.41	4.93	7.44	4	2.0

E_r (keV)	J^π	$\omega\gamma$ (eV)			
		WI80	others	adopt	
20 ± 1	$5/2^+$		$6^{+594}_{-6} \times 10^{-22}$*	$6^{+594}_{-6} \times 10^{-22}$	I
89 ± 3		$\leqslant 5 \times 10^{-8}$	$(2 \pm 2) \times 10^{-8}$ [VO90]	$(2 \pm 2) \times 10^{-8}$	I
143.5 ± 1.2	$1/2^+$	$(1.0 \pm 0.1) \times 10^{-3}$	$(1.1 \pm 0.1) \times 10^{-3}$ [BE82] $(0.92 \pm 0.06) \times 10^{-3}$ [VO90]	$(0.97 \pm 0.05) \times 10^{-3}$	I
204.8 ± 1.3	$(5/2^+)$	$\geqslant 0.8 \times 10^{-5}$	$(5.0 \pm 1.0) \times 10^{-6}$ [VO90]	$(5.0 \pm 1.0) \times 10^{-6}$	M
260.0 ± 2.8	$(3/2 - 7/2)^-$	$(3.7 \pm 0.5) \times 10^{-5}$		$(3.7 \pm 0.5) \times 10^{-5}$	M
315.8 ± 1.5	$5/2^+$	$(0.95 \pm 0.08) \times 10^{-3}$		$(0.95 \pm 0.08) \times 10^{-3}$	M
589.2 ± 1.8	$5/2^+$	$(10 \pm 2) \times 10^{-3}$		$(10 \pm 2) \times 10^{-3}$	M
597.7 ± 1.3	$3/2^-$	0.10 ± 0.02		0.10 ± 0.02	M
799.0 ± 1.7	$1/2^+$	1.4 ± 0.2		1.4 ± 0.2	M
932.5 ± 0.7	$3/2^+$	$(1.5 \pm 0.2) \times 10^{-2}$		$(1.5 \pm 0.2) \times 10^{-2}$	M
1105.5 ± 0.7	$7/2^-$	0.31 ± 0.10	0.29 ± 0.03 [BE82]	0.29 ± 0.03	M
1323.8 ± 2.2	$3/2^+$	0.08 ± 0.01		0.08 ± 0.01	M
1542.1 ± 2.2	$5/2^+$	0.025 ± 0.005		0.025 ± 0.005	M
1572 ± 3	$3/2^-$	0.041 ± 0.010		0.041 ± 0.010	M
1581 ± 4	$3/2^-$	0.06 ± 0.01		0.06 ± 0.01	M
1592 ± 3	$7/2$	0.025 ± 0.004		0.025 ± 0.004	M
1673.3 ± 1.5	$3/2^+$	1.2 ± 0.2		1.2 ± 0.2	M
1825.8 ± 1.0	$5/2^-$	2.8 ± 0.7		2.8 ± 0.7	M
1879.8 ± 1.8	$11/2^-$	0.13 ± 0.04		0.13 ± 0.04	M
1893 ± 3	$1/2^+$	0.14 ± 0.05		0.14 ± 0.05	M

*see comments

Reaction $^{18}O(p,\alpha)^{15}N$

A total of 50 resonances between $E_r = 20$ and 6746 keV [CA61,YA62, MA78b, LO79, WI82, CH86a,BE95] are considered for the calculation of the reaction rates. The resonances at 20, 143.5 and 656 keV dominate the rates. The $E_r = 20$ keV resonance strength is based on proton spectroscopic factors ($\omega\gamma \approx \omega\Gamma_p$) extracted by DWBA analysis from (^{3}He,d) tranfer reactions [SC70,CH86a] and from direct capture measurements [WI80]. A large part of the error on the reaction rates comes from the energy determination of that resonance. The resonance at $E_r = 143.5$ keV is fairly well established. The broad resonance at $E_r = 655.8$ keV gives strong contributions both at low and high temperatures. The total width of that high energy resonance is badly known. The two sets of widths available from YA62 and LO79 are used for numerical integration, and the average of the resulting rates is adopted. For the other broad resonance at $E_r = 799$ keV, which gives a significant contribution at high temperatures, the partial widths from YA62 are adopted. The contribution of this resonance is obtained by numerical integration. The table shows the adopted strengths for the first 24 resonances. In the energy range from 3.0 to 6.05 MeV, the adopted resonance strengths are weighted averages between the values of OR73 and AL75a. Between 6.1 and 6.75 MeV, the values from MU79 are adopted. For the upper and lower bounds of the rates at low temperatures, the limits given by MA78b for the S-factor are adopted. By transfer reaction, CH86a have derived an upper limit for the possible contribution of the sub-threshold level at $E_x = 7.9$ MeV ($E_r = -94$ keV) which turns out to be negligible. The updated contribution of the 656 keV broad resonance accounts for the differences with the CA88 rates at high ($T_9 > 0.45$) temperatures.

T_9	low	adopt	high	exp	ratio	T_9	low	adopt	high	exp	ratio
0.007	1.53	8.32	18.3	−25	0.9	0.18	3.00	3.50	4.09	1	1.1
0.008	0.65	4.13	73.9	−23	0.9	0.2	6.52	7.57	8.78	1	1.1
0.009	1.49	8.85	135	−22	1.0	0.25	2.52	2.90	3.35	2	1.1
0.01	0.21	1.05	14.3	−20	1.0	0.3	6.00	6.91	8.05	2	1.1
0.011	2.02	8.34	101	−20	1.0	0.35	1.10	1.29	1.54	3	1.1
0.012	1.50	5.00	54.4	−19	1.1	0.4	1.78	2.14	2.65	3	1.1
0.013	0.90	2.48	23.7	−18	1.1	0.45	2.77	3.45	4.46	3	1.0
0.014	0.47	1.08	8.83	−17	1.2	0.5	4.45	5.70	7.56	3	0.9
0.015	2.04	4.31	29.1	−17	1.2	0.6	1.36	1.72	2.21	4	0.6
0.016	0.80	1.58	8.73	−16	1.3	0.7	4.29	5.09	6.08	4	0.5
0.018	0.92	1.71	6.35	−15	1.3	0.8	1.17	1.31	1.47	5	0.4
0.02	0.76	1.40	3.83	−14	1.4	0.9	2.69	2.89	3.12	5	0.4
0.025	5.45	9.94	20.1	−13	1.4	1	5.31	5.58	5.86	5	0.3
0.03	1.43	2.61	5.07	−11	1.3	1.25	1.84	1.87	1.91	6	0.3
0.04	1.68	3.07	5.98	−9	1.3	1.5	4.15	4.20	4.25	6	0.3
0.05	0.56	1.01	1.93	−7	1.3	1.75	7.29	7.39	7.48	6	0.4
0.06	1.90	2.91	4.70	−6	1.2	2	1.09	1.11	1.13	7	0.4
0.07	5.82	7.93	11.0	−5	1.1	2.5	1.86	1.91	1.95	7	0.4
0.08	0.90	1.17	1.52	−3	1.1	3	2.56	2.65	2.74	7	0.4
0.09	7.60	9.63	12.2	−3	1.1	3.5	3.14	3.27	3.42	7	0.4
0.1	4.17	5.19	6.44	−2	1.1	4	3.60	3.79	3.99	7	0.4
0.11	1.66	2.04	2.49	−1	1.1	5	4.27	4.58	4.92	7	0.5
0.12	5.19	6.30	7.62	−1	1.1	6	4.73	5.20	5.72	7	0.5
0.13	1.35	1.62	1.95	0	1.1	7	5.13	5.79	6.53	7	0.5
0.14	3.04	3.62	4.31	0	1.1	8	5.51	6.42	7.43	7	0.6
0.15	6.09	7.22	8.54	0	1.1	9	5.92	7.11	8.42	7	0.7
0.16	1.11	1.31	1.54	1	1.1	10	6.37	7.85	9.48	7	0.8
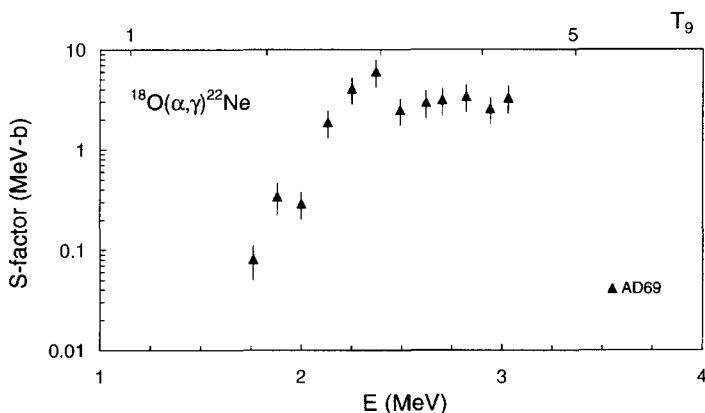
E_r (keV)	J^π	$\omega\gamma$ (eV)					I
		YA62	KA65	LO79	others	adopt	
20 ± 1	5/2+				1.5×10^{-19} [SC70] 2×10^{-18} [WI80] 6×10^{-19} [CH86a]	$6^{+17}_{-5} \times 10^{-19\star}$	I
89 ± 3				$(1.6 \pm 0.5) \times 10^{-7}$		$(1.6 \pm 0.5) \times 10^{-7}$	M
143.5 ± 1.2	1/2+			0.17 ± 0.02	0.167 ± 0.012 [BE95]	0.167 ± 0.012	I
204.8 ± 1.0	(5/2+)			$(2.3 \pm 0.6) \times 10^{-3}$		$(2.3 \pm 0.6) \times 10^{-3}$	M
315.8 ± 1.2	5/2+			0.057 ± 0.010		0.05 ± 0.01	M
597.7 ± 0.4	3/2-	118 ± 19		420 ± 80	110 [MA78b]	116 ± 18	M
655.8	1/2+	4500		$\approx 1.22 \times 10^5$		$(5.5 \pm 1.0) \times 10^{3\star}$	M
799.0 ± 1.5	1/2+	$(11 \pm 1) \times 10^3$		$(4.1 \pm 1.0) \times 10^4$	11.6×10^3 [CA61]	$(11.2 \pm 0.4) \times 10^3$	M
932.5 ± 0.7	3/2-	147 ± 19				147 ± 19	M
1106.8 ± 0.5	7/2+	18 ± 5				18 ± 5	M
1172.8 ± 1.4	1/2+	351 ± 41				351 ± 41	M
1326.8 ± 1.1	1/2+	213 ± 27				213 ± 27	M
				SE69			
1673.3 ± 1.5	3/2+		1910	1658		1773 ± 115	M
1825.8 ± 1.0	5/2			127		127 ± 23	M
1893 ± 3	1/2+		7470	6968	6809 [CA61]	7150 ± 340	M
2168 ± 3	1/2+			660		660 ± 330	M
2238 ± 3	1/2+		1054	1002		1028 ± 26	M
2260 ± 3	3/2+		11×10^3	11.3×10^3		$(11.15 \pm 0.15) \times 10^3$	M
2314 ± 4	3/2+		4573	4571		4572 ± 300	M
2503.8 ± 1.3	3/2+			988		988 ± 494	M
2620.8 ± 1.6	5/2+			547 ± 273		547 ± 273	M
2769.8 ± 2.5	1/2-			897.5		898 ± 60	M
2867.2 ± 1.9	5/2+			$(12 \pm 6) \times 10^3$		$(12 \pm 6) \times 10^3$	M
2980.8 ± 2.5	(3/2,5/2)+			$(3.3 \pm 1.7) \times 10^3$		$(3.3 \pm 1.7) \times 10^3$	M
Res. 3000–6750 keV				see comments			

*see comments

Reaction: $^{18}O(\alpha,\gamma)^{22}Ne$

The experimental data from AD69, GR68, CH70, TR78, VO90, and GI94 up to $E_r = 4025$ keV are adopted. Resonance data for $E_r = 2814 - 4025$ keV come from CH70. These data complement each other and allow the calculation of the rates at $T_9 \leqslant 6$. Up to $T_9 = 1$, the reaction rates are determined by the resonant contributions, the direct capture and resonant tail contributions being predicted to be negligible [TR78]. Above $T_9 = 6$, the rates are calculated using HF rates as explained in Section 2.5. The adopted rates agree with those obtained by GI94. The difference between the adopted rates and the CA88 ones are due to the contribution of the new low energy resonances from GI94. In CA88, a low energy resonance has been considered, but with a strength and energy that differ from those of GI94. Our thermalization corrections cannot account for these differences ($r_{tt} = 0.94 - 0.88$ for $T_9 = 7$ to 10; CA88 adopted $r_{tt} = 1$ at all T_9).
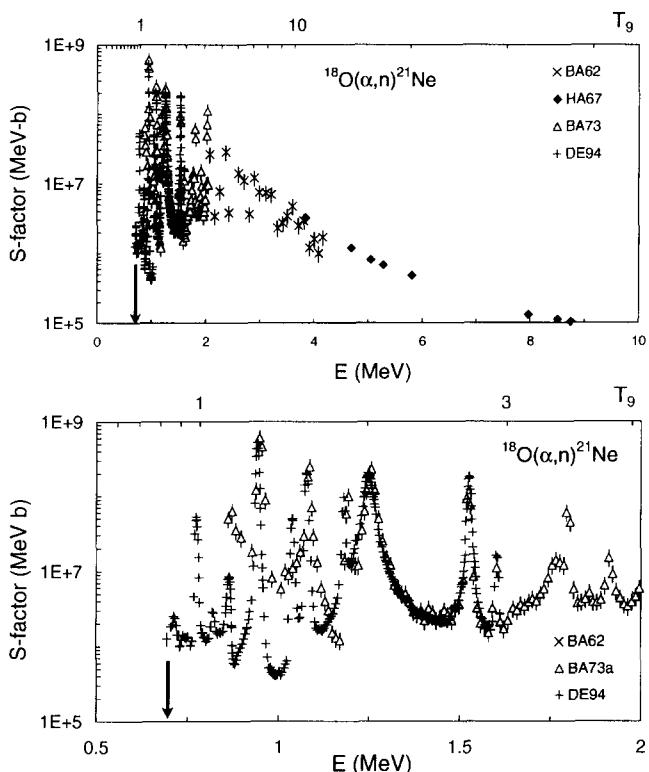
T_9	low	adopt	high	exp	ratio	T_9	low	adopt	high	exp	ratio
0.07	0.92	1.53	2.14	−24	0.1	0.7	3.53	3.94	4.42	−3	1.1
0.08	3.04	5.08	7.17	−23	0.1	0.8	1.00	1.11	1.24	−2	1.2
0.09	5.36	9.20	15.3	−22	0.1	0.9	2.21	2.46	2.74	−2	1.2
0.1	1.45	2.73	6.73	−20	0.4	1	4.15	4.63	5.14	−2	1.2
0.11	0.55	1.09	2.98	−18	3.0	1.25	1.34	1.51	1.69	−1	1.3
0.12	1.38	2.72	7.56	−17	19	1.5	3.64	4.34	5.04	−1	1.3
0.13	2.14	4.20	11.7	−16	86	1.75	1.10	1.42	1.76	0	1.4
0.14	2.22	4.36	12.1	−15	225	2	3.43	4.71	6.01	0	1.6
0.15	1.68	3.29	9.17	−14	219	2.5	2.27	3.27	4.25	1	1.8
0.16	0.98	1.92	5.35	−13	125	3	0.87	1.27	1.65	2	1.9
0.18	1.86	3.62	9.98	−12	38	3.5	2.30	3.34	4.38	2	2.0
0.2	1.99	3.79	10.3	−11	15	4	4.74	6.88	9.02	2	1.9
0.25	1.78	2.95	7.04	−9	3.0	5	1.28	1.85	2.42	3	1.7
0.3	5.30	7.33	13.7	−8	1.5	6	2.39	3.47	4.54	3	1.5
0.35	7.58	9.38	14.1	−6	1.1	7	3.68	6.05	8.41	3	1.5
0.4	6.10	7.16	9.38	−6	1.1	8	4.75	9.22	13.7	3	1.4
0.45	3.17	3.63	4.43	−5	1.0	9	0.52	1.27	2.02	4	1.3
0.5	1.19	1.35	1.59	−4	1.1	10	0.47	1.64	2.79	4	1.3
0.6	8.68	9.74	11.1	−4	1.1						

E_r (keV)	J^π	$\omega\gamma$ (eV)				
		CH70	TR78	others	adopt	
178.3 ± 3.3	2^+			$(7.5 \pm 3.0) \times 10^{-18}$ [GI94]	$(7.5 \pm 3.0) \times 10^{-18}$	I
384.5 ± 3.3	0^+			$(0.6^{+1.1}_{-0.3}) \times 10^{-6}$ [GI94]	$(0.6^{+1.1}_{-0.3}) \times 10^{-6}$	I
541.6 ± 8.2	1^-		$(2.9 \pm 0.5) \times 10^{-4}$	$(2.12 \pm 0.42) \times 10^{-4}$ [GI94] $(2.30 \pm 0.25) \times 10^{-4}$ [VO90]	$(2.39 \pm 0.23) \times 10^{-4}$	I
613.5 ± 8.2			$(4.7 \pm 0.8) \times 10^{-4}$	$(5.6 \pm 0.6) \times 10^{-4}$ [VO90]	$(5.3 \pm 0.5) \times 10^{-4}$	M
628.0 ± 8.2			$\geqslant 6.7 \times 10^{-4}$	$(1.20 \pm 0.12) \times 10^{-3}$ [VO90]	$(1.20 \pm 0.12) \times 10^{-3}$	I
947.3 ± 4.2			$(4.1 \pm 1.0) \times 10^{-4}$		$(4.1 \pm 1.0) \times 10^{-4}$	M
1026.0 ± 3.3			$(1.3 \pm 0.2) \times 10^{-3}$		$(1.3 \pm 0.2) \times 10^{-3}$	M
1255.0 ± 4.1			$(6.5 \pm 0.8) \times 10^{-2}$		$(6.5 \pm 0.8) \times 10^{-2}$	M
1800.0 ± 4.1	1^-	2.7 ± 0.4	0.48 ± 0.07		0.48 ± 0.07	M
2015.0 ± 5.0	2^+	31 ± 10			31 ± 10	M
2084.0 ± 5.0	1^-	0.87 ± 0.31			0.87 ± 0.31	M
		GR68				
2217.0 ± 5.0	1^-	2.13 ± 0.6			2.13 ± 0.6	M
2610.0 ± 5.0	1^-	14.1 ± 4.0			14.1 ± 4.0	M
Res. 2814–4025 keV				see comments		

Reaction: $^{18}O(\alpha,n)^{21}Ne$

The rates are calculated from the data of BA62, HA67, BA73a and DE94b using a spline interpolation, covering the energy range from threshold ($Q = -0.697$ MeV) to 10.2 MeV. The results of DE94b are partially documented in KU95. At low energy, the data of DE94b are used only as the BA73 data may be affected by some background problems. The upper and lower limits of the rates are based on the uncertainties set by the experiments. The differences (up to a factor of 10) between the CA88 and adopted rates in the temperature range $0.14 \leqslant T_9 \leqslant 0.70$ are due to recent experimental data down to the threshold energy.

T_9	low	adopt	high	exp	ratio	T_9	low	adopt	high	exp	ratio
0.14	1.26	1.41	1.56	−24	0.1	1	1.31	1.36	1.40	0	1.0
0.15	6.11	6.80	7.49	−23	0.1	1.25	1.64	1.75	1.85	1	1.0
0.16	1.85	2.04	2.24	−21	0.1	1.5	1.07	1.20	1.32	2	0.9
0.18	5.61	6.14	6.66	−19	0.1	1.75	4.82	5.69	6.55	2	1.0
0.2	5.62	6.08	6.54	−17	0.1	2	1.69	2.07	2.45	3	1.0
0.25	2.50	2.66	2.81	−13	0.2	2.5	1.17	1.50	1.83	4	1.1
0.3	7.98	8.36	8.73	−11	0.2	3	4.79	6.26	7.72	4	1.1
0.35	5.86	6.07	6.29	−9	0.2	3.5	1.39	1.83	2.27	5	1.1
0.4	1.69	1.74	1.80	−7	0.2	4	3.22	4.25	5.29	5	1.1

<div align="center">continued on next page</div>

T_9	low	adopt	high	exp	ratio	T_9	low	adopt	high	exp	ratio
0.45	2.54	2.61	2.68	−6	0.3	5	1.12	1.47	1.83	6	1.1
0.5	2.35	2.41	2.47	−5	0.4	6	2.71	3.55	4.38	6	1.1
0.6	7.36	7.53	7.70	−4	0.6	7	5.33	6.89	8.45	6	1.2
0.7	9.53	9.76	9.98	−3	0.8	8	0.91	1.16	1.42	7	1.3
0.8	7.00	7.18	7.35	−2	0.9	9	1.42	1.78	2.15	7	1.4
0.9	3.48	3.58	3.68	−1	1.0	10	2.04	2.54	3.04	7	1.6
T_9	low	adopt	high	exp	ratio	T_9	low	adopt	high	exp	ratio

Reaction: $^{19}F(p,\gamma)^{20}Ne$
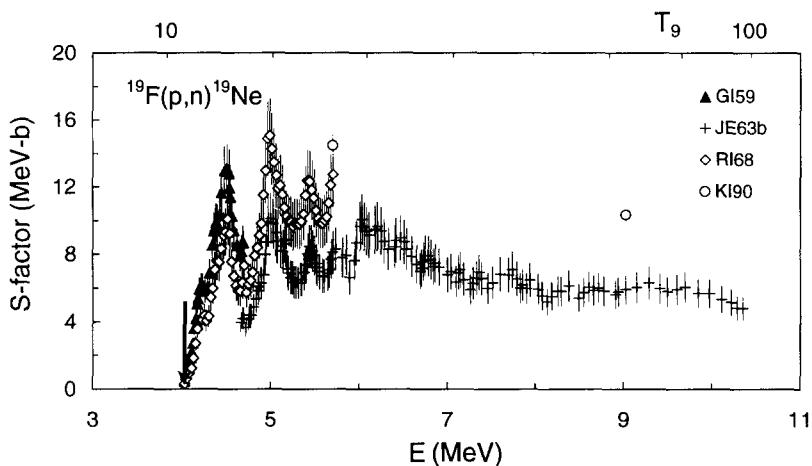
The available experimental data allow the calculation of the reaction rates in the temperature range between $T_9 = 0.2$ and 1.5. The resonance energies are the same as in the $^{19}F(p,\alpha\gamma)^{16}O$ case. The relative (p,γ) to $(p,\alpha\gamma)$ resonance strengths from SI54, FA55, KE62 and BE63 are used together with the adopted $(p,\alpha\gamma)$ strengths in order to extract the (p,γ) strengths. The more recent data from unpublished works of CL75 and KI90b are not considered in the present compilation. The adopted $\omega\gamma$ strengths are the weighted averages of these values and the absolute values from SU79. For $T_9 < 0.2$, the reaction rates are calculated from the resonance tails. The contribution from the tail of the giant dipole resonance is also included. Its parameters are obtained from TA64 and SE67b. However, due to the lack of experimental information on possible interferences between resonances, a 50% error is adopted in this temperature region. Above $T_9 = 1.5$, the adopted rates are calculated using HF rates as explained in Section 2.5. The present rates are in good agreement with those of CA88 at $T_9 < 1.5$, except in the range $0.14 \leqslant T_9 \leqslant 0.4$, where the present rates are slightly larger. This is mainly due to the higher adopted strength for the $E_r = 323$ keV resonance. For $T_9 > 1.5$, the HF estimate are larger than the CA88 rates.

T_9	low	adopt	high	exp	ratio	T_9	low	adopt	high	exp	ratio
0.013	2.07	4.13	6.20	−25	1.0	0.3	0.75	1.93	3.05	−2	1.3
0.014	1.29	2.59	3.88	−24	1.0	0.35	3.61	9.13	14.4	−2	1.2
0.015	0.68	1.37	2.05	−23	1.0	0.4	1.20	2.93	4.58	−1	1.1
0.016	3.14	6.27	9.41	−23	0.9	0.45	3.25	7.42	11.4	−1	0.9
0.018	4.64	9.28	13.9	−22	0.9	0.5	0.79	1.63	2.43	0	0.8
0.02	4.72	9.45	14.2	−21	0.9	0.6	3.78	6.19	8.60	0	0.7
0.025	4.93	9.86	14.8	−19	0.9	0.7	1.37	1.92	2.47	1	0.7
0.03	1.70	3.41	5.11	−17	0.9	0.8	3.79	4.88	5.98	1	0.7
0.04	2.97	5.95	8.92	−15	0.9	0.9	0.85	1.04	1.24	2	0.7
0.05	1.17	2.34	3.50	−13	0.9	1	1.61	1.93	2.25	2	0.8
0.06	1.92	3.84	5.76	−12	0.9	1.25	4.98	5.81	6.64	2	0.9
0.07	1.80	3.60	5.39	−11	0.9	1.5	1.03	1.19	1.35	3	1.0
0.08	1.14	2.28	3.42	−10	0.9	1.75	1.43	1.73	2.02	3	0.9
0.09	0.55	1.10	1.64	−9	0.9	2	1.85	2.32	2.78	3	0.9
0.1	2.15	4.31	6.46	−9	0.9	2.5	2.66	3.59	4.53	3	0.9
0.11	0.73	1.47	2.20	−8	0.9	3	3.41	4.94	6.48	3	0.9
0.12	2.26	4.52	6.79	−8	1.0	3.5	4.10	6.34	8.57	3	1.0
0.13	0.65	1.30	1.94	−7	1.0	4	4.71	7.75	10.8	3	1.1
0.14	1.78	3.56	5.34	−7	1.2	5	0.58	1.06	1.55	4	1.4
0.15	4.77	9.55	14.3	−7	1.3	6	0.67	1.36	2.05	4	1.7
0.16	1.26	2.52	3.78	−6	1.4	7	0.74	1.66	2.57	4	2.2
0.18	0.81	1.62	2.43	−5	1.4	8	0.81	1.97	3.13	4	2.8
0.2	4.34	8.67	13.0	−5	1.4	9	0.88	2.30	3.72	4	3.5
0.25	0.80	2.16	3.38	−3	1.3	10	0.94	2.64	4.34	4	4.3

E_r (keV)	J^π	$\omega\gamma$ (eV)						
		SI54	FA55	KE62	BE63	SU79	adopt	
212.71 ± 0.07	2^-			$(1.3 \pm 1.3) \times 10^{-6}$			$(1.3 \pm 1.3) \times 10^{-6}$	N
323.31 ± 0.04	1^+			$(3.5 \pm 1.2) \times 10^{-3}$		$(10 \pm 2) \times 10^{-3}$	$(5 \pm 3) \times 10^{-3}$	I
459.53 ± 0.09	1^+				$(5 \pm 1) \times 10^{-3}$	$(1.6 \pm 0.4) \times 10^{-3}$	$(2 \pm 1) \times 10^{-3}$	M
564.42 ± 0.90	2^-				$(20 \pm 2) \times 10^{-3}$	$(5.6 \pm 0.8) \times 10^{-3}$	$(8 \pm 5) \times 10^{-3}$	M
635.31 ± 0.62	1^+	1.58 ± 0.36	1.58 ± 0.36			1.61 ± 0.24	1.60 ± 0.17	M
828.17 ± 0.19	2^-		0.24 ± 0.08			0.41 ± 0.06	0.35 ± 0.08	M
887.14 ± 0.49	1^+		0.14 ± 0.05			0.12 ± 0.02	0.12 ± 0.02	M
1032.24 ± 0.48	2^+	0.14 ± 0.03				0.25 ± 0.04	0.25 ± 0.04	M
1214.78 ± 0.48		0.12 ± 0.02					0.14 ± 0.03	M
1254							0.12 ± 0.02	M
1276.73 ± 0.54	2^-		0.42 ± 0.08				0.42 ± 0.08	M
1301.90 ± 0.51	2^-		1.60 ± 0.42				1.60 ± 0.42	M
1350	1^+	1.35 ± 0.27					1.35 ± 0.27	M

Reaction: ^{19}F(p,n)^{19}Ne

The relative data of GI59 and RI68 are consistent in their common energy interval $E = 4.0–4.7$ MeV. However, their absolute values differ by about 25%. RI68 quotes an error of 10%, while we estimate an error of 10% in GI59, mainly due to target uncertainties. For this energy region, the average of the two data sets is adopted. At $4.7 \leqslant E \leqslant 5.8$ MeV, the data of RI68 renormalized ($\times 1.20$) to the average of GI59 and RI68 at lower energies are adopted. The selected data above 5.8 MeV are those of JE63b multiplied by 1.78 in order to bring the data in agreement with both RI68 and KI90a. The differences with CA88 at low temperatures are partly due to their adoption of the GI59 data, which are larger than those adopted here. Our thermalization effects are also important at all temperatures (from a factor of 3 at $T_9 = 0.7$ down to 1.5 at $T_9 = 10$). CA88 adopted the equal strength approximation ($r_{tt} = 1$).

T_9	low	adopt	high	exp	ratio	T_9	low	adopt	high	exp	ratio
0.7	7.07	8.13	9.19	−22	1.8	3	2.28	2.62	2.96	1	2.1
0.8	3.20	3.68	4.16	−18	1.9	3.5	2.22	2.54	2.87	2	2.1
0.9	2.25	2.58	2.92	−15	2.0	4	1.23	1.41	1.58	3	2.1
1	4.27	4.91	5.56	−13	2.0	5	1.36	1.55	1.74	4	2.1
1.25	5.47	6.29	7.12	−9	2.1	6	6.77	7.71	8.65	4	2.1
1.5	3.02	3.48	3.93	−6	2.1	7	2.14	2.43	2.72	5	2.1
1.75	2.76	3.18	3.60	−4	2.1	8	5.09	5.77	6.44	5	2.1
2	8.20	9.43	10.7	−3	2.1	9	1.00	1.13	1.26	6	2.1
2.5	0.95	1.09	1.24	0	2.1	10	1.71	1.93	2.15	6	2.0
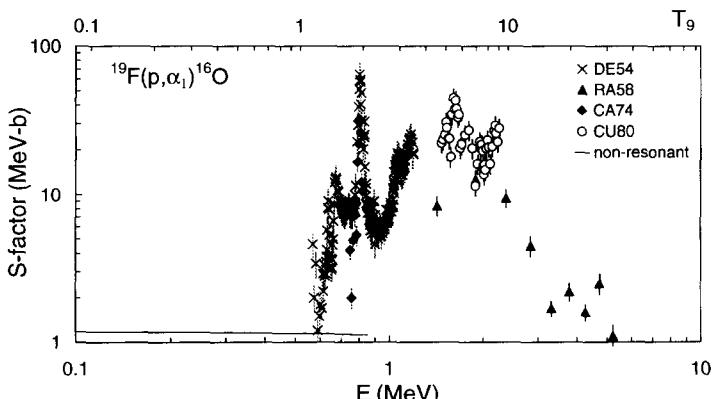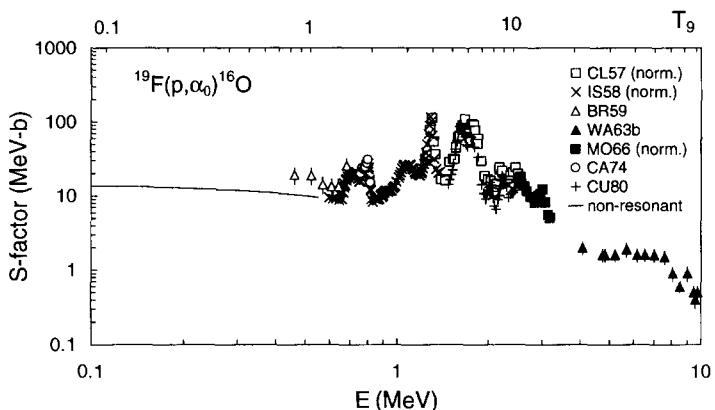
Reaction: $^{19}F(p,\alpha)^{16}O$

The S-factor for the (p,α_0) channel is obtained from BR59, WA63b, CA74 and CU80. The relative cross sections of CL57 and IS58 are normalized to $\sigma = 42$ mb at the 1.3 MeV resonance, while the data of MO66 are normalized to $\sigma = 28$ mb at 2.5 MeV. Below $E = 460$ keV, where no data exist in the (p,α_0) channel, a non-resonant contribution is calculated for s-wave capture. The theoretical S-factors for the (p,α_0) non-resonant contribution of HE91 and YA93 have been obtained using the unpublished data of LO78. The later work was focused mainly in the relative energy dependence of the cross section with no serious check on the absolute reported cross sections which may be underestimated by a factor of 2. Hence in the present compilation these data are not taken into account and the non-resonant contribution at the low energies is estimated with the procedure described in CH50 and adopted by CA88 as follows. The S-factor is adjusted to the lower experimental points in the $460 \leqslant E \leqslant 600$ keV range. The S-factor for the (p,α_1) channel is obtained from DE54, RA58, CA74 and CU80. A non-resonant extrapolation of the S-factor to lower energies is computed for the ground state channel. In the $(p,\alpha\gamma)$ channel, the resonance strength data of BO48, CH50, AS65, BE82, GR84, CR91, ZA95a and SP97 are used. Usefull background information related to this reaction may be found in the unpublished work of KI90b. Between 0.957 and 3.438 MeV, the non-resonant data of SP97 are used, while above $E = 3.44$ MeV, the relative yields at 90° of WI52 are adopted, normalized to $\sigma = 300$ mb at $E = 2.2$ MeV from SP97. For the cases where resonance strengths are not quoted by the authors, we calculate them as follows. The cross sections, resonance energies and total widths quoted by BO48 are used, assuming a 15% error. Data are normalized to the adopted resonance strength for the 828 keV resonance. Resonance strengths are calculated from the thick target yield of CH50, assuming a 15% error and a 48.66% fluorine content for the CaF_2 target. The strengths are estimated in BE75 from the cross section data. For the 323 keV resonance, the quoted (p,α_2) strength in BE82 is divided by its branching ratio of 0.97 [CR91]. For the 828 keV resonance, a branching ratio of 0.73 is used [AJ87]. The available experimental data allow a computation of the rates at $T_9 > 0.3$. Below this temperature, the rates are determined mainly from the non-resonant (p,α_0) channel. Hence, uncertainties progressively increase to about 50% at the lowest temperatures. The differences between our rates and the CA88 ones can be explained by the effect of thermalization, which is estimated by CA88 to be a factor 2.4 at $T_9 = 0.5$ in comparison with the values obtained from our HF predictions.
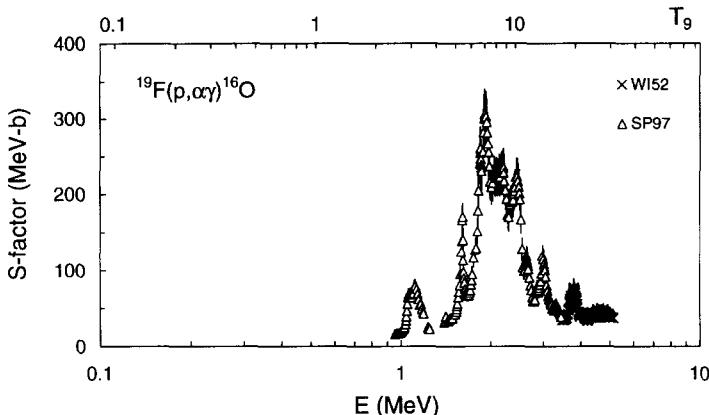
T_9	low	adopt	high	exp	ratio	T_9	low	adopt	high	exp	ratio
0.009	0.69	1.03	1.37	−25	0.8	0.2	4.57	5.12	5.67	−1	1.4
0.01	1.23	1.78	2.34	−24	0.7	0.25	1.02	1.09	1.16	1	1.1
0.011	1.57	2.28	2.98	−23	0.7	0.3	8.79	9.26	9.73	1	1.1
0.012	1.52	2.20	2.89	−22	0.7	0.35	4.06	4.26	4.46	2	1.0
0.013	1.16	1.68	2.20	−21	0.7	0.4	1.26	1.32	1.38	3	1.0

continued from previous page

T_9	low	adopt	high	exp	ratio	T_9	low	adopt	high	exp	ratio
0.014	0.72	1.05	1.37	−20	0.7	0.45	3.00	3.14	3.28	3	1.0
0.015	3.81	5.52	7.23	−20	0.7	0.5	5.94	6.21	6.48	3	0.9
0.016	1.74	2.53	3.31	−19	0.6	0.6	1.62	1.70	1.78	4	0.7
0.018	2.56	3.72	4.87	−18	0.6	0.7	3.30	3.47	3.63	4	0.5
0.02	2.60	3.76	4.93	−17	0.6	0.8	5.65	5.96	6.27	4	0.4
0.025	2.67	3.88	5.09	−15	0.6	0.9	8.73	9.25	9.76	4	0.3
0.03	0.91	1.33	1.74	−13	0.6	1	1.27	1.35	1.43	5	0.3
0.04	1.56	2.27	2.98	−11	0.6	1.25	2.72	2.92	3.11	5	0.2
0.05	5.97	8.72	11.5	−10	0.6	1.5	5.09	5.48	5.87	5	0.2
0.06	0.96	1.41	1.85	−8	0.5	1.75	8.61	9.31	10.0	5	0.3
0.07	0.88	1.30	1.71	−7	0.5	2	1.36	1.47	1.58	6	0.3
0.08	5.53	8.13	10.7	−7	0.5	2.5	2.87	3.13	3.39	6	0.4
0.09	2.70	3.95	5.20	−6	0.5	3	5.25	5.77	6.28	6	0.5
0.1	1.15	1.65	2.16	−5	0.6	3.5	8.63	9.53	10.4	6	0.7
0.11	4.57	6.40	8.23	−5	0.7	4	1.30	1.44	1.58	7	0.9
0.12	1.72	2.33	2.94	−4	0.8	5	2.42	2.70	2.98	7	1.4
0.13	5.96	7.83	9.70	−4	1.0	6	3.74	4.19	4.64	7	1.9
0.14	1.90	2.43	2.96	−3	1.3	7	5.13	5.76	6.39	7	2.4
0.15	5.55	6.92	8.30	−3	1.5	8	6.49	7.30	8.11	7	2.9
0.16	1.51	1.83	2.16	−2	1.7	9	7.75	8.74	9.72	7	3.3
0.18	0.93	1.08	1.23	−1	1.6	10	0.89	1.00	1.12	8	3.7

E_r (keV)	J^π	$\omega\gamma$ (eV)					
		BO48	CH50	SP97	others	adopt	
11 ± 1	1^+				$(7.5 \pm 3.0) \times 10^{-29}$ [BE75]	$(7.5 \pm 3.0) \times 10^{-29}$	N
212.71 ± 0.07	2^-		0.022 ± 0.004			0.022 ± 0.004	M
323.31 ± 0.04	1^+	37 ± 6	24 ± 4		23.0 ± 0.8[BE82] 22 ± 2 [CR91] 24 ± 3 [ZA95a]	23.1 ± 0.9	1
459.53 ± 0.09	1^+	10 ± 1	9 ± 1			9.5 ± 0.7	M
564.42 ± 0.90	2^-	52 ± 8	48 ± 10			50 ± 6	M
635.31 ± 0.62	1^+	86 ± 13	90 ± 14			88 ± 10	M
790.53 ± 0.29		27 ± 4	41 ± 6	17 ± 5		27 ± 6	M
828.17 ± 0.19	2^-		839 ± 125	760 ± 70	872 ± 130[AS65] 780 ± 40 [BE82]	785 ± 32	M
853.71 ± 0.71		28 ± 4	32 ± 5	27 ± 7		29 ± 3	M
887.14 ± 0.49	1^+	514 ± 77	429 ± 64	430 ± 50	472 ± 70[AS65]	452 ± 31	M
1032.24 ± 0.48	2^+	6 ± 1	6 ± 1	7.9 ± 1.0	8.2 ± 1.2 [GR84]	6.9 ± 0.6	M
1078.77 ± 0.88		20 ± 3	23 ± 4	29 ± 4		23 ± 3	M
1214.78 ± 0.48		298 ± 45	222 ± 33	202 ± 26		225 ± 24	M
1276.73 ± 0.54	2^-	415 ± 62	337 ± 50	280 ± 70	470 ± 70[AS65]	347 ± 35	M
1301.90 ± 0.51	2^-	2383 ± 357	2031 ± 305	1860 ± 230	1962 ± 295[BE82]	2005 ± 143	M
1522.03 ± 0.55				44 ± 12		44 ± 12	M

^{19}F(p,αγ)^{16}O

× WI52
△ SP97

Reaction: ^{20}Ne(p,γ)^{21}Na

The non-resonant reaction rate is obtained from the experimental S-factor of RO75b. Below the low energy limit, the theoretical extrapolation of RO75b is used, which takes account of the $1/2^+$ subthreshold state at $E_r = -7$ keV in ^{21}Na. The γ width of this state is given as 0.31 ± 0.07 eV by RO75b, and 0.17 ± 0.05 eV by AN77. The former experiment gives however a "formal" width which must be converted to an "observed" width (see LA58) to be compared with the AN77 result. After correction of the RO75b value (0.14 ± 0.03 eV), both data agree within the error bars. Since the non-resonant reaction rate involves a subthreshold state contribution and a direct capture term, the analytical fit contains a free parameter α in T_9^α. The optimal value is $\alpha = -1.84$, which is close to $\alpha = -2$, valid for a subthreshold state contribution only. The resonant reaction rate involves eight resonances up to $E_r = 2035$ keV. The present reaction rate are larger than those of CA88 at low temperatures, probably because the reduced proton width of the subthreshold state in CA88 is lower than in RO75b.
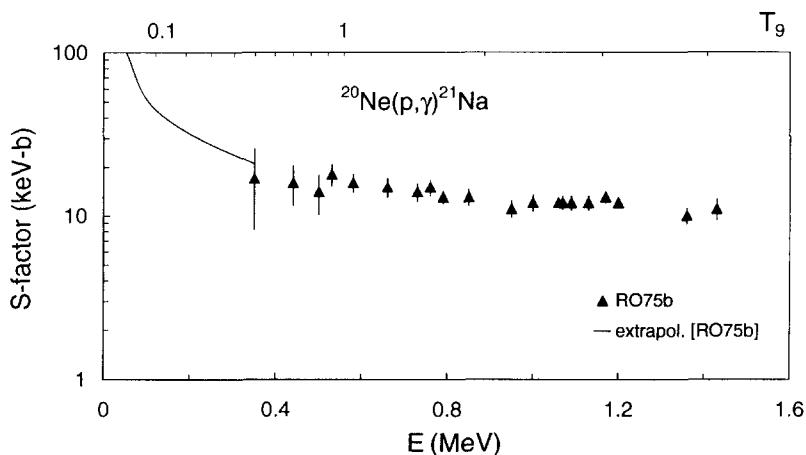
T_9	low	adopt	high	exp	ratio	T_9	low	adopt	high	exp	ratio
0.011	0.61	1.08	1.55	−27	1.6	0.25	2.98	5.50	8.03	−5	1.1
0.012	0.65	1.15	1.64	−26	1.6	0.3	1.99	3.32	4.64	−4	1.0
0.013	5.42	9.41	13.4	−26	1.6	0.35	0.93	1.42	1.92	−3	1.0
0.014	3.64	6.28	8.92	−25	1.6	0.4	3.15	4.60	6.05	−3	1.0
0.015	2.06	3.52	4.98	−24	1.6	0.45	0.84	1.19	1.54	−2	1.0
0.016	1.00	1.70	2.40	−23	1.6	0.5	1.88	2.60	3.32	−2	1.0
0.018	1.63	2.75	3.87	−22	1.5	0.6	6.53	8.73	10.9	−2	1.0
0.02	1.79	3.01	4.23	−21	1.5	0.7	1.67	2.18	2.69	−1	1.0
0.025	2.13	3.61	5.08	−19	1.5	0.8	3.68	4.66	5.64	−1	1.0
0.03	0.79	1.37	1.96	−17	1.5	0.9	7.56	9.28	11.0	−1	1.0
0.04	1.47	2.72	3.97	−15	1.4	1	1.51	1.79	2.08	0	1.0
0.05	0.60	1.15	1.71	−13	1.4	1.25	7.28	8.17	9.07	0	1.0
0.06	1.02	2.00	2.97	−12	1.3	1.5	2.50	2.75	3.00	1	1.0

continued from previous page
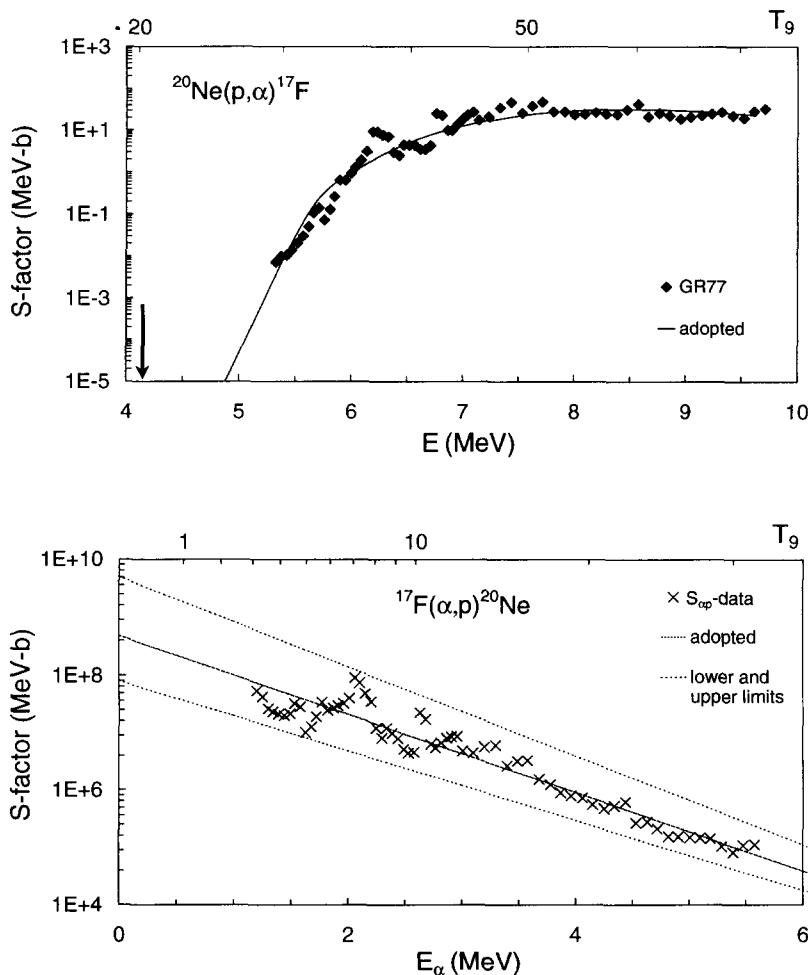
T_9	low	adopt	high	exp	ratio	T_9	low	adopt	high	exp	ratio
0.07	0.99	1.94	2.89	−11	1.3	1.75	6.30	6.91	7.51	1	1.0
0.08	0.64	1.26	1.89	−10	1.3	2	1.27	1.40	1.53	2	1.0
0.09	3.11	6.15	9.19	−10	1.2	2.5	3.40	3.81	4.22	2	1.0
0.1	1.20	2.40	3.59	−9	1.2	3	6.51	7.49	8.46	2	0.9
0.11	3.91	7.87	11.8	−9	1.2	3.5	1.03	1.22	1.41	3	0.9
0.12	1.11	2.25	3.39	−8	1.2	4	1.46	1.77	2.07	3	0.9
0.13	2.82	5.74	8.67	−8	1.2	5	2.38	2.98	3.59	3	0.9
0.14	0.65	1.34	2.02	−7	1.2	6	3.33	4.26	5.19	3	0.9
0.15	1.40	2.88	4.35	−7	1.2	7	4.27	5.52	6.76	3	0.8
0.16	2.83	5.80	8.77	−7	1.2	8	5.23	6.75	8.27	3	0.8
0.18	0.99	2.01	3.03	−6	1.1	9	6.20	7.95	9.71	3	0.8
0.2	2.94	5.91	8.88	−6	1.1	10	7.21	9.14	11.1	3	0.8

E_r (keV)	J^π	adopted $\omega\gamma$ (eV)		
366 ± 1	$1/2^-$	$(1.1 \pm 0.2) \times 10^{-4}$	RO75b	I
398 ± 1	$9/2^+$	$(6 \pm 1) \times 10^{-5}$	RO75b	I
1113 ± 1	$5/2^+$	1.13 ± 0.07	BL69	M
1248 ± 1	$3/2^-$	0.035 ± 0.010	BL69	M
1432 ± 1	$5/2^-$	0.050 ± 0.015	BL69	M
1742 ± 1	$3/2^-$	1.0 ± 0.3	RO75b	M
1861 ± 1	$5/2^+$	2.4 ± 0.7	BL69	M
2035 ± 1	$3/2^+$	1.6	EN78	M

Reaction: ^{20}Ne(p,α)^{17}F

For this endoergic reaction ($Q = -4.130$ MeV), the experimental data are missing between the threshold and $E = 5.33$ MeV. The rates are calculated from the unique set of available cross section data [GR77]. The existing data at the lowest energies do not allow a clear picture of the behavior of the S-factor curve. In order to extrapolate the cross section down to the threshold, the S-factor $S_{\alpha,p}$ for the reverse reaction ^{17}F(α,p)^{20}Ne is approximated by an exponential function $S_{\alpha,p} = 4.83 \times 10^8 \exp(-1.5693E_\alpha)$, where E_α is the center of mass energy in the channel $\alpha + {}^{17}$F, and extrapolated down to the threshold. For the calculation of the lower and upper limits of the rates, exponential fits $S_{\alpha,p}^{max} = 5.0 \times 10^9 \exp(-1.7829E_\alpha)$ and $S_{\alpha,p}^{min} = 8.0 \times 10^7 \exp(-1.3993E_\alpha)$, that corresponds to the lower and upper bounds of $S_{\alpha,p}$ are obtained and extrapolated similar to $S_{\alpha,p}$. Our thermalization corrections are important, $r_{tt} = 5.0$ to 4.8 for $T_9 = 0.9$ to 10 (CA88 adopted $r_{tt} = 1$ for all T_9).

T_9	low	adopt	high	exp	ratio	T_9	low	adopt	high	exp	ratio
0.9	0.23	1.22	10.6	−24	0.3	3.5	0.78	3.24	21.2	−1	0.7
1	0.22	1.14	9.72	−21	0.4	4	1.07	4.30	27.0	0	0.7
1.25	0.64	3.22	26.6	−16	0.4	5	0.44	1.69	9.95	2	0.8
1.5	0.35	1.72	13.7	−12	0.5	6	0.55	2.01	11.3	3	0.8
1.75	1.89	9.03	69.9	−10	0.5	7	0.34	1.19	6.40	4	0.8
2	0.23	1.08	8.11	−7	0.6	8	1.33	4.53	23.6	4	0.8
2.5	0.23	1.01	7.22	−4	0.6	9	0.39	1.28	6.48	5	0.8
3	0.25	1.08	7.37	−2	0.7	10	0.90	2.93	14.5	5	0.9

Reaction: ^{20}Ne$(\alpha,\gamma)^{24}$Mg

Experimental data concern resonances only. Twelve of them are observed by SC83 up to 1.4 MeV, but only the 0^+ states at $E_r = 0.799$ MeV and 1.367 MeV play a significant role. Partial data above $E = 3$ MeV are available [HI68,FI78,FI79], but no data are reported in the $1.4 < E < 3$ MeV range. An estimate of the non-resonant contribution is made here in the potential model, using a Gaussian potential. The two parameters of this potential are selected in order to reproduce the energy $E_r = 1.367$ MeV of the 0^+ resonance, which is known to have an $\alpha + ^{20}$Ne structure, and the quadrupole moment of the 2^+ first excited state of ^{24}Mg. Only capture to that state is considered. The non-resonant S-factor is parametrized as $S(E) = (7.43 + 3.21E + 14.85E^2) \times 10^3$ MeV b (E in MeV). This term contributes for about 10% to the reaction rates at the lowest temperature ($T_9 = 0.15$), but is completely negligible above. The resonant data allow the calculation of the rates up to $T_9 = 1$. HF estimates are used above, using the prescription given in Section 2.5.

T_9	low	adopt	high	exp	ratio	T_9	low	adopt	high	exp	ratio
0.15	1.74	2.26	3.24	−25	0.7	1.25	1.38	2.32	3.58	−2	0.7
0.16	6.38	8.19	11.2	−24	0.7	1.5	0.84	1.81	3.10	−1	0.7
0.18	3.24	4.13	5.36	−21	0.7	1.75	3.27	8.52	15.6	−1	0.8
0.2	4.77	6.05	7.68	−19	0.8	2	0.94	2.89	5.51	0	0.8
0.25	3.63	4.60	5.74	−15	0.9	2.5	0.44	1.77	3.56	1	1.0
0.3	1.34	1.69	2.12	−12	0.9	3	1.31	6.45	13.4	1	1.2
0.35	0.88	1.11	1.40	−10	1.0	3.5	0.29	1.71	3.63	2	1.4
0.4	1.97	2.51	3.18	−9	1.0	4	0.55	3.70	7.96	2	1.6
0.45	2.18	2.77	3.54	−8	1.0	5	0.13	1.16	2.54	3	2.0
0.5	1.47	1.87	2.40	−7	1.0	6	0.25	2.62	5.81	3	2.5
0.6	2.52	3.21	4.15	−6	1.0	7	0.39	4.84	10.8	3	3.0
0.7	1.93	2.45	3.18	−5	1.0	8	0.55	7.84	17.7	3	3.5
0.8	0.93	1.17	1.51	−4	0.9	9	0.07	1.16	2.63	4	4.0
0.9	3.45	4.26	5.42	−4	0.8	10	0.09	1.61	3.65	4	4.5
1	1.08	1.31	1.62	−3	0.7						

E_r (MeV)	J^π	adopted $\omega\gamma$ (eV)		
0.203	4^+	$1.6^{+14}_{-1.6} \times 10^{-29}$	SC83	M
0.216	6^+	$3.0^{+27}_{-3.0} \times 10^{-26}$	SC83	M
0.714	5^-	$1.1^{+10}_{-1.1} \times 10^{-8}$	SC83	M
0.747	2^+	$4.0^{+36}_{-4.0} \times 10^{-9}$	SC83	M
0.799	0^+	$(2.9 \pm 0.6) \times 10^{-4}$	SC83	M
0.849	$(0\text{-}3)^-$	$0.8^{+7.2}_{-0.8} \times 10^{-5}$	SC83	M
1.022	3^-	$(3.0 \pm 0.6) \times 10^{-4}$	SC83	M
1.05	2^+	$(4.8 \pm 1.0) \times 10^{-4}$	SC83	M
1.266	$(3,4)^+$	$0.2^{+1.8}_{-0.2} \times 10^{-4}$	SC83	M
1.348	$(3,4)^+$	$0.2^{+1.8}_{-0.2} \times 10^{-4}$	SC83	M
1.367	0^+	0.17 ± 0.02	SC83	M
1.42	$2^+;1$	$(2.6 \pm 0.5) \times 10^{-3}$	SC83	M

Reaction: ^{21}Ne(p,γ)^{22}Na

The contributions of 46 resonances [AN70, BE77, KE77, GÖ82, GÖ83, BE92b] in the energy range from E_r = 93.5 to 1936.2 keV are taken into account. For the resonances between 943.7 and 1225.6 keV, the resonance strengths are the weigthed averages of those given by GÖ82, GÖ83 and BE92b, while for those between 1237 and 1936 keV, the strengths are the weigthed averages of those given by BE77 and KE77. The non-resonant contribution is calculated using the S-factors from RO75b for direct capture and from GÖ82 for the tails of the broad resonances. A major contribution at low temperatures comes from the resonance at E_r = 93.5 keV, for which only an upper limit of the strength is estimated [GÖ82, GÖ83]. Above $T_9 = 2$, HF estimates are used (see Section 2.5). The differences between the present rates and the CA88 ones in the temperature region around $T_9 = 0.03$ are due to the 93.5 keV resonance, for which the adopted strength [GÖ83] is two orders of magnitude smaller than the value used in CA88. Our thermalization effects reduce the ratio between 10 to 14% at $T_9 = 2.5$ to 10 (CA88 adopt $r_{tt} = 1$ at all temperatures).

E_r (keV)	J^π	$\omega\gamma$ (eV)				
		GÖ82	GÖ83	BE92b	adopt	
93.5 ± 6.7	$(0-1)^+$	$\leqslant 5 \times 10^{-6}$	$\leqslant 5 \times 10^{-8}$		$5^{+45}_{-5} \times 10^{-9}$	I
120.5 ± 0.6	$(1-3)^-$	$(3.75 \pm 0.75) \times 10^{-5}$			$(3.75 \pm 0.75) \times 10^{-5}$	I
216.6 ± 5.7		$\leqslant 5 \times 10^{-6}$			$5^{+45}_{-5} \times 10^{-7}$	M
258.3 ± 0.4	(4^+)			$(2.12 \pm 0.37) \times 10^{-3}$	$(2.12 \pm 0.37) \times 10^{-3}$	M
259.3 ± 0.4	3^+	$(8.25 \pm 1.25) \times 10^{-2}$			$(8.25 \pm 1.25) \times 10^{-2}$	I
277.6 ± 0.4	3	$(2.00 \pm 0.37) \times 10^{-3}$			$(2.00 \pm 0.37) \times 10^{-3}$	M
336.1 ± 0.4	$(1^-,2)$	$(8.12 \pm 1.37) \times 10^{-3}$			$(8.12 \pm 1.37) \times 10^{-3}$	M

E_r (keV)	J^π	$\omega\gamma$ (eV)					
		AN70	BE77	KE77	GÖ83	adopt	
413.2 ± 3.8	$(3,4)^+$		$(1.9 \pm 0.4) \times 10^{-2}$			$(1.9 \pm 0.4) \times 10^{-2}$	M
481.3 ± 1.9	$(1^+,2)$	0.13 ± 0.07	0.20 ± 0.04	0.14 ± 0.03		0.16 ± 0.02	M
500.7 ± 1.4	(2^+-4^+)	0.73 ± 0.30	0.76 ± 0.15	0.98 ± 0.19		0.83 ± 0.11	M
539.1 ± 2.9	$(1^-,2^+)$		0.15 ± 0.04		0.13 ± 0.02	0.13 ± 0.02	M
540.1 ± 2.9	(4^+-6^+)		$(3.5 \pm 0.9) \times 10^{-2}$		0.03 ± 0.01	$(3.2 \pm 0.5) \times 10^{-2}$	M
621.2 ± 2.9	$(3^+,4^-)$		$(5.2 \pm 1.2) \times 10^{-2}$		0.03 ± 0.01	$(3.5 \pm 0.5) \times 10^{-2}$	M
632.6 ± 1.9	2		$(5.2 \pm 1.2) \times 10^{-2}$		0.03 ± 0.01	$(3.5 \pm 0.5) \times 10^{-2}$	M
639.3 ± 1.0	$(2,3)^+$	0.08 ± 0.04	$(7.6 \pm 1.5) \times 10^{-2}$	$(6.0 \pm 1.2) \times 10^{-2}$	0.06 ± 0.01	$(6.5 \pm 0.7) \times 10^{-2}$	M
662.2 ± 1.9	$(1,2^+)$		0.19 ± 0.04		0.14 ± 0.04	0.16 ± 0.03	M
669.7 ± 0.5	1^+	0.93 ± 0.37	1.50 ± 0.37	0.89 ± 0.18	0.85 ± 0.17	0.94 ± 0.11	M
684.2 ± 1.9	2				0.03 ± 0.01	$(2.6 \pm 0.6) \times 10^{-2}$	M
732.7 ± 0.5	2^+	3.95 ± 0.79	6.38 ± 1.88	3.82 ± 0.16	3.37 ± 0.87	3.95 ± 0.79	M
776.2 ± 1.0	3^+	0.36 ± 0.17	0.29 ± 0.06	0.37 ± 0.07		0.32 ± 0.05	M
808.0 ± 1.1	$0(1-3^+)$	0.54 ± 0.24	0.34 ± 0.06	0.52 ± 0.1		0.39 ± 0.05	M
834.6 ± 1.1	(3^+-5^+)	0.21 ± 0.1	0.17 ± 0.04	0.23 ± 0.04		0.19 ± 0.03	M
859.7 ± 2.9	2^-		0.16 ± 0.04			0.16 ± 0.04	M
865.9 ± 1.0	$(1,2)^+$	0.14 ± 0.07	0.10 ± 0.02	$(9.5 \pm 1.9) \times 10^{-2}$		0.10 ± 0.02	M
896.9 ± 1.0	$(2^+,3)$		0.11 ± 0.02			0.11 ± 0.02	M
943.7 ± 1.0	$(2^+,4^+)$		$(3.0 \pm 0.6) \times 10^{-2}$			$(3.0 \pm 0.6) \times 10^{-2}$	M
Res. 1039–1936 keV				see comments			

T_9	low	adopt	high	exp	ratio	T_9	low	adopt	high	exp	ratio
0.015	2.50	4.03	5.41	−25	0.9	0.35	1.11	1.32	1.54	1	1.1
0.016	1.30	2.08	2.82	−24	0.9	0.40	2.65	3.14	3.66	1	1.1
0.018	2.37	3.81	5.30	−23	0.9	0.45	5.19	6.14	7.14	1	1.1
0.02	2.90	4.66	10.0	−22	0.8	0.50	0.87	1.05	1.22	2	1.1
0.025	0.44	1.00	66.5	−19	0.03	0.60	1.99	2.35	2.73	2	1.1
0.03	0.63	4.06	409	−17	0.01	0.70	3.66	4.32	5.01	2	1.1
0.04	3.39	6.70	124	−13	0.04	0.80	5.99	7.08	8.21	2	1.0
0.05	2.73	4.17	18.3	−10	0.1	0.90	0.91	1.08	1.25	3	1.0
0.06	2.24	3.21	7.04	−8	0.3	1.00	1.31	1.54	1.79	3	0.9
0.07	5.05	7.03	11.7	−7	0.5	1.25	2.68	3.18	3.69	3	0.9
0.08	5.09	6.96	10.2	−6	0.6	1.5	4.53	5.39	6.26	3	0.8
0.09	3.00	4.06	5.64	−5	0.7	1.75	6.67	7.95	9.25	3	0.8
0.10	1.22	1.64	2.20	−4	0.8	2	0.89	1.07	1.24	4	0.8
0.11	3.80	5.06	6.67	−4	0.9	2.5	1.27	1.56	1.83	4	0.7
0.12	0.97	1.28	1.67	−3	0.9	3	1.61	2.01	2.40	4	0.7
0.13	2.13	2.81	3.61	−3	0.9	3.5	1.90	2.43	2.93	4	0.7
0.14	4.19	5.49	7.01	−3	0.9	4	2.16	2.81	3.43	4	0.7
0.15	7.58	9.88	12.5	−3	0.9	5	2.58	3.50	4.36	4	0.7
0.16	1.30	1.68	2.11	−2	1.0	6	2.92	4.10	5.22	4	0.8
0.18	3.45	4.39	5.44	−2	1.0	7	3.21	4.67	6.04	4	0.8
0.20	0.87	1.09	1.32	−1	1.0	8	3.46	5.20	6.85	4	0.9
0.25	7.01	8.46	10.0	−1	1.1	9	3.68	5.72	7.64	4	1.0
0.30	3.46	4.13	4.84	0	1.1	10	3.88	6.22	8.44	4	1.0

Reaction: ^{21}Ne$(\alpha,$n$)^{24}$Mg
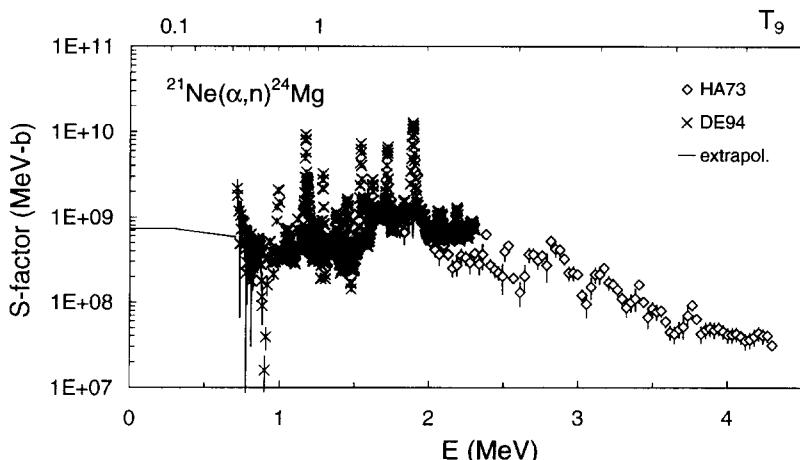
Use is made of the experimental cross sections from HA73 and DE94b covering the energy range $0.714 \leqslant E \leqslant 4.3$ MeV. The adopted rates result from a low energy extrapolation based on a HF calculation from DE94b. The results of DE94b are partially documented in KU95. For the lower limit of the rates, the S-factor curve without any resonance below $E = 0.714$ MeV is considered, and only the tails of observed resonances at energies $E > 0.714$ MeV are assumed to contribute. The upper limit is determined by assuming that all the known states in the compound nucleus [EN90] give rise to resonances in the S-factor. The strengths of these resonances are calculated by the Wigner limit. HF rates are used for $T_9 > 2.5$, following the procedure explained in Section 2.5. The differences between the adopted rates and the CA88 ones are due to the differences in the average S-factor, which is higher in CA88.

T_9	low	adopt	high	exp	ratio	T_9	low	adopt	high	exp	ratio
0.1	0.03	6.32	498	−25	0.3	0.8	1.44	1.57	4.75	−3	0.5
0.11	0.01	1.38	100	−23	0.3	0.9	1.03	1.11	2.05	−2	0.6
0.12	0.01	2.12	156	−22	0.3	1	5.57	5.99	8.35	−2	0.6
0.13	0.01	2.44	183	−21	0.3	1.25	1.59	1.71	1.91	0	0.8
0.14	0.01	2.20	159	−20	0.3	1.5	1.83	1.98	2.15	1	0.9
0.15	0.01	1.62	105	−19	0.3	1.75	1.17	1.28	1.40	2	0.9

T_9	low	adopt	high	exp	ratio	T_9	low	adopt	high	exp	ratio
0.16	0.01	1.01	55.5	−18	0.3	2	5.04	5.61	6.19	2	1.0
0.18	0.02	2.55	88.0	−17	0.3	2.5	4.50	5.18	5.86	3	1.0
0.2	0.06	4.11	81.0	−16	0.3	3	2.29	2.70	3.12	4	1.1
0.25	0.07	1.10	11.5	−13	0.3	3.5	7.84	9.54	11.2	4	1.1
0.3	1.35	7.93	188	−12	0.3	4	2.05	2.57	3.09	5	1.1
0.35	0.71	2.33	90.2	−10	0.3	5	0.83	1.11	1.39	6	1.0
0.4	1.60	3.65	164	−9	0.3	6	2.13	3.09	4.05	6	1.0
0.45	2.14	3.74	155	−8	0.3	7	4.12	6.57	9.02	6	0.9
0.5	2.00	2.90	92.3	−7	0.3	8	0.65	1.17	1.69	7	0.8
0.6	7.87	9.38	134	−6	0.3	9	0.89	1.84	2.79	7	0.7
0.7	1.40	1.56	9.55	−4	0.4	10	1.05	2.64	4.22	7	0.7

Reaction: $^{22}Ne(p,\gamma)^{23}Na$

The contribution of 55 resonances between E_r = 36 and 1822 keV [PI71, DU71, DU72, ME73, SM79, GÖ82, GÖ83] is calculated. For the resonances between 1096.2 and 1208.5 keV, weighted averages of the strengths given by PI71 and SM79 are selected, while these averages are based on the data of DU71 and SM79 for the resonances between 1223.9 and 1821.8 keV. The standard values from MO60 and KE77 are used to normalize the relative resonance strengths. The contributions of the direct capture process and of the subthreshold resonance at E_r = −129 keV are calculated using the S-factors given by RO75b and GÖ83 and are found to be negligible. Above T_9 = 2, HF estimates are used (see Section 2.5). Our rates are significantly different from the CA88 ones at T_9 < 0.3. This is mainly due to the contribution of the resonance at E_r = 36.3 keV. With respect to CA88, the energy of this resonance is different and its adopted strength [GÖ83] is two orders of magnitude larger. The tentative states at E_r = 69.8 and 102.3 keV are also taken into account here with a weighting factor of 0.1. The resonance at E_r = 153 keV has a measured strength [GÖ83], while only an

E_r (keV)	J^π	GÖ82	GÖ83	PI71	DU71	DU72	ME73	SM79	adopt	
36.3±2.9	1/2+	6.0×10^{-17}	6.8×10^{-15}						$(6.8 \pm 1.0) \times 10^{-15}$	I
(69.8)		$\leqslant 3.2 \times 10^{-6}$	$\leqslant 4.2 \times 10^{-9}$						$4.2^{+38}_{-4.2} \times 10^{-10}$	I
(102.3)		$\leqslant 6.0 \times 10^{-7}$	$\leqslant 6.0 \times 10^{-7}$						$6.0^{+54}_{-6.0} \times 10^{-8}$	I
153.0±2.9	7/2-	$\leqslant 1.0 \times 10^{-6}$	6.5×10^{-7}						$(6.5 \pm 1.9) \times 10^{-7}$	I
179.8±2.9		$\leqslant 2.6 \times 10^{-6}$	$\leqslant 2.6 \times 10^{-6}$						$2.6^{+23}_{-2.6} \times 10^{-7}$	M
207.5±2.9		$\leqslant 1.4 \times 10^{-6}$	$\leqslant 1.4 \times 10^{-6}$						$1.4^{+13}_{-1.4} \times 10^{-7}$	M
248.6±2.9		$\leqslant 2.6 \times 10^{-6}$							$2.6^{+23}_{-2.6} \times 10^{-7}$	M
280.2±2.9		$\leqslant 2.2 \times 10^{-6}$							$2.2^{+9.8}_{-2.2} \times 10^{-7}$	M
310.8±4.8		$\leqslant 2.2 \times 10^{-6}$							$2.2^{+9.8}_{-2.2} \times 10^{-7}$	M
321.3±2.9		$\leqslant 3.0 \times 10^{-6}$							$3.0^{+27}_{-3.0} \times 10^{-7}$	M
416.9±1.0	3/2-						0.07 ± 0.02		0.07 ± 0.02	M
458.0±1.0	1/2+			0.50 ± 0.25			0.49 ± 0.15		0.49 ± 0.13	M
603.3±1.0	7/2-						0.03 ± 0.01		0.03 ± 0.01	M
612±1	1/2			2.70 ± 0.25		2.15 ± 0.85	2.70 ± 0.25		2.70 ± 0.25	M
630±1	(1/2 − 5/2+)			0.30 ± 0.15			0.35 ± 0.10		0.34 ± 0.09	M
693.3±0.8	3/2			0.10 ± 0.05			0.14 ± 0.04		0.12 ± 0.04	M
813.7±0.7	3/2+			5.25 ± 2.50			7.35 ± 2.20		6.45 ± 1.65	M
857.7±1.0	(3/2,5/2)+			1.6 ± 0.8			1.90 ± 0.95		1.75 ± 0.60	M
861.5±1.0	1/2+			0.70 ± 0.35			1.10 ± 0.55		0.8 ± 0.3	M
879.7±1.0	(3/2+,5/2)			0.45 ± 0.25			0.85 ± 0.25		0.65 ± 0.20	M
887.3±1.0	3/2+			0.4 ± 0.2			0.38 ± 0.12		0.4 ± 0.1	M
906.5±1.0	3/2+			3.1 ± 1.6		4.6 ± 1.6	6.1 ± 1.9		4.5 ± 0.9	M
938.3±0.5	7/2			0.25 ± 0.15			0.43 ± 0.13		0.35 ± 0.10	M
961.1±0.4	3/2+			1.90 ± 0.95			2.50 ± 0.75		2.20 ± 0.55	M
1021.1±0.8	5/2+			0.65 ± 0.35	0.95 ± 0.40		0.85 ± 0.25		0.8 ± 0.2	M
1041.1±1.0	3/2+			1.8 ± 0.9	1.65 ± 0.60		2.95 ± 0.90		2.00 ± 0.45	M
1056.4±1.0	1/2+			1.45 ± 0.75	2.4 ± 0.9		1.9 ± 0.3	2.05 ± 0.55	1.9 ± 0.3	M
Res. 1096–1822 keV									see comments	

T_9	low	adopt	high	exp	ratio	T_9	low	adopt	high	exp	ratio
0.01	0.19	5.39	150	−25	0.1	0.25	1.47	2.60	10.2	−3	3.3
0.011	0.11	2.10	44.5	−23	0.1	0.3	1.51	2.19	4.10	−2	1.5
0.012	0.29	4.62	74.0	−22	0.2	0.35	1.21	1.68	2.37	−1	1.3
0.013	0.47	6.11	79.1	−21	0.4	0.4	6.16	8.49	11.2	−1	1.3
0.014	0.52	5.55	59.8	−20	0.6	0.45	2.23	3.05	3.94	0	1.3
0.015	0.41	3.73	34.3	−19	0.8	0.5	6.30	8.52	10.9	0	1.3
0.016	0.25	1.96	15.7	−18	1.1	0.6	3.05	4.04	5.08	1	1.3
0.018	0.48	3.07	19.5	−17	1.9	0.7	0.96	1.25	1.55	2	1.3
0.02	0.52	2.73	14.4	−16	2.8	0.8	2.31	2.97	3.65	2	1.3
0.025	0.38	1.34	5.27	−14	6.0	0.9	4.63	5.90	7.20	2	1.2
0.03	0.55	1.92	7.55	−13	11	1	0.82	1.04	1.26	3	1.2
0.04	0.16	1.75	14.7	−11	85	1.25	2.35	2.96	3.58	3	1.1
0.05	0.12	6.28	61.0	−10	680	1.5	4.87	6.15	7.43	3	1.0
0.06	0.05	8.15	80.7	−9	2000	1.75	0.83	1.05	1.27	4	1.0
0.07	0.03	5.78	57.4	−8	1800	2	1.25	1.59	1.93	4	1.0
0.08	0.02	2.78	27.5	−7	870	2.5	2.06	2.76	3.46	4	1.0
0.09	0.01	1.00	9.87	−6	410	3	2.94	4.14	5.34	4	1.0
0.1	0.06	2.90	28.1	−6	220	3.5	3.85	5.68	7.51	4	1.0
0.11	0.27	7.04	67.2	−6	130	4	4.75	7.33	9.91	4	1.1
0.12	0.09	1.50	13.9	−5	83	5	0.64	1.08	1.52	5	1.1
0.13	0.25	2.86	25.8	−5	57	6	0.79	1.43	2.08	5	1.2
0.14	0.59	5.03	43.8	−5	42	7	0.91	1.78	2.65	5	1.3
0.15	1.27	8.30	69.2	−5	33	8	1.02	2.12	3.22	5	1.3
0.16	0.25	1.30	10.3	−4	26	9	1.10	2.44	3.78	5	1.3
0.18	0.75	2.79	20.1	−4	18	10	1.17	2.75	4.33	5	1.3
0.2	1.87	5.36	34.4	−4	13						

upper limit is selected by CA88. Our thermalization factor r_{tt} is 0.89 to 0.73 between $T_9 = 5$ to 10, reducing the ratio between our adopted rates and those of CA88, who adopt $r_{tt} = 1$ at all temperatures.

Reaction: $^{22}Ne(\alpha,\gamma)^{26}Mg$

The contribution of 31 resonances in the energy region between $E_r = 500.8$ and 1728.4 keV is calculated using the resonance strengths reported by WO89. For the low energy resonances at $E_r = 82$ and 338 keV, the values from GI93 are adopted. The angular distribution in GI93 suggests that $J^\pi = 3^-$ for the resonance at $E_r = 338$ keV, but the values $J^\pi = 2^+$ and 4^+ cannot be excluded. The adopted value for $\omega\gamma$ corresponds to $J^\pi = 3^-$, the other two J^π values being used for the upper and lower limits of the rates, respectively. The contributions of the direct capture process and of the tails of the broad resonances at $E_r = 700$, 1213 and 1280 keV are calculated using the S-factors of WO89. Above $T_9 = 1.25$, the rates are calculated using HF rates as explained in Section 2.5. The large differences between our rates and the CA88 ones at $0.3 \leqslant T_9 \leqslant 1$, are due to the differences between the WO89 data and the theoretical estimate used by CA88. For $T_9 \geqslant 1.25$, the HF rates are lower than the CA88 estimate.

E_r (keV)	J^π	$\omega\gamma$ (eV)		E_r (keV)	J^π	$\omega\gamma$ (eV)	
		adopt [GI93]				adopt [WO89]	
82	$4^+(7^-,8^+)$	$5.2^{+2.1\times10^5}_{-4.9} \times 10^{-47}$	N	718.3 ± 1.7	1^-	$4.7^{+42}_{-4.7} \times 10^{-7}$	M
338.4 ± 1.7	$(3^-,2^+,4^+)$	$1.4^{+11.6}_{-1.4} \times 10^{-13}$	I	732.6 ± 1.7		$4.7^{+42}_{-4.7} \times 10^{-7}$	M
		adopt [WO89]					
500.8 ± 1.7	2^+	$1.1^{+9.9}_{-1.1} \times 10^{-11}$	M	1011.0 ± 8.5		$5.9^{+53}_{-5.9} \times 10^{-7}$	M
541.4 ± 1.7	2^+	$8.5^{+77}_{-8.5} \times 10^{-9}$ $9.7^{+87}_{-9.7} \times 10^{-9}$ [GI93]	M	1040.6 ± 8.5		$5.9^{+53}_{-5.9} \times 10^{-7}$	M
551.6 ± 1.7	0^+	$1.0^{+9.0}_{-1.0} \times 10^{-9}$	M	1180.2 ± 8.5		$8.5^{+76}_{-8.5} \times 10^{-6}$	M
559.2 ± 1.7	0^+	$5.2^{+47}_{-5.2} \times 10^{-9}$	M	1186.1 ± 5.1		$8.5^{+76}_{-8.5} \times 10^{-6}$	M
560.0 ± 1.7	2^+	$1.2^{+11}_{-1.2} \times 10^{-8}$	M	1213.2 ± 2.5	$1^-,2^+,3^-$	$(2.11 \pm 0.35) \times 10^{-3}$	M
571.9 ± 1.7	1^-	$1.9^{+17}_{-1.9} \times 10^{-7}$	M	1265.6 ± 4.2		$6.8^{+61}_{-6.8} \times 10^{-6}$	M
577.8 ± 1.7	1^-	$1.9^{+17}_{-1.9} \times 10^{-7}$	M	1280.0 ± 4.2	$1^-,2^+,3^-$	$(1.69 \pm 0.17) \times 10^{-3}$	M
632.8 ± 1.7	1^-	$3.6^{+32}_{-3.6} \times 10^{-7}$	M	1296.9 ± 2.5	$1^-,2^+$	$(1.15 \pm 0.34) \times 10^{-3}$	M
664.1 ± 1.7	1^-	$4.0^{+36}_{-4.0} \times 10^{-7}$	M	1338.4 ± 2.5	$2^+,3^-,4^+$	$(1.15 \pm 0.34) \times 10^{-3}$	M
669.2 ± 1.7	1^-	$4.0^{+36}_{-4.0} \times 10^{-7}$	M	1436.5 ± 2.5	$2^+,3^-$	$(5.08 \pm 0.59) \times 10^{-3}$	M
676.0 ± 1.7	1^-	$4.0^{+36}_{-4.0} \times 10^{-7}$	M	1501.7 ± 6.8	(0^+)	$1.9^{+17}_{-1.9} \times 10^{-5}$	M
677.9 ± 1.7	1^-	$4.0^{+36}_{-4.0} \times 10^{-7}$	M	1524.5 ± 2.5		$(0.85 \pm 0.17) \times 10^{-3}$	M
683.6 ± 1.7	3^-	$5.8^{+52}_{-5.8} \times 10^{-9}$	M	1569.4 ± 6.8	(0^+)	$(0.93 \pm 0.17) \times 10^{-3}$	M
700.5 ± 4.2	1^-	$(30.4 \pm 3.4) \times 10^{-6}$	M	1658.2 ± 6.8	(0^+)	$(7.52 \pm 0.85) \times 10^{-3}$	M
				1728.4 ± 4.2	0^+	$(45.7 \pm 5.9) \times 10^{-3}$	M

T_9	low	adopt	high	exp	ratio	T_9	low	adopt	high	exp	ratio
0.1	0.67	9.90	113	−25	0.7	0.8	3.69	5.30	14.4	−5	46
0.11	0.21	3.05	34.3	−23	1.0	0.9	1.08	1.49	3.65	−4	21
0.12	0.37	5.24	58.1	−22	1.1	1	2.73	3.63	7.95	−4	11
0.13	0.41	5.77	63.2	−21	1.1	1.25	1.81	2.41	4.02	−3	3.4
0.14	0.32	4.52	49.1	−20	1.0	1.5	1.17	1.57	2.64	−2	2.1
0.15	0.19	2.73	29.5	−19	0.8	1.75	5.60	7.61	13.0	−2	1.7
0.16	0.09	1.38	15.0	−18	0.7	2	2.11	2.90	5.01	−1	1.4
0.18	0.13	2.96	32.8	−17	0.7	2.5	1.66	2.33	4.12	0	1.2
0.2	0.22	6.04	66.5	−16	1.0	3	0.74	1.07	1.94	1	1.0
0.25	0.34	3.12	30.1	−13	2.9	3.5	2.34	3.44	6.42	1	0.9
0.3	0.59	2.56	20.3	−11	5.6	4	5.83	8.84	16.9	1	0.8
0.35	2.30	6.58	42.3	−10	9.2	5	2.29	3.69	7.46	2	0.7
0.4	3.49	7.89	42.1	−9	14	6	0.59	1.02	2.19	3	0.6
0.45	2.84	5.56	25.4	−8	23	7	1.14	2.17	4.95	3	0.6
0.5	1.49	2.67	10.8	−7	39	8	1.78	3.83	9.32	3	0.6
0.6	1.74	2.80	9.49	−6	110	9	2.36	5.92	15.5	3	0.5
0.7	0.99	1.49	4.48	−5	100	10	2.67	8.31	23.4	3	0.5
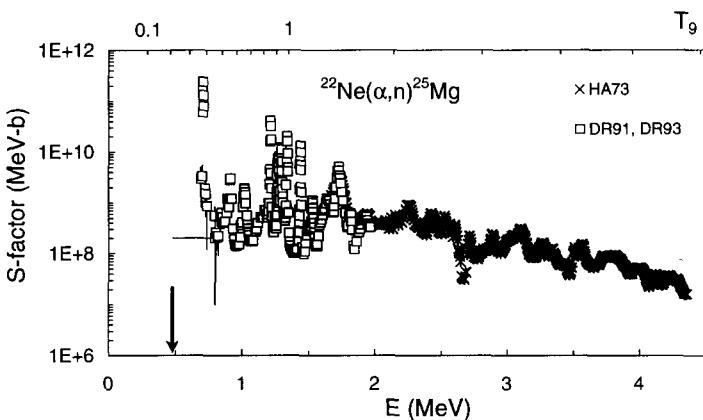
Reaction: ^{22}Ne(α,n)^{25}Mg

The rates for this endoergic reaction ($Q = -0.478$ MeV) are based on the cross section data of HA73, DR91 and DR93. The data of HA91 are not included since unexplained discrepancies exist between them and the other data. Between the threshold and 0.69 MeV, a constant S-factor $S(E) = 2 \times 10^8$ MeV b is adopted. The choise of this rather low value is motivated by the fact that only upper limits of the S-factor can be derived from the low-energy experimental data. The assumption of constancy of the S-factor takes into account in an average way the probable existence of resonances in this energy range [GI93,KÄ94]. For the lower limit of the rates, only tails from measured resonances are used. For the upper limit, the contribution from known states are considered with $\omega\gamma$ values estimated in the Wigner limit [WO89, DR93]. Above $T_9 = 2$, HF rates are used (see Section 2.5). In the temperature range between $T_9 = 0.1$ and 0.2, the present rates are up to a factor 10 smaller than the CA88 ones. This results from our lower extrapolation values. The enhancement of a factor 3 around $T_9 = 0.35$ is due to the resonance at $E_r = 700$ keV.

T_9	low	adopt	high	exp	ratio	T_9	low	adopt	high	exp	ratio
0.12	0.10	2.33	1200	−25	0.2	0.8	2.39	2.69	3.63	−3	1.2
0.13	0.40	8.64	5370	−24	0.2	0.9	1.50	1.68	2.00	−2	1.2
0.14	0.11	1.96	1440	−22	0.2	1	6.99	7.81	8.91	−2	1.2
0.15	0.26	3.03	2550	−21	0.2	1.25	1.33	1.50	1.68	0	1.0
0.16	0.48	3.51	3200	−20	0.1	1.5	1.12	1.30	1.48	1	0.9
0.17	0.75	3.31	3010	−19	0.1	1.75	5.87	7.04	8.21	1	0.8

continued from previous page

0.18	0.91	2.68	2220	−18	0.1	2	2.22	2.76	3.30	2	0.7
0.19	0.89	1.92	1330	−17	0.2	2.5	2.03	2.55	3.07	3	0.6
0.2	0.70	1.23	670	−16	0.2	3	1.01	1.28	1.55	4	0.6
0.25	1.82	2.30	314	−13	1.0	3.5	3.46	4.44	5.42	4	0.6
0.3	3.37	4.06	192	−11	2.2	4	0.94	1.22	1.50	5	0.5
0.35	1.37	1.64	36.8	−9	2.9	5	4.30	5.70	7.11	5	0.6
0.4	2.18	2.60	34.3	−8	2.9	6	1.28	1.74	2.20	6	0.6
0.45	1.90	2.27	19.8	−7	2.4	7	2.88	4.02	5.16	6	0.6
0.5	1.12	1.33	8.26	−6	1.9	8	5.37	7.69	10.0	6	0.6
0.6	2.10	2.45	7.97	−5	1.3	9	0.88	1.29	1.70	7	0.6
0.7	2.67	3.04	5.60	−4	1.1	10	1.29	1.96	2.63	7	0.6
T_9	low	adopt	high	exp	ratio	T_9	low	adopt	high	exp	ratio

Reaction: ^{22}Na(p,γ)^{23}Mg

The rate contribution of 21 resonances between E_r = 2.6 and 1213.6 keV is considered. The adopted resonance strengths come from the reported values of GÖ89a, SE90, SC95b and ST96b. The resonance energies are taken from SE90 and SC95b. For the lowest 3 resonances, only lower and upper limits of the strength are determined. The adopted values are averages of these limits. For the resonances at E_r = 215.6 and 273.6 keV, the values of ST96b are selected because of their measurement of some new γ-branching ratios. The direct capture contribution is calculated using the S-factor of SE90 and is found to be negligible. For the resonances analyzed by transfer reaction [SC95b], the energy dependence of the penetration factor is also taken into account. Above T_9 = 1, the rates are calculated using HF rates (see Section 2.5). The large differences between the present rates and the CA88 ones are due to the estimated resonance strengths [WI86] used by CA88.

E_r (keV)	J^π	$\omega\gamma$ (meV)						
		GÖ89a	SE90	SC95b low	SC95b high	ST96b	adopt	N
2.6 ± 6.0	$5/2^+$			0	1.3×10^{-63}		$1.4^{+13}_{-1.4} \times 10^{-64}$	N
41.6 ± 8.0	$(7/2, 9/2)^+$			1.7×10^{-14}	2.7×10^{-12}		$7.2^{+20}_{-7.0} \times 10^{-13}$	I
61.6 ± 8.0	$3/2^+, 5/2^+$			5.8×10^{-11}	1.5×10^{-8}		$2.9^{+12}_{-2.8} \times 10^{-9}$	I
204.1 ± 2.3	$1/2^+ - 11/2^+, 5/2^- - 7/2^-$		$\leqslant 0.36$	0.33	22	1.8 ± 0.7	1.8 ± 0.7	I
215.6 ± 6.0	$5/2^+$		$\leqslant 1.3$	0.05	29	$\leqslant 2.6$	$2.6^{+23}_{-2.6} \times 10^{-1}$	M
274.0 ± 6.0	$(7/2, 9/2)^+$		14 ± 3	1	58	15.8 ± 3.4	15.8 ± 3.4	M
436.6 ± 6.0	$3/2^-$	$\leqslant 18$	68 ± 20				68 ± 20	M
478.6 ± 7.0	$5/2^-$	$\leqslant 39$	37 ± 12				37 ± 12	M
496.3 ± 8.0	$5/2^+$	$\leqslant 44$	$\leqslant 7.5$				$7.5^{+67}_{-7.5} \times 10^{-1}$	M
575.6 ± 6.0	$3/2^+$	$\leqslant 50$	$\leqslant 8.3$				$8.3^{+75}_{-8.3} \times 10^{-1}$	M
585.1 ± 1.6	$5/2^+$	$\leqslant 38$	235 ± 33				235 ± 33	M
613.6 ± 8.0	$7/2^-$	$\leqslant 36$	$\leqslant 8.9$				$8.9^{+80}_{-8.9} \times 10^{-1}$	M
705.6 ± 8.0		$\leqslant 74$	364 ± 60				364 ± 60	M
754.6 ± 8.0		$\leqslant 83$	95 ± 30				95 ± 30	M
813.6 ± 6.0		$\leqslant 90$	$\leqslant 20$				2^{+18}_{-2}	M
840.6 ± 6.0		$\leqslant 140$	$\leqslant 20$				2^{+18}_{-2}	M
873.6 ± 5.0	$(3/2 - 13/2)^+$	$\leqslant 99$	$\leqslant 21$				$2.1^{+19}_{-2.1}$	M
977.6 ± 6.0		$\leqslant 97$	$\leqslant 15$				$1.5^{+13}_{-1.5}$	M
1037.6 ± 6.0		$\leqslant 79$	$\leqslant 44$				$4.4^{+40}_{-4.4}$	M
1178.6 ± 6.0		$\leqslant 87$	$\leqslant 51$				$5.1^{+46}_{-5.1}$	M
1213.6 ± 8.0		$\leqslant 69$	$\leqslant 51$				$5.1^{+46}_{-5.1}$	M

T_9	low	adopt	high	exp	ratio	T_9	low	adopt	high	exp	ratio
0.012	0.01	2.90	52.1	−25	12	0.3	0.67	1.07	2.28	0	0.1
0.013	0.03	5.68	58.2	−24	7.4	0.35	2.02	3.08	6.22	0	0.1
0.014	0.06	7.21	50.7	−23	4.9	0.4	4.64	6.86	13.2	0	0.1
0.015	0.06	6.48	35.7	−22	3.4	0.45	0.89	1.28	2.37	1	0.1
0.016	0.05	4.40	21.0	−21	2.4	0.5	1.50	2.13	3.79	1	0.1
0.018	0.01	1.06	4.71	−19	1.4	0.6	3.38	4.66	7.81	1	0.1
0.02	0.02	1.36	6.63	−18	0.8	0.7	6.22	8.42	13.5	1	0.1
0.025	0.01	1.61	12.0	−16	0.4	0.8	1.02	1.35	2.09	2	0.1
0.03	0.07	6.15	52.1	−15	0.4	0.9	1.53	2.01	3.01	2	0.1
0.04	0.01	1.06	9.35	−12	0.6	1	2.16	2.81	4.11	2	0.1
0.05	0.02	2.57	30.2	−11	0.7	1.25	4.67	6.32	9.62	2	0.1
0.06	0.02	2.09	32.6	−10	0.8	1.5	0.80	1.12	1.77	3	0.1
0.07	0.21	9.36	180	−10	0.6	1.75	1.19	1.73	2.81	3	0.1
0.08	0.86	4.40	68.6	−9	0.2	2	1.61	2.43	4.06	3	0.1
0.09	1.95	4.57	27.4	−8	0.1	2.5	2.48	4.00	7.04	3	0.1
0.1	2.37	4.86	15.9	−7	0.1	3	3.34	5.72	10.5	3	0.1
0.11	1.82	3.59	9.83	−6	0.2	3.5	4.13	7.51	14.3	3	0.1
0.12	0.98	1.91	4.96	−5	0.1	4	4.84	9.31	18.3	3	0.1
0.13	4.07	7.79	19.9	−5	0.1	5	0.61	1.29	2.66	4	0.1
0.14	1.37	2.59	6.55	−4	0.1	6	0.71	1.65	3.53	4	0.1
0.15	3.93	7.33	18.4	−4	0.1	7	0.79	2.00	4.42	4	0.1
0.16	0.99	1.82	4.52	−3	0.1	8	0.85	2.34	5.32	4	0.1
0.18	4.57	8.23	20.1	−3	0.1	9	0.91	2.68	6.23	4	0.1
0.2	1.57	2.76	6.61	−2	0.1	10	0.95	3.02	7.15	4	0.1
0.25	1.48	2.45	5.55	−1	0.1						

Reaction: ^{23}Na(p,γ)^{24}Mg
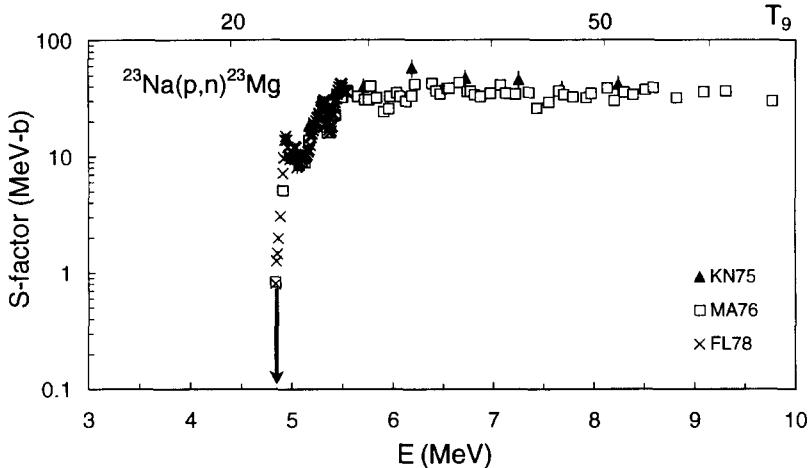
More than 80 resonances are identified up to $E = 3.7$ MeV. The reaction rates are computed using the $\omega\gamma$ values of SW75 and GÖ89b and normalized to the $E_r = 491$ keV resonance yield [PA78,PA79]. Two subthreshold states with $J^\pi = 2^+$ ($\ell = 0$) are included [SW75,SC83] with a reduced width $\gamma_p^2 = 305$ keV (10% of the Wigner limit at $a = 4.6$ fm). These subthreshold states determine the rate up to $T_9 \approx 0.03$. The lower and upper limits on γ_p^2 are taken as 0 and 3.05 MeV (the Wigner limit). Since interference effects cannot be evaluated, they are neglected, and a factor of 2 is included in the uncertainty on the contribution of subthreshold and low-energy states. Between $T_9 = 0.04$ and $T_9 = 0.14$, the rate is essentially determined by the properties of the 138 keV resonance, for which an upper limit on the $\omega\gamma$ value is available [GÖ89b]. Two other 2^+ resonances ($E_r = 0.238$ and 0.294 MeV) also contribute substantially. Above $T_9 = 5$, HF estimates are used (see Section 2.5). As the CA88 and FO75 rates are identical, it is likely that the data of FI78, SC83, and probably also of SW75 have not been taken into account in CA88. The large differences between our rates and the CA88 rates between $T_9 = 0.04$ and $T_9 = 0.14$ are due to the 138 keV resonance, which was not included in CA88. Moreover, the direct-capture term in CA88 is obtained with $S_1 > 0$, which implies that subthreshold states have been disregarded. Our thermalization effects reduce the ratio to CA88 by a factor $r_{tt} = 0.90$ to 0.77 for $T_9 = 3.5$ to 10 (CA88 adopt $r_{tt} = 1$ at all temperatures).

E_r (keV)	J^π	Γ_{tot} (keV)	Γ_γ (eV)	γ_p^2 (keV)
-238 ± 1	2^+	< 2 [SC83]	0.24 ± 0.04 [SC83]	305
-171 ± 1	2^+	< 3 [SC83]	0.16 ± 0.04 [SC83]	305

			$\omega\gamma$ (eV)	
138 ± 3			$5^{+45}_{-5} \times 10^{-7}$ [GÖ89b]	1
238 ± 1	2^+	< 0.02	$(5.3 \pm 1.8) \times 10^{-4}$ [SW75]	1
294 ± 1	2^+	< 0.02	0.11 ± 0.02 [SW75]	1

Res. 294–3700 keV			see comments	

T_9	low	adopt	high	exp	ratio	T_9	low	adopt	high	exp	ratio
0.018	0.02	4.39	86.8	−26	0.2	0.4	0.50	1.23	2.90	1	0.9
0.02	0.03	6.16	122	−25	0.2	0.45	1.10	2.69	6.35	1	0.9
0.025	0.01	1.21	23.9	−22	0.2	0.5	2.06	4.97	11.7	1	0.9
0.03	0.04	6.81	133	−21	0.2	0.6	0.52	1.22	2.85	2	0.9
0.04	1.6e-3	4.43	46.5	−17	3.3	0.7	1.02	2.29	5.25	2	0.9
0.05	1.1e-4	9.04	90.5	−14	97	0.8	1.73	3.67	8.21	2	0.9
0.06	4.2e-6	1.43	14.3	−11	600	0.9	2.69	5.32	11.6	2	0.9
0.07	6.4e-5	5.13	51.3	−10	150	1	3.93	7.25	15.2	2	0.9
0.08	7.7e-4	7.34	73.3	−9	1300	1.25	0.85	1.33	2.53	3	0.9
0.09	3.5e-3	5.69	56.9	−8	370	1.5	1.51	2.11	3.71	3	0.9
0.1	0.01	2.90	28.8	−7	94	1.75	2.38	3.09	5.10	3	0.9
0.11	0.01	1.10	10.8	−6	29	2	3.40	4.25	6.76	3	1.0
0.12	0.10	3.42	32.2	−6	9.7	2.5	5.79	7.00	10.8	3	1.0
0.13	0.67	9.59	82.6	−6	4.1	3	0.84	1.01	1.56	4	1.1
0.14	0.36	2.61	19.1	−5	2.2	3.5	1.10	1.32	2.05	4	1.2
0.15	1.53	7.19	42.2	−5	1.4	4	1.34	1.61	2.51	4	1.3
0.16	0.55	1.99	9.19	−4	1.1	5	1.76	2.10	3.24	4	1.1
0.18	0.48	1.35	4.36	−3	0.9	6	2.13	2.79	5.00	4	1.3
0.2	2.67	6.97	19.0	−3	0.8	7	2.44	3.49	7.00	4	1.4
0.25	0.58	1.44	3.52	−1	0.8	8	2.73	4.22	9.21	4	1.5
0.3	0.44	1.07	2.57	0	0.8	9	2.99	4.97	11.6	4	1.7
0.35	1.78	4.37	10.4	0	0.9	10	3.22	5.74	14.2	4	1.8

Reaction: ^{23}Na(p,n)^{23}Mg

For this endoergic reaction ($Q = -4.839$ MeV), the reaction rates are calculated using a linear interpolation between the experimental data points [KN75,MA76,FL78]. Below $T_9 \approx 8$, our rates are larger than the CA88 ones, while at the highest temperatures they come progressively in agreement. Thermalization effects ($r_{tt} = 2.6 - 2.0$ for $0.7 \leqslant T_9 \leqslant 10$) accounts for these differences at the lower temperatures (CA88 adopt $r_{tt} = 1$ at all temperatures). Our results are in agreement with those of FL78.

T_9	low	adopt	high	exp	ratio	T_9	low	adopt	high	exp	ratio
0.7	3.18	3.46	3.74	−27	2.9	3	1.83	2.00	2.17	0	1.5
0.8	7.23	7.86	8.49	−23	2.7	3.5	2.75	3.01	3.26	1	1.4
0.9	1.77	1.93	2.08	−19	2.6	4	2.09	2.29	2.49	2	1.3
1.0	9.08	9.88	10.7	−17	2.4	5	3.59	3.93	4.27	3	1.2
1.25	6.90	7.50	8.11	−12	2.2	6	2.44	2.67	2.91	4	1.1
1.5	1.22	1.33	1.44	−8	1.9	7	0.94	1.03	1.13	5	1.1
1.75	2.64	2.87	3.11	−6	1.8	8	2.62	2.89	3.15	5	1.0
2	1.47	1.60	1.73	−4	1.7	9	5.92	6.53	7.14	5	1.0
2.5	4.20	4.58	4.97	−2	1.6	10	1.10	1.22	1.33	6	0.9
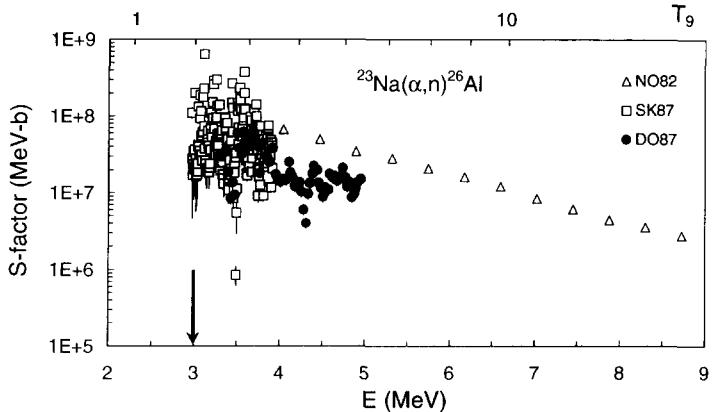
Reaction: ^{23}Na(p,α)^{20}Ne

Resonance strengths of 75 resonances in the energy region between E_r = 36 and 3813 keV are adopted from the data reported by FL54, FI63, KU63, LU70, ME72, ZY81, VA87 and GÖ89b. For resonances above 880.4 keV, adopted strengths are from VA87. The non-resonant contribution is calculated using the S-factor from ZY81 for the tails of the broad resonances. Above T_9 = 5, HF estimates are used (see Section 2.5). The differences between the adopted rates and the CA88 ones arise from the contribution of the resonances at 138 keV and 217 keV that are not taken into account in CA88. Moreover, the contribution of resonances with energies above 2 MeV is neglected by CA88, which leads to their underestimate of the rates at high temperatures.

E_r (keV)	J^π	$\omega\gamma$ (eV)						
		FL54	FI63	KU63	ZY81	GÖ89b	adopt	
36.2	0^+				$\leqslant 1.9 \times 10^{-17}$		$1.9^{+17}_{-1.9} \times 10^{-18}$	I
138.0 ± 2.9						$\leqslant 5.0 \times 10^{-7}$	$5.0^{+45}_{-5.0} \times 10^{-8}$	I
166.7 ± 1.9	$(6^+, 7^-, 8^+)$				$(26 \pm 7) \times 10^{-6}$	$(28 \pm 7) \times 10^{-6}$	$(27 \pm 7) \times 10^{-6}$	I
217.5 ± 1.9						$(70 \pm 16) \times 10^{-6}$	$(70 \pm 16) \times 10^{-6}$	M
240.3 ± 0.2	$(2-4)$		$\leqslant 10^{-3}$	$\leqslant 0.08$			$1^{+9}_{-1} \times 10^{-4}$	M
273.9 ± 0.4	2^+	40×10^{-3}	$(37 \pm 7) \times 10^{-3}$	0.08		$(40 \pm 8) \times 10^{-3}$	$(40 \pm 8) \times 10^{-3}$	M
297.2 ± 0.4	2^+	$\leqslant 10^{-3}$		$\leqslant 0.06$			$1^{+9}_{-1} \times 10^{-4}$	M
324.4 ± 0.5	3^-	6.4×10^{-2}	8.7×10^{-2}	0.11		$(97 \pm 19) \times 10^{-3}$	$(97 \pm 19) \times 10^{-3}$	M
358.2 ± 0.3	4^+		3.7×10^{-3}	$\leqslant 0.01$			$3.7 \pm 0.7 \times 10^{-3}$	M
426.3 ± 0.1	2^+		8.7×10^{-3}	$\leqslant 0.03$			$8.7 \pm 1.7 \times 10^{-3}$	M
490.0 ± 0.3	$(1,2^+)$	$\leqslant 2.5 \times 10^{-2}$		$\leqslant 0.08$			$2.5^{+27}_{-2.5} \times 10^{-3}$	M
566.8 ± 0.4	3^-	40 ± 8		40	40 ± 3		40 ± 3	M
648.3 ± 0.4	3^+			$\leqslant 0.16$			$1.6^{+14}_{-1.6} \times 10^{-2}$	M
692.6 ± 0.3	0^-			$\leqslant 0.26$			$2.6^{+23}_{-2.6} \times 10^{-2}$	M
707.9 ± 0.3	3^+			$\leqslant 0.14$			$1.4^{+13}_{-1.4} \times 10^{-2}$	M
712.6 ± 0.3	2^+			8.4	10.4		9.4 ± 1.9	M
761.6 ± 0.5	1^-			4	3.8		3.9 ± 0.8	M
776.2 ± 0.5	2^+			2.2	2.4		2.3 ± 0.5	M
813.2 ± 4.8	4^+			0.63			0.63 ± 0.13	M
Res. 880–3813 keV					see comments			

(LU70 applies to the ZY81 column values for the 712.6–776.2 keV resonances)

T_9	low	adopt	high	exp	ratio	T_9	low	adopt	high	exp	ratio
0.012	0.001	1.46	14.6	−25	9.4	0.30	1.10	1.42	1.66	0	0.9
0.013	0.001	1.91	19.2	−24	7.9	0.35	4.42	5.60	6.49	0	0.9
0.014	0.001	1.72	17.3	−23	6.8	0.4	1.32	1.65	1.89	1	0.9
0.015	0.001	1.15	11.5	−22	6.0	0.45	3.37	4.11	4.67	1	0.9
0.016	0.004	6.00	60.3	−22	5.4	0.5	7.83	9.32	10.5	1	0.9
0.018	0.008	9.31	73.5	−21	4.5	0.6	3.37	3.86	4.27	2	0.9
0.02	0.01	8.21	82.4	−20	3.8	0.7	1.09	1.21	1.33	3	1.0
0.025	0.03	3.95	39.4	−18	2.9	0.8	2.74	3.02	3.30	3	1.0
0.03	0.18	5.09	49.6	−17	2.3	0.9	5.77	6.31	6.90	3	1.0
0.04	0.76	1.82	11.5	−15	1.4	1	1.07	1.16	1.27	4	1.0
0.05	5.83	7.67	26.2	−14	1.3	1.25	3.51	3.77	4.16	4	1.0
0.06	2.97	5.86	25.9	−12	2.3	1.5	8.53	9.08	10.1	4	1.1
0.07	1.47	3.06	10.3	−10	2.6	1.75	1.70	1.81	2.03	5	1.2
0.08	3.59	7.00	17.8	−9	2.4	2	2.94	3.13	3.54	5	1.3
0.09	4.47	8.20	17.3	−8	2.1	2.5	6.53	7.14	8.13	5	1.4
0.1	3.36	5.90	11.0	−7	2.0	3	1.12	1.29	1.47	6	1.4
0.11	1.75	2.97	5.13	−6	1.8	3.5	1.67	2.01	2.30	6	1.5
0.12	0.70	1.16	1.89	−5	1.7	4	2.28	2.88	3.30	6	1.5
0.13	2.35	3.76	5.88	−5	1.6	5	3.60	4.95	5.69	6	1.6
0.14	0.69	1.07	1.62	−4	1.4	6	6.16	8.50	9.78	6	1.9
0.15	1.85	2.78	4.08	−4	1.3	7	0.94	1.30	1.49	7	2.1
0.16	4.64	6.77	9.80	−4	1.2	8	1.31	1.82	2.10	7	2.3
0.18	2.45	3.41	4.69	−3	1.0	9	1.73	2.41	2.79	7	2.4
0.20	1.04	1.40	1.81	−2	0.9	10	2.18	3.05	3.53	7	2.6
0.25	1.65	2.15	2.59	−1	0.9						

Reaction: ^{23}Na$(\alpha,n)^{26}$Al

Depending upon the astrophysical situation, it is necessary to evaluate either the production of the ^{26}Al ground (g) and isomeric (m) states separately, or the total production of ^{26}Al, irrespective of its state [WA80]. The three corresponding reaction rates are noted $N_A\langle\sigma v\rangle^g$, $N_A\langle\sigma v\rangle^m$ and $N_A\langle\sigma v\rangle^t$. They are calculated by numerical integration of the cross section data of SK87 ($E = 2.97 - 3.83$ MeV), NO82 ($E = 3.0 - 8.9$ MeV), and DO87 ($E = 3.3 - 5.0$ MeV) from threshold energies ($Q^g = -2.968$ MeV and $Q^m = -3.196$ MeV) up to $E = 8.9$ MeV. The NO82 data are divided by a factor of 3 in order to normalize them to the DO87 data. The DO87 time of flight experiment is indeed considered to be more reliable than the NO82 thick target measurements. Total S-factor data are shown in the figure. As experimental data are available down to threshold and up to more than 8.5 MeV, neither low energy nor high energy extrapolations are required. The upper and lower limits of the rates are set by the experimental uncertainties. Our rates differ from the CA88 ones by up to a factor of 6.5.

$N_A \langle \sigma v \rangle_{gs}^t$

T_9	low	adopt	high	exp	ratio	T_9	low	adopt	high	exp	ratio
0.5	1.02	1.36	1.71	−23	6.5	2.5	1.61	1.78	1.95	1	3.8
0.6	1.03	1.34	1.65	−18	6.3	3	1.76	1.93	2.10	2	3.4
0.7	3.89	4.95	6.01	−15	6.0	3.5	0.98	1.07	1.16	3	2.9
0.8	1.89	2.36	2.83	−12	5.8	4	3.59	3.92	4.25	3	2.6
0.9	2.33	2.87	3.41	−10	5.6	5	2.26	2.47	2.68	4	2.0
1	1.11	1.34	1.58	−8	5.5	6	7.96	8.76	9.55	4	1.6
1.25	1.18	1.39	1.60	−5	5.1	7	2.02	2.24	2.45	5	1.4
1.5	1.26	1.45	1.65	−3	4.8	8	4.18	4.63	5.09	5	1.2
1.75	3.61	4.11	4.61	−2	4.5	9	7.49	8.32	9.15	5	1.2
2	4.55	5.11	5.67	−1	4.3	10	1.21	1.35	1.48	6	1.3

$N_A \langle \sigma v \rangle_{gs}^g$

T_9	low	adopt	high	exp	ratio	T_9	low	adopt	high	exp	ratio
0.5	1.02	1.36	1.71	−23	6.5	2.5	1.34	1.53	1.72	1	4.3
0.6	1.03	1.33	1.65	−18	6.3	3	1.42	1.61	1.81	2	3.8
0.7	3.86	4.93	6.01	−15	6.1	3.5	7.77	8.79	9.81	2	3.3
0.8	1.87	2.34	2.83	−12	6.0	4	2.81	3.17	3.54	3	2.8
0.9	2.29	2.84	3.39	−10	5.8	5	1.75	1.99	2.23	4	2.1
1	1.08	1.32	1.57	−8	5.7	6	6.19	7.10	8.02	4	1.7
1.25	1.12	1.34	1.57	−5	5.4	7	1.58	1.83	2.08	5	1.4
1.5	1.16	1.37	1.58	−3	5.2	8	3.28	3.83	4.39	5	1.2
1.75	3.24	3.78	4.33	−2	5.0	9	5.88	6.94	8.01	5	1.2
2	3.97	4.59	5.21	−1	4.8	10	0.95	1.13	1.31	6	1.3

$N_A \langle \sigma v \rangle_{gs}^m$

T_9	low	adopt	high	exp	ratio	T_9	low	adopt	high	exp	ratio
0.5	4.21	5.39	7.14	−27	0.8	2.5	5.61	6.40	7.23	−1	0.6
0.6	1.12	1.40	1.79	−21	0.8	3	7.16	8.15	9.17	0	0.6
0.7	0.83	1.03	1.29	−17	0.8	3.5	4.48	5.10	5.73	1	0.5
0.8	6.69	8.17	10.0	−15	0.8	4	1.80	2.05	2.31	2	0.5
0.9	1.22	1.48	1.79	−12	0.8	5	1.32	1.52	1.71	3	0.5
1	7.91	9.49	11.4	−11	0.8	6	5.31	6.11	6.92	3	0.5
1.25	1.47	1.73	2.03	−7	0.7	7	1.50	1.73	1.97	4	0.5
1.5	2.25	2.63	3.04	−5	0.7	8	3.38	3.92	4.46	4	0.6
1.75	8.30	9.59	11.0	−4	0.7	9	6.49	7.55	8.62	4	0.6
2	1.25	1.43	1.63	−2	0.6	10	1.11	1.29	1.48	5	0.6

Reaction: ^{24}Mg(p,γ)^{25}Al
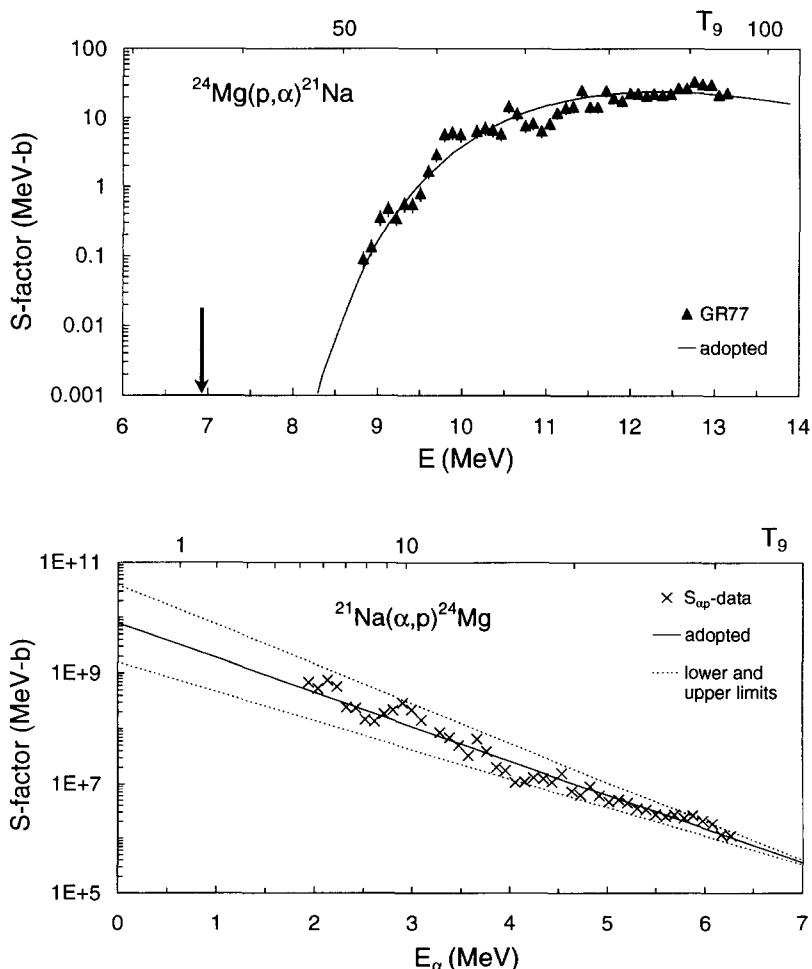
Resonance data are available for 13 resonances in the $214.0 \leqslant E_r \leqslant 5698.7$ keV range [LI56,VA69, TR75b, RO77,KE80]. The strengths of the $E_r = 790.4$ and 1424.4 keV resonances in LI56 are disregarded because of the large discrepancies with the other data sets, probably due to uncertainties in the used stopping power. The level at $E_x = 452$ keV in ^{25}Al is not observed in MO68 data, which are therefore omitted. The relative resonance strengths in VA69 are renormalized, taking as a standard the strength of the 790.4 keV resonance given by TR75b. The non-resonant contribution from the direct capture process is calculated with the S-factor given by TR75a. Above $T_9 = 7$, the rates are calculated using HF rates as explained in Section 2.5. The present rates are in agreement with those of CA88, except at the highest temperatures, where the HF rates are larger.

T_9	low	adopt	high	exp	ratio	T_9	low	adopt	high	exp	ratio
0.025	1.00	1.25	1.49	−23	1.0	0.45	1.72	2.17	2.64	1	1.1
0.03	7.47	9.34	11.2	−21	1.0	0.5	2.60	3.27	3.96	1	1.1
0.04	4.01	5.01	6.01	−19	1.0	0.6	4.75	5.92	7.15	1	1.1
0.05	6.18	8.21	10.7	−17	1.0	0.7	7.22	8.95	10.7	1	1.1
0.06	0.84	1.17	1.62	−13	1.1	0.8	0.99	1.22	1.45	2	1.1
0.07	2.47	3.39	4.60	−11	1.1	0.9	1.27	1.55	1.84	2	1.0
0.08	1.72	2.33	3.12	−9	1.1	1	1.56	1.89	2.23	2	1.0
0.09	4.58	6.15	8.13	−8	1.1	1.25	2.36	2.81	3.27	2	1.0
0.1	6.22	8.29	10.8	−6	1.1	1.5	3.33	3.89	4.45	2	1.0
0.11	5.19	6.87	8.91	−6	1.1	1.75	4.45	5.12	5.79	2	1.0
0.12	3.00	3.96	5.10	−5	1.1	2	5.70	6.49	7.26	2	1.0
0.13	1.31	1.72	2.21	−4	1.1	2.5	8.34	9.37	10.4	2	1.0
0.14	4.62	6.03	7.69	−4	1.1	3	1.09	1.22	1.35	3	1.0
0.15	1.36	1.77	2.25	−3	1.1	3.5	1.33	1.49	1.64	3	1.0
0.16	3.49	4.53	5.73	−3	1.1	4	1.55	1.73	1.91	3	1.0
0.18	1.65	2.13	2.68	−2	1.1	5	1.90	2.14	2.37	3	1.0
0.2	5.62	7.23	9.03	−2	1.1	6	2.16	2.44	2.71	3	1.0
0.25	4.85	6.20	7.68	−1	1.1	7	2.32	2.63	2.93	3	1.5
0.3	1.94	2.47	3.04	0	1.1	8	2.70	3.44	4.15	3	2.1
0.35	5.07	6.42	7.87	0	1.1	9	3.09	4.35	5.57	3	2.9
0.4	1.02	1.29	1.57	1	1.1	10	3.48	5.39	7.23	3	4.0

C. Angulo et al./Nuclear Physics A 656 (1999) 3–183

E_r (keV)	J^π	$\omega\gamma$ (meV)						
		LI56	VA69	TR75b	RO77	KE80	adopt	
214.0 ± 0.8	1/2+	13.9 ± 6.9		9.5 ± 2.0			10.0 ± 2.0	I
402.2 ± 0.6	3/2+	28.4 ± 5.6		33 ± 5			31 ± 4	M
790.4 ± 0.6	3/2−	220 ± 44	490 ± 100	490 ± 70		580 ± 60	532 ± 41	M
1153.0 ± 0.5	(5/2+, 9/2+)	27.5 ± 5.5	38 ± 8				31 ± 5	M
1177.7 ± 0.5					68 ± 14		68 ± 14	M
1424.4 ± 0.5	7/2−	52 ± 10	155 ± 31	140 ± 20			144 ± 17	M
1551.7 ± 1.6	1/2−	520 ± 100	283 ± 57	700 ± 100			410 ± 120	M
1587.5 ± 0.8	5/2+	165 ± 33	188 ± 36	190 ± 30			181 ± 19	M
1754.7 ± 3.0	(5/2+, 9/2+)				19 ± 4		19 ± 4	M
1924.7 ± 5.0	3/2+	700 ± 140		520 ± 80			564 ± 78	M
2311.7 ± 4.0	5/2+	180 ± 36					180 ± 36	M
			MO68					
5629.7 ± 2.0	5/2+		1200 ± 500		255 ± 60		255 ± 60	M
5698.7 ± 2.0	3/2+ (5/2+)		1500 ± 800		395 ± 90		395 ± 90	M

Reaction: ^{24}Mg(p,α)^{21}Na

For this endoergic reaction ($Q = -6.884$ MeV), a unique set of cross section data [GR77] is available, with no information between the threshold and $E = 8.83$ MeV. In order to extrapolate the cross section down to the threshold, the S-factor $S_{\alpha,p}$ for the reverse reaction ^{21}Na(α,p)^{24}Mg is approximated by an exponential function $S_{\alpha,p} = 7.92 \times 10^9 \exp(-1.4271E_\alpha)$, where E_α is the center of mass energy in the channel $\alpha + ^{21}$Na, and extrapolated down to the threshold. For the calculation of the lower and upper limits of the rates, exponential fits $S_{\alpha,p}^{max} = 4.00 \times 10^{10} \exp(-1.5786E_\alpha)$ and $S_{\alpha,p}^{min} = 2.00 \times 10^9 \exp(-1.2758E_\alpha)$, that corresponds to the lower and upper bounds of $S_{\alpha,p}$ are obtained and extrapolated to the threshold in a way similar to $S_{\alpha,p}$. Our thermalization effects are $r_{tt} = 6$ to 20 at $T_9 = 0.2$ to 10 while CA88 adopted the equal strength approximation here ($r_{tt} = 1$ for all temperatures). A more accurate extrapolation needs data at lower energies.

T_9	low	adopt	high	exp	ratio	T_9	low	adopt	high	exp	ratio
1.5	0.51	1.65	6.82	−23	0.2	5	1.81	4.48	14.3	−2	0.8
1.75	0.83	2.61	10.5	−19	0.3	6	0.82	1.94	5.90	0	0.9
2	1.33	4.09	16.1	−16	0.3	7	1.29	2.91	8.54	1	1.0
2.5	0.50	1.47	5.54	−11	0.5	8	1.02	2.24	6.36	2	1.1
3	0.66	1.85	6.71	−8	0.6	9	0.52	1.10	3.04	3	1.2
3.5	1.21	3.30	11.5	−6	0.6	10	1.89	3.91	10.6	3	1.4
4	0.64	1.69	5.70	−4	0.7						

Reaction: ^{25}Mg(p,γ)^{26}Al

Three reaction rates, $N_A\langle\sigma v\rangle^g$, $N_A\langle\sigma v\rangle^m$ and $N_A\langle\sigma v\rangle^t$ have to be evaluated. They correspond to the production of the ^{26}Al ground (g) state, ^{26}Al isomeric (m) state, and to the sum over all possible exit channels, respectively. The contribution of 89 resonances ranging from 37.5 to 1920.5 keV is considered. For the low energy resonances ($E_r \leqslant$ 130.4 keV), the strengths of IL96, obtained by a new analysis of the CH89 and RO90 data, are adopted. For resonances above 130.4 keV, the adopted resonance strengths are the weighted averages of the values reported in EN66, DE74, EL79b, AN80, KE80, AN82, CH83, KA84, CH86b, EN86, EN87, CH89, KA89, IL90, and RO90. The relative resonance strengths in DE74 are renormalized, taking as a standard the strength of the $E_r = 658.4$ keV resonance in KE80. The data of CH83 and KA84 differ substantially from the data of the other authors, and are neglected. The non-resonant contribution from the direct capture process into the bound states of ^{26}Al and the contribution of the subthreshold state at $E_r = -25.7$ keV are calculated with the S-factors given by EN87. The branching ratios for forming the ^{26}Al ground state reported by EN87 and CH89 are used. Above $T_9 = 2$, HF rates are used for $N_A\langle\sigma v\rangle^t$ (see Section 2.5). For the calculation of $N_A\langle\sigma v\rangle^g$ and $N_A\langle\sigma v\rangle^m$, the total rate has been multiplied by the corresponding branching ratios at $T_9 = 2$. The present rates at low temperatures are smaller than the CA88 ones. This is mainly due to the smaller strengths of the resonances at $E_r = 37.5$ and 58 keV. Our thermalization effects reduce the ratio by a factor $r_{tt} = 0.92 - 0.69$ for $T_9 = 4$ to 10. (CA88 adopt $r_{tt} = 1$ at all temperatures).

E_r (keV)	J^π		$\omega\gamma$ (eV)					
		CH86b	EN87	CH89	RO90	IL96	adopt	
37.5 ± 0.5	4^-		1.9×10^{-18}	$\leqslant 2.1\ 10^{-20}$	$(3.1 \pm 0.8) \times 10^{-20}$	$\leqslant 2.4 \times 10^{-20}$	$2.4^{+21.6}_{-2.4} \times 10^{-21}$	I
58.0 ± 0.5	3^+	$(1.6 \pm 0.6)10^{-13}$	1.2×10^{-12}	2.6×10^{-13}	$(2.6 \pm 0.3) \times 10^{-13}$	$2.82^{+1.41}_{-0.94} \times 10^{-13}$	$2.82^{+1.41}_{-0.94} \times 10^{-13}$	I
		EL79b						
92.6 ± 0.5	2^-	$\leqslant 4 \times 10^{-8}$	4.3×10^{-10}	8.5×10^{-11}	$(2.2 \pm 0.5) \times 10^{-10}$	$1.16^{+1.16}_{-0.39} \times 10^{-10}$	$1.16^{+1.16}_{-0.39} \times 10^{-10}$	I
108.5 ± 0.5	0^+	$\leqslant 4 \times 10^{-8}$	$\leqslant 1.9 \times 10^{-10}$	$\leqslant 2.0 \times 10^{-12}$	$(6.3 \pm 0.5) \times 10^{-12}$	2.1×10^{-11}	$2.1^{+2.1}_{-0.7} \times 10^{-11}$	M
130.4 ± 0.5	4^-	$\leqslant 4 \times 10^{-8}$	1.7×10^{-7}	$\leqslant 1.3 \times 10^{-9}$	$\leqslant 5.0 \times 10^{-9}$	$\leqslant 1.4 \times 10^{-10}$	$1.4^{+1.3}_{-1.4} \times 10^{-11}$	M
Res. 189.9–1920.5 keV					see comments			

$N_A \langle \sigma v \rangle^t$:

T_9	low	adopt	high	exp	ratio	T_9	low	adopt	high	exp	ratio
0.015	3.90	8.87	25.9	−25	0.02	0.35	1.22	1.33	1.43	0	0.9
0.016	0.59	1.28	3.08	−23	0.04	0.4	3.97	4.29	4.62	0	0.9
0.018	0.55	1.12	2.36	−21	0.1	0.45	1.00	1.08	1.16	1	0.9
0.02	2.02	4.01	8.01	−20	0.2	0.5	2.12	2.28	2.46	1	0.9
0.025	1.27	2.39	4.48	−17	0.2	0.6	6.67	7.18	7.71	1	0.9
0.03	0.89	1.61	2.91	−15	0.2	0.7	1.54	1.66	1.78	2	0.9
0.04	1.67	2.89	5.02	−13	0.2	0.8	2.92	3.15	3.39	2	0.9
0.05	3.96	6.66	11.6	−12	0.2	0.9	4.85	5.24	5.63	2	0.9
0.06	3.86	6.37	11.7	−11	0.2	1	7.31	7.92	8.51	2	1.0
0.07	2.38	3.88	7.56	−10	0.2	1.25	1.55	1.70	1.82	3	1.0
0.08	1.06	1.71	3.46	−9	0.2	1.5	2.61	2.87	3.08	3	1.0
0.09	3.60	5.77	12.0	−9	0.1	1.75	3.82	4.24	4.55	3	1.0
0.1	1.03	1.62	3.40	−8	0.1	2	5.16	5.75	6.17	3	1.0
0.11	2.79	4.22	8.51	−8	0.1	2.5	0.83	1.00	1.12	4	1.1
0.12	0.85	1.18	2.12	−7	0.2	3	1.16	1.51	1.74	4	1.2
0.13	3.21	4.03	6.03	−7	0.3	3.5	1.49	2.06	2.45	4	1.3
0.14	1.37	1.60	2.05	−6	0.4	4	1.80	2.66	3.24	4	1.4
0.15	5.61	6.37	7.50	−6	0.6	5	2.39	3.95	5.01	4	1.5
0.16	2.06	2.30	2.61	−5	0.7	6	2.93	5.35	7.00	4	1.7
0.18	1.91	2.11	2.33	−4	0.8	7	3.41	6.84	9.17	4	1.9
0.2	1.16	1.27	1.39	−3	0.8	8	3.86	8.40	11.5	4	2.1
0.25	2.97	3.24	3.52	−2	0.9	9	0.43	1.00	1.39	5	2.3
0.3	2.59	2.81	3.04	−1	0.9	10	0.46	1.17	1.65	5	2.5

$N_A \langle \sigma v \rangle^g$:
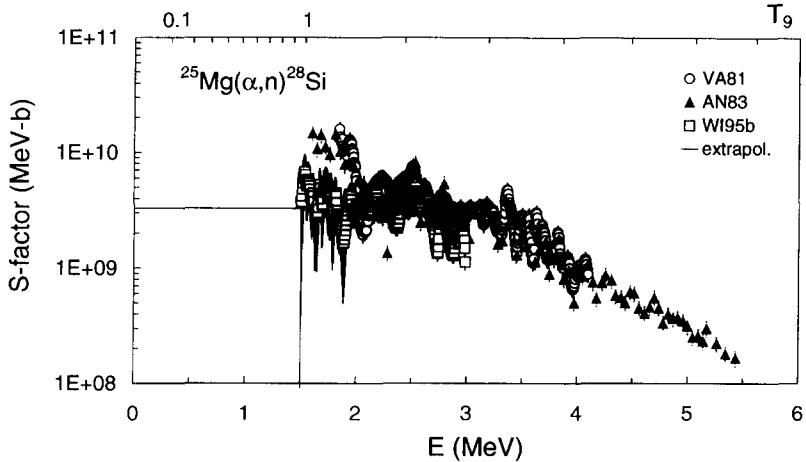
T_9	low	adopt	high	exp	ratio	T_9	low	adopt	high	exp	ratio
0.015	3.16	7.18	20.9	−25	0.02	0.35	1.03	1.12	1.21	0	0.9
0.016	0.48	1.03	2.48	−23	0.04	0.4	3.33	3.59	3.86	0	0.9
0.018	4.42	9.09	19.1	−22	0.1	0.45	8.32	8.97	9.64	0	0.9
0.02	1.63	3.25	6.48	−20	0.2	0.5	1.75	1.88	2.02	1	0.9
0.025	1.03	1.93	3.63	−17	0.2	0.6	5.39	5.79	6.21	1	0.9
0.03	0.72	1.30	2.36	−15	0.2	0.7	1.22	1.31	1.40	2	0.9
0.04	1.36	2.34	4.07	−13	0.2	0.8	2.27	2.44	2.61	2	0.9
0.05	3.23	5.43	9.48	−12	0.2	0.9	3.69	3.97	4.25	2	0.9
0.06	3.18	5.24	9.65	−11	0.2	1	5.46	5.89	6.30	2	0.9
0.07	1.98	3.23	6.30	−10	0.2	1.25	1.12	1.21	1.30	3	0.9
0.08	0.89	1.43	2.90	−9	0.2	1.5	1.84	2.00	2.14	3	0.9
0.09	3.02	4.83	10.1	−9	0.1	1.75	2.66	2.90	3.11	3	0.8
0.1	0.86	1.35	2.83	−8	0.1	2	3.51	3.91	4.20	3	0.9
0.11	2.30	3.48	7.02	−8	0.1	2.5	5.64	6.80	7.62	3	0.9
0.12	6.94	9.64	17.3	−8	0.2	3	0.79	1.03	1.18	4	1.0
0.13	2.65	3.32	4.94	−7	0.3	3.5	1.01	1.40	1.67	4	1.1
0.14	1.15	1.34	1.71	−6	0.5	4	1.22	1.81	2.20	4	1.2
0.15	4.77	5.40	6.34	−6	0.6	5	1.63	2.69	3.41	4	1.3
0.16	1.76	1.97	2.23	−5	0.7	6	1.99	3.64	4.76	4	1.4
0.18	1.64	1.81	2.00	−4	0.8	7	2.32	4.65	6.24	4	1.6
0.2	1.00	1.09	1.20	−3	0.9	8	2.62	5.71	7.82	4	1.8
0.25	2.54	2.78	3.02	−2	0.9	9	2.92	6.80	9.45	4	2.0
0.3	2.20	2.39	2.59	−1	0.9	10	3.13	7.96	11.2	4	2.1

$N_A \langle \sigma v \rangle^m$:

T_9	low	adopt	high	exp	ratio	T_9	low	adopt	high	exp	ratio
0.015	0.74	1.69	5.02	−25	0.02	0.35	1.94	2.10	2.22	−1	0.7
0.016	1.12	2.50	5.98	−24	0.04	0.4	6.38	7.04	7.58	−1	0.7
0.018	1.04	2.11	4.54	−22	0.12	0.45	1.68	1.83	1.96	0	0.8
0.02	3.93	7.62	15.3	−21	0.2	0.5	3.71	4.01	4.42	0	0.8
0.025	2.43	4.56	8.50	−18	0.2	0.6	1.28	1.39	1.50	1	0.9
0.03	1.69	3.12	5.48	−16	0.2	0.7	3.23	3.52	3.82	1	1.0
0.04	3.11	5.52	9.53	−14	0.2	0.8	6.52	7.10	7.78	1	1.0
0.05	0.73	1.23	2.12	−12	0.2	0.9	1.16	1.27	1.38	2	1.1
0.06	0.68	1.13	2.05	−11	0.2	1	1.85	2.03	2.21	2	1.2
0.07	3.95	6.54	12.6	−11	0.2	1.25	4.30	4.88	5.22	2	1.4
0.08	1.71	2.82	5.60	−10	0.1	1.5	7.70	8.72	9.40	2	1.5
0.09	0.58	9.43	1.92	−10	0.1	1.75	1.16	1.34	1.44	3	1.5
0.1	1.71	2.67	5.67	−9	0.1	2	1.65	1.84	1.97	3	1.6
0.11	4.90	7.38	14.9	−9	0.1	2.5	2.66	3.20	3.58	3	1.8
0.12	1.56	2.16	3.91	−8	0.2	3	3.71	4.83	5.57	3	1.9
0.13	5.60	7.11	10.9	−8	0.3	3.5	4.77	6.59	7.84	3	2.1
0.14	2.21	2.60	3.43	−7	0.4	4	5.76	8.51	10.4	3	2.2
0.15	8.37	9.72	11.6	−7	0.4	5	0.76	1.26	1.60	4	2.4
0.16	2.98	3.30	3.80	−6	0.5	6	0.94	1.71	2.24	4	2.7
0.18	2.70	3.03	3.33	−5	0.6	7	1.09	2.19	2.93	4	3.0
0.2	1.65	1.80	1.91	−4	0.6	8	1.24	2.69	3.68	4	3.4
0.25	4.31	4.56	5.02	−3	0.6	9	1.38	3.20	4.45	4	3.7
0.3	3.89	4.18	4.53	−2	0.7	10	1.47	3.74	5.28	4	4.0

Reaction: ^{25}Mg(α,n)^{28}Si

The experimental data of VA81, AN83 and WI95b are adopted. They cover the energy ranges between 1.8 and 4.1 MeV, 1.6 and 5.4 MeV, and 0.86 and 3 MeV, respectively. The AN83 and VA81 data are disregarded in the WI95b data range: (1) Below 2.2 MeV, the background contribution from the target backing [mainly from ^{13}C(α,n)^{16}O] indeed dominates the neutron yield in the AN83 and VA81 experiments. (2) In contrast, WI95b minimize the background by using gold plated backings. In addition, this background is measured and substracted. Below 1.5 MeV, we adopt a constant S-factor of 3.3×10^9 MeV b, which is an average of the measured S-factors between 1.5 and 3 MeV. The lower limit of the rates is obtained by assuming that the S-factor is the sum of the tails of the measured resonances. The upper limit of the rates results from the selection of the value $S = 10^{11}$ MeV b, which is the WI95b highest measured S-factor at $E < 1.29$ MeV. Above $T_9 = 2$, HF rates are used as explained in Section 2.5. The differences with the CA88 rates are most likely due to the new WI95b data.

T_9	low	adopt	high	exp	ratio	T_9	low	adopt	high	exp	ratio
0.14	0.005	3.37	120	−25	0.2	1	1.48	3.48	24.5	−4	0.5
0.15	0.005	3.34	119	−24	0.2	1.25	0.83	1.37	4.31	−2	0.6
0.16	0.004	2.72	97.0	−23	0.2	1.5	1.59	2.15	4.01	−1	0.7
0.18	0.002	1.12	39.6	−21	0.2	1.75	1.56	1.90	2.66	0	0.7
0.2	0.005	2.74	96.6	−20	0.2	2	0.98	1.12	1.37	1	0.8
0.25	0.003	1.67	58.0	−17	0.2	2.5	1.34	1.52	1.85	2	0.8
0.3	0.006	2.22	76.2	−15	0.2	3	0.91	1.03	1.25	3	0.8
0.35	0.004	1.09	37.4	−13	0.2	3.5	3.97	4.49	5.42	3	0.8
0.4	0.01	2.71	92.5	−12	0.2	4	1.28	1.44	1.73	4	0.8
0.45	0.03	4.10	138	−11	0.3	5	7.35	8.23	9.80	4	0.7
0.5	0.07	4.26	139	−10	0.3	6	2.56	2.84	3.36	5	0.7
0.6	0.12	2.05	58.1	−8	0.3	7	6.53	7.21	8.43	5	0.7
0.7	0.66	4.63	100	−7	0.3	8	1.36	1.49	1.72	6	0.7
0.8	1.49	6.14	93.0	−6	0.4	9	2.45	2.67	3.06	6	0.7
0.9	1.83	5.42	55.8	−5	0.4	10	3.98	4.31	4.89	6	0.7

Reaction: ^{26}Mg(p,γ)^{27}Al

A total of 132 resonances in the energy region $15.4 \leqslant E_r \leqslant 2865.8$ keV are considered in the calculation of the rates. The adopted resonance strengths are the weighted averages of the strengths reported by VA56, VA63, VA66, EN66, LY69, TR75b, MA78c, PA79, BU80, KE80, SM82, CH90 and IL90. For the resonance at $E_r = 148.7$ keV, the value from the only direct measurement [IL90] is adopted. The relative strengths from MA78c, originally normalized to the EN66 strength of the resonance at $E_r = 436.9$ keV, are presently renormalized to the KE80 strength of the same resonance. The direct capture contribution is calculated using the S-factor given by IL90, and is found to be negligible. Above $T_9 = 3.5$, HF estimates are used (see Section 2.5). In the low temperature region, our rates are lower than the CA88 ones, due to the smaller resonance strengths of the low energy resonances used here.

E_r (keV)	J^π	$\omega\gamma$ (eV)				
		BU80	CH90	IL90	adopt	
15.4	$9/2^-$		$\leqslant 1.5 \times 10^{-38}$		$1.5^{+14}_{-1.5} \times 10^{-39}$	N
52.1 ± 0.6	$5/2^+$		$(5.3 \pm 1.7) \times 10^{-17}$		$(5.3 \pm 1.7) \times 10^{-17}$	I
90.0 ± 2.0		$\leqslant 1.0 \times 10^{-8}$	$\leqslant 1.2 \times 10^{-10}$		$1.2^{+11}_{-1.2} \times 10^{-11}$	I
105.0 ± 2.0	$(3/2,5/2)^+$	$\leqslant 2.0 \times 10^{-8}$	$(1.7 \pm 0.5) \times 10^{-11}$		$(1.7 \pm 0.5) \times 10^{-11}$	M
124.2 ± 2.9	$11/2$	$\leqslant 3.0 \times 10^{-8}$	$\leqslant 1.3 \times 10^{-15}$		$1.3^{+12}_{-1.3} \times 10^{-16}$	M
136.7 ± 2.9		$\leqslant 3.0 \times 10^{-8}$	$\leqslant 3.0 \times 10^{-8}$		$3.0^{+27}_{-3.0} \times 10^{-9}$	M
148.7 ± 1.0	$(3/2,5/2)^+$	$\leqslant 8.0 \times 10^{-7}$	$(5.5 \pm 1.7) \times 10^{-8}$		$(6.0 \pm 1.5) \times 10^{-8}$	I
171.4 ± 2.9	$7/2$	$\leqslant 6.0 \times 10^{-8}$	$\leqslant 6.0 \times 10^{-11}$	$(7.7 \pm 3.0) \times 10^{-8}$	$6.0^{+54}_{-6.0} \times 10^{-12}$	M
		BU80	others	IL90	adopt	
218.4 ± 1.2	$5/2^+$	$(5 \pm 2) \times 10^{-5}$		$(4.7 \pm 1.0) \times 10^{-5}$	$(4.8 \pm 1.8) \times 10^{-5}$	M
250.3 ± 2.9	$(1/2 - 7/2)^+$	$\leqslant 2.0 \times 10^{-6}$			$2.0^{+18}_{-2.0} \times 10^{-7}$	M
264.9 ± 1.8	$5/2^+$	$(1.0 \pm 0.8) \times 10^{-6}$			$(1.0 \pm 0.8) \times 10^{-6}$	M
281.2 ± 0.1	$3/2^+$	$(8.6 \pm 2.2) \times 10^{-3}$	$(9.6 \pm 4.8) \times 10^{-3}$ [VA56] $(2.4 \pm 0.7) \times 10^{-2}$ [KE80] $(7.7 \pm 2.4) \times 10^{-3}$ [SM82]	$(5.8 \pm 0.8) \times 10^{-3}$	$(6.5 \pm 1.5) \times 10^{-3}$	M
316.7 ± 2.9	$7/2$	$\leqslant 3.0 \times 10^{-5}$			$3.0^{+27}_{-3.0} \times 10^{-6}$	M
325.8 ± 0.1	$3/2^-$	0.25 ± 0.11	0.77 ± 0.19 [VA56] 0.67 ± 0.34 [VA63] 0.67 ± 0.14 [KE80] 0.67 ± 0.14 [SM82]	0.24 ± 0.03	0.59 ± 0.01	I
Res. 436.9–2865.8 keV			see comments			

T_9	low	adopt	high	exp	ratio	T_9	low	adopt	high	exp	ratio
0.016	0.72	1.64	3.34	−25	0.1	0.4	3.21	3.32	3.43	1	1.1
0.018	4.21	9.13	17.8	−24	0.1	0.45	7.88	8.15	8.43	1	1.1
0.02	1.08	2.24	4.20	−22	0.1	0.5	1.61	1.66	1.72	2	1.1
0.025	3.49	6.82	12.7	−20	0.1	0.6	4.59	4.77	4.94	2	1.1
0.03	1.56	3.19	11.1	−18	0.1	0.7	9.57	9.97	10.4	2	1.2
0.04	0.17	1.42	20.6	−15	0.1	0.8	1.64	1.71	1.79	3	1.2
0.05	0.06	1.59	24.1	−13	0.1	0.9	2.48	2.60	2.72	3	1.2
0.06	0.28	4.25	57.0	−12	0.1	1	3.42	3.60	3.78	3	1.2
0.07	0.87	5.28	57.3	−11	0.1	1.25	6.04	6.41	6.78	3	1.2
0.08	1.38	4.54	36.0	−10	0.1	1.5	8.77	9.41	10.0	3	1.1
0.09	1.28	3.05	17.3	−9	0.1	1.75	1.15	1.25	1.34	4	1.1
0.1	0.84	1.67	6.91	−8	0.1	2	1.42	1.55	1.69	4	1.1
0.11	4.55	8.08	24.7	−8	0.2	2.5	1.94	2.18	2.43	4	1.1
0.12	2.37	3.75	8.51	−7	0.3	3	2.48	2.86	3.28	4	1.1
0.13	1.24	1.74	3.02	−6	0.4	3.5	3.06	3.63	4.29	4	1.1
0.14	6.17	7.88	11.2	−6	0.6	4	4.00	4.96	6.07	4	1.3
0.15	2.76	3.30	4.15	−5	0.7	5	5.98	8.07	10.5	4	1.7
0.16	1.08	1.23	1.45	−4	0.8	6	0.80	1.16	1.59	5	2.1
0.18	1.11	1.21	1.33	−3	0.9	7	0.99	1.55	2.20	5	2.5
0.2	7.33	7.83	8.37	−3	0.9	8	1.17	1.96	2.87	5	2.8
0.25	2.19	2.29	2.39	−1	1.0	9	1.33	2.37	3.58	5	3.0
0.3	2.05	2.13	2.21	0	1.0	10	1.47	2.78	4.31	5	3.1
0.35	1.00	1.03	1.07	1	1.1						
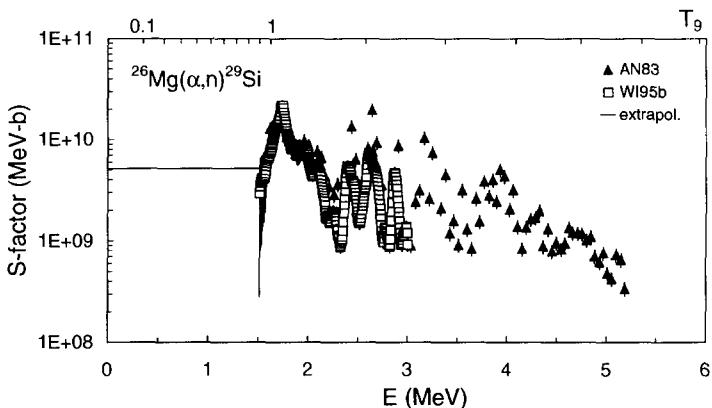
Reaction: ^{26}Mg$(\alpha,n)^{29}$Si

The experimental data of AN83 and WI95b are adopted. They cover the energy ranges from 1.51 to 5.2 MeV and from 0.87 to 3 MeV, respectively. The AN83 data are disregarded in the WI95b data range: (1) Below 2.2 MeV, the background contribution from the target backing [mainly from ^{13}C$(\alpha,n)^{16}$O] indeed dominates the neutron yield in the AN83 and VA81 experiments. (2) In contrast, WI95b minimize the background by using gold plated backings. In addition, this background is measured and subtracted. Below 1.5 MeV, we adopt a constant S-factor of 5.15×10^9 MeV b, which is an average of the measured S-factors between 1.5 and 3 MeV. The lower limit of the rates is obtained by assuming that the S-factor is the sum of the tails of the measured resonances. The upper limit of the rates results from the selection of the value $S = 10^{11}$ MeV b, which is the WI95b highest measured S-factor at $E < 1.19$ MeV. Above $T_9 = 2$, HF estimates are used (see Section 2.5). The differences with CA88 are probably due to the new data of WI95b.

T_9	low	adopt	high	exp	ratio	T_9	low	adopt	high	exp	ratio
0.14	0.003	5.19	102	−25	0.1	1	3.63	6.28	18.9	−4	1.1
0.15	0.004	5.15	102	−24	0.1	1.25	1.77	2.41	4.13	−2	1.5
0.16	0.003	4.20	83.0	−23	0.1	1.5	2.68	3.31	4.45	−1	1.7
0.18	0.001	1.72	34.1	−21	0.1	1.75	2.17	2.53	3.04	0	1.9
0.2	0.003	4.22	83.6	−20	0.1	2	1.20	1.36	1.54	1	2.0

continued from previous page

T_9	low	adopt	high	exp	ratio	T_9	low	adopt	high	exp	ratio
0.25	0.003	2.56	50.8	−17	0.1	2.5	1.68	1.90	2.15	2	2.5
0.3	0.004	3.38	67.3	−15	0.2	3	1.19	1.34	1.51	3	2.8
0.35	0.003	1.67	33.2	−13	0.2	3.5	5.37	6.03	6.79	3	3.1
0.4	0.01	4.16	82.3	−12	0.2	4	1.78	2.00	2.24	4	3.4
0.45	0.02	6.30	122	−11	0.3	5	1.08	1.20	1.34	5	3.9
0.5	0.06	6.54	120	−10	0.3	6	3.90	4.33	4.82	5	4.3
0.6	0.16	3.13	46.7	−8	0.4	7	1.03	1.14	1.26	6	4.8
0.7	1.18	7.19	75.2	−7	0.5	8	2.21	2.43	2.67	6	5.4
0.8	3.23	10.0	67.3	−6	0.7	9	4.08	4.46	4.89	6	5.9
0.9	4.39	9.38	40.7	−5	0.9	10	6.77	7.37	8.04	6	6.5

Reaction: ^{26}Al(p,γ)^{27}Si

Of astrophysical relevance are the proton capture rates on to the ground and isomeric states of ^{26}Al, noted $N_A\langle\sigma v\rangle_{gs}$ and $N_A\langle\sigma v\rangle_{ms}$, respectively [see WA89]. For the calculation of $N_A\langle\sigma v\rangle_{gs}$, the resonance strengths are adopted from BU84, VO96 and the theoretical calculations of CH93. The calculations of WA89, based on the Wigner limit, are not taken into account, neither the hypothetical 226 keV resonance, found only in WA89. For the E_r = 68 and 93 keV resonances, the theoretical estimates of CH93 are used for the lower and upper limits of the rates. The adopted values are taken as 1/10 of the upper limits. For the 128 keV resonance, the value of VO96 is taken for the upper limit. The adopted strength is taken as 1/10 of this limit. The lower limit is taken as zero. However, the results of CO95, based on a single-particle estimate taking a real Woods–Saxon potential, give $\omega\gamma \leqslant 5.4 \times 10^{-9}, \leqslant 6.1 \times 10^{-6}, \leqslant 1.2 \times 10^{-5}$ meV for the resonances at 68, 93 and 128 keV, respectively. The discrepancy between the results of the different theoretical approaches indicates that the parameters of the low energy resonances in this reaction are model dependent and not well-known experimentally. For the 188 keV resonance, the adopted $\omega\gamma$ and upper limit are taken from VO96 for the ℓ = 1 and 0 pure transfers, respectively, while the lower limit is taken as 1/10 of the value for ℓ = 3. For the 238 and 328 keV resonances, the lower and upper limits of

the strengths are taken from CH93, using the average value for the adopted $\omega\gamma$. For the 275.6, 363 to 894 keV resonances, the values are adopted from BU84. The resonance data allow the calculation of the rates at $T_9 \leqslant 0.9$. Above $T_9 = 0.9$, HF estimates are used (see Section 2.5). The $N_A\langle\sigma v\rangle_{ms}$ rates are calculated by multiplying the $N_A\langle\sigma v\rangle_{gs}$ values by the HF ratio $\langle\sigma v\rangle_{ms}/\langle\sigma v\rangle_{gs}$. The thermalized reaction rate applies when $^{26}Al^g$ and $^{26}Al^m$ may be considered to be in thermal equilibrium (see [WA89] for details) and is calculated by multiplying $N_A\langle\sigma v\rangle_{gs}$ by the ratio r_{tt}, as usual. Differences in the adopted strengths account for the differences between our rates and those of CA88 up to $T_9 \approx 1$. At high temperatures, the HF estimates are larger than the CA88 rates while thermalization effects account for 10 to 65% of the differences at $T_9 = 1.5$ to 10.

$N_A\langle\sigma v\rangle_{gs}$:

T_9	low	adopt	high	exp	ratio	T_9	low	adopt	high	exp	ratio
0.018	0.002	1.34	92.6	−25	0.1	0.4	1.34	2.16	4.06	0	1.0
0.02	0.01	9.17	523	−24	0.2	0.45	3.24	5.04	8.62	0	1.0
0.025	0.004	1.76	70.7	−20	1.2	0.5	6.54	9.96	16.0	0	1.0
0.03	0.01	2.61	83.3	−18	1.9	0.6	1.85	2.75	4.12	1	0.9
0.04	0.01	1.40	35.6	−15	1.4	0.7	3.83	5.61	8.07	1	0.9
0.05	0.09	7.78	367	−14	0.8	0.8	6.47	9.40	13.2	1	0.8
0.06	0.02	1.59	230	−12	0.5	0.9	0.96	1.39	1.93	2	0.7
0.07	0.03	3.11	545	−11	0.6	1	1.55	2.24	3.12	2	0.9
0.08	0.02	7.52	616	−10	1.4	1.25	3.83	5.54	7.68	2	1.1
0.09	0.01	1.19	43.2	−8	3.1	1.5	0.72	1.05	1.45	3	1.4
0.1	0.002	1.12	22.3	−7	5.6	1.75	1.16	1.68	2.32	3	1.8
0.11	0.03	7.09	93.5	−7	8.0	2	1.68	2.41	3.34	3	2.1
0.12	0.03	3.28	33.1	−6	9.7	2.5	2.84	4.08	5.64	3	2.8
0.13	0.02	1.20	10.1	−5	10	3	4.07	5.84	8.06	3	3.6
0.14	0.11	3.65	27.2	−5	9.3	3.5	5.30	7.57	10.4	3	4.3
0.15	0.43	9.61	65.5	−5	7.9	4	6.47	9.23	12.7	3	5.0
0.16	0.15	2.26	14.3	−4	6.5	5	0.86	1.22	1.68	4	6.2
0.18	1.19	9.63	53.9	−4	4.3	6	1.05	1.49	2.04	4	7.1
0.2	0.62	3.21	15.9	−3	3.0	7	1.23	1.73	2.36	4	7.8
0.25	1.26	3.34	12.1	−2	1.7	8	1.39	1.95	2.65	4	8.3
0.3	0.97	1.93	5.19	−1	1.3	9	1.55	2.15	2.92	4	8.9
0.35	4.32	7.47	16.2	−1	1.1	10	1.69	2.35	3.18	4	9.9

$N_A\langle\sigma v\rangle_{ms}$:

T_9	low	adopt	high	exp	ratio	T_9	low	adopt	high	exp	ratio
0.018	0.002	1.34	92.6	−25	0.03	0.12	0.03	3.30	33.3	−6	5.5
0.02	0.01	9.17	523	−24	0.1	0.13	0.02	1.21	10.2	−5	6.5
0.025	0.004	1.76	70.7	−20	0.6	0.14	0.11	3.71	27.7	−5	7.3
0.03	0.01	2.61	83.3	−18	0.9	0.15	0.45	9.86	67.3	−5	7.7
0.04	0.01	1.40	35.6	−15	0.7	0.16	0.16	2.34	14.9	−4	8.0
0.05	0.09	7.78	367	−14	0.4	0.18	0.13	1.03	5.76	−3	8.1
0.06	0.02	1.59	230	−12	0.2	0.2	0.69	3.55	17.7	−3	8.1
0.07	0.03	3.11	545	−11	0.3	0.25	1.58	4.19	15.1	−2	8.2
0.08	0.02	7.52	616	−10	0.7	0.3	1.41	2.79	7.53	−1	8.7
0.09	0.01	1.19	43.2	−8	1.5	0.35	0.72	1.25	2.72	0	9.4
0.1	0.002	1.12	22.3	−7	2.8	0.4	2.56	4.14	7.78	0	9.9
0.11	0.03	7.09	93.5	−7	4.2						

E_r (keV)	J^π	WA89	CH93* low	CH93* upper	VO96	lower	adopt	upper
					$\omega\gamma$ (meV)			
4 ± 3	N	$< 1.8 \times 10^{-60}$	2.9×10^{-76}	2.7×10^{-75}	$\leqslant 5.4 \times 10^{-9}$ [CO95]	2.9×10^{-76}	1.5×10^{-75}	2.7×10^{-75}
68 ± 3	1	$< 2.3 \times 10^{-10}$	2×10^{-13}	2.2×10^{-10}	$\leqslant 6.1 \times 10^{-6}$ [CO95]	2×10^{-13}	2.2×10^{-11}	2.2×10^{-10}
93 ± 3	1	$< 1.9 \times 10^{-7}$	2.3×10^{-10}	5.3×10^{-8}	$< 5.9 \times 10^{-6}$	2.3×10^{-10}	5.3×10^{-9}	5.3×10^{-8}
128 ± 3	N	$< 5.7 \times 10^{-3}$	0	2.4×10^{-5}	$\leqslant 1.2 \times 10^{-5}$ [CO95]	0	5.9×10^{-7}	5.9×10^{-6}
188 ± 3	1	$< 4.2 \times 10^{-2}$		1.6×10^{-3}	0.29; 0.064**; $< 3.2 \times 10^{-3}$; $< 9.9 \times 10^{-5}$	9.9×10^{-6}	0.064	0.29
226 ± 3		< 0.62				0	0	0
238 ± 3	N	< 1.2	4.3×10^{-3}	5.0×10^{-3}		4.3×10^{-3}	4.7×10^{-3}	5.0×10^{-3}
275.6 ± 0.3	1	3.8 ± 1.0 (BU84)	1.9	14	19; 3.6; 0.17; $< 7 \times 10^{-3}$		3.8 ± 1.0	
328 ± 4	N		0.19	0.22		0.19	0.2	0.22
363 ± 3	1	65 ± 18	4.5	42			65 ± 18	
693 ± 2	N	51 ± 27					51 ± 27	
701 ± 2	N	16 ± 6					16 ± 6	
762 ± 2	N	35 ± 13					35 ± 13	
825 ± 3	N	41 ± 16					41 ± 16	
894 ± 2	N	67 ± 28					67 ± 28	

*Shell model calculation

**$\omega\gamma = 0.055 \pm 0.009$ meV in VO89

Reaction: ^{27}Al(p,γ)^{28}Si

The contribution of 122 resonances between 195 and 3817.4 keV is taken into account. For resonances above 956 keV, the adopted strengths are the averages of those given by SM58, AN63, NO63, AN64, NO64, SI65, EN66, GI68, KU69, ME70, TV72, DA73, ME75, and BR95. Several of the reported values are renormalized. For the resonances at $E < 195$ keV, the data of CH86c, CH88, TI88 and CH97 ($< 2.4 \times 10^{-14}$ eV for the 72 keV resonance and $< 1.0 \times 10^{-14}$ eV for the 84 keV resonance from CH97, respectively) are used to set upper limits on the resonance strengths. The direct capture contribution is adopted from the calculations of TI88, which are in agreement with available experimental data [LY69,HA88]. The contributions of resonance tails are found to be negligible with respect to the direct capture one. The available data allow the reaction rate calculation for $T_9 \leqslant 6$. Above $T_9 = 6$, HF estimates are used as explained in Section 2.5. Below $T_9 = 0.05$, the differences with the CA88 rates are due to the availability of more recent upper limits on resonance strengths, as well as the inclusion of a direct capture contribution neglected by CA88.

T_9	low	adopt	high	exp	ratio	T_9	low	adopt	high	exp	ratio
0.025	0.03	1.67	16.4	−23	0.7	0.45	0.86	1.05	1.25	0	1.1
0.03	0.03	3.39	33.5	−21	0.6	0.5	1.88	2.27	2.66	0	1.0
0.04	0.03	2.44	24.1	−18	0.5	0.6	6.97	8.20	9.43	0	0.8
0.05	0.05	1.25	11.9	−16	0.5	0.7	1.97	2.28	2.59	1	0.8
0.06	3.72	8.37	25.1	−15	0.9	0.8	4.56	5.21	5.87	1	0.7
0.07	0.73	1.31	1.96	−12	1.1	0.9	0.90	1.03	1.15	2	0.7
0.08	3.89	6.73	9.59	−11	1.1	1	1.60	1.80	2.00	2	0.7
0.09	0.87	1.45	2.04	−9	1.1	1.25	4.66	5.20	5.75	2	0.7
0.1	1.04	1.69	2.35	−8	1.1	1.5	0.99	1.10	1.21	3	0.8
0.11	0.79	1.26	1.73	−7	1.1	1.75	1.71	1.91	2.10	3	0.8
0.12	4.29	6.71	9.13	−7	1.1	2	2.63	2.93	3.23	3	0.8
0.13	1.79	2.75	3.72	−6	1.1	2.5	4.86	5.45	6.04	3	0.8
0.14	6.07	9.21	12.3	−6	1.1	3	7.39	8.35	9.31	3	0.7
0.15	1.75	2.62	3.49	−5	1.1	3.5	1.00	1.14	1.28	4	0.7
0.16	4.40	6.52	8.65	−5	1.1	4	1.25	1.44	1.62	4	0.7
0.18	2.06	2.99	3.92	−4	1.2	5	1.71	1.99	2.27	4	0.6
0.2	0.71	1.01	1.32	−3	1.2	6	2.08	2.45	2.82	4	0.6
0.25	6.93	9.55	12.2	−2	1.4	7	2.47	4.03	5.59	4	0.7
0.3	3.49	4.64	5.79	−2	1.5	8	2.82	5.88	8.94	4	0.8
0.35	1.23	1.58	1.94	−1	1.5	9	3.13	7.96	12.8	4	0.9
0.4	3.49	4.38	5.27	−1	1.3	10	0.34	1.02	1.71	5	1.0

E_r (keV)	J^π	adopted $\omega\gamma$ (eV)	Ref.	
71.9 ± 0.5	2^+	$(0.15^{+1.35}_{-0.15}) \times 10^{-15}$	CH86c, CH88, CH97	I
84.8 ± 0.4	1^-	$(0.15^{+1.35}_{-0.15}) \times 10^{-15}$	CH86c, CH88, CH97	M
195.5 ± 0.9	2^+	$(1.40 \pm 0.7) \times 10^{-5}$	SM62	M
214.7 ± 0.4		$(9.00 \pm 0.2) \times 10^{-5}$	BR47, EN60, OK60a	M
282.1 ± 0.4	4^+	$(3.80 \pm 0.7) \times 10^{-4}$	BR47, EN60, OK60a	M
314.8 ± 0.4		0.0015 ± 0.0003	BR47, EN60, OK60a, SM62, LY69, ME75	M
390.9 ± 0.3		0.009 ± 0.001	SM62	M
430.6 ± 0.5		0.0014 ± 0.0002	BR47, LY69, ME75	M
486.72 ± 0.07	2^+	0.061 ± 0.007	BR47, EN60, OK60a, SM62 LY69, ME75, SW75	M
488.15 ± 0.07	2	0.042 ± 0.009	EN60, OK60a, ME75	M
589.40 ± 0.04		0.004 ± 0.001	BR47, EN60, OK60a, LY69, ME75	M
609.47 ± 0.04	3^-	0.266 ± 0.014	BR47, SM58, EN60, OK60a, SM62, NO63, NO64, EN66, LY69, LE71, DA73, AL74, ME75, SW75, PA79, BR95	M
631.08 ± 0.04	2^-	0.120 ± 0.009	BR47, EN60, OK60a, LY69, SW75	M
654.85 ± 0.04	3^+	0.045 ± 0.005	BR47, EN60, OK60a, LY69, ME75	M
705.06 ± 0.04	2^-	0.12 ± 0.01	BR47, EN60, OK60a, LY69, ME75	M
709.97 ± 0.04		0.160 ± 0.016	BR47, EN60, OK60a, LY69, ME75	M
716.21 ± 0.04		0.021 ± 0.003	BR47, SM62, EN60, OK60a, LY69, ME75	M
733.02 ± 0.04	2^-	0.135 ± 0.016	BR47, EN60, OK60a, LY69, ME75	M
739.56 ± 0.04	4^+	0.16 ± 0.02	BR47, EN60, OK60a, LY69, ME75	M
745.79 ± 0.04		0.41 ± 0.03	BR47, SM58, EN60, OK60a, NO63, NO64, EN66, LY69, LE71, DA73, AL74, ME75, BR95	M
855.82 ± 0.05	2^+	0.015 ± 0.002	BR47, LY69, ME75	M
889.73 ± 0.05	2^+	0.140 ± 0.018	LY69, ME75	M
903.50 ± 0.05	3^-	0.176 ± 0.021	SM58, NO63, NO64, EN66, LY69, LE71, DA73, ME75	M
956.20 ± 0.03	3^+	1.90 ± 0.10	SM58, NO63, NO64, EN66, LE71, PA70, DA73	M
Res. 1130–3817 keV			see comments	

Reaction: ^{27}Al(p,α)^{24}Mg

A total of 78 resonances at energies below 3064.6 keV are included in the calculation of the rates. The adopted strengths for the first 20 resonances below 900 keV are shown in the table. The adopted resonance parameters for $E > 900$ keV are the weighted averages of the data reported by AN61, AB63, AW65, NE84 and CO92 for the (p,α_0) channel, and by TV72, DA73, ME75 and NE84 for the (p,α_1) channel. Tail contributions are also included. The available data allow the rates to be calculated for $T_9 \leqslant 6$. Above $T_9 = 6$, HF estimates are used (see Section 2.5). The large differences between the present rates and the CA88 ones below $T_9 = 0.6$ are mainly due to the adoption by CA88 of a strength for the $E_r = 215$ keV resonance which exceeds the upper limit of TI88. Below $T_9 = 0.05$, the difference is due to updated upper limits of resonance

strengths that were not available to CA88. Above $T_9 = 4$, thermalization effects account
for about 30% of the differences.

E_r (keV)	J^π	adopted $\omega\gamma$ (eV)	Ref.	
71.9 ± 0.5	2^+	$(0.6^{+5.4}_{-0.6}) \times 10^{-15}$	CH88, CH97	I
84.8 ± 0.4	1^-	$(0.1^{+0.9}_{-0.1}) \times 10^{-15}$	CH88, CH97	M
195.5 ± 0.9	2^+	$(1.30^{+1.20}_{-1.29}) \times 10^{-8}$	SM62, MA78d, CH88	I
214.7 ± 0.4		$(0.18^{+1.72}_{-0.18}) \times 10^{-7}$	CH88, TI88	M
282.1 ± 0.4	4^+	$(0.11^{+0.99}_{-0.11}) \times 10^{-6}$	CH88, TI88	I
314.8 ± 0.4		$(1.10^{+0.70}_{-0.78}) \times 10^{-6}$	CH88, TI88	M
390.9 ± 0.3		$(1.25 \pm 0.75) \times 10^{-5}$	MA78d, CH88, EN90	M
486.72 ± 0.07	2^+	0.10 ± 0.02	AN61, KU63, MA78d, CH88, TI88, EN90	M
488.15 ± 0.07	2	$(0.2^{+1.8}_{-0.2}) \times 10^{-2}$	AN61, KU63, MA78d, CH88, TI88, EN90	M
609.47 ± 0.04	3^-	0.28 ± 0.05	AN61, KU63, MA78d, CH88, TI88, EN90	M
631.08 ± 0.04	2^-	$(0.20^{+1.8}_{-0.2}) \times 10^{-3}$	AN61, KU63, MA78d, CH88, TI88, EN90	M
654.85 ± 0.04	3^+	$(1.80 \pm 1.6) \times 10^{-3}$	CH88, EN90	M
705.06 ± 0.04	2^-	0.53 ± 0.1	AN61, KU63, MA78d, CH88, TI88, EN90	M
709.97 ± 0.04		$(0.20^{+1.8}_{-0.2}) \times 10^{-3}$	AN61, KU63, MA78d, CH88, TI88, EN90	M
716.21 ± 0.04		$(0.10^{+0.9}_{-0.1}) \times 10^{-2}$	AN61, KU63, MA78d, CH88, TI88, EN90	M
733.02 ± 0.04	2^-	$(0.10^{+0.9}_{-0.1}) \times 10^{-2}$	AN61, KU63, MA78d, CH88, TI88, EN90	M
739.56 ± 0.04	4^+	$(0.10^{+0.9}_{-0.1}) \times 10^{-2}$	AN61, KU63, MA78d, CH88, TI88, EN90	M
745.79 ± 0.04		$(0.10^{+0.9}_{-0.1}) \times 10^{-2}$	AN61, KU63, MA78d, CH88, TI88, EN90	M
855.82 ± 0.05	2^+	0.83 ± 0.20	AN61	M
889.73 ± 0.05		0.33 ± 0.09	AN61	M

Res. 903.5–3065 keV	see comments

T_9	low	adopt	high	exp	ratio	T_9	low	adopt	high	exp	ratio
0.025	2E-5	7.80	78.0	-23	0.05	0.45	1.73	2.19	2.96	-1	0.1
0.03	2E-6	1.55	15.5	-20	0.05	0.5	5.45	6.91	9.26	-1	0.2
0.04	2E-6	1.05	10.5	-17	0.04	0.6	3.10	3.91	5.18	0	0.5
0.05	2E-5	4.92	49.2	-16	0.04	0.7	1.10	1.39	1.81	1	0.8
0.06	5E-4	6.07	60.7	-15	0.03	0.8	2.99	3.73	4.82	1	0.9
0.07	7E-3	3.63	35.6	-14	0.01	0.9	6.88	8.52	10.8	1	0.9
0.08	0.03	1.78	14.1	-13	1E-3	1	1.43	1.75	2.18	2	0.9
0.09	0.06	1.32	6.17	-12	4E-4	1.25	6.92	8.17	9.69	2	1.0
0.1	0.07	1.14	3.93	-11	2E-4	1.5	2.49	2.87	3.30	3	1.2
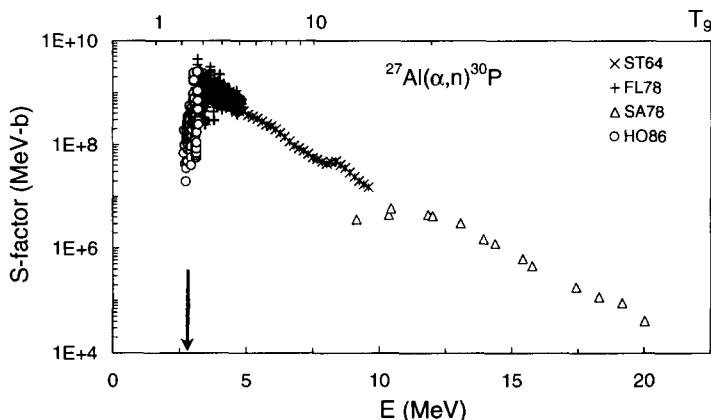
continued from previous page

0.11	0.49	7.64	25.2	−11	2E-4	1.75	6.98	7.93	8.96	3	1.4
0.12	0.24	3.80	13.0	−10	2E-4	2	1.60	1.81	2.03	4	1.6
0.13	0.09	1.48	5.29	−9	1E-4	2.5	5.56	6.25	6.95	4	1.8
0.14	0.29	4.74	17.7	−9	1E-4	3	1.34	1.50	1.67	5	1.9
0.15	0.08	1.30	5.05	−8	1E-4	3.5	2.57	2.89	3.21	5	1.9
0.16	0.19	3.14	12.6	−8	1E-4	4	4.23	4.76	5.30	5	1.9
0.18	0.12	1.41	5.89	−7	1E-4	5	8.59	9.69	10.8	5	1.6
0.2	1.08	5.45	21.3	−7	1E-4	6	1.37	1.55	1.73	6	1.3
0.25	1.65	2.46	4.66	−5	6E-4	7	2.52	2.90	3.28	6	1.4
0.3	5.39	7.03	10.2	−4	4E-3	8	4.10	4.82	5.53	6	1.5
0.35	6.44	8.24	11.4	−3	0.02	9	6.14	7.33	8.52	6	1.5
0.4	4.10	5.22	7.10	−2	0.05	10	0.86	1.04	1.23	7	1.4
T_9	low	adopt	high	exp	ratio	T_9	low	adopt	high	exp	ratio

Reaction: ^{27}Al(α,n)^{30}P

The experimental cross sections of ST64, FL78, SA78 and HO86 from threshold ($Q = -2.643$ MeV) to $E = 24$ MeV are used in the calculation of the rates. Thick target experiments [HO74] with larger uncertainties are disregarded. The reaction rate uncertainties relate to the experimental uncertainties. In the $0.4 \leqslant T_9 \leqslant 1$ range, our

T_9	low	adopt	high	exp	ratio	T_9	low	adopt	high	exp	ratio
0.45	0.79	1.34	1.89	−25	0.5	2.5	3.68	3.92	4.16	0	1.0
0.5	0.74	1.20	1.66	−22	0.5	3	4.68	4.98	5.27	1	1.0
0.6	2.25	3.37	4.50	−18	0.6	3.5	3.07	3.27	3.47	2	1.1
0.7	3.88	5.41	6.94	−15	0.6	4	1.31	1.40	1.50	3	1.1
0.8	1.11	1.46	1.81	−12	0.7	5	1.09	1.18	1.27	4	1.2
0.9	0.97	1.21	1.45	−10	0.7	6	4.81	5.29	5.76	4	1.3
1	3.59	4.33	5.07	−9	0.8	7	1.46	1.62	1.78	5	1.4
1.25	2.75	3.14	3.52	−6	0.9	8	3.47	3.89	4.32	5	1.5
1.5	2.60	2.88	3.16	−4	0.9	9	6.96	7.88	8.80	5	1.6
1.75	7.26	7.90	8.54	−3	0.9	10	1.24	1.41	1.58	6	1.6
2	0.93	1.00	1.07	−1	1.0						

rates are 20 to 60% smaller than the CA88 ones. Our thermalization effects are a factor $r_{tt} = 1.10 - 1.19$ for $T_9 = 4$ to 10 (CA88 adopt $r_{tt} = 1$ at all temperatures).

Reaction: $^{28}Si(p,\gamma)^{29}P$

Parameters for the resonances at $357 \leqslant E_r \leqslant 2778$ keV are obtained from NE60, OK60b, VA61, EJ64, EN66, BE70, ZU71, BA73b, BY74, AL75b, RI79, TE79 and GR90. Tail contributions are also taken into account. The non-resonant contribution is calculated by using the S-factor reported by GR90. Above $T_9 = 3$, HF estimates are used following the procedure explained in Section 2.5. The difference between the adopted rates and the CA88 ones are probably due to the different resonance parameters used here. At low temperatures, where the direct capture contribution is significant, the differences are larger.

E_r (keV)	J^π	$\omega\gamma$ (meV)					
		BY74	RI79	GR90	others	adopt	
357 ± 4	$5/2^+$	1.3 ± 0.3	2.7 ± 0.2	1.7 ± 0.4	2.3 ± 0.3 [OK60b] 2.3 ± 0.4 [VA61] 1.6 ± 0.2 [EN66]	2.0 ± 0.2	I
698.9 ± 0.7	$7/2^-$	0.21 ± 0.08		0.15 ± 0.03	$\leqslant 2$ [VA61] 0.34 ± 0.06 [ZU71] $\leqslant 0.23$ [BA73] 0.12 ± 0.04 [AL75b]	0.17 ± 0.04	M
1332.6 ± 0.5	$7/2^+$	30 ± 6	43 ± 4	29 ± 5	$7.7 \pm 4^*$ [EJ64] $13.5 \pm 3^*$ [ZU71]	36.3 ± 2.8	M
1595 ± 0.7	$3/2^-$	2500 ± 400	4200 ± 340	2500 ± 400	3400 ± 700 [NE60] 3600 ± 800 [VA61] 4000 ± 1000 [EJ64] 3100 ± 500 [TE79] 3600 ± 800 [KI85]	3300 ± 270	M
1894 ± 1					0.45 ± 0.13 [NE60]	0.45 ± 0.13	M
2012.4 ± 1.3	$1/2^+$	410 ± 60	440 ± 70	440 ± 70	430 ± 200 [NE60] 420 ± 80 [VA61] 320 ± 100 [EJ64] 530 ± 100 [TE79] 540 ± 200 [KI85]	430 ± 30	M
2206.9 ± 1.5	$5/2^+$	220 ± 50			130 ± 50 [KA75]	180 ± 50	M
2545 ± 2	$7/2^+$	50 ± 10			320 ± 100 [KA75]	50 ± 10	M
2779 ± 10	$1/2^-$			2500 ± 400	$\leqslant 2000$ [EJ64] 2700 ± 1700 [TE79] 3100 ± 400 [KI85]	2800 ± 300	M
2994 ± 2	$7/2^-$				460 ± 70 [EJ64]	460 ± 70	M

* disregarded

T_9	low	adopt	high	exp	ratio	T_9	low	adopt	high	exp	ratio
0.03	3.02	5.97	11.9	−25	8.1	0.5	2.09	2.35	2.62	−1	1.0
0.04	3.34	6.61	13.1	−22	9.0	0.6	6.36	7.14	7.94	−1	1.0
0.05	4.86	9.63	19.1	−20	10	0.7	1.36	1.52	1.69	0	1.0
0.06	2.16	4.29	8.52	−18	11	0.8	2.34	2.62	2.91	0	1.0
0.07	4.48	8.87	17.6	−17	12	0.9	3.51	3.92	4.35	0	1.0
0.08	0.55	1.08	2.14	−15	13	1	4.77	5.33	5.92	0	1.0
0.09	4.59	9.01	17.8	−15	12	1.25	7.99	8.97	10.0	0	1.0
0.1	3.56	6.44	12.0	−14	4.6	1.5	1.14	1.29	1.48	1	0.9
0.11	4.40	6.33	9.66	−13	1.6	1.75	1.61	1.87	2.21	1	0.8
0.12	6.82	8.55	11.0	−12	1.1	2	2.47	2.93	3.58	1	0.7
0.13	8.21	9.88	11.9	−11	1.0	2.5	6.43	7.86	10.1	1	0.6
0.14	7.13	8.45	9.96	−10	1.0	3	1.48	1.85	2.46	2	0.6
0.15	4.64	5.46	6.38	−9	0.9	3.5	1.98	2.75	4.01	2	0.5
0.16	2.39	2.79	3.24	−8	0.9	4	2.51	3.82	5.98	2	0.4
0.18	3.60	4.18	4.82	−7	0.9	5	3.64	6.51	11.2	2	0.4
0.2	3.10	3.59	4.11	−6	0.9	6	4.82	9.92	18.3	2	0.4
0.25	1.43	1.64	1.86	−4	0.9	7	0.60	1.41	2.73	3	0.5
0.3	1.74	1.98	2.24	−3	0.9	8	0.73	1.90	3.83	3	0.6
0.35	1.00	1.14	1.28	−2	0.9	9	0.86	2.48	5.14	3	0.7
0.4	3.64	4.11	4.60	−2	1.0	10	1.01	3.16	6.70	3	0.8
0.45	0.97	1.09	1.22	−1	0.9						

Table 3. Analytical approximations of the reaction rates

^{1}**H(p,νe$^+$)^{2}H**, $Q = 1.442$ MeV, (3%)

$$N_A\langle\sigma v\rangle_{gs} = 4.08 \times 10^{-15}T_9^{-2/3}\exp(-3.381T_9^{-1/3})$$
$$\times(1 + 3.82T_9 + 1.51T_9^2 + 0.144T_9^3 - 1.14 \times 10^{-2}T_9^4)$$
$$N_A\langle\sigma v\rangle_{tt} = N_A\langle\sigma v\rangle_{gs}$$

^{2}**H(p,γ)^{3}He**, $Q = 5.493$ MeV, (3%)

For $T_9 \leqslant 0.11$: $N_A\langle\sigma v\rangle_{gs} = 1.81 \times 10^3T_9^{-2/3}\exp(-3.721T_9^{-1/3})$
$$\times(1 + 14.3T_9 - 90.5T_9^2 + 395T_9^3)$$
For $T_9 > 0.11$: $N_A\langle\sigma v\rangle_{gs} = 2.58 \times 10^3T_9^{-2/3}\exp(-3.721T_9^{-1/3})$
$$\times(1 + 3.96T_9 + 0.116T_9^2)$$

$$N_A\langle\sigma v\rangle_{tt} = N_A\langle\sigma v\rangle_{gs}$$
Rev. ratio $= 1.630 \times 10^{10}T_9^{3/2}\exp(-63.749/T_9)$

^{2}**H(d,γ)^{4}He**, $Q = 23.847$ MeV, (3%)

$$N_A\langle\sigma v\rangle_{gs} = 42.1T_9^{-2/3}\exp(-4.259T_9^{-1/3})$$
$$\times(1 + 0.514T_9 + 0.339T_9^2 - 1.18 \times 10^{-2}T_9^3)$$
$$N_A\langle\sigma v\rangle_{tt} = N_A\langle\sigma v\rangle_{gs}$$
Rev. ratio $= 4.488 \times 10^{10}T_9^{3/2}\exp(-276.73/T_9)$

^{2}**H(d,n)^{3}He**, $Q = 3.269$ MeV, (4%)

$$N_A\langle\sigma v\rangle_{gs} = 4.67 \times 10^8T_9^{-2/3}\exp(-4.259T_9^{-1/3})$$
$$\times(1 + 1.079T_9 - 0.1124T_9^2 + 5.68 \times 10^{-3}T_9^3)$$
$$N_A\langle\sigma v\rangle_{tt} = N_A\langle\sigma v\rangle_{gs}$$
Rev. ratio $= 1.730\exp(-37.935/T_9)$

^{2}**H(d,p)^{3}H**, $Q = 4.033$ MeV, (5%)

$$N_A\langle\sigma v\rangle_{gs} = 4.66 \times 10^8T_9^{-2/3}\exp(-4.259T_9^{-1/3})$$
$$\times(1 + 0.759T_9 - 0.0612T_9^2 + 2.78 \times 10^{-3}T_9^3)$$
$$N_A\langle\sigma v\rangle_{tt} = N_A\langle\sigma v\rangle_{gs}$$
Rev. ratio $= 1.732\exp(-46.797/T_9)$

^{2}**H(α, γ)^{6}Li**, $Q = 1.474$ MeV, (4%)

$$N_A \langle \sigma v \rangle_{gs} = 14.82 T_9^{-2/3} \exp(-7.435 T_9^{-1/3})(1 + 6.572 T_9 + 0.076 T_9^2 + 0.0248 T_9^3)$$
$$+82.8 T_9^{-3/2} \exp(-7.904/T_9)$$
$$N_A \langle \sigma v \rangle_{tt} = N_A \langle \sigma v \rangle_{gs}$$

Rev. ratio $= 1.531 \times 10^{10} T_9^{3/2} \exp(-17.108/T_9)$

^{3}**H(d,n)^{4}He**, $Q = 17.589$ MeV, (8%)

$$N_A \langle \sigma v \rangle_{gs} = 8.29 \times 10^{10} T_9^{-2/3} \exp(-4.524 T_9^{-1/3} - (T_9/0.08)^2)$$
$$\times (1 + 17.2 T_9 + 175 T_9^2) + 8.12 \times 10^8 T_9^{-0.712} \exp(-0.506/T_9)$$
$$N_A \langle \sigma v \rangle_{tt} = N_A \langle \sigma v \rangle_{gs}$$

Rev. ratio $= 5.506 \exp(-204.12/T_9)$

^{3}**H(α, γ)^{7}Li**, $Q = 2.467$ MeV, (5%)

$$N_A \langle \sigma v \rangle_{gs} = 8.20 \times 10^5 T_9^{-2/3} \exp(-8.081 T_9^{-1/3})$$
$$\times (1 - 0.389 T_9 + 0.134 T_9^2 - 1.81 \times 10^{-2} T_9^3 + 9.23 \times 10^{-4} T_9^4)$$
$$N_A \langle \sigma v \rangle_{tt} = N_A \langle \sigma v \rangle_{gs}$$

Rev. ratio $= 1.113 \times 10^{10} T_9^{3/2} \exp(-28.629/T_9)$

^{3}**He(^{3}He,2p)^{4}He**, $Q = 12.859$ MeV, (2%)

$$N_A \langle \sigma v \rangle_{gs} = 5.59 \times 10^{10} T_9^{-2/3} \exp(-12.277 T_9^{-1/3})$$
$$\times (1 - 0.135 T_9 + 2.54 \times 10^{-2} T_9^2 - 1.29 \times 10^{-3} T_9^3)$$
$$N_A \langle \sigma v \rangle_{tt} = N_A \langle \sigma v \rangle_{gs}$$

Rev. ratio $= 3.392 \times 10^{-10} T_9^{-3/2} \exp(-149.23/T_9)$

^{3}**He(α, γ)^{7}Be**, $Q = 1.587$ MeV, (6%)

$$N_A \langle \sigma v \rangle_{gs} = 5.46 \times 10^6 T_9^{-2/3} \exp(-12.827 T_9^{-1/3})$$
$$\times (1 - 0.307 T_9 + 8.81 \times 10^{-2} T_9^2 - 1.06 \times 10^{-2} T_9^3 + 4.46 \times 10^{-4} T_9^4)$$
$$N_A \langle \sigma v \rangle_{tt} = N_A \langle \sigma v \rangle_{gs}$$

Rev. ratio $= 1.113 \times 10^{10} T_9^{3/2} \exp(-18.412/T_9)$

^{4}**He(αn,γ)^{9}Be** [11] , $Q = 1.573$ MeV, (19%)

$$N_A \langle \sigma v \rangle_{gs}^{\alpha\alpha} = 2.43 \times 10^9 T_9^{-2/3} \exp(-13.490\, T_9^{-1/3} - (T_9/0.15)^2) \times (1 + 74.5\, T_9)$$
$$+ 6.09 \times 10^5 T_9^{-3/2} \exp(-1.054/T_9)$$

For $T_9 \leqslant 0.03$: $N_A^2 \langle \sigma v \rangle_{gs}^{\alpha\alpha n} = N_A \langle \sigma v \rangle_{gs}^{\alpha\alpha} \times 6.69 \times 10^{-12}$
$$\times (1 - 192 T_9 + 2.48 \times 10^4 T_9^2 - 1.50 \times 10^6 T_9^3$$
$$+ 4.13 \times 10^7 T_9^4 - 3.90 \times 10^8 T_9^5)$$

For $T_9 > 0.03$: $N_A^2 \langle \sigma v \rangle_{gs}^{\alpha\alpha n} = N_A \langle \sigma v \rangle_{gs}^{\alpha\alpha} \times 2.42 \times 10^{-12} \times (1 - 1.52 \log_{10} T_9$
$$+ 0.448 (\log_{10} T_9)^2 + 0.435 (\log_{10} T_9)^3)$$

$N_A \langle \sigma v \rangle_{tt} = N_A \langle \sigma v \rangle_{gs}$
Rev. ratio $= 5.844 \times 10^{19} T_9^3 \exp(-18.258/T_9)$

^{4}**He($\alpha\alpha$, γ)^{12}C**, $Q = 7.274$ MeV, (23%)

$$N_A \langle \sigma v \rangle_{gs}^{\alpha^8 Be} = 2.76 \times 10^7 T_9^{-2/3} \exp(-23.570 T_9^{-1/3}$$
$$- (T_9/0.4)^2) \times (1 + 5.47 T_9 + 326 T_9^2)$$
$$+ 130.7 T_9^{-3/2} \exp(-3.338/T_9) + 2.51 \times 10^4 T_9^{-3/2} \exp(-20.307/T_9)$$

For $T_9 \leqslant 0.03$: $N_A^2 \langle \sigma v \rangle_{gs}^{\alpha\alpha\alpha} = N_A \langle \sigma v \rangle_{gs}^{\alpha\alpha} \times N_A \langle \sigma v \rangle_{gs}^{\alpha^8 Be}$
$$\times 3.07 \times 10^{-16} \times (1 - 29.1 T_9 + 1308 T_9^2)$$

For $T_9 > 0.03$: $N_A^2 \langle \sigma v \rangle_{gs}^{\alpha\alpha\alpha} = N_A \langle \sigma v \rangle_{gs}^{\alpha\alpha} \times N_A \langle \sigma v \rangle_{gs}^{\alpha^8 Be}$
$$\times 3.44 \times 10^{-16} \times (1 + 0.0158 T_9^{-0.65})$$

$N_A \langle \sigma v \rangle_{tt} = N_A \langle \sigma v \rangle_{gs}$
Rev. ratio $= 2.003 \times 10^{20} T_9^3 \exp(-84.415/T_9)$

^{6}**Li(p,γ)^{7}Be**, $Q = 5.606$ MeV, (7%)

$$N_A \langle \sigma v \rangle_{gs} = 1.25 \times 10^6 T_9^{-2/3} \exp(-8.415 T_9^{-1/3})$$
$$\times (1 - 0.252 T_9 + 5.19 \times 10^{-2} T_9^2 - 2.92 \times 10^{-3} T_9^3)$$

$N_A \langle \sigma v \rangle_{tt} = N_A \langle \sigma v \rangle_{gs}$
Rev. ratio $= 1.187 \times 10^{10} T_9^{3/2} \exp(-65.052/T_9)$

---

[11] The rate $N_A \langle \sigma v \rangle_{gs}^{\alpha\alpha}$ has no physical meaning but is convenient for the definitions of $N_A \langle \sigma v \rangle^{\alpha\alpha n}$ and $N_A \langle \sigma v \rangle^{\alpha\alpha\alpha}$.

^{6}**Li(p,α)^{3}He**, $Q = 4.019$ MeV, (2%)

$$N_A \langle \sigma v \rangle_{gs} = 3.54 \times 10^{10} T_9^{-2/3} \exp(-8.415 T_9^{-1/3})$$
$$\times (1 - 0.137 T_9 + 2.41 \times 10^{-2} T_9^2 - 1.28 \times 10^{-3} T_9^3)$$
$$N_A \langle \sigma v \rangle_{tt} = N_A \langle \sigma v \rangle_{gs}$$

Rev. ratio $= 1.067 \exp(-46.641/T_9)$

^{7}**Li(p,γ)^{8}Be**, $Q = 17.255$ MeV, (11%)

$$N_A \langle \sigma v \rangle_{gs} = 1.75 \times 10^7 T_9^{-2/3} \exp(-8.473 T_9^{-1/3} - (T_9/0.8)^2)$$
$$\times (1 - 1.47 T_9 + 4.43 T_9^2) + 1.60 \times 10^6 T_9^{-3/2} \exp(-4.441/T_9)$$
$$+ 4.32 \times 10^4 T_9^{0.309} \exp(-2.811/T_9)$$
$$N_A \langle \sigma v \rangle_{tt} = N_A \langle \sigma v \rangle_{gs}$$

Rev. ratio $= 6.531 \times 10^{10} T_9^{3/2} \exp(-200.23/T_9)$

^{7}**Li(p,α)^{4}He**, $Q = 17.347$ MeV, (6%)

$$N_A \langle \sigma v \rangle_{gs} = 7.20 \times 10^8 T_9^{-2/3} \exp(-8.473 T_9^{-1/3} - (T_9/6.5)^2)$$
$$\times (1 + 1.05 T_9 - 0.653 T_9^2 + 0.185 T_9^3$$
$$- 2.12 \times 10^{-2} T_9^4 + 9.30 \times 10^{-4} T_9^5)$$
$$+ 9.85 \times 10^6 T_9^{0.576} \exp(-10.415/T_9)$$
$$N_A \langle \sigma v \rangle_{tt} = N_A \langle \sigma v \rangle_{gs}$$
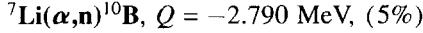
Rev. ratio $= 4.676 \exp(-201.30/T_9)$

^{7}**Li(α,γ)^{11}B**, $Q = 8.664$ MeV, (17%)

$$N_A \langle \sigma v \rangle_{gs} = 9.72 \times 10^7 T_9^{-2/3} \exp(-19.163 T_9^{-1/3} - (T_9/0.4)^2)$$
$$\times (1 + 2.84 T_9 - 7.89 T_9^2) + 3.35 \times 10^2 T_9^{-3/2} \exp(-2.959/T_9)$$
$$+ 1.04 \times 10^4 T_9^{-0.023} \exp(-4.922/T_9)$$

$$N_A \langle \sigma v \rangle_{tt} = N_A \langle \sigma v \rangle_{gs}$$
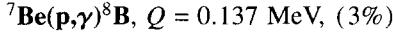
Rev. ratio $= 4.015 \times 10^{10} T_9^{3/2} \exp(-100.55/T_9)$

^{7}Li(α,n)^{10}B, $Q = -2.790$ MeV, (5%)

$$N_A \langle \sigma v \rangle_{\mathrm{gs}} = 1.66 \times 10^7 \exp(-32.371/T_9) \times (1 + 1.064T_9)$$

$$N_A \langle \sigma v \rangle_{\mathrm{tt}} = N_A \langle \sigma v \rangle_{\mathrm{gs}}$$
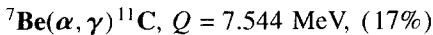
Rev. ratio $= 1.325 \exp(32.371/T_9)$

^{7}Be(p,γ)^{8}B, $Q = 0.137$ MeV, (3%)

$$\begin{aligned}
N_A \langle \sigma v \rangle_{\mathrm{gs}} &= 2.61 \times 10^5 T_9^{-2/3} \exp(-10.264T_9^{-1/3}) \\
&\quad \times (1 - 5.11 \times 10^{-2}T_9 + 4.68 \times 10^{-2}T_9^2 - 6.60 \times 10^{-3}T_9^3 \\
&\quad + 3.12 \times 10^{-4}T_9^4) + 2.05 \times 10^3 T_9^{-3/2} \exp(-7.345/T_9)
\end{aligned}$$

$$N_A \langle \sigma v \rangle_{\mathrm{tt}} = N_A \langle \sigma v \rangle_{\mathrm{gs}}$$

Rev. ratio $= 1.306 \times 10^{10} T_9^{3/2} \exp(-1.594/T_9)$

^{7}Be(α,γ)^{11}C, $Q = 7.544$ MeV, (17%)
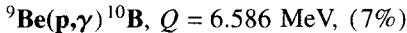
$$\begin{aligned}
\text{For } T_9 \leqslant 2: \quad N_A \langle \sigma v \rangle_{\mathrm{gs}} &= 1.29 \times 10^{10} T_9^{-2/3} \exp(-23.214T_9^{-1/3} - (T_9/0.8)^2) \\
&\quad \times (1 - 6.47T_9 + 19.5\,T_9^2 - 19.3T_9^3) \\
&\quad + 1.25 \times 10^4 T_9^{-3/2} \exp(-6.498/T_9) \\
&\quad + 1.44 \times 10^5 T_9^{-3/2} \exp(-10.177/T_9) \\
&\quad + 1.63 \times 10^4 T_9^{0.178} \exp(-15.281/T_9)
\end{aligned}$$

$$\text{For } T_9 > 2: \quad N_A \langle \sigma v \rangle_{\mathrm{gs}} = 1.41 \times 10^3 T_9^{0.636} \exp(-3.015/T_9)$$

$$N_A \langle \sigma v \rangle_{\mathrm{tt}} = N_A \langle \sigma v \rangle_{\mathrm{gs}}$$
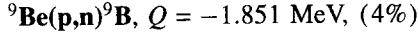
Rev. ratio $= 4.016 \times 10^{10} T_9^{3/2} \exp(-87.541/T_9)$

^{9}Be(p,γ)^{10}B, $Q = 6.586$ MeV, (7%)

$$\begin{aligned}
N_A \langle \sigma v \rangle_{\mathrm{gs}} &= 1.36 \times 10^7 T_9^{-2/3} \exp(-10.361T_9^{-1/3} - (T_9/1.5)^2) \\
&\quad \times (1 + 2.71T_9 - 1.95T_9^2 + 0.594T_9^3) \\
&\quad + 4.80 \times 10^3 T_9^{-3/2} \exp(-3.102/T_9) \\
&\quad + 2.75 \times 10^6 T_9^{-3/2} \exp(-10.615/T_9)
\end{aligned}$$

$$N_A \langle \sigma v \rangle_{\mathrm{tt}} = N_A \langle \sigma v \rangle_{\mathrm{gs}}$$
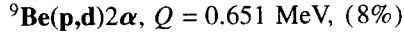
Rev. ratio $= 9.734 \times 10^9 T_9^{3/2} \exp(-76.424/T_9)$

^{9}**Be(p,n)**^{9}**B**, $Q = -1.851$ MeV, (4%)

$$N_A \langle \sigma v \rangle_{gs} = 5.06 \times 10^7 \exp(-21.474/T_9) \times (1 + 1.26T_9 - 0.0302T_9^2)$$

$$N_A \langle \sigma v \rangle_{tt} = N_A \langle \sigma v \rangle_{gs}$$
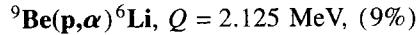
Rev. ratio $= 9.989 \times 10^{-1} \exp(21.474/T_9)$

^{9}**Be(p,d)2α**, $Q = 0.651$ MeV, (8%)

$$N_A \langle \sigma v \rangle_{gs} = 2.18 \times 10^{11} T_9^{-2/3} \exp(-10.361T_9^{-1/3} - (T_9/0.42)^2)$$
$$\times (1 - 0.427T_9 + 34.055T_9^2) + 6.24 \times 10^8 T_9^{-3/2} \exp(-3.446/T_9)$$
$$+ 3.53 \times 10^8 T_9^{-0.205} \exp(-3.889/T_9)$$
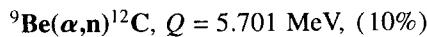
$$N_A \langle \sigma v \rangle_{tt} = N_A \langle \sigma v \rangle_{gs}$$

Rev. ratio $= 8.071 \times 10^{-11} T_9^{-3/2} \exp(-7.556/T_9)$

^{9}**Be(p,α)^{6}Li**, $Q = 2.125$ MeV, (9%)

$$N_A \langle \sigma v \rangle_{gs} = 2.11 \times 10^{11} T_9^{-2/3} \exp(-10.361T_9^{-1/3} - (T_9/0.4)^2)$$
$$\times (1 - 0.189T_9 + 35.2T_9^2) + 5.24 \times 10^8 T_9^{-3/2} \exp(-3.446/T_9)$$
$$+ 4.65 \times 10^8 T_9^{-0.293} \exp(-4.396/T_9)$$
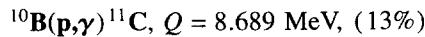
$$N_A \langle \sigma v \rangle_{tt} = N_A \langle \sigma v \rangle_{gs}$$

Rev. ratio $= 6.177 \times 10^{-1} \exp(-24.663/T_9)$

^{9}**Be(α,n)^{12}C**, $Q = 5.701$ MeV, (10%)

$$N_A \langle \sigma v \rangle_{gs} = 5.00 \times 10^{13} T_9^{-2/3} \exp(-23.872T_9^{-1/3} - (T_9/0.154)^2)$$
$$\times (1 + 27.3T_9 + 1632T_9^2)$$
$$+ 0.70T_9^{-3/2} \exp(-1.832/T_9)$$
$$+ 1.77 \times 10^5 T_9^{-3/2} \exp(-4.385/T_9)$$
$$+ 4.12 \times 10^7 T_9^{0.65} \exp(-10.060/T_9)$$
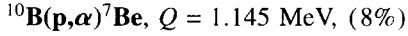
$$N_A \langle \sigma v \rangle_{tt} = N_A \langle \sigma v \rangle_{gs}$$

Rev. ratio $= 10.28 \exp(-66.158/T_9)$

^{10}**B(p,γ)^{11}C**, $Q = 8.689$ MeV, (13%)
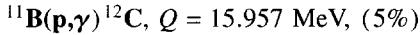
$$N_A \langle \sigma v \rangle_{gs} = 1.68 \times 10^6 T_9^{-2/3} \exp(-12.064T_9^{-1/3})$$

$$\times ((T_9^{2/3} - 0.0273)^2 + 4.69 \times 10^{-4})^{-1}$$

$$\times (1 + 0.977T_9 + 1.87T_9^2 - 0.272T_9^3 + 1.30 \times 10^{-2}T_9^4)$$

$$N_A \langle \sigma v \rangle_{tt} = N_A \langle \sigma v \rangle_{gs}$$

$$\text{Rev. ratio} = 3.026 \times 10^{10} T_9^{3/2} \exp(-100.83/T_9)$$

^{10}**B(p,α)^{7}Be**, $Q = 1.145$ MeV, (8%)
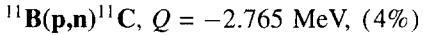
For $T_9 \leqslant 0.8$: $N_A \langle \sigma v \rangle_{gs} = 2.56 \times 10^{10} T_9^{-2/3} \exp(-12.064 T_9^{-1/3})$

$$\times ((T_9^{2/3} - 0.026)^2 + 4.70 \times 10^{-4})^{-1}$$

$$\times (1 + 5.95T_9 + 29.2T_9^2 - 316T_9^3 + 914T_9^4$$

$$-1085T_9^5 + 465T_9^6)$$

For $T_9 > 0.8$: $N_A \langle \sigma v \rangle_{gs} = 1.01 \times 10^{10} T_9^{-2/3} \exp(-12.064 T_9^{-1/3})$

$$\times (-1 + 15.8T_9 - 2.60T_9^2 + 0.125T_9^3)$$
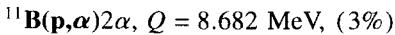
$$N_A \langle \sigma v \rangle_{tt} = N_A \langle \sigma v \rangle_{gs}$$

$$\text{Rev. ratio} = 7.537 \times 10^{-1} \exp(-13.291/T_9)$$

^{11}**B(p,γ)^{12}C**, $Q = 15.957$ MeV, (5%)

$$N_A \langle \sigma v \rangle_{gs} = 4.58 \times 10^7 T_9^{-2/3} \exp(-12.097 T_9^{-1/3} - (T_9/0.6)^2)$$

$$\times (1 + 0.353T_9 + 0.842T_9^2) + 6.82 \times 10^3 T_9^{-3/2} \exp(-1.738/T_9)$$

$$+2.80 \times 10^4 T_9^{0.104} \exp(-3.892/T_9)$$

$$N_A \langle \sigma v \rangle_{tt} = N_A \langle \sigma v \rangle_{gs}$$

$$\text{Rev. ratio} = 7.004 \times 10^{10} T_9^{3/2} \exp(-185.17/T_9)$$

^{11}**B(p,n)^{11}C**, $Q = -2.765$ MeV, (4%)

$$N_A \langle \sigma v \rangle_{gs} = 1.36 \times 10^8 \exp(-32.085/T_9)$$

$$\times (1 + 0.963T_9 - 0.285T_9^2 + 3.36 \times 10^{-2}T_9^3 - 1.37 \times 10^{-3}T_9^4)$$

$$N_A \langle \sigma v \rangle_{tt} = N_A \langle \sigma v \rangle_{gs}$$

$$\text{Rev. ratio} = 9.988 \times 10^{-1} \exp(32.085/T_9)$$

^{11}**B(p,α)2α**, $Q = 8.682$ MeV, (3%)
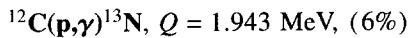
For $T_9 \leqslant 2$: $N_A \langle \sigma v \rangle_{gs} = 2.68 \times 10^{12} T_9^{-2/3} \exp(-12.097 T_9^{-1/3})$

$$\times (1 + 1.62T_9 - 1.31T_9^2 + 0.260T_9^3)$$
$$+2.12 \times 10^6 T_9^{-3/2} \exp(-1.724/T_9)$$

For $T_9 > 2$:
$$N_A \langle \sigma v \rangle_{gs} = 5.84 \times 10^{11} T_9^{-2/3} \exp(-12.097T_9^{-1/3})$$
$$\times ((T_9^{2/3} - 1.47)^2 + 0.187)^{-1}$$
$$\times (-1 + 0.883T_9 + 0.012T_9^2)$$
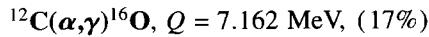
$$N_A \langle \sigma v \rangle_{tt} = N_A \langle \sigma v \rangle_{gs}$$
$$\text{Rev. ratio} = 3.501 \times 10^{-10} T_9^{-3/2} \exp(-100.76/T_9)$$

^{12}**C(p,γ)^{13}N**, $Q = 1.943$ MeV, (6%)

$$N_A \langle \sigma v \rangle_{gs} = 2.00 \times 10^7 T_9^{-2/3} \exp(-13.692T_9^{-1/3} - (T_9/0.46)^2)$$
$$\times (1 + 9.89T_9 - 59.8T_9^2 + 266T_9^3)$$
$$+1.00 \times 10^5 T_9^{-3/2} \exp(-4.913/T_9)$$
$$+4.24 \times 10^5 T_9^{-3/2} \exp(-21.62/T_9)$$
$$N_A \langle \sigma v \rangle_{tt} = N_A \langle \sigma v \rangle_{gs}$$
$$\text{Rev. ratio} = 8.847 \times 10^9 T_9^{3/2} \exp(-22.553/T_9)$$

^{12}**C(α,γ)^{16}O**, $Q = 7.162$ MeV, (17%)
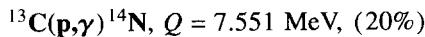
$$N_A \langle \sigma v \rangle_{gs} = N_A \langle \sigma v \rangle_{E1} + N_A \langle \sigma v \rangle_{E2} + N_A \langle \sigma v \rangle_{res}$$
$$N_A \langle \sigma v \rangle_{E1} = 6.66 \times 10^7 T_9^{-2} \exp(-32.123T_9^{-1/3} - (T_9/4.6)^2)$$
$$\times (1 + 2.54T_9 + 1.04T_9^2 - 0.226T_9^3)$$
$$+1.39 \times 10^3 T_9^{-3/2} \exp(-28.930/T_9)$$
$$N_A \langle \sigma v \rangle_{E2} = 6.56 \times 10^7 T_9^{-2} \exp(-32.123T_9^{-1/3} - (T_9/1.3)^2)$$
$$\times (1 + 9.23T_9 - 13.7T_9^2 + 7.4T_9^3)$$
$$N_A \langle \sigma v \rangle_{res} = 19.2T_9^2 \exp(-26.9/T_9)$$
$$N_A \langle \sigma v \rangle_{tt} = N_A \langle \sigma v \rangle_{gs}$$
$$\text{Rev. ratio} = 5.132 \times 10^{10} T_9^{3/2} \exp(-83.109/T_9)$$
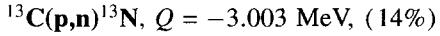
^{13}**C(p,γ)^{14}N**, $Q = 7.551$ MeV, (20%)
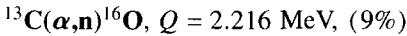
$$N_A \langle \sigma v \rangle_{gs} = 9.57 \times 10^7 T_9^{-2/3} (1 + 3.56T_9) \exp(-13.720T_9^{-1/3} - T_9^2)$$
$$+1.50 \times 10^6 T_9^{-3/2} \exp(-5.930/T_9)$$

$$+6.83 \times 10^5 T_9^{-0.864} \exp(-12.057/T_9)$$

$$N_A \langle \sigma v \rangle_{tt} = N_A \langle \sigma v \rangle_{gs} \times (1 - 2.070 \exp(-37.938/T_9))$$

Rev. ratio $= 1.190 \times 10^{10} T_9^{3/2} \exp(-87.619/T_9)$

^{13}C(p,n)^{13}N, $Q = -3.003$ MeV, (14%)
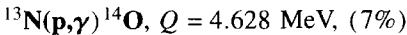
$$N_A \langle \sigma v \rangle_{gs} = 1.18 \times 10^8 \exp(-34.846/T_9)$$
$$\times (1 + 0.336 T_9 - 3.79 \times 10^{-2} T_9^2 + 2.02 \times 10^{-3} T_9^3)$$

$$N_A \langle \sigma v \rangle_{tt} = N_A \langle \sigma v \rangle_{gs} \times (1 + 1.131 \exp(-12.892/T_9 + 0.019 T_9))$$

Rev. ratio $= 9.988 \times 10^{-1} \exp(34.846/T_9)$

^{13}C(α,n)^{16}O, $Q = 2.216$ MeV, (9%)
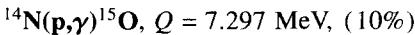
For $T_9 \leqslant 4.0$: $\quad N_A \langle \sigma v \rangle_{gs} = 3.78 \times 10^{14} T_9^{-2} \exp(-32.333 T_9^{-1/3} - (T_9/0.71)^2)$
$$\times (1 + 46.8 T_9 - 292 T_9^2 + 738 T_9^3)$$
$$+2.30 \times 10^7 T_9^{0.45} \exp(-13.03/T_9)$$

For $T_9 > 4.0$: $\quad N_A \langle \sigma v \rangle_{gs} = 7.59 \times 10^6 T_9^{1.078} \exp(-12.056/T_9)$

$$N_A \langle \sigma v \rangle_{tt} = N_A \langle \sigma v \rangle_{gs} \times (1 + 73.318 \exp(-58.176/T_9 - 0.198 T_9))$$

Rev. ratio $= 5.793 \exp(-25.710/T_9)$

^{13}N(p,γ)^{14}O, $Q = 4.628$ MeV, (7%)

$$N_A \langle \sigma v \rangle_{gs} = 4.02 \times 10^7 T_9^{-2/3} \exp(-15.205 T_9^{-1/3} - (T_9/0.54)^2)$$
$$\times (1 + 3.81 T_9 + 18.6 T_9^2 + 32.3 T_9^3)$$
$$+3.25 \times 10^5 T_9^{-1.35} \exp(-5.926/T_9)$$

$$N_A \langle \sigma v \rangle_{tt} = N_A \langle \sigma v \rangle_{gs}$$

Rev. ratio $= 3.571 \times 10^{10} T_9^{3/2} \exp(-53.705/T_9)$

^{14}N(p,γ)^{15}O, $Q = 7.297$ MeV, (10%)

$$N_A \langle \sigma v \rangle_{gs} = 4.83 \times 10^7 T_9^{-2/3} \exp(-15.231 T_9^{-1/3} - (T_9/0.8)^2)$$
$$\times (1 - 2.00 T_9 + 3.41 T_9^2 - 2.43 T_9^3)$$
$$+2.36 \times 10^3 T_9^{-3/2} \exp(-3.010/T_9)$$
$$+6.72 \times 10^3 T_9^{0.380} \exp(-9.530/T_9)$$

$$N_A \langle \sigma v \rangle_{tt} = N_A \langle \sigma v \rangle_{gs}$$

Rev. ratio $= 2.699 \times 10^{10} T_9^{3/2} \exp(-84.677/T_9)$

^{14}**N(p,n)**^{14}**O**, $Q = -5.925$ MeV, (2%)

$$N_A\langle\sigma v\rangle_{gs} = 6.40 \times 10^5 \exp(-68.761/T_9) \times (-1 + 8.74T_9 - 0.431T_9^2)$$

$$N_A\langle\sigma v\rangle_{tt} = N_A\langle\sigma v\rangle_{gs} \times (1 + 1.206\exp(0.007/T_9 + 0.046T_9))$$

Rev. ratio $= 2.996\exp(68.761/T_9)$

^{14}**N(p,α)**^{11}**C**, $Q = -2.923$ MeV, (19%)

$$N_A\langle\sigma v\rangle_{gs} = 3.01 \times 10^{16} \exp(-31.884T_9^{-1/3} - 33.920/T_9)$$
$$\times \exp(-1.379T_9 + 0.215T_9^2 - 2.13 \times 10^{-2}T_9^3 + 8.00 \times 10^{-4}T_9^4)$$

$$N_A\langle\sigma v\rangle_{tt} = N_A\langle\sigma v\rangle_{gs} \times (1 + 0.140\exp(-0.275/T_9 - 0.210T_9))$$

Rev. ratio $= 2.719 \times 10^{-1} \exp(33.920/T_9)$

^{14}**N(α,γ)**^{18}**F**, $Q = 4.415$ MeV, (5%)

For $T_9 \leqslant 2$:
$$N_A\langle\sigma v\rangle_{gs} = 7.93 \times 10^{11}T_9^{-2/3} \exp(-36.035T_9^{-1/3} - (T_9/0.07)^2)$$
$$+ 1.85 \times 10^{-10}T_9^{-3/2}\exp(-2.750/T_9)$$
$$+ 2.62T_9^{-3/2}\exp(-5.045/T_9)$$
$$+ 2.93 \times 10^3 T_9^{0.344}\exp(-10.561/T_9)$$

For $T_9 > 2$:
$$N_A\langle\sigma v\rangle_{gs} = 1.52 \times 10^2 T_9^{1.567}\exp(-6.315/T_9)$$

$$N_A\langle\sigma v\rangle_{tt} = N_A\langle\sigma v\rangle_{gs} \times (1 - 0.340\exp(-26.885/T_9 - 0.012T_9))$$

Rev. ratio $= 5.420 \times 10^{10}T_9^{3/2}\exp(-51.231/T_9)$

^{14}**N(α,n)**^{17}**F**, $Q = -4.735$ MeV, (8%)

$$N_A\langle\sigma v\rangle_{gs} = 1.38 \times 10^8 T_9^{0.053}\exp(-55.0/T_9)$$

$$N_A\langle\sigma v\rangle_{tt} = N_A\langle\sigma v\rangle_{gs} \times (1 + 0.039\exp(-0.012/T_9 + 0.217T_9))$$

Rev. ratio $= 1.478\exp(54.943/T_9)$
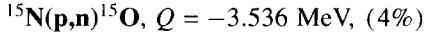
^{15}**N(p,γ)**^{16}**O**, $Q = 12.127$ MeV, (15%)

For $T_9 \leqslant 3.5$:
$$N_A\langle\sigma v\rangle_{gs} = 1.08 \times 10^9 T_9^{-2/3}\exp(-15.254T_9^{-1/3}$$
$$- (T_9/0.34)^2) \times (1 + 6.15T_9 + 16.4T_9^2)$$
$$+ 9.23 \times 10^3 T_9^{-3/2}\exp(-3.597/T_9)$$
$$+ 3.27 \times 10^6 T_9^{-3/2}\exp(-11.024/T_9)$$

For $T_9 > 3.5$:
$$N_A\langle\sigma v\rangle_{gs} = 3.54 \times 10^4 T_9^{0.095}\exp(-2.306/T_9)$$

$$N_A \langle \sigma v \rangle_{tt} = N_A \langle \sigma v \rangle_{gs}$$

Rev. ratio $= 3.622 \times 10^{10} T_9^{3/2} \exp(-140.73/T_9)$

^{15}N(p,n)^{15}O, $Q = -3.536$ MeV, (4%)
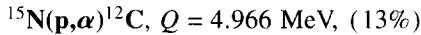
$$N_A \langle \sigma v \rangle_{gs} = 1.16 \times 10^8 \exp(-41.037/T_9)$$
$$\times (1 + 0.219 T_9 - 0.029 T_9^2 + 1.73 \times 10^{-3} T_9^3)$$
$$N_A \langle \sigma v \rangle_{tt} = N_A \langle \sigma v \rangle_{gs} \times (1 + 0.387 \exp(-26.171/T_9 + 0.118 T_9))$$

Rev. ratio $= 9.988 \times 10^{-1} \exp(41.037/T_9)$

^{15}N(p,α)^{12}C, $Q = 4.966$ MeV, (13%)
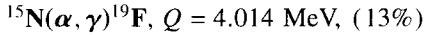
For $T_9 \leqslant 2.5$: $\quad N_A \langle \sigma v \rangle_{gs} = 1.12 \times 10^{12} T_9^{-2/3} \exp(-15.253 T_9^{-1/3}$
$$-(T_9/0.28)^2) \times (1 + 4.95 T_9 + 143 T_9^2)$$
$$+1.01 \times 10^8 T_9^{-3/2} \exp(-3.643/T_9)$$
$$+1.19 \times 10^9 T_9^{-3/2} \exp(-7.406/T_9)$$

For $T_9 > 2.5$: $\quad N_A \langle \sigma v \rangle_{gs} = 4.17 \times 10^7 T_9^{0.917} \exp(-3.292/T_9)$

$$N_A \langle \sigma v \rangle_{tt} = N_A \langle \sigma v \rangle_{gs}$$
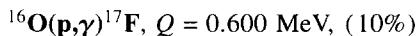
Rev. ratio $= 7.060 \times 10^{-1} \exp(-57.622/T_9)$

^{15}N(α,γ)^{19}F, $Q = 4.014$ MeV, (13%)

$$N_A \langle \sigma v \rangle_{gs} = 1.10 \times 10^{11} T_9^{-2/3} \exp(-36.214 T_9^{-1/3} - (T_9/0.6)^2)$$
$$+1.65 \times 10^{-4} T_9^{-3/2} \exp(-4.224/T_9)$$
$$+2.66 T_9^{-3/2} \exp(-6.220/T_9) + 1.56 \times 10^2 T_9^{-3/2} \exp(-7.764/T_9)$$
$$+3.92 \times 10^4 T_9^{-0.333} \exp(-14.522/T_9)$$
$$N_A \langle \sigma v \rangle_{tt} = N_A \langle \sigma v \rangle_{gs}$$

Rev. ratio $= 5.542 \times 10^{10} T_9^{3/2} \exp(-46.577/T_9)$

^{16}O(p,γ)^{17}F, $Q = 0.600$ MeV, (10%)

$$N_A \langle \sigma v \rangle_{gs} = 7.37 \times 10^7 \exp(-16.696 T_9^{-1/3}) \times T_9^{-0.82}$$
$$N_A \langle \sigma v \rangle_{tt} = N_A \langle \sigma v \rangle_{gs} \times (1 + 202 \exp(-70.348/T_9 - 0.161 T_9))$$

Rev. ratio $= 3.037 \times 10^9 T_9^{3/2} \exp(-6.966/T_9)$

$^{16}\mathbf{O}(\boldsymbol{\alpha},\boldsymbol{\gamma})^{20}\mathbf{Ne}$, $Q = 4.730$ MeV, (3%)

$$N_A\langle\sigma v\rangle_{gs} = 2.68 \times 10^{10}T_9^{-2/3}\exp(-39.760T_9^{-1/3} - (T_9/1.6)^2)$$
$$+51.1T_9^{-3/2}\exp(-10.32/T_9) + 616.1T_9^{-3/2}\exp(-12.200/T_9)$$
$$+0.41T_9^{2.966}\exp(-11.900/T_9)$$

$$N_A\langle\sigma v\rangle_{tt} = N_A\langle\sigma v\rangle_{gs}$$

Rev. ratio $= 5.653 \times 10^{10}T_9^{3/2}\exp(-54.886/T_9)$

$^{17}\mathbf{O}(\mathbf{p},\boldsymbol{\gamma})^{18}\mathbf{F}$, $Q = 5.606$ MeV, (10%)

For $T_9 \leqslant 3$: $N_A\langle\sigma v\rangle_{gs} = 1.50 \times 10^8T_9^{-2/3}\exp(-16.710T_9^{-1/3} - (T_9/0.2)^2)$
$$+9.79 \times 10^{-6}T_9^{-3/2}\exp(-0.7659/T_9)$$
$$+4.15T_9^{-3/2}\exp(-2.083/T_9)$$
$$+7.74 \times 10^4T_9^{1.16}\exp(-6.342/T_9)$$

For $T_9 > 3$: $N_A\langle\sigma v\rangle_{gs} = 1.74 \times 10^3T_9^{0.700}\exp(-1.072/T_9)$

$$N_A\langle\sigma v\rangle_{tt} = N_A\langle\sigma v\rangle_{gs} \times (1 - 0.287\exp(-10.011/T_9 - 0.062T_9))$$

Rev. ratio $= 3.663 \times 10^{10}T_9^{3/2}\exp(-65.060/T_9)$
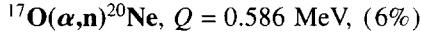
$^{17}\mathbf{O}(\mathbf{p},\boldsymbol{\alpha})^{14}\mathbf{N}$, $Q = 1.192$ MeV, (11%)

For $T_9 \leqslant 6$: $N_A\langle\sigma v\rangle_{gs} = 9.20 \times 10^8T_9^{-2/3}\exp(-16.715T_9^{-1/3} - (T_9/0.06)^2)$
$$\times (1 - 80.31T_9 + 2211T_9^2)$$
$$+9.13 \times 10^{-4}T_9^{-3/2}\exp(-0.7667/T_9)$$
$$+9.68T_9^{-3/2}\exp(-2.083/T_9)$$
$$+8.13 \times 10^6T_9^{-3/2}\exp(-5.685/T_9)$$
$$+1.85 \times 10^6T_9^{1.591}\exp(-4.848/T_9)$$
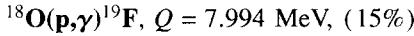
For $T_9 > 6$: $N_A\langle\sigma v\rangle_{gs} = 8.73 \times 10^6T_9^{0.950}\exp(-7.508/T_9)$

$$N_A\langle\sigma v\rangle_{tt} = N_A\langle\sigma v\rangle_{gs} \times (1 + 1.033\exp(-10.034/T_9 - 0.165T_9))$$

Rev. ratio $= 6.759 \times 10^{-1}\exp(-13.829/T_9)$

^{17}**O(α,n)^{20}Ne**, $Q = 0.586$ MeV, (6%)
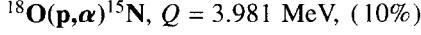
$$N_A \langle \sigma v \rangle_{gs} = 4.38 \times 10^{17} T_9^{-2/3} \exp(-39.918 T_9^{-1/3} - (T_9/1.1)^2)$$
$$+ 1.73 \times 10^3 T_9^{-3/2} \exp(-8.55/T_9) + 7.50 \times 10^5 T_9^{1.83} \exp(-13.8/T_9)$$
$$N_A \langle \sigma v \rangle_{tt} = N_A \langle \sigma v \rangle_{gs}$$

Rev. ratio $= 18.59 \exp(-6.806/T_9)$

^{18}**O(p,γ)^{19}F**, $Q = 7.994$ MeV, (15%)
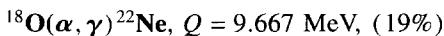
For $T_9 \leqslant 2$:
$$N_A \langle \sigma v \rangle_{gs} = 4.59 \times 10^8 T_9^{-2/3} \exp(-16.732 T_9^{-1/3} - (T_9/0.15)^2)$$
$$\times (1 - 9.02 T_9 + 506 T_9^2 - 2400 T_9^3)$$
$$+ 9.91 \times 10^{-17} T_9^{-3/2} \exp(-0.232/T_9)$$
$$+ 3.30 \times 10^{-3} T_9^{-3/2} \exp(-1.033/T_9)$$
$$+ 1.61 \times 10^2 T_9^{-3/2} \exp(-1.665/T_9)$$
$$+ 1.25 \times 10^4 T_9^{0.458} \exp(-5.297/T_9)$$

For $T_9 > 2$:
$$N_A \langle \sigma v \rangle_{gs} = 1.38 \times 10^4 T_9^{0.829} \exp(-5.919/T_9)$$

$$N_A \langle \sigma v \rangle_{tt} = N_A \langle \sigma v \rangle_{gs} \times (1 - 0.475 \exp(-15.513/T_9 - 0.102 T_9))$$

Rev. ratio $= 9.201 \times 10^9 T_9^{3/2} \exp(-92.769/T_9)$

^{18}**O(p,α)^{15}N**, $Q = 3.981$ MeV, (10%)

$$N_A \langle \sigma v \rangle_{gs} = 5.58 \times 10^{11} T_9^{-2/3} \exp(-16.732 T_9^{-1/3} - (T_9/0.51)^2)$$
$$\times (1 + 3.2 T_9 + 21.8 T_9^2) + 9.91 \times 10^{-14} T_9^{-3/2} \exp(-0.232/T_9)$$
$$+ 2.58 \times 10^4 T_9^{-3/2} \exp(-1.665/T_9)$$
$$+ 3.24 \times 10^8 T_9^{-0.378} \exp(-6.395/T_9)$$
$$N_A \langle \sigma v \rangle_{tt} = N_A \langle \sigma v \rangle_{gs} \times (1 - 1.968 \exp(-25.673/T_9 - 0.083 T_9))$$

Rev. ratio $= 1.660 \times 10^{-1} \exp(-46.192/T_9)$

^{18}**O(α, γ)^{22}Ne**, $Q = 9.667$ MeV, (19%)

For $T_9 \leqslant 6$:
$$N_A \langle \sigma v \rangle_{gs} = 1.95 \times 10^{-13} T_9^{-3/2} \exp(-2.069/T_9)$$
$$+ 1.56 \times 10^{-2} T_9^{-3/2} \exp(-4.462/T_9)$$
$$+ 10.1 T_9^{-3/2} \exp(-6.391/T_9)$$

$$+44.1T_9^{-3/2}\exp(-7.389/T_9)$$
$$+3.44\times 10^5 T_9^{-0.5}\exp(-22.103/T_9)$$

For $T_9 > 6$: $N_A\langle\sigma v\rangle_{gs} = 3.31\times 10^5 T_9^{-0.221}\exp(-24.990/T_9)$

$$N_A\langle\sigma v\rangle_{tt} = N_A\langle\sigma v\rangle_{gs}\times(1-1.411\exp(-20.533/T_9-0.038T_9))$$
Rev. ratio $= 5.847\times 10^{10}T_9^{3/2}\exp(-112.18/T_9)$

^{18}**O(α,n)^{21}Ne**, $Q = -0.697$ MeV, (12%)

$$N_A\langle\sigma v\rangle_{gs} = 49.1\exp(-8.085/T_9)\times(-1+18.7T_9-85.6T_9^2+146.8T_9^3)$$
$$+6.94\times 10^5 T_9^{2.24}\exp(-15.444/T_9)$$
$$N_A\langle\sigma v\rangle_{tt} = N_A\langle\sigma v\rangle_{gs}\times(1+0.427\exp(-22.836/T_9-0.009T_9))$$
Rev. ratio $= 7.845\times 10^{-1}\exp(8.085/T_9)$

^{19}**F(p,γ)^{20}Ne**, $Q = 12.843$ MeV, (11%)

For $T_9 \leqslant 1.5$: $N_A\langle\sigma v\rangle_{gs} = 6.37\times 10^7 T_9^{-2/3}\exp(-18.116T_9^{-1/3})$
$$\times(1+0.775T_9+36.1T_9^2)$$
$$+8.27\times 10^2 T_9^{-3/2}\exp(-3.752/T_9)$$
$$+1.28\times 10^6 T_9^{-3.667}\exp(-9.120/T_9)$$

For $T_9 > 1.5$: $N_A\langle\sigma v\rangle_{gs} = 3.66\times 10^3 T_9^{0.947}\exp(-2.245/T_9)$

$$N_A\langle\sigma v\rangle_{tt} = N_A\langle\sigma v\rangle_{gs}\times(1-0.990\exp(-1.207/T_9-0.0886T_9))$$
Rev. ratio $= 3.696\times 10^{10}T_9^{3/2}\exp(-149.04/T_9)$

^{19}**F(p,n)^{19}Ne**, $Q = -4.021$ MeV, (7%)

$$N_A\langle\sigma v\rangle_{gs} = 4.42\times 10^7\ \exp(-46.659/T_9)$$
$$\times(1+1.19T_9-0.150T_9^2+6.68\times 10^{-3}T_9^3)$$
$$N_A\langle\sigma v\rangle_{tt} = N_A\langle\sigma v\rangle_{gs}\times(1.536+2.848\times\exp(-0.0331/T_9-0.943T_9))$$
Rev. ratio $= 9.988\times 10^{-1}\exp(46.659/T_9)$

^{19}**F(p,α)^{16}O**, $Q = 8.114$ MeV, (18%)

$$N_A\langle\sigma v\rangle_{gs} = 2.62\times 10^{11}T_9^{-2/3}\exp(-18.116T_9^{1/3}-(T_9/0.185)^2)$$
$$\times(1+6.26\times 10^{-2}T_9+0.285T_9^2+4.94\times 10^{-3}T_9^3+11.5T_9^4$$
$$+7.40\times 10^4 T_9^5)+3.80\times 10^6 T_9^{-3/2}\exp(-3.752/T_9)$$

$$+3.27 \times 10^7 T_9^{-0.193} \exp(-6.587/T_9)$$

$$+7.30 \times 10^8 T_9^{-0.201} \exp(-16.249/T_9)$$

$$N_A \langle \sigma v \rangle_{tt} = N_A \langle \sigma v \rangle_{gs} \times (1 + 0.755 \exp(-1.755/T_9 - 0.174 T_9))$$

$$\text{Rev. ratio} = 6.538 \times 10^{-1} \exp(-94.154/T_9)$$

^{20}**Ne(p,γ)**^{21}**Na**, $Q = 2.431$ MeV, (12%)

$$N_A \langle \sigma v \rangle_{gs} = 2.35 \times 10^7 T_9^{-1.84} \exp(-19.451 T_9^{-1/3})$$

$$\times (1 + 10.80 T_9) + 18.0 T_9^{-3/2} \exp(-4.247/T_9)$$

$$+9.83 T_9^{-3/2} \exp(-4.619/T_9) + 6.76 \times 10^4 T_9^{-0.641} \exp(-11.922/T_9)$$

$$N_A \langle \sigma v \rangle_{tt} = N_A \langle \sigma v \rangle_{gs} \times (1 - 7.929 \exp(-20.108/T_9 - 0.327 T_9))$$

$$\text{Rev. ratio} = 4.637 \times 10^9 T_9^{3/2} \exp(-28.214/T_9)$$

^{20}**Ne(p,α)**^{17}**F**, $Q = -4.130$ MeV, (6%)

$$N_A \langle \sigma v \rangle_{gs} = 3.75 \times 10^{18} T_9^{-2/3} \exp(-43.180 T_9^{-1/3} - 47.920/T_9)$$

$$\times \exp(-1.40 \times 10^{-3} T_9^4 + 3.44 \times 10^{-2} T_9^3 - 0.278 T_9^2 + 0.354 T_9)$$

$$N_A \langle \sigma v \rangle_{tt} = N_A \langle \sigma v \rangle_{gs} \times (5.341 - 0.549 T_9 + 0.363 T_9^2$$

$$-0.0603 T_9^3 + 2.90 \times 10^{-3} T_9^4)$$

$$\text{Rev. ratio} = 5.372 \times 10^{-2} \exp(47.920/T_9)$$

^{20}**Ne(α, γ)**^{24}**Mg**, $Q = 9.316$ MeV, (12%)

For $T_9 \leqslant 1$: $\quad N_A \langle \sigma v \rangle_{gs} = 8.72 T_9^{-0.532} \exp(-8.995/T_9)$

For $T_9 > 1$: $\quad N_A \langle \sigma v \rangle_{gs} = 3.74 \times 10^2 T_9^{2.229} \exp(-12.681/T_9)$

$$N_A \langle \sigma v \rangle_{tt} = N_A \langle \sigma v \rangle_{gs} \times (1 - 7.787 \exp(-19.821/T_9 - 0.114 T_9))$$

$$\text{Rev. ratio} = 6.010 \times 10^{10} T_9^{3/2} \exp(-108.11/T_9)$$

^{21}**Ne(p,γ)**^{22}**Na**, $Q = 6.739$ MeV, (5%)

For $T_9 \leqslant 2$: $\quad N_A \langle \sigma v \rangle_{gs} = 4.68 \times 10^8 T_9^{-2/3} \exp(-19.465 T_9^{-1/3} - (T_9/0.2)^2)$

$$+8.18 \times 10^{-4} T_9^{-3/2} \exp(-1.085/T_9)$$

$$+6.11 T_9^{-3/2} \exp(-1.399/T_9)$$

$$+1.34 \times 10^4 T_9^{-3/2} \exp(-3.009/T_9)$$

$$+1.26 \times 10^5 T_9^{-0.128} \exp(-4.962/T_9)$$

For $T_9 > 2$: $\quad N_A \langle \sigma v \rangle_{gs} = 3.04 \times 10^4 T_9^{0.420} \exp(-2.650/T_9)$

$$N_A \langle \sigma v \rangle_{tt} = N_A \langle \sigma v \rangle_{gs} \times (1 - 0.708 \exp(-3.851/T_9 - 0.156T_9))$$

$$\text{Rev. ratio} = 1.064 \times 10^{10} T_9^{3/2} \exp(-78.205/T_9)$$

^{21}Ne(α,n)^{24}Mg, $Q = 2.555$ MeV, (7%)

$$\text{For } T_9 \leqslant 2.5 : \quad N_A \langle \sigma v \rangle_{gs} = 1.00 \times 10^{19} T_9^{-2/3} \exp(-46.880 T_9^{-1/3} - (T_9/1.5)^2)$$
$$\times (1 - 0.15T_9) + 7.00 \times 10^5 T_9^{-3/2} \exp(-16.9/T_9)$$
$$+ 3.7 \times 10^6 T_9^{1.61} \exp(-20.20/T_9)$$

$$\text{For } T_9 > 2.5 : \quad N_A \langle \sigma v \rangle_{gs} = 7.50 \times 10^6 T_9^{1.511} \exp(-21.764/T_9)$$

$$N_A \langle \sigma v \rangle_{tt} = N_A \langle \sigma v \rangle_{gs}$$

$$\text{Rev. ratio} = 12.94 \exp(-29.651/T_9)$$

^{22}Ne(p,γ)^{23}Na, $Q = 8.794$ MeV, (12%)

$$\text{For } T_9 \leqslant 2 : \quad N_A \langle \sigma v \rangle_{gs} = 1.11 \times 10^{-9} T_9^{-3/2} \exp(-0.422/T_9)$$
$$+ 6.83 \times 10^{-5} T_9^{-3/2} \exp(-0.810/T_9)$$
$$+ 9.76 \times 10^{-3} T_9^{-3/2} \exp(-1.187/T_9)$$
$$+ 1.06 \times 10^{-1} T_9^{-3/2} \exp(-1.775/T_9)$$
$$+ 8.51 \times 10^4 T_9^{0.725} \exp(-4.315/T_9)$$

$$\text{For } T_9 > 2 : \quad N_A \langle \sigma v \rangle_{gs} = 6.30 \times 10^4 T_9^{0.816} \exp(-3.910/T_9)$$

$$N_A \langle \sigma v \rangle_{tt} = N_A \langle \sigma v \rangle_{gs} \times (1 - 1.410 \exp(-14.651/T_9 - 0.020T_9))$$

$$\text{Rev. ratio} = 4.668 \times 10^9 T_9^{3/2} \exp(-102.05/T_9)$$

^{22}Ne(α,γ)^{26}Mg, $Q = 10.615$ MeV, (22%)

$$\text{For } T_9 \leqslant 1.25 : \quad N_A \langle \sigma v \rangle_{gs} = 3.55 \times 10^{-9} T_9^{-3/2} \exp(-3.927/T_9)$$
$$+ 7.07 \times 10^{-1} T_9^{-1.064} \exp(-7.759/T_9)$$
$$+ 1.27 \times 10^{-3} T_9^{-2.556} \exp(-6.555/T_9)$$

$$\text{For } T_9 > 1.25 : \quad N_A \langle \sigma v \rangle_{gs} = 1.76 T_9^{3.322} \exp(-12.412/T_9)$$

$$N_A \langle \sigma v \rangle_{tt} = N_A \langle \sigma v \rangle_{gs} \times (1 - 0.005 \exp(-5.109/T_9 + 0.373T_9))$$

$$\text{Rev. ratio} = 6.150 \times 10^{10} T_9^{3/2} \exp(-123.18/T_9)$$

^{22}**Ne(α,n)^{25}Mg**, $Q = -0.478$ MeV, (4%)

For $T_9 \leqslant 2$: $N_A \langle \sigma v \rangle_{gs} = 7.40 \exp(-7.79/T_9) + 1.30 \times 10^{-4} T_9^{0.83} \exp(-5.52/T_9)$

$$+ 9.41 \times 10^3 T_9^{2.78} \exp(-11.7/T_9)$$

$$+ 8.59 \times 10^6 T_9^{0.892} \exp(-24.4/T_9)$$

For $T_9 > 2$: $N_A \langle \sigma v \rangle_{gs} = 1.51 \times 10^5 T_9^{2.879} \exp(-16.717/T_9)$

$N_A \langle \sigma v \rangle_{tt} = N_A \langle \sigma v \rangle_{gs} \times (1 + 2.674 \exp(-15.025/T_9 - 0.321 T_9))$

Rev. ratio $= 5.440 \times 10^{-1} \exp(5.547/T_9)$

^{22}**Na(p,γ)^{23}Mg**, $Q = 7.579$ MeV, (11%)

For $T_9 \leqslant 1$: $N_A \langle \sigma v \rangle_{gs} = 1.12 \times 10^{-10} T_9^{-3/2} \exp(-0.483/T_9)$

$$+ 4.51 \times 10^{-7} T_9^{-3/2} \exp(-0.715/T_9)$$

$$+ 2.80 \times 10^2 T_9^{-3/2} \exp(-2.369/T_9)$$

$$+ 4.15 \times 10^3 T_9^{0.152} \exp(-2.775/T_9)$$

For $T_9 > 1$: $N_A \langle \sigma v \rangle_{gs} = 7.55 \times 10^3 T_9^{0.744} \exp(-3.299/T_9)$

$N_A \langle \sigma v \rangle_{tt} = N_A \langle \sigma v \rangle_{gs} \times (1 - 0.769 \exp(-7.854/T_9 + 0.016 T_9))$

Rev. ratio $= 3.268 \times 10^{10} T_9^{3/2} \exp(-87.955/T_9)$

^{23}**Na(p,γ)^{24}Mg**, $Q = 11.693$ MeV, (7%)

For $T_9 \leqslant 5$: $N_A \langle \sigma v \rangle_{gs} = 9.55 \times 10^7 T_9^{-2/3} \exp(-20.770 T_9^{-1/3} - (T_9/0.3)^2)$

$$\times (1 - 10.80 T_9 + 61.08 T_9^2)$$

$$+ 8.20 \times 10^{-2} T_9^{-3/2} \exp(-1.601/T_9)$$

$$+ 85.2 T_9^{-3/2} \exp(-2.808/T_9)$$

$$+ 1.70 \times 10^4 T_9^{-3/2} \exp(-3.458/T_9)$$

$$+ 5.94 \times 10^4 \exp(-5.734/T_9)$$

For $T_9 > 5$: $N_A \langle \sigma v \rangle_{gs} = 5.60 \times 10^3 T_9^{1.112} \exp(-2.337/T_9)$

$N_A \langle \sigma v \rangle_{tt} = N_A \langle \sigma v \rangle_{gs} \times (1 - 0.560 \exp(-5.119/T_9 - 0.050 T_9))$

Rev. ratio $= 7.490 \times 10^{10} T_9^{3/2} \exp(-135.69/T_9)$

^{23}**Na(p,n)**^{23}**Mg**, $Q = -4.839$ MeV, (3%)

$$N_A \langle \sigma v \rangle_{gs} = 2.26 \times 10^8 \exp(-56.156/T_9) \times (1 + 0.071T_9 - 2.26 \times 10^{-3}T_9^2)$$
$$N_A \langle \sigma v \rangle_{tt} = N_A \langle \sigma v \rangle_{gs} \times (1 + 1.651 \exp(-0.014/T_9 - 0.054T_9))$$
Rev. ratio $= 9.988 \times 10^{-1} \exp(56.156/T_9)$

^{23}**Na(p,α)**^{20}**Ne**, $Q = 2.377$ MeV, (12%)

For $T_9 \leqslant 5$: $N_A \langle \sigma v \rangle_{gs} = 8.39 \times 10^9 T_9^{-2/3} \exp(-20.770T_9^{-1/3} - (T_9/0.1)^2)$
$$\times (1 + 45.2T_9) + 3.09 \times 10^{-13}T_9^{-3/2} \exp(-0.420/T_9)$$
$$+ 8.12 \times 10^{-3}T_9^{-3/2} \exp(-1.601/T_9)$$
$$+ 4.37T_9^{-3/2} \exp(-1.934/T_9)$$
$$+ 7.50 \times 10^3 T_9^{-1.48} \exp(-3.150/T_9)$$
$$+ 1.05 \times 10^6 T_9^{1.456} \exp(-4.482/T_9)$$

For $T_9 > 5$: $N_A \langle \sigma v \rangle_{gs} = 3.96 \times 10^6 T_9^{1.291} \exp(-9.277/T_9)$

$$N_A \langle \sigma v \rangle_{tt} = N_A \langle \sigma v \rangle_{gs}$$

Rev. ratio $= 1.246 \exp(-27.578/T_9)$

^{23}**Na(α,n)**^{26}**Al^g**, $Q = -2.966$ MeV (6%)

$$N_A \langle \sigma v \rangle_{gs}^g = 2.74 \times 10^6 T_9^{-2/3} \exp(-34.440/T_9)$$
$$\times (1 + 2.86T_9 + 0.38T_9^2 - 3.00 \times 10^{-2}T_9^3)$$
$$+ 1.45 \times 10^{10} T_9^{-1.36} \exp(-74.00/T_9)$$
$$N_A \langle \sigma v \rangle_{tt}^g = N_A \langle \sigma v \rangle_{gs}^g \times (1 + 1.14 \exp(-0.0097/T_9 - 0.246T_9))$$
Rev. ratio $= 1.196 \exp(34.414/T_9)$
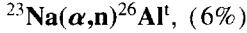
^{23}**Na(α,n)**^{26}**Al^m**, $Q = -3.194$ MeV (5%)
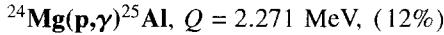
$$N_A \langle \sigma v \rangle_{gs}^m = 5.55 \times 10^2 T_9^{-2/3} \exp(-37.090/T_9)$$
$$\times (1 + 1.80 \times 10^3 T_9 + 5.40 \times 10^2 T_9^2 - 1.50 \times 10^2 T_9^3)$$
$$+ 1.38 \times 10^6 T_9^{1.5} \exp(-48.00/T_9)$$
$$N_A \langle \sigma v \rangle_{tt}^m = N_A \langle \sigma v \rangle_{gs}^m \times (1 + 1.14 \exp(-0.0097/T_9 - 0.246T_9))$$
Rev. ratio $= 13.16 \exp(37.062/T_9)$

^{23}**Na(α,n)^{26}Al^{t}**, (6%)

$$N_A\langle\sigma v\rangle_{gs}^{t} = 1.30 \times 10^4 T_9^{-2/3}\exp(-34.440/T_9)(1 - 20.0T_9^2 + 7.80T_9^3)$$
$$+1.17 \times 10^7 T_9^{0.35}\exp(-34.350/T_9)$$
$$N_A\langle\sigma v\rangle_{tt}^{t} = N_A\langle\sigma v\rangle_{gs}^{t} \times (1 + 1.14\exp(-0.0097/T_9 - 0.246T_9))$$

^{24}**Mg(p,γ)^{25}Al**, $Q = 2.271$ MeV, (12%)
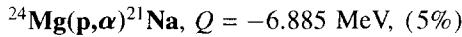
For $T_9 \leqslant 7$: $\quad N_A\langle\sigma v\rangle_{gs} = 5.97 \times 10^8 T_9^{-2/3}\exp(-22.023T_9^{-1/3} - (T_9/0.1)^2)$
$$+1.59 \times 10^3 T_9^{-3/2}\exp(-2.483/T_9)$$
$$+3.33 \times 10^3 T_9^{0.122}\exp(-3.981/T_9)$$
For $T_9 > 7$: $\quad N_A\langle\sigma v\rangle_{gs} = 3.81 \times 10^1 T_9^{2.113}\exp(0.860/T_9)$
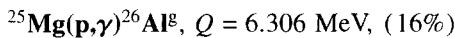
$$N_A\langle\sigma v\rangle_{tt}^{t} = N_A\langle\sigma v\rangle_{gs}^{t}$$
Rev. ratio $= 3.129 \times 10^9 T_9^{3/2}\exp(-26.357/T_9)$

^{24}**Mg(p,α)^{21}Na**, $Q = -6.885$ MeV, (5%)

$$N_A\langle\sigma v\rangle_{gs} = 3.72 \times 10^{16} T_9^{-2/3}\exp(-44.480T_9^{-1/3} - 79.897/T_9) \times$$
$$\times \exp(1.88T_9 - 0.516T_9^2 + 5.17 \times 10^{-2}T_9^3 - 1.86 \times 10^{-3}T_9^4)$$
$$N_A\langle\sigma v\rangle_{tt} = N_A\langle\sigma v\rangle_{gs} \times (4.555 + 2.790T_9 - 0.127T_9^2)$$
Rev. ratio $= 7.716 \times 10^{-2}\exp(79.897/T_9)$

^{25}**Mg(p,γ)^{26}Al^{g}**, $Q = 6.306$ MeV, (16%)

For $T_9 \leqslant 2$: $\quad N_A\langle\sigma v\rangle_{gs} = 3.07 \times 10^{-16} T_9^{-3/2}\exp(-0.435/T_9)$
$$+3.70 \times 10^{-8} T_9^{-3/2}\exp(-0.673/T_9)$$
$$+1.60 \times 10^{-5} T_9^{-3/2}\exp(-1.074/T_9)$$
$$+1.27 \times 10^4 T_9^{0.647}\exp(-3.055/T_9)$$
For $T_9 > 2$: $\quad N_A\langle\sigma v\rangle_{gs} = 8.75 \times 10^3 T_9\exp(-2.997/T_9)$

$$N_A\langle\sigma v\rangle_{tt}^{g} = N_A\langle\sigma v\rangle_{gs}^{g} \times (1 - 0.352\exp(-7.221/T_9 + 0.068T_9))$$
Rev. ratio $= 1.026 \times 10^{11} T_9^{3/2}\exp(-73.183/T_9)$

^{25}**Mg(p,γ)^{26}Al^{m}**, $Q = 6.078$ MeV, (28%)

$$\text{For } T_9 \leqslant 2: \quad N_A \langle \sigma v \rangle_{gs} = 8.15 \times 10^{-17} T_9^{-3/2} \exp(-0.435/T_9)$$
$$+ 8.68 \times 10^{-9} T_9^{-3/2} \exp(-0.673/T_9)$$
$$+ 2.82 \times 10^{-6} T_9^{-3/2} \exp(-1.074/T_9)$$
$$+ 3.48 \times 10^3 T_9^{1.362} \exp(-2.906/T_9)$$
$$\text{For } T_9 > 2: \quad N_A \langle \sigma v \rangle_{gs} = 3.91 \times 10^3 T_9^{1.262} \exp(-3.229/T_9)$$

$$N_A \langle \sigma v \rangle_{tt}^{m} = N_A \langle \sigma v \rangle_{gs}^{m} \times (1 - 0.352 \exp(-7.221/T_9 + 0.068T_9))$$
$$\text{Rev. ratio} = 1.129 \times 10^{11} T_9^{3/2} \exp(-70.535/T_9)$$

^{25}**Mg(p,γ)^{26}Al^{t}**, (16%)

$$N_A \langle \sigma v \rangle_{gs}^{t} = N_A \langle \sigma v \rangle_{gs}^{g} + N_A \langle \sigma v \rangle_{gs}^{m}$$
$$N_A \langle \sigma v \rangle_{tt}^{t} = N_A \langle \sigma v \rangle_{gs}^{t} \times (1 - 0.352 \exp(-7.221/T_9 + 0.068T_9))$$

^{25}**Mg(α,n)^{28}Si**, $Q = 2.654$ MeV, (9%)

$$\text{For } T_9 \leqslant 2: \quad N_A \langle \sigma v \rangle_{gs} = 3.84 \times 10^{19} T_9^{-2/3} \exp(-53.415 T_9^{-1/3})$$
$$\times (1 + 6.993 \times 10^{-1} T_9 - 4.538 \times 10^{-1} T_9^2$$
$$+ 8.853 \times 10^{-2} T_9^3 - 7.387 \times 10^{-3} T_9^4$$
$$+ 2.276 \times 10^{-4} T_9^5)$$
$$\text{For } T_9 > 2: \quad N_A \langle \sigma v \rangle_{gs} = 5.37 \times 10^4 T_9^{2.852} \exp(-21.052/T_9)$$

$$N_A \langle \sigma v \rangle_{tt} = N_A \langle \sigma v \rangle_{gs} \times (1 - 0.397 \exp(-12.153/T_9 - 0.093T_9))$$
$$\text{Rev. ratio} = 20.01 \exp(-30.794/T_9)$$

^{26}**Mg(p,γ)^{27}Al**, $Q = 8.271$ MeV, (21%)

$$\text{For } T_9 \leqslant 3.5: \quad N_A \langle \sigma v \rangle_{gs} = 8.54 \times 10^{-12} T_9^{-3/2} \exp(-0.605/T_9)$$
$$+ 1.93 \times 10^{-6} T_9^{-3/2} \exp(-1.044/T_9)$$
$$+ 9.67 \times 10^{-3} T_9^{-3/2} \exp(-1.726/T_9)$$
$$+ 9.50 \times 10^4 T_9^{-3/2} \exp(-3.781/T_9)$$
$$+ 10.2 T_9^{-1.565} \exp(-2.521/T_9)$$
$$+ 7.07 \times 10^4 T_9^{0.215} \exp(-3.947/T_9)$$
$$\text{For } T_9 > 3.5: \quad N_A \langle \sigma v \rangle_{gs} = 3.95 \times 10^4 T_9^{1.068} \exp(-4.990/T_9)$$

$$N_A \langle \sigma v \rangle_{tt} = N_A \langle \sigma v \rangle_{gs} \times (1 - 1.259 \exp(-20.076/T_9 + 0.069 T_9))$$

$$\text{Rev. ratio} = 3.144 \times 10^9 T_9^{3/2} \exp(-95.983/T_9)$$

^{26}**Mg(α,n)^{29}Si**, $Q = 0.034$ MeV, (7%)

For $T_9 \leqslant 2$: $N_A \langle \sigma v \rangle_{gs} = 8.09 \times 10^{19} T_9^{-2/3} \exp(-53.505 T_9^{-1/3} - (T_9/7.3)^2)$

$$\times (1 - 0.17 T_9 + 8.9 \times 10^{-3} T_9^2)$$

$$+ 2.80 \times 10^4 T_9^{-0.43} \exp(-18.73/T_9)$$

For $T_9 > 2$: $N_A \langle \sigma v \rangle_{gs} = 4.92 \times 10^4 T_9^{3.117} \exp(-20.864/T_9)$

$$N_A \langle \sigma v \rangle_{tt} = N_A \langle \sigma v \rangle_{gs}$$

$$\text{Rev. ratio} = 1.678 \exp(-0.396/T_9)$$

^{26}**Al^g(p,γ)^{27}Si**, $Q = 7.463$ MeV, (10%)

For $T_9 \leqslant 0.9$: $N_A \langle \sigma v \rangle_{gs} = 3.54 \times 10^{-9} T_9^{-3/2} \exp(-0.789/T_9)$

$$+ 8.54 \times 10^{-7} T_9^{-3/2} \exp(-1.079/T_9)$$

$$+ 10.3 T_9^{-3/2} \exp(-2.182/T_9)$$

$$+ 6.12 \times 10^2 T_9^{-3/2} \exp(-3.203/T_9)$$

$$+ 1.05 \times 10^4 T_9^{-3/2} \exp(-4.213/T_9)$$

For $T_9 > 0.9$: $N_A \langle \sigma v \rangle_{gs} = 1.63 \times 10^4 T_9^{0.348} \exp(-4.285/T_9)$

$$N_A \langle \sigma v \rangle_{tt} = N_A \langle \sigma v \rangle_{gs} \times (1 + 2.17 \exp(-4.616/T_9 - 0.076 T_9))$$

$$\text{Rev. ratio} = 3.459 \times 10^{10} T_9^{3/2} \exp(-86.608/T_9)$$

^{26}**Al^{ms}(p,γ)^{27}Si**, $Q = 7.691$ MeV, (10%)

For $T_9 \leqslant 0.4$: $N_A \langle \sigma v \rangle_{ms} = N_A \langle \sigma v \rangle_{gs} \times (1 + 7.80 \exp(-0.854/T_9 - 0.019 T_9))$

$$N_A \langle \sigma v \rangle_{tt} = N_A \langle \sigma v \rangle_{gs} \times (1 + 2.17 \exp(-4.616/T_9 - 0.076 T_9))$$

$$\text{Rev. ratio} = 3.459 \times 10^{10} T_9^{3/2} \exp(-89.254/T_9)$$

^{27}**Al(p,γ)^{28}Si**, $Q = 11.585$ MeV, (10%)

For $T_9 \leqslant 6$: $N_A \langle \sigma v \rangle_{gs} = 2.51 \times 10^{-11} T_9^{-3/2} \exp(-0.839/T_9)$

$$+ 48.2 T_9^{-0.2} \exp(-2.223/T_9)$$

$$+ 1.76 \times 10^3 T_9^{1.12} \exp(-3.196/T_9)$$

$$+3.25 \times 10^4 T_9^{0.251} \exp(-5.805/T_9)$$

For $T_9 > 6$: $\quad N_A \langle \sigma v \rangle_{gs} = 1.62 \times 10^5 T_9^{0.549} \exp(-17.222/T_9)$

$$N_A \langle \sigma v \rangle_{tt} = N_A \langle \sigma v \rangle_{gs} \times (1 - 0.669 \exp(-10.426/T_9 + 0.008 T_9))$$

Rev. ratio $= 1.134 \times 10^{11} T_9^{3/2} \exp(-134.440/T_9)$

^{27}Al(p,α)^{24}Mg, $Q = 1.601$ MeV, (11%)

For $T_9 \leqslant 6$: $\quad N_A \langle \sigma v \rangle_{gs} = 4.76 \times 10^{10} T_9^{-2/3} \exp(-23.265 T_9^{-1/3} - (T_9/0.15)^2)$

$$\times (1 - 22.3 T_9 + 126.7 T_9^2)$$

$$+9.65 \times 10^{-11} T_9^{-3/2} \exp(-0.834/T_9)$$

$$+2.09 \times 10^{-3} T_9^{-3/2} \exp(-2.269/T_9)$$

$$+1.17 \times 10^{-2} T_9^{-3/2} \exp(-3.273/T_9)$$

$$+2.84 \times 10^4 \exp(-5.623/T_9)/T_9$$

$$+1.38 \times 10^6 T_9 \exp(-10.01/T_9)$$

For $T_9 > 6$: $\quad N_A \langle \sigma v \rangle_{gs} = 6.02 \times 10^5 T_9^{1.862} \exp(-14.352/T_9)$

$$N_A \langle \sigma v \rangle_{tt} = N_A \langle \sigma v \rangle_{gs} \times (1 + 3.471 \exp(-11.091/T_9 - 0.129 T_9))$$

Rev. ratio $= 1.809 \exp(-18.574/T_9)$

^{27}Al(α,n)^{30}P, $Q = -2.643$ MeV, (3%)

$$N_A \langle \sigma v \rangle_{gs} = 8.15 \times 10^4 \exp(-30.667/T_9)$$

$$\times (1 - 1.351 T_9 + 1.086 T_9^2 + 0.354 T_9^3 + 0.014 T_9^4 - 2.13 \times 10^{-3} T_9^5)$$

$$N_A \langle \sigma v \rangle_{tt} = N_A \langle \sigma v \rangle_{gs} \times (1 + 0.227 \exp(-3.588/T_9 + 0.0172 T_9))$$

Rev. ratio $= 6.751 \exp(30.677/T_9)$

^{28}Si(p,γ)^{29}P, $Q = 2.748$ MeV, (1%)

For $T_9 \leqslant 3$: $\quad N_A \langle \sigma v \rangle_{gs} = 8.71 \times 10^8 T_9^{-2/3} \exp(-24.453 T_9^{-1/3} - (T_9/1.1)^2)$

$$\times (1 + 0.301 T_9 + 0.069 T_9^2)$$

$$+3.37 \times 10^2 T_9^{-3/2} \exp(-4.155/T_9)$$

$$+1.14 \times 10^3 T_9^{1.654} \exp(-11.055/T_9)$$

For $T_9 > 3$: $\quad N_A \langle \sigma v \rangle_{gs} = 32.4 T_9^{2.052} \exp(-1.525/T_9)$

$$N_A \langle \sigma v \rangle_{tt} = N_A \langle \sigma v \rangle_{gs} \times (1 - 23.813 \exp(-22.872/T_9 - 0.353 T_9))$$

Rev. ratio $= 9.468 \times 10^9 T_9^{3/2} \exp(-31.889/T_9)$

Table 4. Analytical approximations of the partition functions

$$G(T_9) = 1 + a_1 T_9^{a_2} \exp(a_3/T_9 + a_4 T_9 + a_5 T_9^{2/3})$$
$G(T_9) = 1$ for H and He isotopes, as well as for ^{8}B and ^{9}B

Isotope	a_1	a_2	a_3	a_4	a_5
^{6}Li	3.47×10^0	-3.43×10^{-1}	-2.59×10^1	5.58×10^{-2}	—
^{7}Li	5.20×10^{-1}	-5.75×10^{-2}	-5.59×10^0	1.27×10^{-2}	—
^{7}Be	5.16×10^{-1}	-5.18×10^{-2}	-5.02×10^0	1.20×10^{-2}	—
^{8}Be	4.52×10^0	5.29×10^{-2}	-3.51×10^1	-3.79×10^{-3}	—
^{9}Be	1.73×10^{-2}	2.25×10^0	-1.54×10^1	-1.08×10^{-1}	—
^{10}B	5.04×10^{-1}	-3.19×10^{-1}	-8.59×10^0	9.40×10^{-2}	—
^{11}B	2.16×10^0	-1.19×10^0	-2.67×10^1	1.74×10^{-1}	—
^{11}C	2.89×10^0	-1.38×10^0	-2.57×10^1	1.95×10^{-1}	—
^{12}C	4.55×10^0	1.64×10^{-2}	-5.13×10^1	3.91×10^{-3}	—
^{13}C	4.44×10^{-1}	1.06×10^0	-3.57×10^1	-4.57×10^{-2}	—
^{13}N	4.68×10^{-2}	1.69×10^0	-2.33×10^1	-3.84×10^{-2}	—
^{14}N	1.23×10^0	-1.48×10^0	-2.85×10^1	2.97×10^{-1}	—
^{15}N	1.61×10^0	1.60×10^{-1}	-5.94×10^1	7.03×10^{-2}	—
^{14}O	3.16×10^{-1}	1.38×10^0	-5.75×10^1	-4.25×10^{-2}	—
^{15}O	2.95×10^0	-3.40×10^{-2}	-6.04×10^1	7.82×10^{-2}	—
^{16}O	2.38×10^0	5.15×10^{-1}	-6.87×10^1	1.53×10^{-2}	—
^{17}O	6.47×10^{-1}	-7.03×10^{-1}	-1.10×10^1	1.29×10^{-1}	—
^{18}O	8.11×10^0	-6.71×10^{-1}	-2.37×10^1	1.59×10^{-1}	—
^{17}F	4.16×10^{-1}	-3.07×10^{-1}	-6.03×10^0	6.64×10^{-2}	—
^{18}F	4.36×10^0	6.46×10^{-2}	-1.14×10^1	4.81×10^{-2}	—
^{19}F	9.05×10^0	1.66×10^0	-1.05×10^0	6.81×10^{-1}	-2.39×10^0
^{19}Ne	3.73×10^0	-1.33×10^{-1}	-2.87×10^0	7.61×10^{-2}	—
^{20}Ne	1.02×10^1	-6.02×10^{-1}	-1.99×10^1	8.95×10^{-2}	—
^{21}Ne	2.98×10^0	4.86×10^{-1}	-3.97×10^0	4.16×10^{-1}	-1.20×10^0
^{22}Ne	1.00×10^1	-6.92×10^{-1}	-1.57×10^1	1.22×10^{-1}	—
^{21}Na	1.58×10^0	-2.51×10^{-1}	-3.99×10^0	8.92×10^{-2}	—
^{22}Na	3.24×10^{-1}	7.64×10^{-1}	-6.32×10^0	3.87×10^{-2}	—
^{23}Na	1.80×10^0	-4.17×10^{-1}	-5.40×10^0	1.20×10^{-1}	-1.90×10^0
^{23}Mg	4.30×10^0	8.89×10^{-1}	-5.00×10^0	6.16×10^{-1}	-1.90×10^0
^{24}Mg	8.23×10^0	-4.74×10^{-1}	-1.65×10^1	7.87×10^{-2}	—
^{25}Mg	1.51×10^{-1}	6.37×10^{-1}	-6.07×10^0	9.59×10^{-2}	—
^{26}Mg	1.15×10^1	-9.90×10^{-1}	-2.22×10^1	2.17×10^{-1}	—
^{25}Al	5.26×10^{-2}	-1.91×10^0	-5.78×10^0	-5.96×10^{-1}	2.99×10^0
^{26}Al	2.26×10^0	3.98×10^0	-1.58×10^0	1.39×10^0	-5.09×10^0
^{27}Al	9.52×10^{-1}	-4.51×10^{-1}	-1.08×10^1	1.69×10^{-1}	—
^{27}Si	9.24×10^{-1}	-4.28×10^{-1}	-1.01×10^1	1.63×10^{-1}	—
^{28}Si	9.87×10^0	-5.50×10^{-1}	-2.16×10^1	7.73×10^{-2}	—
^{29}Si	1.31×10^0	1.27×10^{-3}	-1.44×10^1	1.32×10^{-1}	—
^{30}Si	1.87×10^1	-1.28×10^0	-2.78×10^1	2.38×10^{-1}	—
^{29}P	1.46×10^0	2.90×10^{-2}	-1.59×10^1	1.33×10^{-1}	—
^{30}P	1.41×10^0	-5.33×10^{-1}	-8.41×10^0	2.36×10^{-1}	—
^{31}P	4.05×10^0	-1.03×10^0	-1.57×10^1	2.69×10^{-1}	—

References

| AB63 | M.A. Abuzeid, F.M. Aly, Y.P. Antoufiev, A.T. Baranik, T.M. Nower and P.V. Sorokin, Nucl. Phys 45 (1963) 123. al27pa.

| AD69 | A. Adams, M.H. Shapiro, W.M. Denny, E.G. Adelberger and C.A. Barnes, Nucl. Phys. A 131 (1969) 430. o18ag.

| AD98 | E.G. Adelberger, S.M. Austin, J.N. Bahcall, A.B. Balantekin, G. Bogaert, L.S. Brown, L. Buchmann, F.E. Cecil, A.E. Champagne, L. de Braeckeleer, C.A. Duba, S.R. Elliot, S.J. Freedman, M. Gai, G. Goldring, C.R. Gould, A. Gruzinov, W.C. Haxton, K.M. Heeger, E. Henley, C.W. Johnson, M. Kamionkowski, R.W. Kavanagh, S.E. Koonin, K. Kubodera, K. Langanke, T. Motobayashi, V. Pandharipande, P. Parker, R.G.H. Robertson, C. Rolfs, R.F. Sawyer, N. Shaviv, T.D. Shoppa, K.A. Snover, E. Swanson, R.E. Tribbl, S. Turck-Chièze and J.F. Wilkerson, Rev. Mod. Phys. 70 (1998) 1265. intro, ppnu, he3he3, he3he4, be7pg, c13pg, n14pg.

| AG89 | P. Aguer, G. Bogaert, M. Kious, V. Landré, A. Lefebvre, J.P. Thibaud, F. Beck and A. Huck, Proc. Int. Symp. on Heavy-Ion Physics and Nuclear Astrophysics, ed. S. Kubono, M. Ishihara and T. Nomura (World Scientific, Singapore, 1989), p. 107. n13pg.

| AI70 | J.H. Aitken, R.E. Azuma, A.E. Litherland, A.M. Charlesworth, D.W.O. Rogers and J.J. Simpson, Can. J. Phys. 48 (1970) 1617. n15ag.

| AJ87 | F. Ajzenberg-Selove, Nucl. Phys. A 475 (1987) 1. f19pg, f19pa.

| AJ88 | F. Ajzenberg-Selove, Nucl. Phys. A 490 (1988) 1. aang.

| AJ90 | F. Ajzenberg-Selove, Nucl. Phys. A 506 (1990) 1. aaag.

| AL64 | R.G. Allas, S.S. Hanna, L. Meyer-Schützmeister and R.E. Segel, Nucl. Phys. 58 (1964) 122. b11pg.

| AL72a | T.K. Alexander, O. Häuser, A.B. McDonald and A.J. Ferguson, Nucl. Phys. A 179 (1972) 477. o16ag.

| AL72b | T.K. Alexander, B.Y. Underwood, N. Anayas-Weiss, N.A. Jelly, J. Szücs, S.P. Dolan, M.R. Wormald and K.W. Allen, Nucl. Phys. A 197 (1972) 1. o16ag.

| AL74 | M.M. Aléonard, C. Boursiquot, P. Hubert and P. Mennrath, Phys. Lett B 49 (1974) 40. al27pg.

| AL75a | R. Almanza, G. Murillo, S.E. Darden and S. Sen, Nucl. Phys. A 248 (1975) 214. o18pa.

| AL75b | M.M. Aléonard, P. Hubert, L. Sarger and P. Mennrath, J. Phys. (Paris) 36 (1975) 913. si28pg.

| AL82 | P.F.A. Alkemade, C. Alderliesten, P. De Wit and C. van der Leun, Nucl. Instr. Meth. 197 (1982) 383. mg25pg.

| AL84 | T.K. Alexander, G.C. Ball, W.N. Lennard, H. Geissel and H.-B. Mak, Nucl. Phys. A 427 (1984) 526. he3ag.

| AN61 | S.L. Andersen, A. Haug, T. Holtebeck, O. Lonsjo and R. Nordhagen, Phys. Norveg. 1 (1961) 7. al27pg, al27pa.

| AN63 | Y.P. Antoufiev, L.M. El Nadi, D.A.E. Darwish, O.E. Badawy and P.V. Sorokin, Nucl. Phys. 46 (1963) 1. al27pg.

| AN64 | Y.P. Antoufiev, D.A.E. Darwish, O.E. Badawy, L.M. El-Nadi and P.V. Sorokin, Nucl. Phys. 56 (1964) 401. al27pg.

| AN70 | A. Anttila, M. Bister and E. Arminen, Z. Phys. 234 (1970) 455. ne21pg.

| AN74 | B.D. Anderson, M.R. Dwarakanath, J.S. Schweitzer and A.V. Nero, Nucl. Phys. A 233 (1974) 286. b11pg, b11pa.

| AN77 | A. Anttila, J. Keinonen and M. Bister, J. Phys. G 3 (1977) 1241. ne20pg.

| AN80 | M.R. Anderson, S.R. Kennett, L.W. Mitchell and D.G. Sargood, Nucl. Phys. A 349 (1980) 154. mg25pg.

| AN82 | M.R. Anderson, L.W. Mitchell, M.E. Sevior, S.R. Kennett and D.G. Sargood, Nucl. Phys. A 373 (1982) 326. mg25pg.

| AN83 | M.R. Anderson, L.W. Mitchell, M.E. Sevior and D.G. Sargood, Nucl. Phys. A 405 (1983) 170. mg25an, mg26an.

| AN93 | C. Angulo, S. Engstler, G. Raimann, C. Rolfs, W.H. Schulte and E. Somorjai, Z. Phys. A 345 (1993) 231. b10pa, b11pa.

| AR52 | H.V. Argo, R.F. Taschek, H.M. Agnew, A. Hemmendinger and W.T. Leland, Phys. Rev. 87 (1952) 612. tdn.

| AR54 | W.R. Arnold, J.A. Phillips, G.A. Sawyer, E.J. Stovall Jr and J.L. Tuck, Phys. Rev. 93 (1954) 483. tdn.

| AR72 | M. Arnould, Astron. Astrophys. 19 (1972) 92. intro.

| AR96 | C. Arpesella, E. Bellotti, C. Broggini, P. Corvisiero, G. Fiorentini, A. Fubini, G. Gervino, U. Greife, C. Gustavino, M. Junker, J. Lambert, P. Prati, W.S. Rodney, C. Rolfs, H.P. Trautvetter, D. Zahnow and S. Zavatarelli, Phys. Lett. B 389 (1996) 452. he3he3.

| AS65 | L. Ask, Ark. Phys. 29 (1965) 195. f19pa.

| AS87 | H.J. Assenbaum, K. Langanke and C. Rolfs, Z. Phys. A 327 (1987) 461. intro.

| AU75 | W. Auwärter and V. Meyer, Nucl. Phys. A 242 (1975) 129. be9pg.

| AU97 | G. Audi, O. Bersillon, J. Blachot and A.H. Wapstra, Nucl. Phys. A 624 (1997) 1. intro.

| AW65 | T. Awaya, J. Phys. Soc. Japan 20 (1965) 669. al27pa.

| AZ94 | R.E. Azuma, L. Buchmann, F.C. Barker, C.A. Barnes, J.M. D'Auria, M. Dombsky, U. Giesen, K.P. Jackson, J.D. King, R.G. Korteling, P. McNeely, J. Powell, G. Roy, J. Vincent, T.R. Wang, S.S.M. Wong and P.R. Wrean, Phys. Rev. C 50 (1994) 1194. c12ag.

| BA50 | C.L. Bailey and W.R. Stratton, Phys. Rev. 77 (1950) 194. c12pg.

| BA55a | G.G. Bach and D.J. Livesey, Philos. Mag. 46 (1955) 824. b10pa.

| BA55b | S. Bashkin, R.R. Carlson and E.B. Nelson, Phys. Rev. 99 (1955) 107. n14pg.

| BA57 | S.J. Bame Jr and J.E. Perry Jr, Phys. Rev. 107 (1957) 1616. tdn.

| BA60 | W.C. Barber, F. Berthold, G. Fricke and F.E. Gudden, Phys. Rev. 120 (1960) 2081. dag.

| BA62 | J.K. Bair and H.B. Willard, Phys. Rev. 128 (1962) 299. o18an.

| BA64 | J.K. Bair, C.M. Jones and H.B. Willard, Nucl. Phys. 53 (1964) 209. be9pn, b11pn.

| BA67 | A.D. Bacher and T.A. Tombrello, *in* Nuclear research with Low-Energy Accelerators, ed. J.B. Marion, D.M. Van Patter (Academic Press, New York, 1967) p. 195. he3he3.

| BA68a | F.C. Barker and B.M. Fitzpatrick, Aust. J. Phys. 21 (1968) 415. aang.

| BA68b | A.R. Barnett, Nucl. Phys. A 120 (1968) 342. n15pn.

| BA69a | N.N. Bahcall and W.A. Fowler, Astrophys. J. 157 (1969) 659. intro.

| BA69b | N.N. Bahcall and W.A. Fowler, Astrophys. J. 157 (1969) 645. intro.

| BA69c | J.N. Bahcall and R.M. May, Astrophys. J. 155 (1969) 501. ppnu.

| BA73a | J.K. Bair and F.X. Haas, Phys. Rev. C 7 (1973) 1356. c13an, o17an, o18an.

| BA73b | D.G. Barnes, J.M. Calvert and T. Joy, J. Phys. (London) A 6 (1973) 1011. si28pg.

| BA79a | C. Bargholtz, Astrophys. J. 233 (1979) L161. ppnu.

| BA79b | I.Ya. Barit, Yu.G. Balashko, L.S. Dulkova and V.P. Zavarzina, Sov. J. Nucl. Phys. 29 (1979) 585. dag.

| BA80 | F.C. Barker, Aust. J. Phys. 33 (1980) 159. li6pg.

| BA81 | J.K. Bair, P.D. Miller and B.W. Wieland, Int. J. Appl. Radiat. Isotop. 32 (1981) 389. b11pn.

| BA83 | F.C. Barker, Can. J. Phys. 61 (1983) 1371. aang.

| BA85 | D. Baye and P. Descouvemont, Ann. Phys. (NY) 165 (1985) 115. intro.

| BA87 | C.A. Barnes, K.H. Chang, T.R. Donoghue, C. Rolfs and J. Kammeraad, Phys. Lett. 197B (1987) 315. ddg.

| BA88a | J.N. Bahcall and R.K. Ulrich, Rev. Mod. Phys. 60 (1988) 297. ppnu.

| BA88b | D. Baye and P. Descouvemont, Phys. Rev. C 38 (1988) 2463. o16ag.

| BA91 | F.C. Barker and T. Kajino, Aust. J. Phys. 44 (1991) 369. c12ag.

| BA92 | J.N. Bahcall and M.H. Pinsonneault, Rev. Mod. Phys. 64 (1992) 885. ppnu.

| BE51 | W.E. Bennett, P.A. Roys and B.J. Toppel, Phys. Rev. 82 (1951) 20. li7ag.

| BE63 | I. Berkes, I. Dezsi, I. Fodor and L. Keszthelyi, Nucl. Phys. 43 (1963) 103. f19pg.

| BE64 | B.L. Berman, L.J. Koester Jr and J.H. Smith, Phys. Rev. 133 (1964) B117. dpg.

| BE67 | B.L. Berman, R.L. Van Hemert and C.D. Bowman, Phys. Rev. 163 (1967) 958. aang.

| BE68 | J. Benn, E.B. Dally, H.H. Müller, R.E. Pixley, H.H. Staub and H. Winkler, Nucl. Phys. A 106 (1968) 296. aaag.

| BE70 | F.A. Beck, T. Byrski, P. Engelstein, A. Knipper and S. Gorodetzky, Proc. Int. Conf. on Angular correlations in nuclear disintegration, ed. H. van Krugten, B. van Nooijen, Delft (The Netherlands) 1970, p. 226. si28pg.

| BE75 | R.R. Betts, H.T. Fortune and R. Middleton, Phys. Rev. C 11 (1975) 19. f19pa.

| BE77 | H.L. Berg, W. Hietzke, C. Rolfs and H. Winkler, Nucl. Phys. A 276 (1977) 168. ne21pg.

| BE82 | H.W. Becker, W.E. Kieser, C. Rolfs, H.P. Trautvetter and M. Wiescher, Z. Phys. A 305 (1982) 319. n14ag, o18pg, f19pa.

| BE87 | H.W. Becker, C. Rolfs and H.P. Trautvetter, Z. Phys. A 327 (1987) 341. b11pa.

| BE92a | M. Berheide, C. Rolfs, U. Schröder and H.P. Trauttvetter, Z. Phys. A 343 (1992) 483. o17pg, o17pa.

[BE92b] H.W. Becker, H. Ebbing, W.H. Schulte, S. Wüstenbecker, M. Berheide, M. Buschmann, C. Rolfs, G.E. Mitchell and J.S. Schweitzer, Z. Phys. A 343 (1992) 361. ne21pg.

[BE95] H.W. Becker, M. Bahr, M. Berheide, L. Borucki, M. Buschmann, C. Rolfs, G. Roters, S. Schmidt, W.H. Schulte, G.E. Mitchell and J.S. Schweitzer, Z. Phys. A 351 (1995) 453. o18pa.

[BI80] G.T. Bida, T.J. Ruth and A.P. Wolf, Radiochimical Acta 27 (1980) 181. n14pa.

[BI81] W. Biesiot, Ph.B. Smith, Phys. Rev. C 24 (1981) 2443. c13pg.

[BL52] J.M. Blatt and V.F. Weisskopf, Theoretical Nuclear Physics (Wiley, New York, 1952). intro.

[BL63] H.R. Blieden, G.M. Temmer and K.L. Warsh, Nucl. Phys. 49 (1963) 209. be9pa.

[BL65] R.J. Blin Stoyle and S. Papageorgiou, Nucl. Phys. 64 (1965) 1. ppnu.

[BL69] R. Block, T. Knellwolf and R.E. Pixley, Nucl. Phys. A 123 (1969) 129. ne20pg.

[BL95] J.C. Blackmon, A.E. Champagne, M.A. Hofstee, M.S. Smith, R.G. Downing and G.P. Lamaze, Phys. Rev. Lett. 74 (1995) 2642. o17pg, o17pa.

[BO48] T.W. Bonner and J.E. Evans, Phys. Rev. 73 (1948) 666. f19pa.

[BO64] R.O. Bondelid and J.W. Butler, Nucl. Phys. 53 (1964) 618. be9pg.

[BO92] H.-S. Bosch and G.M. Hale, Nucl. Fusion 32 (1992) 611. ddn, ddp.

[BR47] K.J. Broström, T. Huus and R. Tangen, Phys. Rev. 71 (1947) 661. al27pg.

[BR51a] J.E. Brolley, J.L. Fowler and E.J. Stovall Jr, Phys. Rev. 82 (1951) 502. tdn.

[BR51b] A.B. Brown, C.W. Snyder, W.A. Fowler and C.C. Lauritsen, Phys. Rev. 82 (1951) 159. b10pa.

[BR59] G. Breuer, Z. Phys. 154 (1959) 339. f19pa.

[BR62] R.E. Brown, Phys. Rev. 125 (1962) 347. o17pa.

[BR71] J.E. Brolley, Solar Physics 20 (1971) 249. ppnu.

[BR87a] R.E. Brown, N. Jarmie and G.M. Hale, Phys. Rev. C 35 (1987) 1999. tdn.

[BR87b] R.E. Brown, F.D. Correll, P.M. Hegland, J.A. Koepke and C.H. Poppe, Phys. Rev. C 35 (1987) 383. he3he3.

[BR90] R.E. Brown and N. Jarmie, Phys. Rev. C 41 (1990) 1391. ddn, ddp.

[BR93] C.R. Brune, I. Licot and R.W. Kavanagh, Phys. Rev. C 48 (1993) 3119. c13an.

[BR94] C.R. Brune, R.W. Kavanagh and C. Rolfs, Phys. Rev. C 50 (1994) 2205. tag.

[BR95] J. Brenneisen, D. Grathwohl, M. Lickert, R. Ott, H. Röpke, J. Schmälzlin, P. Siedle and B.H. Wildenthal, Z. Phys. A 352 (1995) 149. al27pg.

[BU50] W.E. Burcham and J.M. Freeman, Philos. Mag. 41 (1950) 337. b10pa.

[BU80] L. Buchmann, H.W. Becker, K.U. Kettner, W.E. Kieser, P. Schmalbrock and C. Rolfs, Z. Phys. A 296 (1980) 273. mg26pg.

[BU84] L. Buchmann, M. Hilgemeier, A. Krauss, A. Redder, C. Rolfs and H.P. Trautvetter, Nucl. Phys. A 415 (1984) 93. al26pg.

[BU87] S. Burzyński, K. Czerski, A. Marcinkowski and P. Zupranski, Nucl. Phys. A 473 (1987) 179. tag.

[BU88] L. Buchmann, J.M. D'Auria and P. McCorquodale, Astrophys. J. 324 (1988) 953. be7ag.

[BU90] N.A. Burkova, K.A. Zhaksibekova and M.A. Zhusupov, Phys. Lett. B 248 (1990) 15. dag.

[BU93] L. Buchmann, R.E. Azuma, C.A. Barnes, J.M. D'Auria, M. Dombsky, U. Giesen, K.P. Jackson, J.D. King, R.G. Korteling, P. McNeely, J. Powell, G. Roy, J. Vincent, T.R. Wang, S.S.M. Wong and P.R. Wrean, Phys. Rev. Lett. 70 (1993) 726. c12ag.

[BU96] L. Buchmann, R.E. Azuma, C.A. Barnes, J. Humblet and K. Langanke, Phys. Rev. C 54 (1996) 393. c12ag.

[BU98] L. Buchmann, Proceedings of the International Symposium on Origin of Matter and Evolution of Galaxies, ed. S. Kubono, T. Kajino, K.I. Nomoto, I. Tanihata (World Scientific, Singapore, 1998). aang.

[BY74] T. Byrski, F.A. Beck, P. Engelstein, M. Forterre and A. Knipper, Nucl. Phys. A 223 (1974) 125. si28pg.

[BY95] J. Byrne, Phys. Scr. T 59 (1995) 311. ppnu.

[CA61] R.R. Carlson, C.C. Kim, J.A. Jacobs and A.C.L. Barnard, Phys. Rev. 122 (1961) 607. o18pa.

[CA62] Y. Cassagnou, J.M.F. Jeronymo, G.S. Mani, A. Sadeghi and P.D. Forsyth, Nucl. Phys. 33 (1962) 449; 41 (1963) 176. li7pa.

[CA74] R. Caracciolo, P. Cuzzocrea, A. De Rosa, G. Inglima, E. Perillo, M. Sandoli and G. Spadaccini, Lett. Nuovo Cimento 11 (1974) 33. f19pa.

[CA78] V.R. Casella, D.R. Christman, T. Ido and A.P. Wolf, Radiochimica Acta 25 (1978) 17. n14pa.

[CA85] G.R. Caughlan, W.A. Fowler, M.J. Harris and B.A. Zimmerman, At. Data Nucl. Data Tables 32 (1985) 197. intro.

[CA88]	G.R. Caughlan and W.A. Fowler, At. Data Nucl. Data Tables 40 (1988) 283. intro and all compiled reactions.
[CA91]	J. Carlson, D.O. Riska, R. Schiavilla and R.B. Wiringa, Phys. Rev. C 44 (1991) 619. ppnu.
[CA97]	V. Castellani, S. Dell'Innocenti, G. Fiorentini, M. Lissia and B. Ricci, Phys. Rep. 281 (1997) 309. intro.
[CE92]	F.E. Cecil, D. Ferg, H. Liu, J.C. Scorby, J.A. McNeil, P.D. Kunz, Nucl. Phys. A 539 (1992) 75. li6pg, be9pg, b11pg.
[CE96]	F.E. Cecil, J. Yan and C.S. Galovich, Phys. Rev. C 53 (1996) 1967. dag.
[CH50]	C.Y. Chao, A.V. Tollestrup, W.A. Fowler and C.C. Lauritsen, Phys. Rev. 79 (1950) 108. f19pa.
[CH70]	G. Chouraqui, T. Muller, M. Port and J.M. Thirion, J. de Phys. 31 (1970) 249. o18ag.
[CH78]	S.H. Chew, J. Lowe and J.M. Nelson, Nucl. Phys. A 298 (1978) 19. n15pn.
[CH83]	A.E. Champagne, A.J. Howard and P.D. Parker, Nucl. Phys. A 402 (1983) 179. mg25pg.
[CH85]	T.E. Chupp, R.T. Kouzes, A.B. McDonald, P.D. Parker, T.F. Wang and A. Howard, Phys. Rev. C 31 (1985) 1023. n13pg.
[CH86a]	A.E. Champagne and M.L. Pitt, Nucl. Phys. A 457 (1986) 367. o18pg, o18pa.
[CH86b]	A.E. Champagne, A.B. McDonald, T.F. Wang, A.J. Howard, P.V. Magnus and P.D. Parker, Nucl. Phys. A 451 (1986) 498. mg25pg.
[CH86c]	A.E. Champagne, M.L. Pitt, P.H. Zhang, L.L. Lee Jr and M.J. Levine, Nucl. Phys. A 459 (1986) 239. al27pg, al27pa.
[CH88]	A.E. Champagne, C.H. Cella, R.T. Kouzes, M.M. Lowry, P.V. Magnus, M.S. Smith and Z.Q. Mao, Nucl. Phys. A 487 (1988) 433. al27pg, al27pa.
[CH89]	A.E. Champagne, A.J. Howard, M.S. Smith, P.V. Magnus and P.D. Parker, Nucl. Phys. A 505 (1989) 384. mg25pg.
[CH90]	A.E. Champagne, P.V. Magnus, M.S. Smith and A.J. Howard, Nucl. Phys. A 512 (1990) 317. mg26pg.
[CH92]	R.M. Chasteler, R.M. Prior, D.R. Tilley and H.R. Weller, Phys. Rev. Lett. 72 (1992) 3949. li7pg.
[CH93]	A.E. Champagne, B.A. Brown and R. Sherr, Nucl. Phys. A 556 (1993) 123. al26pg.
[CH97]	A.C. Champagne, private communication. al27pg, al27pa.
[CI80]	S. Cierjacks, F. Hinterberger, G. Schmalz, D. Erbe, P. van Rossen and B. Leugers, Nucl. Instr. Meth. 169 (1980) 185. be9an.
[CL57]	R.L. Clarke and E.B. Paul, Can. J. Phys. 35 (1957) 155. f19pa.
[CL68]	H.G. Clerc, K.J. Wetzel and E. Spamer, Nucl. Phys. A 120 (1968) 441. aang.
[CL75]	X. Clifford, University of Toronto, MS Thesis, 1975, unpublished. f19pg.
[CL83]	D.D. Clayton, Principles of Stellar Evolution and Nucleosynthesis (Chicago Press, Chicago, 1983). intro.
[CO52]	J.P. Conner, T.W. Bonner and J.R. Smith, Phys. Rev. 88 (1952) 468. tdn.
[CO72]	R.G. Couch, H. Spinka, T.A. Tombrello and T.A. Weaver, Astrophys. J. 172 (1972) 395. n14ag.
[CO92]	C.T. Coburn, J.F. Shriner Jr and C.R. Westerfeldt, Z. Phys. A 343 (1992) 185. al27pa.
[CO95]	A. Coc, R. Mochkovitch, Y. Oberto, J.P. Thibaud and E. Vangioni-Flam, Astron. Astrophys. 299 (1995) 479. al26pg.
[CR89]	R. Crespo, A.M. Eiró and F.D. Santos, Phys. Rev. C 39 (1989) 305. dag.
[CR90]	R. Crespo, A.M. Eiró and J.A. Tostevin, Phys. Rev. C 42 (1990) 1646. dag.
[CR91]	S. Croft, Nucl. Instr. Meth. A 307 (1991) 353. f19pa.
[CU80]	P. Cuzzocrea, A. De Rosa, G. Inglima, E. Perillo, E. Rosato, M. Sandoli and G. Spadaccini, Lett. Nuovo Cimento 28 (1980) 515. f19pa.
[DA52]	R.B. Day and R.L. Walker, Phys. Rev 85 (1952) 582. be9pa.
[DA61]	P. Dagley, W. Haeberli and J.X. Saladin, Nucl. Phys. 24 (1961) 353. c13pn.
[DA68]	C.N. Davids, Nucl. Phys. A 110 (1968) 619. c13an.
[DA73]	M.J. Dalmas, C.R. Acad. Sc. Paris 277 (1973) B-237. al27pg, al27pa.
[DA76]	F. Dautry, M. Rho and D.O. Riska, Nucl. Phys. A 264 (1976) 507. ppnu.
[DA79]	J.M. Davidson, H.L. Berg, M.M. Lowry, M.R. Dwarakanath, A.J. Sierk and P. Batay-Csorba, Nucl. Phys. A 315 (1979) 253. b11pa.
[DA84]	S.E. Darden, S. Sen, G. Murillo, M. Fernández, J. Ramírez, A. Galindo, P.L. Jolivette and B.P. Hichwa, Nucl. Phys. A 429 (1984) 218. n15pa.
[DA93]	S.O.F. Dababneh, K. Toukan and I. Khubeis, Nucl. Instr. Meth. B 83 (1993) 319. f19pa.
[DE54]	S. Devons, G. Goldring and G.R. Lindsey, Proc. Phys. Soc. A 67 (1954) 134. f19pa.

| DE65 | R.W. Detenbeck, J.C. Armstrong, A.S. Figuera and J.B. Marion, Nucl. Phys. 72 (1965) 552. c13pg.

| DE74 | E.O. De Neijs, M.A. Meyer, J.P.L. Reinecke and D. Reitmann, Nucl. Phys A 230 (1974) 490. mg25pg.

| DE83 | P. Descouvemont and D. Baye, Phys. Lett. B 127 (1983) 286. o16ag.

| DE86 | P. Descouvemont and D. Baye, Nucl. Phys. A 459 (1986) 374. o16ag.

| DE87 | P. Descouvemont and D. Baye, Phys. Rev. C 36 (1987) 54. aaag.

| DE89 | P. Descouvemont, Phys. Rev. C 39 (1989) 1557. aang.

| DE93a | P. Decrock, T. Delbar, W. Galster, M. Huyse, P. Leleux, I. Licot, E. Liénard, P. Lipnik, C. Michotte, P. Van Duppen, J. Vanhorenbeeck and J. Vervier, Phys. Lett. B 304 (1993) 50. n13pg.

| DE93b | P. Decrock, M. Gaelens, M. Huyse, G. Reusen, G. Vancraeynest, P. Van Duppen, J. Wauters, T. Delbar, W. Galster, P. Leleux, I. Licot, E. Liénard, P. Lipnik, C. Michotte, J. Vervier and H. Oberhummer, Phys. Rev. C 48 (1993) 2057. n13pg.

| DE93c | P. Descouvemont, Phys. Rev. C 48 (1993) 2746. o17an.

| DE94a | P. Descouvemont and D. Baye, Nucl. Phys. A 567 (1994) 341. be7pg.

| DE94b | A. Denker, PhD thesis, University of Stuttgart (Aachen: Shaker, 1994), ISBN 3-8265-0191-8. o17an, o18an, ne21an.

| DE95 | P. Descouvemont, Nucl. Phys. A 584 (1995) 532. li7ag, be7ag.

| DI71a | W.R. Dixon and R.S. Storey, Can. J. Phys. 49 (1971) 1714. n15ag.

| DI71b | W.R. Dixon, R.S. Storey, J.H. Aitken, A.E. Litherland and D.W.O. Rogers, Phys. Rev. Lett. 27 (1971) 1460. n15ag.

| DI71c | W.T. Diamond, T.K. Alexander and O. Häusser, Can. J. Phys. 49 (1971) 1589. o16ag.

| DI77 | W.R. Dixon and R.S. Storey, Nucl. Phys. A 284 (1977) 97. n15ag.

| DO87 | G. Doukellis and J. Rapaport, Nucl. Phys. A 467 (1987) 511. na23an.

| DR91 | H.W. Drotleff, A. Denker, J.W. Hammer, H. Knee, S. Küchler, D. Streit, C. Rolfs and H.P. Trautvetter, Z. Phys A 338 (1991) 367. ne22an.

| DR93 | H.W. Drotleff, A. Denker, H. Knee, M. Soiné, G. Wolf, J.W. Hammer, U. Greife, C. Rolfs and H.P. Trautvetter, Astrophys. J. 414 (1993) 735. c13an, ne22an.

| DU51 | D.B. Duncan and J.E. Perry, Phys. Rev. 82 (1951) 809. n14pg.

| DU71 | Z.B. du Toit, P.R. de Kock and W.L. Mouton, Z. Phys. 246 (1971) 170. ne22pg.

| DU72 | Z.B. du Toit, P.R. de Kock, J.H. Hough and W.L. Mouton, Z. Phys. 255 (1972) 97. ne22pg.

| DU94 | M. Dufour, P. Descouvemont and D. Baye, Phys. Rev. C 50 (1994) 795. o16ag.

| DW71 | M.R. Dwarakanath and H. Winkler, Phys. Rev. C 4 (1971) 1532. he3he3.

| DW74 | M.R. Dwarakanath, Phys. Rev. C 9 (1974) 805. he3he3.

| DY74 | P. Dyer and C.A. Barnes, Nucl. Phys. A 233 (1974) 495. c12ag.

| DY81 | P. Dyer, D. Bodansky, A.G. Seamster, E.B. Norman and D.R. Maxson, Phys. Rev. C 23 (1981) 1865. n14pn.

| EI69 | F. Eigenbrod, Z. Phys. 228 (1969) 337. dag.

| EJ64 | H. Ejiri, H. Ohmura, Y. Nakajima, K. Horie, Y. Hashimoto, K. Eto, S. Matsumoto and Y. Nogami, Nucl. Phys. 52 (1964) 561. si28pg.

| EL79a | A.J. Elwyn, R.E. Holland, C.N. Davids, L. Meyer-Schutzmeister, F.P. Mooring and W. Ray Jr, Phys. Rev. C 20 (1979) 1984. li6pa.

| EL79b | K. Elix, H.W. Becker, L. Buchmann, J. Görres, K.U. Kettner, M. Wiescher and C. Rolfs, Z. Phys. A 293 (1979) 261. mg25pg.

| EN60 | P.M. Endt and A. Heyligers, Physica 26 (1960) 230. al27pg.

| EN66 | G.A.P. Engelbertink and P.M. Endt, Nucl. Phys. 88 (1966) 12. mg25pg, mg26pg, al27pg, si28pg.

| EN78 | P.M. Endt and C. van der Leun, Nucl. Phys. A 310 (1978) 1. ne20pg.

| EN86 | P.M. Endt, P. de Wit and C. Alderliesten, Nucl. Phys. A 459 (1986) 61. mg25pg.

| EN87 | P.M. Endt and C. Rolfs, Nucl. Phys. A 467 (1987) 261. mg25pg.

| EN88 | S. Engstler, A. Krauss, K. Neldner, C. Rolfs, U. Schröder and K. Langanke, Phys. Lett. B 202 (1988) 179. intro.

| EN90 | P.M. Endt and C. van der Leun, Nucl. Phys. A 521 (1990) 1. o17pg, ne21an, al27pa.

| EN92 | S. Engstler, G. Raimann, C. Angulo, U. Greife, C. Rolfs, U. Schröder, E. Somorjai, B. Kirch and K. Langanke, Z. Phys. A 342 (1992) 471; Phys. Lett. B 279 (1992) 20. li6pa, li7pa.

| EP71 | M. Epherre and C. Seide, Phys. Rev. C 3 (1971) 2167. n14pa.

| FA55 | G.K. Farney, H.H. Givin, B.D. Kern and T.M. Hahn, Phys. Rev. 97 (1955) 720. f19pg.

| FA64 | U. Fasoli, D. Toniolo and G. Zago, Phys. Lett. 8 (1964) 127. li6pa.

[FE65] V.N. Fetisov, A.N. Gorbunov and A.T. Varfolomeev, Nucl. Phys. 71 (1965) 305. dpg.

[FE72] V.N. Fetisov and Y.S. Kopysov, Phys. Lett. B 40 (1972) 602; Nucl. Phys. A 239 (1972) 511. he3he3.

[FE89] P.B. Fernandez, E.G. Adelberger and A. García, Phys. Rev. C 40 (1989) 1887. n13pg.

[FI63] T.R. Fisher and W. Whaling, Phys. Rev. 131 (1963) 1723. na23pa.

[FI67] O. Fiedler and P. Kunze, Nucl. Phys. A 96 (1967) 513. li6pa, li7pa.

[FI76] G.A. Fisher, P. Paul, F. Riess and S.S. Hanna, Phys. Rev. C 14 (1976) 28. li7pg.

[FI77] L.K. Fifield, F.P. Calaprice, C.H. Zimmerman, M.J. Hurst, A. Pakkanen, T.J.M. Symons, F. Watt and K.W. Allen, Nucl. Phys. A 288 (1977) 57. o16ag.

[FI78] L.K. Fifield, M.J. Hurst, T.J.M. Symons, F. Watt, C.H. Zimmerman and K.W. Allen, Nucl. Phys. A 309 (1978) 77. ne20ag, na23pg.

[FI79] L.K. Fifield, E.F. Garman, M.J. Hurst, T.J.M. Symons, F. Watt, C.H. Zimmerman and K.W. Allen, Nucl. Phys. A 322 (1979) 1. ne20ag.

[FI80] L.K. Fifield, M.J. Hurst, E.F. Garman, T.J.M. Symons, F. Watt and K.W. Allen, Nucl. Phys. A 334 (1980) 109. o16ag.

[FI83a] B.W. Filippone, A.J. Elwyn, C.N. Davids and D.D. Koetke, Phys. Rev. Lett. 50 (1983) 412, and private communication. be7pg.

[FI83b] B.W. Filippone, A.J. Elwyn, C.N. Davids and D.D. Koetke, Phys. Rev. C 28 (1983) 2222. be7pg.

[FI91] M.L. Firouzbakht, D.J. Schlyer and A.P. Wolf, Radiochimica Acta 55 (1991) 1. c13pn.

[FL54] F.C. Flack, J.G. Rutherglen and P.J. Grant, Proc. Phys. Soc. London A 67 (1954) 973. na23pa.

[FL78] D.S. Flynn, K.K. Sekharan, B.A. Hiller, H. Laumer, J.L. Weil and F. Gabbard, Phys. Rev. C 18 (1978) 1566. na23pn, al27an.

[FO49] W.A. Fowler and C.C. Lauritsen, Phys. Rev. 76 (1949) 314. be9pg.

[FO67] W.A. Fowler, G.R. Caughlan and B.A. Zimmerman, Ann. Rev. Astron. Astrophys. 5 (1967) 525. intro.

[FO72] W.A. Fowler, Nature 238 (1972) 24. he3he3.

[FO73] J.L. Fowler, C.H. Johnson and R.M. Feezel, Phys. Rev. C 8 (1973) 545. c13an.

[FO75] W.A. Fowler, G.R. Caughlan and B.A. Zimmerman, Ann. Rev. Astron. Astrophys. 13 (1975) 69. intro, na23pg.

[FR77] T. Freye, H. Lorenz-Wirzba, B. Cleff, H.P. Trautvetter and C. Rolfs, Z. Phys. A 281 (1977) 211. f19pa.

[FR97] R.H. France III, E.L. Wilds, N.B. Jetvic J.E. McDonald and M. Gai, Nucl. Phys. A 621 (1997) 165c. c12ag.

[FU82] M. Fujishiro, T. Tabata, K. Okamoto and T. Tsujimoto, Can. J. Phys. 60 (1982) 1672. aang.

[GA56] A. Galonsky and C.H. Johnson, Phys. Rev. 104 (1956) 421. tdn.

[GA72] M. Gari and A.H. Huffman, Astrophys. J. 178 (1972) 543. ppnu.

[GE66] W. Gemeinhardt, D. Kamke and C. von Rhöneck, Z. Phys. 197 (1966) 58. li6pa.

[GE67] K.N. Geller, E.G. Muirhead and L.D. Cohen, Nucl. Phys. A 96 (1967) 397. dpg.

[GE75] K.W. Geiger, L. Van der Zwan, Nucl. Instr. Meth. 131 (1975) 315. be9an.

[GI59] J.H. Gibbons and R.L. Macklin, Phys. Rev. 114 (1959) 571. li7an, be9pn, b11pn, f19pn.

[GI65] J.H. Gibbons and R.L. Macklin, Phys. Rev. B 137 (1965) 1508. be9an.

[GI68] E.F. Gibson, K. Battleson and D.K. McDaniels, Phys. Rev. 172 (1968) 1004. al27pg.

[GI93] U. Giesen, C.P. Browne, J. Görres, S. Graff, C. Iliadis, H.P. Trautvetter, M. Wiescher, W. Harms, K.L. Kratz, B. Pfeiffer, R.E. Azuma, M. Buckby and J.D. King, Nucl. Phys. A 561 (1993) 95. ne22ag, ne22an.

[GI94] U. Giesen, C.P. Browne, J. Görres, J.G. Ross, M. Wiescher, R.E. Azuma, J.D. King, J.B. Vise and M. Buckby, Nucl. Phys. A 567 (1994) 146. o18ag.

[GO54] W.M. Good, W.E. Kunz and C.D. Moak, Phys. Rev. 94 (1954) 87. he3he3.

[GO61] M.D. Goldberg, J.M. Le Blanc, Phys. Rev. 122 (1961) 164. tdn.

[GO74] C.R. Gould, R.O. Nelson, J.R. Williams and J.R. Boyce, Nucl. Sci. Eng. 55 (1974) 267. li6pa.

[GO90] R.J. Gould and N. Guessoum, Astrophys. J. 359 (1990) L67. ppnu.

[GO96] M.A. Godwin, R.M. Chasteler, C.M. Laymond, R.M. Prior, D.R. Tilley and H.R. Weller, Phys. Rev. C 53 (1996) R1. li7pg.

[GO97] M.A. Godwin, C.M. Laymond, R.M. Prior, D.R. Tilley and H.R. Weller, Phys. Rev. C 56 (1997) 1605. li7pg.

[GÖ82] J. Görres, C. Rolfs, P. Schmalbrock, H.P. Trautvetter and J. Keinonen, Nucl. Phys. A 385 (1982) 57. ne21pg, ne22pg.

[GÖ83] J. Görres, H.W. Becker, L. Buchmann, C. Rolfs, P. Schmalbrock, H.P. Trautvetter, A. Vlieks, J.W. Hammer and T.R. Donoghue, Nucl. Phys. A 408 (1983) 372. ne21pg, ne22pg.

[GÖ89a] J. Görres, M. Wiescher, S. Graff, R.B. Vogelaar, B.W. Filippone, C.A. Barnes, S.E. Kellogg, T.R. Wang and B.A. Brown, Phys. Rev. C 39 (1989) 8. na22pg.

[GÖ89b] J. Görres, M. Wiescher and C. Rolfs, Astrophys. J. 343 (1989) 365. na23pa.

[GÖ95] J. Görres, H. Herndl, I.J. Thompson and M. Wiescher, Phys. Rev. C 52 (1995) 2231. aang.

[GR61] G.M. Griffiths, R.A. Morrow, P.J. Riley and J.B. Warren, Can. J. Phys. 39 (1961) 1397. tag.

[GR62] G.M. Griffiths, E.A. Larson and L.P. Robertson, Can. J. Phys. 40 (1962) 402. dpg.

[GR63] G.M. Griffiths, M. Lal and C.D. Scarfe, Can. J. Phys. 41 (1963) 724. dpg.

[GR68] J. Graff, G. Chouraqui, M. Port, J.M. Thirion, S. Jang and Th. Muller, J. de Phys. 29 (1968) 141 o18ag.

[GR72a] M.B. Greenfield, C.R. Bingham, E. Newman and M.J. Saltmarsh, Phys. Rev. C 6 (1972) 1756. n13pg.

[GR72b] W. Gruhle, W. Schmidt and W. Burgmer, Nucl. Phys. A 186 (1972) 257. n14an.

[GR77] W. Gruhle and B. Kober, Nucl. Phys. A 286 (1977) 523. ne20pa, mg24pa.

[GR84] D. Grambole, C. Bauer, P. Gippner, C. Heiser, W. Rudolph, H.-J. Thomas, J. Radioanal. Nucl. Chem. 83 (1984) 107. f19pa.

[GR90] S. Graff, J. Görres, M. Wiescher, R.E. Azuma, J. King, J. Vise, G. Hardie and T.R. Wang, Nucl. Phys. A 510 (1990) 346. si28pg.

[GR95] U. Greife, F. Gorris, M. Junker, C. Rolfs, D. Zahnow, Z. Phys. A 351 (1995) 107. ddn, ddp.

[HA50] R.N. Hall and W.A. Fowler, Phys. Rev. 77 (1950) 197. c12pg.

[HA57a] F.B. Hagedorn, F.S. Mozer, T.S. Webb, W.A. Fowler and C.C. Lauritsen, Phys. Rev. 105 (1957) 219. n14pg.

[HA57b] F.B. Hagedorn, Phys. Rev. 108 (1957) 735. n15pa.

[HA67] L.F. Hansen, J.D. Anderson, J.W. McClure, B.A. Pohl, M.L. Stelts, J.J. Wesolowski and C. Wong, Nucl. Phys. A 98 (1967) 25. o17an, o18an.

[HA73] F.X. Haas and J.K. Bair, Phys. Rev. C 7 (1973) 2432. ne21an, ne22an.

[HA83] M.J. Harris, W.A. Fowler, G.R. Caughlan and B.A. Zimmerman, Ann. Rev. Astron. Astrophys. 21 (1983) 165. intro.

[HA84] G. Hardie, B.W. Filippone, A.J. Elwyn, M. Wiescher and R.E. Segel, Phys. Rev. C 29 (1984) 1199. be7ag, li7ag.

[HA87] K.H. Hahn, K.H. Chang, T.R. Donoghue and B.W. Filippone, Phys. Rev. C 36 (1987) 892. o16ag.

[HA88] G. Hardie, R.E. Segel, A.J. Elwyn and J.E. Monahan, Phys. Rev. C 38 (1988) 2003. al27pg.

[HA89] J.F. Harmon, Nucl. Inst. Meth. B 40/41 (1989) 507. li7pa.

[HA91] V. Harms, K.-L. Kratz and M. Wiescher, Phys. Rev. C 43 (1991) 2849. ne22an.

[HA96] K.I. Hahn, C.R. Brune and R.W. Kavanagh, Phys. Rev. C 53 (1996) 1273. li7pg.

[HA97] G.M. Hale, Nucl. Phys. A 621 (1997) 177c. c13an.

[HA98] F. Hammache, G. Bogaert, P. Aguer, C. Angulo, S. Barhoumi, L. Brillard, J.F. Chemin, G. Claverie, A. Coc, M. Hussonnois, M. Jacotin, J. Kiener, A. Lefebvre, J.N. Scheurer, J.P. Thibaud and E. Virassamynaïken, Phys. Rev. Lett. 80 (1998) 928. be7pg.

[HE55] A. Hemmendinger and H.V. Argo, Phys. Rev. 98 (1955) 70. tdn.

[HE58] R.E. Hester, R.E. Pixley and W.A. Lamb, Phys. Rev. 111 (1958) 1604. o16pg.

[HE60a] D.F. Hebbard and J.L. Vogl, Nucl. Phys. 21 (1960) 652. c13pg.

[HE60b] D.F. Hebbard, Nucl. Phys. 15 (1960) 289. n15pg.

[HE61] R.E. Hester and W.A.S. Lamb, Phys. Rev. 121 (1961) 584. c13pg.

[HE63] D.F. Hebbard and G.M. Bailey, Nucl. Phys. 49 (1963) 666. n14pg.

[HE91] H. Herndl, H. Abele, G. Staudt, B. Bach, K. Grun, H. Scsribany, H. Oberhummer and G. Raiman, Phys. Rev. C 44 (1991) R952. f19pa.

[HI68] C.J. Highland and T.T. Thwaites, Nucl. Phys. A 109 (1968) 163. ne20ag.

[HI88] M. Hilgemeier, H.W. Becker, C. Rolfs, H.P. Trautvetter and J.W. Hammer, Z. Phys. A 329 (1988) 243. he3ag.

[HO53] W.F. Hornyak and T. Coor, Phys. Rev. 92 (1953) 675. be9pg.

[HO59] H.D. Holmgren and R.L. Johnston, Phys. Rev. 113 (1959) 1556. he3ag.

[HO64] W.F. Hornyak, C.A. Ludemann and M.L. Roush, Nucl. Phys. 50 (1964) 424. be9pg.

[HO74] A.J. Howard, H.B. Jensen, M. Rios, W.A. Fowler and B.A. Zimmerman, Astrophys. J. 188 (1974) 131. al27an.

C. Angulo et al. / Nuclear Physics A 656 (1999) 3–183

| HO86 | B. Holmqvist and E. Ramström, Phys. Scr. 33 (1986) 107. al27an.

| HU53 | T. Huus and R.B. Day, Phys. Rev. 91 (1953) 599. b11pg.

| HU72 | G.M. Hudson, G.B. Crinean, D.T. Kelly and B.M. Spicer, Nucl. Phys. A 184 (1972) 175. be9pd.

| HU75 | R.J. Hughes, R.H. Sambell, E.G. Muirhead and B.M. Spicer, Nucl. Phys. A 238 (1975) 189. aang.

| HU80 | M.J. Hurst, L.K. Fifield, E.F. Garman, T.J. Symons, F. Watt and K.W. Allen, J. Phys. G 6 (1980) 891. o16ag.

| IL90 | C. Iliadis, T. Schange, C. Rolfs, U. Schröder, E. Somorjai, H.P. Trautvetter, K. Wolke, P.M. Endt, S.W. Kikstra, A.E. Champagne, M. Arnould and G. Paulus, Nucl. Phys. A 512 (1990) 509. mg26pg.

| IL96 | C. Iliadis, L. Buchmann, P.M. Endt, H. Herndl and M. Wiescher, Phys. Rev. C 53 (1996) 475. mg25pg.

| IN76a | P.D. Ingalls, J.S. Schweitzer, B.D. Anderson and M. Rios, Phys. Rev. C 13 (1976) 524. n14pa.

| IN76b | P.D. Ingalls, Nucl. Phys. A 265 (1976) 93. o16ag.

| IS58 | A. Isoya, H. Ohmura and T. Momota, Nucl. Phys. 7 (1958) 116. f19pa.

| JA74 | W.W. Jacobs, D. Bodansky, D. Chamberlin and D.L. Oberg, Phys. Rev. C 9 (1974) 2134. n14pa.

| JA84 | N. Jarmie, R.E. Brown and R.A. Hardekopf, Phys. Rev. C 29 (1984) 2031. tdn.

| JE63a | J.M.F. Jeronymo, G.S. Mani and A. Sadeghi, Nucl. Phys. 43 (1963) 424. li6pa.

| JE63b | J.G. Jenkin, L.G. Earwaker and E.W. Titterton, Nucl. Phys. 44 (1963) 453. f19pn.

| JE64 | J.G. Jenkin, L.G. Earwaker and E.W. Titterton, Nucl. Phys. 50 (1964) 516. b10pa.

| JE77 | J.P. Jeukenne, A. Lejeune and C. Mahaux, Phys. Rev. C 16 (1977) 80. intro.

| JO73 | C.H. Johnson, Phys. Rev. C 7 (1973) 561. c13an.

| JU98 | M. Junker, A. D'Alessandro, S. Zavatarelli, C. Arpesella, E. Bellotti, C. Broggini, P. Corvisiero, G. Fiorentini, A. Fubini, G. Gervino, U. Greife, C. Gustavino, J. Lambert, P. Prati, W.S. Rodney, C. Rolfs, F. Strieder, H.P. Trautvetter and D. Zahnow, Phys. Rev. C 57 (1998) 2700. he3he3.

| KA60 | R.W. Kavanagh, Nucl. Phys. 15 (1960) 411. be7pg.

| KA65 | K.V. Karadzhev, V.I. Man'ko and F.E. Chukreev, Sov. Phys. JETP 20 (1965) 800. o18pa.

| KA69 | R.W. Kavanagh, T.A. Tombrello, J.M. Mosher and D.R. Goosman, Bull. Am. Phys. Soc. 14 (1969) 1209. be7pg.

| KA84 | A.S. Kachan and E.G. Kopanetz, Izv. Akad. Nauk. SSSR, Ser. Fiz. 48 (1984) 116. mg25pg.

| KA86 | T. Kajino, Nucl. Phys. A 460 (1986) 559. tag, he3he4.

| KA89 | A.S. Kachan, B.A. Nemashkalo and V.E. Storizhko, Sov. J. Nucl. Phys. 49 (1989) 227. mg25pg.

| KA94 | M. Kamionkowski and J.N. Bahcall, Astrophys. J. 420 (1994) 884. ppnu.

| KÄ94 | F. Käppeler, M. Wiescher, U. Giesen, J. Görres, I. Baraffe, M. El Eid, C.M. Raiteri, M. Busso, R. Gallino, M. Limongi and A. Chieffi, Astrophys. J. 437 (1994) 396. ne22an.

| KE62 | L. Keszthelyi, I. Berkes, I. Demeter and I. Fodor, Nucl. Phys. 29 (1962) 241. f19pg.

| KE77 | J. Keinonen, M. Riihonen and A. Anttila, Phys. Rev. C 15 (1977) 579. ne21pg, ne22pg.

| KE80 | J. Keinonen and S. Brandenburg, Nucl. Phys. A 341 (1980) 345. mg24pg, mg25pg, mg26pg.

| KE82 | K.U. Kettner, H.W. Becker, L. Buchmann, J. Görres, H. Kräwinkel, C. Rolfs, P. Schmalbrock, H.P. Trautvetter, A. Vlieks, Z. Phys. A 308 (1982) 73. c12ag.

| KI79a | W.E. Kieser, R.E. Azuma, I. Berka, K.P. Jackson, A.B. McDonald, H.-B. Mak and W. McLatchie, Nucl. Phys. A 327 (1979) 172. o17pg, o17pa.

| KI79b | W.E. Kieser, R.E. Azuma and K.P. Jackson, Nucl. Phys. A 331 (1979) 155. o17pa.

| KI85 | M. Kicinska-Habior and T. Matulewicz, J. de Phys. 46 (1985) 1881. si28pg.

| KI90a | S. Wa-Kitwanga, P. Leleux, P. Lipnik and J. Vanhorenbeeck, Phys. Rev. C 42 (1990) 748. f19pn.

| KI90b | M. Kious, PhD Thesis, University of Paris XI (1990), unpublished. f19pa.

| KI91 | J. Kiener, H.J. Gils, H. Rebel, S. Zagromski, G. Gsottschneider, N. Heide, H. Jelitto, J. Wentz and G. Baur, Phys. Rev. C 44 (1991) 2195 and private communication. dag.

| KI93 | J. Kiener, A. Lefebvre, P. Aguer, C.O. Bacri, R. Bimbot, G. Bogaert, B. Borderie, F. Clapier, A. Coc, D. Disdier, S. Fortier, C. Grunberg, L. Kraus, I. Linck, G. Pasquier, M.F. Rivet, F.St. Laurent, C. Stephan, L. Tassan-Got and J.P. Thibaud, Nucl. Phys. A 552 (1993) 66. n13pg.

| KI94 | J.D. King, R.E. Azuma, J.B. Vise, J. Görres, C. Rolfs, H.P. Trautvetter and A.E. Vlieks, Nucl. Phys. A 567 (1994) 354. c13pg.

| KN75 | D.W. Kneff, F.M. Mann and Z.E. Switkowski, Nucl. Phys. A 250 (1975) 285. na23pn.

| KN93 | F. Knape, H. Bucka and P. Heide, Proc. 2nd Intern. Symposium on Nuclear Astrophysics, ed. F. Käppeler and K. Wisshak (IOP, Bristol, 1993). b10pa.

| KN94 | H. Knee, PhD thesis, University of Stuttgart (Aachen: Shaker, 1994), ISBN 3-8265-0528-x. o16ag.

[KO66] A.P. Kobzev, V.I. Salatskii and S.A. Telezhnikov, Sov. J. Nucl. Phys. 3 (1966) 774. tdn.

[KR82] H. Kräwinkel, H.W. Becker, L. Buchmann, J. Görres, K.U. Kettner, W.E. Kieser, R. Santo, P. Schmalbrock, H.P. Trautvetter, A. Vlieks, C. Rolfs, J.W. Hammer, R.E. Azuma and W.S. Rodney, Z. Phys. A 304 (1982) 307. he3ag.

[KR87a] A. Krauss, H.W. Becker, H.P. Trautvetter, C. Rolfs and K. Brand, Nucl. Phys. A 465 (1987) 150. ddn, ddp.

[KR87b] A. Krauss, H.W. Becker, H.P. Trautvetter and C. Rolfs, Nucl. Phys. A 467 (1987) 273. he3he3.

[KR88] R.M. Kremer, C.A. Barnes, K.H. Chang, H.C. Evans, B.W. Filippone, K.H. Hahn and L.W. Mitchell, Phys. Rev. Lett. 60 (1988) 1475. c12ag.

[KU63] J. Kuperus, P.W.M. Glaudemans and P.M. Endt, Physica 29 (1963) 1281. na23pa, al27pa.

[KU64] H.-M. Kuan and J.R. Risser, Nucl. Phys. 51 (1964) 518. n14pn.

[KU69] E. Kurtz, K. Battleson, D.K. McDaniels and D.J. Horen, Nucl. Instr. Meth. 69 (1969) 56. al27pg.

[KU70] H.M. Kuan, M. Hasinoff, W.J. O'Connell and S.S. Hanna, Nucl. Phys. A 151 (1970) 129. b10pg.

[KU77] H.M. Kuan, D.G. Shirk and S. Fiarman, Phys. Rev. C 15 (1977) 569. n14pg.

[KU87] G. Kuechler, A. Richter and W. von Witsch, Z. Phys. A 326 (1987) 447. aang.

[KU95] R. Kunz, H.W. Drotleff, M. Grösse, H. Knee, S. Küchler, R. seidel, M. Soin and J.W. Hammer, Proc. Int. Conf. Neutrons and their Applications, ed. G. Vourvopoulos and T. Paradellis, SPIE 2339, Washington 1995, p. 38. o17an, o18an, ne21an.

[KU96] R. Kunz, S. Barth, A. Denker, H.W. Drotleff, J.W. Hammer, H. Knee and A. Mayer, Phys. Rev. C 53 (1996) 2486. be9an.

[KU97] R. Kunz, A. Mayer, K.D. Joss, H. Knee, A. Müller, J. Nickel, Ch. Plettner, J.W. Hammer, D. Baye, P. Descouvemont, M. Jaeger, V. Kölle, S. Wilmes, G. Staudt, P. Mohr, Ch. Chronidou, S. Harissopulos, K. Spyrou and T. Paradellis, Nucl. Phys. A 621 (1997) 149c. o16ag.

[KW89] J.U. Kwon, J.C. Kim and B.N. Sung, Nucl. Phys. A 493 (1989) 112. li6pa.

[LA57a] W.A.S. Lamb and R.E. Hester, Phys. Rev. 107 (1957) 550. c12pg.

[LA57b] W.A.S. Lamb and R.E. Hester, Phys. Rev. 108 (1957) 1304. n14pg.

[LA58] A.M. Lane and R.G. Thomas, Rev. Mod. Phys. 30 (1958) 257. intro.

[LA66] T. Lauritsen and F. Ajzenberg-Selove, Nucl. Phys. 78 (1966) 1. aang.

[LA83] K. Langanke, Phys. Lett. B 131 (1983) 21. o16ag.

[LA85] K. Langanke, O.S. van Rossmalen and W.A. Fowler, Nucl. Phys. A 435 (1985) 657. n13pg.

[LA86a] K. Langanke, Nucl. Phys. A 457 (1986) 351. dag, he3he4.

[LA86b] K. Langanke, C. Rolfs, Z. Phys. A 325 (1986) 193. dag.

[LA86c] K. Langanke, M. Wiescher and F.-K. Thielemann, Z. Phys. A 324 (1986) 147. aaag.

[LA89] V. Landre, P. Aguer, G. Bogaert, A. Lefebvre, J.P. Thibaud, S. Fortier, J.M. Maison and J. Vernotte, Phys. Rev. C 40 (1989) 1972. o17pg, o17pa.

[LE61] G.J.F. Legge and I.F. Bubb, Nucl. Phys. 26 (1961) 616. b11pn.

[LE71] J.R. Leslie, W. McLatchie, C.F. Monahan and J.K. Thrasher, Nucl. Phys. A 170 (1971) 115. al27pg.

[LI56] A.E. Litherland, E.B. Paul, G.A. Bartolomew and H.E. Gove, Phys. Rev. 102 (1956) 208. mg24pg.

[LI67] A.E. Litherland, R.W. Ollerhead, P.J.M. Smulders, T.K. Alexander, C. Broude, A.J. Ferguson and J.A. Kuehner, Can. J. Phys. 45 (1967) 1901. o16ag.

[LI77] C.-S. Lin, W.-S. Hou, M. Wen and J.-C. Chou, Nucl. Phys. A 275 (1977) 93. li6pa.

[LI81] Q.K.K. Liu, H. Kanada and Y.C. Tang, Phys. Rev. C 23 (1981) 645. he3ag.

[LO78] H. Lorenz-Wirzba, PhD thesis, University of Münster (1978), unpublished. f19pa.

[LO79] H. Lorenz-Wirzba, P. Schmalbrock, H.P. Trautvetter, M. Wiescher, C. Rolfs and W.S. Rodney, Nucl. Phys. A 313 (1979) 346. o18pa.

[LU70] A. Luukko, A. Anttila, M. Bister and M. Piiparinen, Phys. Scr. 2 (1970) 159. na23pa.

[LY69] P.B. Lyons, J.W. Toevs and D.G. Sargood, Nucl. Phys. A 130 (1969) 1. mg26pg, al27pg.

[MA56] J.B. Marion, G. Weber and F.S. Mozer, Phys. Rev. 104 (1956) 1402. li6pa.

[MA59] J.B. Marion and J.S. Levin, Phys. Rev. 115 (1959) 144. be9pa.

[MA64] G.S. Mani, R. Freeman, F. Picard, A. Sadeghi and D. Redon, Nucl. Phys. 60 (1964) 588. li7pa.

[MA68] R.L. Macklin and J.H. Gibbons, Phys. Rev. 165 (1968) 1147. li7an.

[MA75] E. Magiera, M. Bormann and W. Scobel, Nucl. Phys. A 246 (1975) 413. tdn.

[MA76] F.M. Mann, D.W. Kneff, Z.E. Switkowski and S.E. Woosley, Nucl. Phys. A 256 (1976) 163. na23pn.

[MA78a] F.M. Mann, Hauser5, a computer code to calculate the nuclear cross sections, Hanford Engineering (HEDL-TME-78-83). intro.

|MA78b| H.-B. Mak, H.C. Evans, G.T. Ewan and J.D. MacArthur, Nucl. Phys. A 304 (1978) 210. o18pa.

|MA78c| J.W. Maas, A.J.C.D. Holvast, A. Baghus, H.J.M. Aarts and P.M. Endt, Nucl. Phys. A 301 (1978) 237. mg26pg.

|MA78d| J.W. Maas, E. Somorjai, H.D. Graber, C.A. Van Den Wijngaart, C. van der Leun and P.M. Endt, Nucl. Phys. A 301 (1978) 213. al27pa.

|MA80| H.-B. Mak, G.T. Ewan, H.C. Evans, J.D. MacArthur, W. McLatchie and R.E. Azuma, Nucl. Phys. A 343 (1980) 79. o17pg, o17pa.

|MA87| P.V. Magnus, M.S. Smith, P.D. Parker, R.E. Azuma, C. Campbell, J.D. King and J. Vise, Nucl. Phys. A 470 (1987) 206. n15ag.

|MA94| P.V. Magnus, E.G. Adelberger and A. García, Phys. Rev. C 49 (1994) R 1755. n13pg.

|MA97| L. Ma, H.J. Karwowski, C.R. Brune, Z. Ayer, T.C. Black, J.C. Blackmon and E.J. Ludwig, Phys. Rev. C 55 (1997) 588. dpg.

|MC73| D.K. McDaniels, M. Drosg, J.C. Hopkins and J.D. Seagrave, Phys. Rev. C 7 (1973) 882. tdn.

|ME59| W.E. Meyerhof, N.W. Tanner and C.M. Hudson, Phys. Rev. 115 (1959) 1227. be9pg.

|ME63| M.K. Mehta, W.E. Hunt, H.S. Plendl and R.H. Davis, Nucl. Phys. 48 (1963) 90. li7an.

|ME69| W.E. Meyerhof, W. Feldman, S. Gilbert and W. O'Connell, Nucl. Phys. A 131 (1969) 489. ddg.

|ME70| M.A. Meyer, N.S. Wolmarans and D. Reitmann, Nucl. Phys. A 144 (1970) 261. al27pg, al27pa.

|ME72| M.A. Meyer, J.P.L. Reinecke and D. Reitmann, Nucl. Phys. A 185 (1972) 625. na23pa.

|ME73| M.A. Meyer and J.J.A. Smit, Nucl. Phys. A 205 (1973) 177. ne22pg.

|ME75| M.A. Meyer, I. Venter and D. Reitmann, Nucl. Phys. A 250 (1975) 235. al27pg, al27pa.

|MO56| F.S. Mozer, Phys. Rev. 104 (1956) 1386. be9pa.

|MO60| W.L. Mouton and P.B. Smith, Nucl. Phys. 16 (1960) 206. ne22pg.

|MO65| S. Morita, T. Tohei, T. Nakagawa, T. Hasegawa, H. Ueno and H. Chu-Chung, Nucl. Phys. 66 (1965) 17. be9pa.

|MO66| S. Morita, T. Nakagawa, C.-C. Hsu and S.-M. Lee, J. Phys. Soc. Japan 21 (1966) 2435. f19pa.

|MO68| G.C. Morrison, D.H. Youngblood, R.C. Bearse and R.E. Segel, Phys. Rev. 174 (1968) 1366. mg24pg.

|MO91| T. Motobayashi, T. Takei, S. Kox, C. Perrin, F. Merchez, D. Rebreyend, K. Ieki, H. Murakami, Y. Ando, N. Iwasa, N. Kurokawa, S. Shirato, J. Ruan (Gen), T. Ichihara, T. Kubo, N. Inabe, A. Goto, S. Kubono, S. Shimoura and M. Ishihara, Phys. Lett. B 264 (1991) 259. n13pg.

|MO93| P. Mohr, H. Abele, R. Zwiebel, G. Staudt, H. Krauss, H. Oberhummer, A. Denker, J.W. Hammer and G. Wolf, Phys. Rev. C 48 (1993) 1420. tag, he3he4.

|MO94a| P. Mohr, V. Kölle, S. Wilmes, U. Atzrott, G. Staudt, J.W. Hammer, H. Krauss and H. Oberhummer, Phys. Rev. C 50 (1994) 1543. dag.

|MO94b| T. Motobayashi, N. Iwasa, Y. Ando, M. Kurokawa, H. Murakami, J. Ruan (Gen), S. Shimoura, S. Shirato, N. Inabe, M. Ishihara, T. Kubo, Y. Watanabe, M. Gai, R.H. France III, K.I. Hahn, Z. Zhao, T. Nakamura, T. Teranishi, Y. Futami, K. Furutaka and T. Delbar, Phys. Rev. Lett. 73 (1994) 2680. be7pg.

|MO97| R. Morlock, R. Kunz, A. Mayer, M. Jaeger, A. Müller, J.W. Hammer, P. Mohr, H. Oberhummer, G. Staudt and V. Kölle, Phys. Rev. Lett. 79 (1997) 3837. o16pg.

|MU79| G. Murillo, M. Fernández, P. Pérez, J. Ramírez, S.E. Darden, M.C. Cobian-Rozak and L. Montestruque, Nucl. Phys. A 318 (1979) 352. o18pa.

|MU81| K. Murphy, R.C. Byrd, P.P. Guss, C.E. Floyd and R.L. Walter, Nucl. Phys. A 355 (1981) 1. n15pn.

|NA69| K. Nagatani, M.R. Dwarakanath and D. Ashery, Nucl. Phys. A 128 (1969) 325. he3ag.

|NE51| J.A. Neuendorffer, D.R. Inglis and S.S. Hanna, Phys. Rev. 82 (1951) 75. be9pd, be9pa.

|NE60| J.O. Newton, Nucl. Phys. 21 (1960) 529. si28pg.

|NE84| R.O. Nelson, E.G. Bilpuch, C.R. Westerfeldt and G.E. Mitchell, Phys. Rev. C 29 (1984) 1656; C 30 (1984) 755. al27pa.

|NI97| S. Niemeyer and H.P. Trautvetter, Jahresbericht of the Dynamitron Tandem Laboratorium 95-97, University of Bochum, 1997. o17pa.

|NO63| R. Nordhagen, Nucl. Phys. 44 (1963) 130. al27pg.

|NO64| R. Nordhagen and A. Tveter, Nucl. Phys. 56 (1964) 337. al27pg.

|NO81| T. Nozaki and M. Iwamoto, Radiochimical Acta 29 (1981) 57. n14pn.

|NO82| E.B. Norman, T.E. Chupp, K.T. Lesko and P. Schwalbach, Nucl. Phys. A 390 (1982) 561. na23an.

|NO85| K. Nomoto, F.-K. Thielemann and S. Miyaji, Astron. Astrophys. 149 (1985) 239. aaag, aang.

|NO97| K.M. Nollet, M. Lemoine and D.N. Schramm, Phys. Rev. C 56 (1997) 1144. dag.

[OK60a] K. Okano, J. Phys. Soc. Japan 15 (1960) 28. al27pg.

[OK60b] K. Okano, T. Tabata and K. Fukuda, J. Phys. Soc. Japan 15 (1960) 1556. si28pg.

[OL84] M.D. Olson and R.W. Kavanagh, Phys. Rev. C 30 (1984) 1375. li7an.

[OL96] F. de Oliveira, A. Coc, P. Aguer, C. Angulo, G. Bogaert, J. Kiener, A. Lefebvre, V. Tatischeff, J.P. Thibaud, S. Fortier, J.M. Maison, L. Rosier, G. Rotbard, J. Vernotte, M. Arnould, A. Jorissen and N. Mowlavi, Nucl. Phys. A 597 (1996) 231. n15ag.

[OL97] F. de Oliveira, A. Coc, P. Aguer, G. Bogaert, J. Kiener, A. Lefebvre, V. Tatischeff, J.P. Thibaud, S. Fortier, J.M. Maison, L. Rosier, G. Rotbard, J. Vernotte, S. Wilmes, P. Mohr, V. Kölle and G. Staudt, Phys. Rev. C 55 (1997) 3149. n15ag.

[OR73] H. Orihara, G. Rudolf and Ph. Gorodetzky, Nucl. Phys. A 203 (1973) 78. o18pa.

[OS84] J.L. Osborne, C.A. Barnes, R.W. Kavanagh, R.M. Kremer, G.J. Mathews, J.L. Zyskind, P.D. Parker and A.J. Howard, Nucl. Phys. A 419 (1984) 115. he3ag.

[OV69] Y.C. Overley, P.D. Parker and D.A. Bromley, Nucl. Instr. Meth. 68 (1969) 61. intro.

[OU92] J.M.L. Ouellet, H.C. Evans, H.W. Lee, J.R. Leslie, J.D. MacArthur, W. McLatchie, H.-B. Mak, P. Skensved, J.L. Whitton, X. Zhao and T.K. Alexander, Phys. Rev. Lett. 69 (1992) 1896. c12ag.

[OU96] J.M.L. Ouellet, M.N. Butler, H.C. Evans, H.W. Lee, J.R. Leslie, J.D. MacArthur, W. McLatchie, H.-B. Mak, P. Skensved, J.L. Whitton, X. Zhao and T.K. Alexander, Phys. Rev. C 54 (1996) 1982. c12ag.

[PA63] P.D. Parker and R.W. Kavanagh, Phys. Rev. 131 (1963) 2578. he3ag.

[PA66] P.D. Parker, Phys. Rev. 150 (1966) 851. be7pg.

[PA67] P. Paul, N.G. Puttaswamy and D. Kohler, Phys. Rev. 164 (1967) 1332. li7ag.

[PA68] P.D. Parker, Phys. Rev. 173 (1968) 1021. n14ag.

[PA78] B.M. Paine, S.R. Kennett and D.G. Sargood, Phys. Rev. C 17 (1978) 1550. na23pa.

[PA79] B.M. Paine and D.G. Sargood, Nucl. Phys. A 331 (1979) 389. na23pa, mg26pg, al27pg.

[PA89] Y.H. Park, B.-N. Sung, C.B. Moon, J.W. Kwon, J.C. Kim, H.C. Bhang, W.H. Chung and S.W. Cho, New Physics (Korean Phys. Soc.) 29 (1989) 430. be9pg.

[PA96] Particle Data Group, Phys. Rev. D 54 (1996) 1. intro, ppnu.

[PE63] R.R. Perry, B. Mainsbridge and J. Rickards, Nucl. Phys. 45 (1963) 586. li7pg.

[PE64] J.D. Pearson and R.H. Spear, Nucl. Phys. C 54 (1964) 434. o16ag.

[PH72] G.W. Phillips, P. Richard, D.O. Elliott, F.F. Hopkins and A.C. Porter, Phys. Rev. C 5 (1972) 297. n14pg.

[PI57] R.E. Pixley, PhD thesis, California Institute of Technology (1957), unpublished. n14pg.

[PI71] M. Piiparinen, A. Anttila, M. Viitasalo, Z. Phys. 247 (1971) 400. ne22pg.

[PL87] R. Plaga, H.W. Becker, A. Redder, C. Rolfs, H.P. Trautvetter and K. Langanke, Nucl. Phys. A 465 (1987) 291. c12ag.

[PR85] C. Pruneau, M.B. Chatterjee, C. Rangacharyulu and C. St-Pierre, Can. J. Phys. 63 (1985) 1141. c13pg.

[RA58] W.A. Ranken, T.W. Bonner and J.H. McCrary, Phys. Rev. 109 (1958) 1646. f19pa.

[RA80] K. Ramavataram, R. Larue, V. Turcotte, C. St-Pierre and S. Ramavataram, Nuovo Cim. A 58 (1980) 342. b11pn.

[RE68] R.V. Reid Jr., Ann. Phys. (N.Y.) 50 (1968) 411. ppnu.

[RE82] A. Redder, H.W. Becker, H. Lorenz-Wirzba, C. Rolfs, P. Schmalbrock and H.P. Trautvetter, Z. Phys. A 305 (1982) 325. n15pg, n15pa.

[RE87] A. Redder, H.W. Becker, C. Rolfs, H.P. Trautvetter, T.R. Donoghue, T.C. Rinckel, J.W. Hammer and K. Langanke, Nucl. Phys. A 462 (1987) 385. c12ag.

[RI63] V. Riech, Phys. Lett. 6 (1963) 267. li7pg.

[RI68] F.L. Riffle, J.D. Goss, D.R. Parsignault and J.C. Harris, Nucl. Phys. A 115 (1968) 120. f19pn.

[RI79] M. Riihonen, J. Keinonen and A. Anttila, Nucl. Phys. A 313 (1979) 251. si28pg.

[RO71] D.W.O. Rogers, J.H. Aitken, A.E. Litherland, W.R. Dixon and R.S. Storey, Can. J. Phys. 49 (1971) 1397. o16ag.

[RO72a] D.W.O. Rogers, J.H. Aitken and A.E. Litherland, Can. J. Phys. 50 (1972) 268. n15ag.

[RO72b] D.W.O. Rogers, R.P. Beukens and W.T. Diamond, Can. J. Phys. 50 (1972) 2428. n15ag.

[RO73a] C. Rolfs, Nucl. Phys. A 217 (1973) 29. o16pg.

[RO73b] C. Rolfs, A.M. Charlesworth and R.E. Azuma, Nucl. Phys. A 199 (1973) 257. n14ag, o17pg, o17pa.

[RO73c] C. Rolfs, I. Berka and R.E. Azuma, Nucl. Phys. A 199 (1973) 306. o17pg, o17pa.

| RO73d | D.W.O. Rogers, W.R. Dixon and R.S. Storey, Can. J. Phys. 51 (1973) 1. n15ag.

| RO74a | C. Rolfs and R.E. Azuma, Nucl. Phys. A 227 (1974) 291. c12pg.

| RO74b | C. Rolfs and W.S. Rodney, Nucl. Phys. A 235 (1974) 450. n15pg.

| RO75a | C. Rolfs and W.S. Rodney, Nucl. Phys. A 250 (1975) 295. o17pg, o17pa.

| RO75b | C. Rolfs, W.S. Rodney, M.H. Shapiro and H. Winkler, Nucl. Phys. A 241 (1975) 460. ne20pg, ne21pg, ne22pg.

| RO76 | D.W.O. Rogers, A.L. Carter, T.M.J. Symons, S.P. Dolan, N. Anyas- Weiss and K.W. Allen, Can. J. Phys. 54 (1976) 938. n15ag.

| RO77 | D.W.O. Rogers, N. Anyas-Weiss, S.P. Dolan, N.A. Jelley and T.K. Alexander, Can. J. Phys. 55 (1977) 206. mg24pg.

| RO79 | N.A. Roughton, M.R. Fritts, R.J. Peterson, C.S. Zaidins and C.J. Hansen, At. Data Nucl. Data Tables 23 (1979) 177. b10pa.

| RO81 | R.G.H. Robertson, P. Dyer, R.A. Warner, R.C. Melin, T.J. Bowles, A.B. McDonald, G.C. Ball, W.G. Davies and E.D. Earle, Phys. Rev. Lett. 47 (1981) 1867. dag.

| RO83a | R.G.H. Robertson, P. Dyer, T.J. Bowles, R.E. Brown, N. Jarmie, C.J. Maggiore and S.M. Austin, Phys. Rev. C 27 (1983) 11. he3ag.

| RO83b | N.A. Roughton, T.P. Intrator, R.J. Peterson, C.S. Zaidins and C.J. Hansen, At. Data Nucl. Data Tables 28 (1983) 341. n14an.

| RO86 | C. Rolfs and R.W. Kavanagh, Nucl. Phys. A 455 (1986) 179. li7pa.

| RO88 | C.E. Rolfs and W.S. Rodney, Cauldrons in the Cosmos (Chicago: Chicago University, 1988). intro.

| RO90 | A.A. Rollefson, V. Wijekumar, C.P. Browne, M. Wiescher, H.J. Hausman, W.Y. Kim and P. Schmalbrock, Nucl. Phys. A 507 (1990) 413. mg25pg.

| RO92 | F.J. Rogers and C.A. Iglesias, Astrophys. J. Supp. 79 (1992) 507. intro.

| SA52 | E.E. Salpeter, Phys. Rev. 88 (1952) 547. ppnu.

| SA78 | S.M. Sahakundu, S.M. Qaim, G. Stöcklin, Int. J. Appl. Radiat. Isotop. 30 (1978) 3. al27an.

| SA84 | M. Sajjad, R.M. Lambrecht and A.P. Wolf, Radiochimical Acta 36 (1984) 159. n15pn.

| SC52 | A.W. Schardt, W.A. Fowler and C.C. Lauritsen, Phys. Rev. 86 (1952) 527. n15pg, n15pa.

| SC70 | C. Schmidt and H. Duhm, Nucl. Phys. A 155 (1970) 644. o18pa.

| SC72 | R.L. Schulte, M. Cosack, A.W. Obst and J.L. Weil, Nucl. Phys. A 192 (1972) 609. ddn.

| SC83 | P. Schmalbrock, H.W. Becker, L. Buchmann, J. Görres, K.U. Kettner, W.E. Kieser, H. Kräwinkel, C. Rolfs, H.P. Trautvetter, J.W. Hammer and R.E. Azuma, Nucl. Phys. A 398 (1983) 279. ne20ag, na23pg.

| SC87a | U. Schröder, A. Redder, C. Rolfs, R.E. Azuma, L. Buchmann, C. Campbell, J.D. King and T.R. Donoghue, Phys. Lett. B 192 (1987) 55. tag.

| SC87b | U. Schröder, H.W. Becker, G. Bogaert, J. Görres, C. Rolfs, H.P. Trautvetter, R.E. Azuma, C. Campbell, J.D. King and J. Vise, Nucl. Phys. A 467 (1987) 240. n14pg.

| SC89 | U. Schröder, S. Engstler, A. Krauss, K. Neldner, C. Rolfs, E. Somorjai and K. Langanke, Nucl. Inst. Meth. 40/41 (1989) 466. intro.

| SC92 | D. Schmidt, R. Böttger, H. Klein and R. Nolte, Reports PTB-N-7 and PTB-N-8, Physikalisch-Technische Bundesanstalt, 1992, unpublished. be9an.

| SC95a | G.J. Schmid, R.M. Chasteler, C.M. Laymon, H.R. Weller, R.M. Prior and D.R. Tilley, Phys. Rev. C 52 (1995) R1732. dpg.

| SC95b | S. Schmidt, C. Rolfs, W.H. Schulte, H.P. Trautvetter, R.W. Kavanagh, C. Hategan, S. Faber, B.D. Valnion and G. Graw, Nucl. Phys. A 591 (1995) 227. na22pg.

| SE52 | J.D. Seagrave, Phys. Rev. 85 (1952) 197. c13pg.

| SE61 | R.E. Segel and M.J. Bina, Phys. Rev. 124 (1961) 814. b11pa.

| SE65 | R.E. Segel, S.S. Hanna and R.G. Allas, Phys. Rev. 139 (1965) B818. b11pg, b11pa.

| SE67a | K.K. Sekharan, A.S. Divatia, M.K. Mehta, S.S. Kerekatte and K.B. Nambiar, Phys. Rev. 156 (1967) 1187. c13an.

| SE67b | R.E. Segel, Z. Vager, L. Meyer-Schutzmeister, P.P. Singh and R.G. Allas, Nucl. Phys. A 93 (1967) 31. f19pg.

| SE69 | D.L. Sellin, H.W. Newson and E.G. Bilpuch, Ann. Phys. 51 (1969) 461. o18pa.

| SE73 | J.C. Sens, A. Pape and R. Armbruster, Nucl. Phys. A 199 (1973) 241. o17pg.

| SE78 | J.C. Sens, S.M. Refaei and A. Pape, Phys. Rev. C 18 (1978) 2007. o17pa.

| SE81 | R.M. Sealock, H.Y. Wu and J.C. Overley, Nucl. Phys. A 357 (1981) 279. li7an.

| SE90 | S. Seuthe, C. Rolfs, U. Schröder, W.H. Schulte, E. Somorjai, H.P. Trautvetter, F.B. Waanders, R.W. Kavanagh, H. Ravn, M. Arnould and G. Paulus, Nucl. Phys. A 514 (1990) 471. na22pg.

| SH68 | P.N. Shrivastava, F. Boreli and B.B. Kinsey, Phys. Rev. 169 (1968) 842. n14pa.

| SH79 | T. Shinozuka, Y. Tanaka and K. Sugiyama, Nucl. Phys. A 326 (1979) 47. li6pa.

| SI54 | R.M. Sinclair, Phys. Rev. 93 (1954) 1082. f19pg.

| SI65 | P.P. Singh, R.E. Segel, L. Meyer-Schützmeister, S.S. Hanna and R.G. Allas, Nucl. Phys. 65 (1965) 577. al27pg.

| SI73 | A.J. Sierk and T.A. Tombrello, Nucl. Phys. A 210 (1973) 341. be9pd, be9pa.

| SK87 | R.T. Skelton, R.W. Kavanagh and D.G. Sargood, Phys. Rev. C 35 (1987) 45. na23an.

| SM58 | P.B. Smith and P.M. Endt, Phys. Rev. 110 (1958) 397. al27pg.

| SM62 | P.J.M. Smulders and P.M. Endt, Physica 28 (1962) 1093. al27pg, al27pa.

| SM79 | J.J.A. Smit, M.A. Meyer, J.P.L. Reinecke and D. Reitmann, Nucl. Phys. A 318 (1979) 111. ne22pg.

| SM82 | J.J.A. Smit, J.P.L. Reinecke, M.A. Meyer, D. Reitmann and P.M. Endt, Nucl. Phys. A 377 (1982) 15. mg26pg.

| SM93 | M.S. Smith, P.V. Magnus, K.I. Hahn, R.M. Curley, P.D. Parker, T.F. Wang, K.E. Rehm, P.B. Fernandez, S.J. Sanders, A. García and E.G. Adelberger, Phys. Rev. C 47 (1993) 2740. n13pg.

| SN83 | K.A. Snover, E.G. Adelberger, P.G. Ikossi and B.A. Brown, Phys. Rev. C 27 (1983) 1837. n15pa.

| SP71 | H. Spinka, T. Tombrello and H. Winkler, Nucl. Phys. A 164 (1971) 1. li6pa, li7pa.

| SP97 | K. Spyrou, C. Chronidou, S. Harissopulos, S. Kossionides and T. Paradellis, Z. Phys. A 357 (1997) 283. f19pa.

| ST52 | T.F. Stratton and G.D. Freier, Phys. Rev. 88 (1952) 261. tdn.

| ST64 | P.H. Stelson and F.K. McGowan, Phys. Rev. B 133 (1964) 911. al27an.

| ST65 | J.R. Stewart, R.C. Morrison and J.S. O'Connell, Phys. Rev. 138 (1965) B372. dpg.

| ST78 | D.J. Steck, Phys. Rev. C 17 (1978) 1034. o16ag.

| ST96a | F. Strieder, L. Gialanella, U. Greife, C. Rolfs, S. Schmidt, W.H. Schulte, H.P. Trautvetter, D. Zahnow, F. Terrasi, L. Campajola, A. D'Onofrio, V. Roca, M. Romano and M. Romoli, Z. Phys. A 355 (1996) 209. be7pg.

| ST96b | F. Stegmüller, C. Rolfs, S. Schmidt, W.H. Schulte, H.P. Trautvetter and R.W. Kavanagh, Nucl. Phys. A 601 (1996) 168. na22pg.

| SU79 | K.M. Subotić, R. Ostojić and B.Z. Stepančić, Nucl. Phys. A 331 (1979) 491. f19pg.

| SW75 | Z.E. Switkowski, R. O'Brien, A.K. Smith and D.G. Sargood, Aust. J. Phys. 28 (1975) 141. na23pg, al27pg.

| SW79 | Z.E. Switkowski, J.C.P. Heggie, D.L. Kennedy, D.G. Sargood, F.C. Barker and R.H. Spear, Nucl. Phys. A 331 (1979) 50. li6pg.

| SY78 | T.J.M. Symons, L.K. Fifield, M.J. Hurst, F. Watt, C.H. Zimmerman and K.W. Allen, J. Phys. G 4 (1978) 411. n15ag.

| SZ72 | J. Szabó, J. Csikai and M. Várnagy, Nucl. Phys. A 195 (1972) 527. b10pa.

| TA59 | N. Tanner, Phys. Rev. 114 (1959) 1060. o16pg.

| TA64 | N.W. Tanner, G.C. Thomas and E.D. Earle, Nucl. Phys. 52 (1964) 29. f19pg.

| TE79 | F. Terrasi, A. Brondi, P. Cuzzocrea, R. Moro and M. Romano, Nucl. Phys. A 324 (1979) 1. si28pg.

| TH49 | R.G. Thomas, S. Rubin, W.A. Fowler and C.C. Lauritsen, Phys. Rev. 75 (1949) 1612. be9pa.

| TH77 | D.R. Thompson, M. LeMere and Y.C. Tang, Nucl. Phys. A 286 (1977) 53. ppnu.

| TH86 | F.K. Thielemann, M. Arnould and J.W. Truran, in Advances in Nuclear Astrophysics, ed. E. Vangioni-Flam, J. Audouze, J-P. Chièze and J. Tran Thanh Van (Editions Frontières, Gif sur Yvette, 1986), p. 525. intro.

| TI73 | G. Ticcioni, S.N. Gardiner, J.L. Matthews and R.O. Owens, Phys. Lett. B 46 (1973) 369. dpg.

| TI88 | R. Timmermann, H.W. Becker, C. Rolfs, U. Schröder and H.P. Trautvetter, Nucl. Phys. A 477 (1988) 105. al27pg, al27pa.

| TI93 | D.R. Tilley, H.R. Weller and C.M. Cheves, Nucl. Phys. A 564 (1993) 1. c12ag.

| TO63 | T.A. Tombrello and P.D. Parker, Phys. Rev. 131 (1963) 2582. he3ag.

| TR75a | H.P. Trautvetter and C. Rolfs, Nucl. Phys. A 242 (1975) 519. mg24pg.

| TR75b | H.P. Trautvetter, Nucl. Phys. A 243 (1975) 37. mg24pg, mg26pg.

| TR78 | H.P. Trautvetter, M. Wiescher, K.U. Kettner, C. Rolfs and J.W. Hammer, Nucl. Phys. A 297 (1978) 489. o18ag.

| TR95 | H.P. Trauttvetter, M. Möhle and S. Schmidt, Proc. 3rd Int. Symposium on Nuclei in the Cosmos, ed. M. Busso, R. Gallino and C.M. Raiteri (AIP Press, New York, 1995) p. 83. o17pg.

| TR97 | H.P. Trauttvetter, G. Roters, C. Rolfs, S. Schmidt and P. Descouvemont, Nucl. Phys. A 621 (1997) 161c. c12ag.

[TV72] A. Tveter, Nucl. Phys. A 185 (1972) 433. al27pg, al27pa.

[TY91] S. Typel, G. Blüge and K. Langanke, Z. Phys. A 339 (1991) 335. dag.

[TY94] S. Typel, PhD thesis, University of Münster (1994), unpublished. dag.

[UN74] B.Y. Underwood, M.R. Wormald, N. Anyas-Weiss, N.A. Jelley and K.W. Allen, Nucl. Phys. A 225 (1974) 253. n15ag.

[VA56] C. van der Leun, P.M. Endt, J.C. Kluyver and L.E. Vrenken, Physica 22 (1956) 1223. mg26pg.

[VA61] K.J. Van Oostrum, N. Hazewindus and A.H. Wapstra, Nucl. Phys. 25 (1961) 409. si28pg.

[VA63] C. van der Leun and P.M. Endt, Physica 29 (1963) 990. mg26pg.

[VA66] C. van der Leun and N.C. Burhoven Jaspers, Nucl. Phys. 88 (1966) 235. mg26pg.

[VA69] R.J. van Reenen, Z.B. du Toit and W.L. Mouton, Z. Phys. 227 (1969) 326. mg24pg.

[VA70a] F.J. Vaughn, R.A. Chalmers, D. Kohler and L.F. Chase Jr, Phys. Rev. C 2 (1970) 1657. be7pg.

[VA70b] L. Van der Zwan and K.W. Geiger, Nucl. Phys. A 152 (1970) 481. be9an.

[VA78] L. Van der Zwan and K.W. Geiger, Nucl. Phys. A 306 (1978) 45. b11pn.

[VA81] L. Van der Zwan and K.W. Geiger, Nucl. Sci. Eng. 79 (1981) 197. mg25an.

[VA87] J.R. Vanhoy, E.G. Bilpuch, C.R. Westerfeldt and G.E. Mitchell, Phys. Rev. C 36 (1987) 920. na23pa.

[VO63] J.L. Vogl, PhD thesis, California Institute of Technology (1963), unpublished. c12pg.

[VO83] H. Volk, H. Kräwinkel, R. Santo and L. Wallek, Z. Phys. A 310 (1983) 91. he3ag.

[VO89] R.B. Vogelaar, PhD thesis, California Institute of Technology, 1989. al26pg.

[VO90] R.B. Vogelaar, T.R. Wang, S.E. Kellogg and R.W. Kavanagh, Phys. Rev. C 42 (1990) 753. o18pg, o18ag.

[VO96] R.B. Vogelaar, L.W. Mitchell, R.W. Kavanagh, A.E. Champagne, P.V. Magnus, M.S. Smith and A.J. Howard, Phys. Rev. C 53 (1996) 1945. al26pg.

[WA54] J.B. Warren, K.A. Laurie, D.B. James and K.L. Erdman, Can. J. Phys. 32 (1954) 563. o16pg.

[WA63a] J.B. Warren, K.L. Erdman, L.P. Robertson, D.A. Axen and J.R. Macdonald, Phys. Rev. 132 (1963) 1691. dpg.

[WA63b] K.L. Warsh, G.M. Temmer and H.R. Blieden, Phys. Rev. 131 (1963) 1690. f19pa.

[WA66] N.-M. Wang, V. Novatskii, G.M. Osetinskii, N.-K. Chien and I.A. Chepurchenko, Sov. J. Nucl. Phys. 3 (1966) 777. he3he3.

[WA80] R.A. Ward and W.A. Fowler, Astr. J. 238 (1980) 266. na23an.

[WA84] H. Walliser, H. Kanada and Y.C. Tang, Nucl. Phys. A 419 (1984) 133. he3ag.

[WA89] T.F. Wang, A.E. Champagne, J.D. Hadden, P.V. Magnus, M.S. Smith, A.J. Howard and P.D. Parker, Nucl. Phys. A 499 (1989) 546. al26pg.

[WE56] G. Weber, L.W. Davis and J.B. Marion, Phys. Rev 104 (1956) 1307. be9pd, be9pa.

[WE86] H.R. Weller, P. Colby, J. Langenbrunner, Z.D. Huang, D.R. Tilley, F.D. Santos, A. Arriaga and A.M. Eiró, Phys. Rev. C 34 (1986) 32. ddg.

[WI52] H.B. Willard, J.K. Bair, J.D. Kington, T.M. Hahn, C.W. Snyder and F.P. Green, Phys. Rev. 85 (1952) 849. f19pa.

[WI77] C. Wiezorek, H. Kräwinkel, R. Santo and L. Wallek, Z. Phys. A 282 (1977) 121. be7pg.

[WI80] M. Wiescher, H.W. Becker, J. Görres, K.U. Kettner, H.P. Trautvetter, W.E. Kieser, C. Rolfs, R.E. Azuma and K.P. Jackson and J.W. Hammer, Nucl. Phys. A 349 (1980) 165. o18pg.

[WI81] R.D. Williams and S.E. Koonin, Phys. Rev. C 23 (1981) 2773. he3ag.

[WI82] M. Wiescher and K.U. Kettner, Astrophys. J. 263 (1982) 891. o18pa.

[WI83] M. Wiescher, R.N. Boyd, S.L. Blatt, L.J. Rybarcyk, J.A. Spizuoco, R.E. Azuma, E.T.H. Clifford, J.D. King, J. Görres, C. Rolfs and A. Vlieks, Phys. Rev. C 28 (1983) 1431. b10pg, b10pa.

[WI85] F.J. Wilkinson III and F.E. Cecil, Phys. Rev. C 31 (1985) 2036. ddg.

[WI86] M. Wiescher and K. Langanke, Z. Phys. A 325 (1986) 309. na22pg.

[WI95a] S. Wilmes, P. Mohr, U. Atzrott, V. Kölle, G. Staudt, A. Mayer and J.W. Hammer, Phys. Rev. C 52 (1995) 2823. n15ag.

[WI95b] O. Wieland, Diplom thesis, University of Stuttgart (1995), unpublished. mg25an, mg26an.

[WI97] S. Wilmes, V. Kölle, U. Kölle, G. Staudt, P. Mohr, J.W. Hammer and A. Mayer, Nucl. Phys. A 621 (1997) 145c. n15ag.

[WO53] H.H. Woodbury, R.B. Day and A.V. Tollestrup, Phys. Rev. 92 (1953) 1199. c13pg.

[WO61] C. Wong, J.D. Anderson, S.D. Bloom, J.W. McClure and B.D. Walker, Phys. Rev. 123 (1961) 598. c13pn, n15pn.

[WO67] W. Wölfli, R. Bösch, J. Lang, R. Müller and P. Marmier, Helv. Phys. Acta 40 (1967) 946. dpg.

[WO89] K. Wolke, V. Harms, H.W. Becker, J.W. Hammer, K.L. Kratz, C. Rolfs, U. Schröder, H.P. Trautvetter, M. Wiescher and A. Wöhr, Z. Phys. A 334 (1989) 491. ne22ag, ne22an.

[WR94] P.R. Wrean, C.R. Brune and R.W. Kavanagh, Phys. Rev. C 49 (1994) 1205. be9an.

[WÜ92] S. Wüstenbecker, H.W. Becker, H. Ebbing, W.H. Schulte, M. Berheide, M. Buschmann, C. Rolfs, G.E. Mitchell and J.S. Schweitzer, Z. Phys. A 344 (1992) 205. aaag.

[YA62] K. Yagi, J. Phys. Soc. Japan 17 (1962) 604. o18pa.

[YA64] T. Yanabu, S. Yamashita, S. Kakigi, D.-C. Nguyen, K. Takimoto, Y. Yamada and K. Ogino, J. Phys. Soc. Japan 19 (1964) 1818. be9pa.

[YA93] Y. Yamashita and Y. Kudo, Prog. Theor. Phys 90 (1993) 1303. f19pa.

[YO91] M. Youn, H.T. Chung, J.C. Kim and H.C. Bhang, Nucl. Phys. A 533 (1991) 321. b10pa.

[ZA95a] D. Zahnow, C. Angulo, C. Rolfs, S. Schmidt, W.H. Schulte and E. Somorjai, Z. Phys. A 351 (1995) 229. li7pg, f19pa.

[ZA95b] D. Zahnow, C. Angulo, M. Junker, C. Rolfs, S. Schmidt, W.H. Schulte and E. Somorjai, Nucl. Phys. A 589 (1995) 95. be9pg.

[ZA97] D. Zahnow, C. Rolfs, S. Schmidt and H.P. Trautvetter, Z. Phys. A 359 (1997) 211. be9pd, be9pa.

[ZH93] Z. Zhao, R.H. France III, K.S. Lai, L. Rugari, M. Gai and E.L. Wilds, Phys. Rev. Lett. 70 (1993) 2066. c12ag.

[ZI85] J.F. Ziegler, J.P. Biersack and U. Littmark, The Stopping Power and Ranges of Ions in Solids (Pergamon Press, New York, 1985). b10pa.

[ZI86] F. Zijderhand and C. van der Leun, Nucl. Phys. A 460 (1986) 181. c13pg.

[ZU63] R.W. Zurmühle, W.E. Stephens and H.H. Staub, Phys. Rev. 132 (1963) 751. ddg.

[ZU65] R.W. Zurmühle, Nucl. Phys. 72 (1965) 225. he3he3.

[ZU71] W.M. Zuk, J.L. Black and W.F. Davidson, Aust. J. Phys. 24 (1971) 37. si28pg.

[ZY79] J.L. Zyskind and P.D. Parker, Nucl. Phys. A 320 (1979) 404. n15pa.

[ZY81] J.L. Zyskind, M. Rios and C. Rolfs, Astrophys. J. 243 (1981) L53. na23pa.